

AN ABSTRACT OF THE THESIS OF

G.A. Bradshaw for the degree of Doctor of Philosophy in Forest Science presented on September 10, 1991.

Title: Hierarchical Analysis of Spatial Pattern and Processes of Douglas-fir Forests.

Abstract approved: \_\_\_\_\_ Signature redacted for privacy.

Susan G. Stafford  
Signature redacted for privacy.

\_\_\_\_\_  
William J. Ripple

There has been an increased interest in the quantification of pattern in ecological systems over the past years. This interest is motivated by the desire to construct valid models which extend across many scales. Spatial methods must quantify pattern, discriminate types of pattern, and relate hierarchical phenomena across scales. Wavelet analysis is introduced as a method to identify spatial structure in ecological transect data. The main advantage of the wavelet transform over other methods is its ability to preserve and display hierarchical information while allowing for pattern decomposition.

Two applications of wavelet analysis are illustrated, as a means to: 1) quantify known spatial patterns in Douglas-fir forests at several scales, and 2) construct spatially-explicit

hypotheses regarding pattern generating mechanisms. Application of the wavelet variance, derived from the wavelet transform, is developed for forest ecosystem analysis to obtain additional insight into spatially-explicit data. Specifically, the resolution capabilities of the wavelet variance are compared to the semi-variogram and Fourier power spectra for the description of spatial data using a set of one-dimensional stationary and non-stationary processes. The wavelet cross-covariance function is derived from the wavelet transform and introduced as an alternative method for the analysis of multivariate spatial data of understory vegetation and canopy in Douglas-fir forests of the western Cascades of Oregon.

° Copyright by G.A. Bradshaw

10 September 1991

All Rights Reserved

Hierarchical Analysis of Spatial Pattern and Processes  
of Douglas-fir Forests Using Wavelet Analysis

by

G.A. Bradshaw

A THESIS

submitted to

Oregon State University

in partial fulfillment of  
the requirements for the  
degree of

Doctor of Philosophy

Completed September 10, 1991

Commencement June 1992

APPROVED:

 Signature redacted for privacy.  
\_\_\_\_\_  
Professor of Forest Resources in charge of major

 Signature redacted for privacy.  
\_\_\_\_\_  
Professor of Forest Science in charge of major

Signature redacted for privacy.  
\_\_\_\_\_  
Head of Department of Forest Science

Signature redacted for privacy.  
Dean of Graduate School \_\_\_\_\_  


Date thesis is presented September 10, 1991

Typed by G.A. Bradshaw

To  
Chauncey S. Goodrich

## Table of Contents

	<u>Page</u>
Chapter 1: Introduction	1
Chapter 2: Satellite Imagery and Time Series Analysis for the Description of Forested Landscapes in Oregon	7
Abstract	7
Introduction	9
Multi-scale Analysis of western Oregon Landscapes	14
Study Area	15
Methods	17
Satellite Imagery	17
Time Series Analysis: Wavelet Transform	18
Results	21
AVHRR Analysis	21
Multi-spectral Scanner Results	23
Thematic Mapper Analysis	24
Discussion	26
Conclusions	29
Literature Cited	66
Chapter 3: Resolution Capabilities of the Wavelet Variance in the Analysis of Spatial Pattern	70
Abstract	70
Introduction	72
Wavelet Variance	76
Calculation of the Wavelet Variance	76
Calibration of the Wavelet Variance in the Frequency Domain	81
Comparison of Wavelet Variance, Power Spectrum, and Semi-Variogram	86
Stationary Processes	
Non-Stationary and Non-Uniform Processes	89
Wavelet Cross-variance	93
Conclusions	97
Literature Cited	130
Chapter 4: Characterising Forest Canopy Gap Structure Using Wavelet Variance	133
Abstract	133
Introduction	135
Wavelet Analysis	139
Wavelet Transform	139
Simulated Example	140

## Table of Contents continued

	Wavelet Variance	142
	Application to Forest Transects	145
	Study Sites	146
	Wavelet Analysis	147
	Canopy Patterns Along a Chronosequence	149
	Conclusions	153
	Literature Cited	177
Chapter 5:	Spatially Correlated Patterns Between Understory Vegetation and Age-Related Gap Structure in Douglas-fir Forests	180
	Abstract	180
	Introduction	182
	Assumptions	186
	Study Area	187
	Methods	189
	Results	192
	Trends in Vegetation and Resource Cover	192
	Spatial Covariance Between Canopy Gap and Understorey Vegetation	194
	Conclusions	198
	Literature Cited	258
Chapter 6:	Conclusions	262
	Bibliography	266

## List of Figures

<u>Figure</u>	<u>Page</u>
2.1 Rectified AVHRR image of western Oregon in the visible red and near-infrared bands. Superimposed blue lines correspond to the three transects selected in the study: T4= western Cascades transect (500 kilometers), T3=Coast Range transect (500 km), and O1=west to east transect across western Oregon.	31
2.2 Rectified MSS image of an approximately 3500 km <sup>2</sup> area located in the western Cascades, Oregon. Superimposed blue lines denote the transects used in the study: P1=private land transect, P2= public land, P3=wilderness land.	33
2.3 Standardized NIR and red visible AVHRR data transects of the west to east transect across Oregon (O1).	34
2.4 Standardized NIR and red visible AVHRR data transects of the Cascade Range (T4).	35
2.5 Standardized NIR and red visible AVHRR data transects of the Coast Range (T3).	36

- 2.6 Standardized NIR and visible red TM data transects of the Starkey Experimental Forest. 37
- 2.7 Standardized NIR TM data transect of the western Cascades Range. 38
- 2.8 Wavelet variance for NIR AVHRR band of the west-east transect across western Oregon (O1). y-axis corresponds to wavelet variance amplitude; x-axis corresponds to scale of pattern (km). 39
- 2.9 Wavelet transform of west-east transect (O1). y-axis corresponds to scale (km); x-axis corresponds to distance along the transect (km). Grey-scale denotes signal intensity. 40
- 2.10 Small-scale wavelet transform of west-east transect (O1) ranging from one to twenty kilometer scale to illustrate fine-scale structure. 42
- 2.11 Wavelet cross-covariance between visible red and NIR spectral bands for west-east transect (O1). Dark values denote high covariance. Light values denote negative covariance. y-axis corresponds to scale of interaction (km); x-axis corresponds to lag (km). 44

2.12	Wavelet variance for NIR and visible red AVHRR band of the western Cascades transect in western Oregon (T4).	46
2.13	Wavelet variance for NIR and visible red AVHRR band of the Coast Range transect across western Oregon (T3).	47
2.14	Wavelet transform of western Cascades transect (T4).	48
2.15	Wavelet transform of Coast Range transect (T3).	49
2.16	Wavelet cross-covariance between visible red and NIR spectral bands for western Cascades transect (T4).	50
2.17	Wavelet cross-covariance between visible red and NIR spectral bands for Coast Range transect (T3).	51
2.18	Wavelet variance for MSS private lands transect in 1972. Visible red correponds to solid line and NIR to the dashed line.	52
2.19	Wavelet variance for MSS public lands transect in 1972. Visible red correponds to solid line and NIR to the dashed line.	53

- 2.20 Wavelet variance for MSS wilderness lands transect in 1972. Visible red corresponds to solid line and NIR to the dashed line. 54
- 2.21 Wavelet variance for MSS private lands transect in 1988. Visible red corresponds to solid line and NIR to the coarse dashed line. 55
- 2.22 Wavelet variance for MSS public lands transect in 1988. Visible red corresponds to solid line and NIR to the dashed line. 56
- 2.23 Wavelet variance for MSS wilderness lands transect in 1988. Visible red corresponds to solid line and NIR to the coarse dashed line. 57
- 2.24 Wavelet transform for MSS NIR transect on private lands in 1988. 58
- 2.25 Wavelet transform for MSS NIR transect on public lands in 1988. 59
- 2.26 Wavelet variance for Starkey Experimental Forest for visible red (solid line) and NIR (dashed line). Note peak centred at 350 meters. 60
- 2.27 Wavelet cross-covariance for the Starkey

transect between the visible red and NIR TM bands.  
Notice high covariance at 350 meters.

61

2.28: Wavelet variance for western Cascades TM transect for visible red (solid line) and NIR (dashed line). Note peaks centred at 100 meters and 350 meters.

63

2.29: Wavelet cross-covariance for the western Cascades TM transect between the visible red and NIR TM bands. Notice high covariance at the fine scale.

64

3.1 Mexican hat (solid line), Haar (heavy solid line) and French hat (dashed line) analysing wavelets.

99

3.2 Sample data transect used in wavelet transform construction for figure 3.3. x-axis represents distance along transect (meters); y-axis represents magnitude of variable.

100

3.3 Wavelet transform of data transect shown in figure 3.2 calculated using the mexican hat analysing wavelet. x-axis represents distance along transect while y-axis represents scale (meters). Brightness of transform increases with increasing intensity of

feature magnitude of signal at given location.	101
3.4 Transfer functions of mexican hat (solid line), Haar (heavy solid line), and french hat (dashed line) analysing wavelets and semi-variogram (dotted line).	103
3.5 Calibrated transfer functions of figure 3.4.	104
3.6 Transfer function of the mexican hat analysing function at several scales of the scaling parameter a.	105
3.7 AR(1) process of parameter $\alpha=0.5$ : wavelet variances (mexican hat (solid), Haar (heavy solid), French hat (dashed)) and semi-variogram (heavy dashed) responses.	106
3.8 AR(1) process of parameter $\alpha=0.5$ : power spectrum.	107
3.9 Additive moving average process of parameter $m+1=5$ : wavelet variances (mexican hat (solid), Haar (heavy solid), french hat (dashed)) and semi-variogram (heavy dashed) responses.	108

3.10 Additive moving average process of parameter $m+1=5$ : power spectrum response.	109
3.11 Non-additive moving average process of parameter $m + 1=5$ : wavelet variances (mexican hat (solid), Haar (heavy solid), french hat (dashed)) and semi-variogram (heavy dashed) responses.	110
3.12 Non-additive moving average process of parameter $m+1=5$ power spectrum.	111
3.13 AR Harmonic process of parameter $p=0.9$ , period=10 meters: wavelet variances (mexican hat (solid), Haar (heavy solid), french hat (dashed)) and semi-variogram (heavy dashed ) responses.	112
3.14 AR Harmonic process of parameter $p=0.9$ , period=10 meters: power spectrum.	113
3.15 Simulated data transect composed of two cosine functions of period 10 and 30 meters.	114
3.16 Power spectrum of transect in figure 3.15.	115
3.17 Wavelet variance for figure 3.15.	116
3.18 Simulated data transect composed of two cosine functions of period 10 and 30 meters.	117

3.19 Power spectrum of transect in figure 3.18.	118
3.20 Wavelet variance for figure 3.18.	119
3.21 Power spectra for family of square waves of varying period ratios.: 1 (solid line), 2 (light dashed line), 3 (heavy solid line), 4 (heavy solid line).	120
3.22 Haar wavelet variance for period ratios as described in figure 3.21 above.	121
3.23 Mexican hat wavelet variance for period ratios as described in figure 3.21 above.	122
3.24 Two cosine functions of period ten offset by five meters relative to each other.	123
3.25 Wavelet cross-covariance function for variables in figure 3.24. Grey-scale indicates correlation values. x- axis corresponds to lag (offset) between variables at which a given correlation occurs. y-axis corresponds to the scale of interaction (m).	124
3.26 Transect of canopy gap (upper panel) and tall	

shrub (lower panel) data from the young Douglas-fir.	126
3.27 Wavelet cross-covariance function for variables in figure 3.26.	127
3.28 Transect of canopy gap (upper panel) and tall shrub (lower panel) data from the old-growth Douglas fir stand.	128
3.29 Wavelet cross-covariance for variables in figure 3.28.	129
4.1 The mexican hat (solid line) and Haar (heavy solid line) analysing wavelets used in the simulation and empirical analyses.	158
4.2 Simulated forest canopy-gap transect of simple pattern.	159
4.3 Haar wavelet transform for data in figure 4.2. Grey-scale indicates values of wavelet transform. y-axis corresponds to scale (m); x-axis corresponds to distance along transect (m). Viewing the figure nearly-parallel to plane of the page emphasises the transform structure.	160

4.4 Mexican hat wavelet transform for data in figure 4.2.	162
4.5 Simulated forest canopy transect of nested, two-scale pattern.	163
4.6 Wavelet transform of data in figure 4.6.	164
4.7 Wavelet variance of the nested, two-scale transect in figure 4.5.	165
4.8 Data transect of forest canopy gap of a young stand (Y1).	166
4.9 Wavelet transform of canopy gap data of young stand (Y1) shown in figure 4.8.	167
4.10 Wavelet variance of canopy gap data of young stand (Y1) shown in figure 4.8.	168
4.11 Data transect of forest canopy gaps of an old-growth stand (O1).	169
4.12 Wavelet transform of canopy gap data of old growth stand (O1) shown in figure 4.11.	170

4.13 Wavelet variance of canopy gap data of old growth stand (O1) shown in figure 4.11.	171
4.14 Data transect of forest canopy gaps of a second young stand (Y4).	172
4.15 Wavelet transform of canopy gap data of second young stand (Y4) shown in figure 4.14.	173
4.16 Wavelet variance of canopy gap data of second young stand (Y4) shown in figure 4.14.	174
4.17 Composite plot of wavelet variances calculated for canopy gap transects established in twelve <u>Pseudotsuga menziesii</u> stands representing three age classes: young, mature, and old growth. The twelve wavelet variances are grouped according to group I (multi-scale, open gaps (5-30 m)) heavy dashed lines to group II (small (<8 m), diffuse gaps), light dashed lines to group III (small to moderately sized (4-15 m), open gaps), and heavy solid lines to group IV (moderately sized, diffuse gaps).	175
5.1 Transect data for young stand Y1. Canopy gap measured in percent canopy opening.	209

5.2	Transect data for mature stand M1. Canopy gap measured in percent canopy opening.	211
5.3	Transect data for old growth stand O1. Canopy gap measured in percent canopy opening.	213
5.4	Transect data for young stand Y4. Canopy gap measured in percent canopy opening.	216
5.5	Transect data for mature stand M3. Canopy gap measured in percent canopy opening.	217
5.6	Transect data for old growth stand O2. Canopy gap measured in percent canopy opening.	219
5.7	Wavelet variance for herb cover in all twelve stands. x-axis corresponds to scale of patch size; y-axis corresponds to the magnitude of the wavelet variance at a given patch size. Y1-Y4=young stands (dashed lines), M1-M4=mature stands (solid lines), O1-O4=old growth stands (heavy solid lines).	221
5.8	Total wavelet variance for herb class as a function of stand age. Total wavelet variance is in units of (% <sup>2</sup> cover).	223

5.9 Scale at which maximum wavelet variance occurs in meters (average patch size) as a function of relative stand age for herb class.	224
5.10 Total wavelet variance for hemlock seedling class as a function of stand age. Total wavelet variance is in units of (% <sup>2</sup> cover).	225
5.11 Total wavelet variance of woody debris cover versus total wavelet variance of hemlock seedling (% <sup>2</sup> ).	226
5.12 Total wavelet variance of canopy gap cover versus total wavelet variance of hemlock seedling (% <sup>2</sup> ).	227
5.13 Wavelet variance for woody debris in all twelve stands.	228
5.14 Wavelet variance for hemlock seedling in all twelve stands.	229
5.15 Scale at which maximum wavelet variance occurs in meters (average patch size) as a function of relative stand age for hemlock seedling class.	230

- 5.16 Scale at which maximum wavelet variance occurs in meters (average patch size) as a function of relative stand age for total woody debris class. 231
- 5.17 Total wavelet variance for total woody debris class as a function of stand age. Total wavelet variance is in units of (%<sup>2</sup> cover). 232
- 5.18 Total wavelet variance for low shrub class as a function of stand age. Total wavelet variance is in units of (%<sup>2</sup> cover). 233
- 5.19 Total wavelet variance for tall shrub class as a function of stand age. Total wavelet variance is in units of (%<sup>2</sup> cover). 234
- 5.20 Scale at which maximum wavelet variance occurs in meters (average patch size) as a function of relative stand age for low shrub class. 235
- 5.21 Scale at which maximum wavelet variance occurs in meters (average patch size) as a function of relative stand age for tall shrub class. 236
- 5.22 Total wavelet variance of tall shrub cover versus total wavelet variance of canopy gap (%<sup>2</sup>). 237

5.23 Wavelet variance for tall shrub in all twelve stands.	238
5.24 Wavelet variance for canopy gap opening in all twelve stands.	239
5.25 Total wavelet variance of canopy gap opening versus total wavelet variance of canopy gap opening (% <sup>2</sup> ).	240
5.26 Wavelet variance for low shrub class in all twelve stands.	241
5.27 Scale at which maximum wavelet variance occurs in meters (average patch size) as a function of relative stand age for canopy gap opening.	242
5.28 Total wavelet variance for canopy gap opening as a function of stand age. Total wavelet variance is in units of (% <sup>2</sup> cover).	243
5.29 Wavelet cross-covariance between canopy gap and low shrub cover for young stand Y1. x-axis corresponds to the lag or offset between the two variables in meters; the y-axis corresponds to the scale at which the variables are correlated. The	

grey-scale bar at the right of the figure indicates the magnitude of the spatial covariance. Positive covariance values are dark grey while negative correlations are white. 244

5.30 Wavelet cross-covariance between canopy gap and low shrub cover for mature stand M3. 246

5.31 Wavelet cross-covariance between canopy gap and low shrub cover for old growth stand O1. 247

5.32 Wavelet cross-covariance between canopy gap and tall shrub cover for young stand Y4. 248

5.33 Wavelet cross-covariance between canopy gap and tall shrub cover for young stand Y1. 249

5.34 Wavelet cross-covariance between canopy gap and hemlock seedlings for old growth stand O1. Note two distinct scales of interaction at 5 and 25 meters. 250

5.35 Wavelet cross-covariance between woody debris and hemlock seedlings for stand O1. Note two distinct scales of pattern. 252

5.36 Wavelet cross-covariance between woody debris

and hemlock seedlings for mature stand M1. 254

5.37 Wavelet cross-covariance between canopy gap and  
hemlock seedlings for mature stand M1. 255

5.38 Wavelet cross-covariance between canopy gap and  
hemlock seedlings for mature stand M3. Note lack of  
structure. 256

## List of Tables

	<u>Page</u>
Table 4.1: Description of canopy structure of the twelve <u>Pseudotsuga</u> stands.	156
Table 5.1: Total woody debris, canopy gap and overstorey hemlock of each stand ranked by overall amount of cover. Woody debris and canopy gap estimates were obtained using the wavelet variance. Overstorey hemlock represents a qualitative estimate based on field observations. Y1-Y4 are young stands, M1-M4 are mature stands, and O1-O4 are old growth stands.	203
Table 5.2: The mean, maximum, minimum, and interquartile range for each variable according to age class (O=old, M=mature, Y=young). Summary statistics are in transformed units; low values of percent cover are negative, high values of percent cover are positive. Results of nested ANOVA performed on each variable are included (Sig=Significance level $Pr>F=0.0001$ at 0.5).	205

**List of Tables continued**

Table 5.3: Total wavelet variance for twelve  
Pseudotsuga stands (%<sup>2</sup> cover) by variable.  
Y1-Y4=young stands, M1-M4= mature stands,  
O1-O4=old growth stands.

**HIERARCHICAL ANALYSIS OF SPATIAL PATTERN AND PROCESSES  
OF DOUGLAS-FIR FORESTS USING  
WAVELET ANALYSIS**

**Chapter 1**

**INTRODUCTION**

When the titles of published articles in the natural and physical sciences are reviewed over the past few years, terms such as "pattern", "hierarchical", "intergration", "scale", "spatial", "temporal", and "patch dynamics" appear with increasing frequency in journals from disciplines as disparate as geophysics, ecology, oceanography, and biology. In the broadest sense, this attention to pattern merely reflects an effort to unravel the complexity of observed phenomena and discriminate the signal from the noise (Levin, 1988). However, as viewed from a historical perspective, the recent interest behind the study of pattern and scale is only a part of a general trend to integrate research across disciplines (MacIntosh, 1985). This shift is exemplified by the evolution and present usage of the concept of a plant community in the field of ecology. The changing definitions and perception of a plant community parallels the history of

plant ecology over the past century.

Plant ecology began as a descriptive discipline focusing on isolated parts of the ecosystem and classification (Sears, 1955). This approach gradually evolved into a discipline which encompasses both the isolated and the integrated, the quantitative and the descriptive. Reflecting this trend, the term "plant community" has shifted from a purely floristically based classification to a broader, more abstract concept in deference to recognition of the importance of spatial (e.g. landscape features), temporal (e.g. disturbance frequency), and environmental variability (e.g. site moisture heterogeneity; Hemstrom and Logan, 1986). Plant ecology now focusses on the identification and integration of abiotic and biotic processes which govern community structure and composition; a plant community is not viewed as a static condition but rather as an ongoing expression of the underlying processes of succession, disturbance history, and plant-plant interactions (Barbour et al, 1980). The concept of the ecosystem has nearly supplanted the dichotomy of the Clements' holistic and Gleason-Whittaker individual-based approaches (MacIntosh, 1985).

Concurrent with the shift in conceptual approach, there has been a dramatic ascendancy of technology in the natural sciences. Computer accessibility and the development of accurate and innovative measurement tools have broadened the scope of field and laboratory experimentation previously

hindered by feasibility constraints. The use and application of techniques developed in other fields has functioned to bridge the communication gap between disciplines as well. Transfer of technology has increased the exchange of ideas and the introduction of perspectives from a spectrum of disciplines.

Finally, the realization of the impact of humans on the ecosystem and social demands from various quarters has further galvanized the integration of methods and concepts in science. For example, recognition of the cumulative effects of pollution on global climate has underscored the realization that conditions of the local environment are linked to events occurring at distances and scales outside everyday perception; the range of human impact on the biosphere extends well beyond the artificial bounds of county or state. The consideration of all three of these factors (i.e. conceptual, technological advances and social considerations) has motivated current research and management interest in the spatial relationships of the forest ecosystem. To accomplish the integration of concepts and data across scales, the ecologist will need to use multi-scale data along with spatial pattern analyses.

A number of extant methods for the analysis of spatial pattern have been used in ecology over the past fifteen years (Pielou, 1977). Because the majority of spatial methods have derive from fields outside of ecology, there is still a great

need to develop and test extant methods for specific application to ecological data. Many of these techniques belong to a group of methods designed to describe point processes. A spatial point process is "any stochastic mechanism which generates a countable set of events in space" (e.g. tree locations; Diggle, 1987). In contrast, a continuously-valued process is one generated by a stochastic mechanism which assigns a value to every point in the area of interest (e.g. elevation). A second group of spatial methods, time-series analysis, is used for the description of continuously-valued processes. These methods include Fourier power spectra and the semi-variogram (Priestley, 1977; Journel and Huijbregts, 1978) and only have begun to be applied in terrestrial ecology over the past ten years (e.g. Cohen, Spies, and Bradshaw, 1991; Kenkel, 1988; Ford and Renshaw, 1984).

A third time-series method, the wavelet transform, has recently been introduced to the physical sciences for signal processing and description of structure in turbulent flow (Mallet, 1988; Gamage, 1990). The wavelet transform differs from other time-series methods in that it preserves locational information as a function of pattern scale. As a result, the transform and its derivative functions, the wavelet variance and, introduced here, the wavelet cross-covariance, preserve hierarchical relationships in the data. In contrast to many other methods, the wavelet transform is

not subject to prior assumptions of stationarity (i.e. uniformity of pattern in the data).

This thesis explores the concepts and application of hierarchical analysis of spatial pattern and the processes related to their generation in the context of Douglas-fir forest systems using the wavelet transform. The first manuscript, Chapter 2, introduces the application of multi-scale analysis of pattern using wavelet analysis. Satellite imagery of the western Cascade Range, Oregon is used in conjunction with wavelet analysis to identify and describe dominant spatial patterns in the forest landscape across several scales; specifically, wavelet analysis of imagery at three resolutions is used to describe the nested pattern characterising these Douglas-fir forests. Because such landscape-level patterns are well-known, Chapter 2 is primarily intended as a tutorial to illustrate such an approach to the analysis of multi-scale pattern.

The second manuscript, Chapter 3, defines wavelet analysis more rigorously and compares its abilities to resolve spatial pattern with Fourier spectral analysis and the semi-variogram. The wavelet cross-covariance function is introduced as a method for the analysis of spatial pattern using multivariate data. The third manuscript, Chapter 4, extends the discussion to an ecological data set. The utility of wavelet analysis is illustrated with an application to characterise canopy gap structure of Douglas-fir forests.

Specifically, the wavelet variance is used to discern similarities among forest canopy structure in a chronosequence as a function of average stand age and disturbance history.

While much attention has focussed on overstory species and their response to structure, the role and form of understory vegetation through succession in Douglas-fir forests has only been recently studied (Zamoro, 1981; Halpern and Franklin, 1990). However, the species composition and abundances of the understory play an important role in succession. The fourth manuscript, Chapter 5, uses wavelet analysis to explore the spatial relationship between canopy gap structure and understory vegetation and discuss the implications of gap patterns on understory life-form distributions. Spatial correlations between canopy gap structure and understory vegetation are elucidated using the wavelet cross-covariance function.

## Chapter 2

SATELLITE IMAGERY AND TIME SERIES ANALYSIS  
FOR THE DESCRIPTION OF  
FORESTED LANDSCAPES IN OREGON

by

G.A. Bradshaw

**ABSTRACT**

The use of satellite imagery in conjunction with time series analysis provides an objective measure to quantify known spatial patterns and identify hierarchical structure across scales. The application of satellite imagery used in conjunction with a new analytical technique, wavelet analysis, is presented for the case of forested landscapes in western Oregon. The objectives of this study are two-fold: 1) to provide the ecological context motivating analysis of multi-scale imagery using time series analysis, and 2) to identify dominant patterns across scales in forested landscapes of western Oregon.

While both the Cascade and Coast Ranges lie within the Tsuga heterophylla vegetation zone, variations in their climate, geologic, and disturbance histories contribute to the pattern of structures characterising conifer landscapes.

Within scales resolved by AVHRR data, the Coast Range is dominated by several scales of pattern ranging from three to thirty-five kilometers. In contrast, the Cascade Range is dominated by two distinct scales of pattern (three and fifty kilometers) lacking the intermediate structure of the Coast Range. The difference between these patterns are inferred to reflect corresponding differences in the fire and timber harvesting histories of the two areas.

Nested within this large-scale pattern, the structure of the western Cascades forests is dominated by various scales of features from 100 meters to several kilometers resulting from recent human disturbance (i.e. varying land practices as a function of ownership). In contrast, the major factor governing the dominant scale of biomass pattern observed in the Starkey Experimental Forest, northeastern Oregon, is attributed to a topographically-linked response to a steep environmental gradient or critical moisture threshold restricting vegetation distribution. This pattern is in marked contrast to the western Cascades where vegetation appears more uniform and less closely coupled to topographic trends.

## INTRODUCTION

An important challenge confronting natural resource managers and scientists is how to relate forest ecosystem components and properties observed at the familiar, ground-level scale (e.g. <100 m) to scales only recently captured by satellite technology ( $10^1$ - $10^6$  meters). While the majority of past forest research in the Pacific Northwest has focused on the single tree to stand levels, activity in the evaluation and integration of stand level data to the landscape level has recently increased in government agencies and university research. Research questions have been extended from intensive study of the components of the ecosystem to how they are related to each other in space and time.

The complexity of changing social and environmental issues requires resource managers to view the ecosystem across both spatial and temporal scales. For example, the task of defining viable habitat for the spotted owl has required the consideration of biological factors and habitat locations which transcend both individual National Forest district boundaries and ownerships. Remote sensing data represents a technology which provides the necessary temporal and spatial coverage for such integrated, multi-scalar research. The availability of technology has made it possible to address these questions. As a result, the use of satellite imagery and GIS (Geographical Information Systems) has become

more commonplace.

Analysis across several scales often requires the identification or definition of additional variables to accommodate the changing resolution in the data; an increase in areal coverage generally implies a loss in spatial resolution. For instance, at resolutions greater than the average crown diameter, the integrity of individual trees are no longer discernible (Cohen et al, 1990). The alternative use of surrogate variables such as spectral indices can provide additional insight into the physiology and function of the forest stand (Lillesand and Kiefer, 1987; Gholz et al, 1991).

While many properties at the stand level may be viewed as the sum of the individual trees comprising the stand (e.g. net primary productivity), certain properties of the stand will vary as a function of the spatial arrangement of trees (e.g. stand moisture retention and fire susceptibility) requiring a synthetic rather than individual-based approach. Once scene objects and properties are identified in the image, there must be some means by which the spatial arrangement are objectively documented and related to functional properties (Jupp et al, 1988; Curran, 1988). For example, the western Cascades landscape of Oregon presently resembles a mosaic of forest stands of varying ages as a result of the extensive and intensive clearcutting which has occurred over the past forty years (Franklin and Forman,

1987; Ripple et al, 1991). As a result, a significantly larger proportion of the forest is subject to "edge effects" as compared with projected, historical amounts (Harris, 1984). The extent and type of edge effects (e.g. amount and quality of interior habitat, wind fetch magnitude, and seed source-sink relations) will differ depending on such factors as the distance between forested units and geometry (Yahner, 1988; Forman and Godron, 1986). The demand for objective measures that compare spatial relationships has precipitated the recent application and research of spatial statistics and time series analysis in plant ecology (Milne, 1988; Pielou, 1977; Cohen et al, 1990; Jupp et al, 1988)

Spatial pattern may be described by such variables as texture, patch size or distribution, number of units, degree of aggregation and contrast between units. Because pattern implies many attributes, the choice and appropriateness of a given spatial technique depends on the available data and study goals. First, one must understand the type of processes which underlie the data. Processes underlying the data distribution and which are responsible for generating pattern may be "continuous-valued" or "point" processes. A spatial point process is "any stochastic mechanism which generates a countable set of events in space" (Diggle, 1987). A typical example of a point process is a map of tree locations where the events are individual trees. In contrast, continuous-valued processes are generated by a stochastic mechanism

which assigns a value to every point in the area of interest (e.g. biomass).

Time series analysis (e.g. spectral analysis, wavelet analysis) is one set of several extant methods which may be used for the description and quantification of spatial and temporal patterns. It may be loosely considered to fall into a category of techniques referred to as "spatial statistics" (Diggle, 1987; Ripley, 1977). Similar to applications in satellite imagery, these techniques function to confirm and quantify what is already perceived or known, or they are used as an exploratory tool revealing hitherto undetected phenomena. In the capacity of the second function, spatial methods are useful for generating spatially-explicit models and hypotheses for detailed field testing; analysis of pattern can be used for the analysis of processes which have generated these structures.

Methods such as the wavelet transform, spectral analysis, and autocorrelation functions are appropriate methods for the analysis of continuous-valued data such as digitized spectral imagery. In particular, the wavelet transform and its derivative functions, the wavelet variance and wavelet cross-covariance are well-suited to the analysis of digital data across scales because of their property of preserving locational information with scale information (discussed in full in chapters 2 and 3). By preserving locational (i.e. distance along a transect) and scale (i.e.

patch size) information, multi-scale and hierarchical relationships are also preserved and elucidated (Gamage, 1990; Daubechies, 1987).

## MULTISCALE ANALYSIS OF WESTERN OREGON LANDSCAPES

To demonstrate the use of time series analysis and multi-scalar satellite imagery for landscape analysis, a simple study of the forested landscape of Oregon was undertaken. The forested landscape of western Oregon is composed of a composite pattern of many spatial scales resulting from the interaction between climate, geology, and disturbance regimes. Wavelet analysis was applied using imagery of several resolutions to isolate separate components of pattern at various scales and relate them to physical factors. AVHRR (Advance Very High Resolution Radiometer) imagery was used to identify and describe known physiographic domains in western Oregon, namely the Coast and Cascade Ranges, based on spatial pattern of the near infrared (NIR) spectral band. A second aspect of the study entailed the use of multi-spectral scanner data (MSS) to identify the scale and type of patterns imposed by the land-use practices of various ownerships within the western Cascades over a sixteen year period (1972-1988). Finally, a comparison of TM (Thematic mapper) data from the western Cascades and Starkey Experimental forest in northeastern Oregon was used to explore the use of spectral and spatial analysis to contrast vegetation patterns in climatic extremes.

## STUDY AREA

Seven transects were located in western Oregon. At the regional level, the most notable features in western Oregon are the north-south oriented linear structures of the Coast Range, Willamette Valley, and Western Cascade Range (figure 2.1). The Willamette Valley is bounded to the east and west by the two mountain ranges. The major physiographic features were formed by orogenic events beginning with intrusion in the late Mesozoic and continuing with volcanic events throughout the Pliocene (Baldwin, 1976). These tectonic events created a basin-arc complex by a combination of mechanisms of compression, convection, and extension. Extrusion of volcanic basalts further modified the terrain. Specifically, the Coast Range is characterised by relatively low elevations (average crestline altitude 450-750 meters; Baldwin, 1976) and steep, dissected slopes dominated by marine sediments and intrusions (e.g. Marys Peak). In contrast, the average crestline in the Western Cascades is approximately 1000 meters, topographic relief is steep, and is composed of Tertiary flows, tuffs and intrusive rocks.

While all three physiographic domains are located in the Tsuga heterophylla vegetation zone, their vegetation varies as a function of differing climate, geologic, and disturbance histories (Franklin and Dyrness, 1985). Recently, the signature of natural vegetation has become subordinated to a

dominant pattern effected by intensive timber harvesting on public and private lands (Ripple et al, 1991; Spies, Ripple, and Bradshaw, unpublished ms; figure 2.2). Of the eight satellite image transects used in the study, only one transect was selected from the eastside of the Cascade Range; specifically the Starkey Experimental Forest located south of LaGrande in the Blue River Province of northeastern Oregon.

## METHODS

### Satellite Imagery

Satellite imagery at several scales were used in the analysis of landscape pattern to describe the western portion of the state of Oregon, namely the Willamette Valley, Western Cascades and Coast Range vegetation zone (figure 2.1; Franklin and Dyrness, 1985). Rectified imagery at three scales of resolution were used: AVHRR (one kilometer resolution), MSS (multi-spectral scanner; resampled at 50 meter by 50 meter resolution), and TM (Thematic mapper; resampled at 30 meters by 30 meters ground resolution). MSS images from two dates, 1972 and 1988, were used for the ownership and temporal analyses (figure 2.2). The two MSS images form a subset from a series of rectified images of the same location during 1972, 1976, 1981, 1984, and 1988 which were used to evaluate landscape change over the sixteen year period. The transects selected from the 1972 and the 1988 images were from the same location: a private holding, a National Forest holding, and a wilderness holding. Each transect was chosen to represent the average pattern in the landscape for each holding.

The analysis was initially performed using two spectral bands, red visible (AVHRR 580-680 nm; MSS 580-680; TM 630-690 nm) and near infrared (AVHRR 720-1100 nm; MSS 690-830 nm; TM

760-900 nm), chosen for their sensitivity to vegetation biomass (Lillesand and Kiefer, 1987; Curran, 1980; Knipling, 1970). Results using two spectral indices derived from the red and NIR bands, NDVI (normalized difference vegetation index) and the simple NIR and red band ratio were found to be very similar to the single band results. However, because the near infrared band was found to be most sensitive at detecting changes in vegetation, the present discussion focuses on the this band.

#### **Time Series Analysis: Wavelet Transform**

The wavelet transform, wavelet variance, and wavelet cross-covariance were used to identify similarities and differences in dominant spatial patterns observed across scales in western Oregon. Wavelet analyses were performed on the eight transects from AVHRR, MSS and TM data throughout the western portion of the state. Each of the three wavelet functions yielded slightly different information regarding spatial pattern in the data. The wavelet transform is a graphical representation by which the landscape spatial pattern is effectively decomposed into its dominant scalar components as a function of location along the transect. The two-dimensional contour plot quantifies the contribution of each scale of pattern to the overall data "signal". Preservation of locational information allows fine-scale

structure to be related to coarser features in the data. For example, within-stand variability is observed to occur nested within the landscape pattern effected by aspect.

Similar to Fourier spectral analysis, the wavelet variance provides a measure of the average, dominant scales of pattern in the data and facilitates comparison between variables and data sets. The wavelet variance is calculated by integrating over the transect at each scale. The wavelet variance quantifies the average energy or magnitude contributed by features at each scale of analysis. While there is loss of the hierarchical and locational information, there is a gain in the ability to compare data sets more easily.

The wavelet cross-covariance is a multivariate technique used to quantify the magnitude of spatial covariance between two variables as a function of scale (e.g. patch size) and lag (i.e. spatial offset between the two variables). This method is used to measure the scale and the degree to which two variables are linked in space.

A wavelet analysis was performed on each of three transects (i.e. a north-south transect through the Coast Range, a north-south transect through the Cascade Range, and an east-west transect through across Oregon from the coast to west of Bend). The three transects were selected from the AVHRR image to compare the gross spatial features and hierarchical structure of the major physiographic domains

across Oregon (figures 2.3, 2.4, and 2.5).

A second, similar analysis was performed on three MSS transects within the mid-elevation western Cascade Range from figure 2.2 to evaluate the effect of land-use practice by ownership on forested pattern (i.e. private versus general National Forest land and public wilderness areas) over a sixteen year period. A third set of analyses were performed on two TM transects; one transect was selected from the western Cascades and the other from the eastern Oregon (Starkey Experimental Forest) to explore the use of multi-scale pattern in the analysis of the climatic gradients and biomass patterns (figures 2.6 and 2.7). Replicate analyses were performed on additional transects in all cases to insure that the transect representations accurately reflected the structure of the two-dimensional study area.

## RESULTS

### AVHRR Analysis

The peak in the wavelet variance calculated for the AVHRR transect traversing the state west to east identified the large-scale features ranging from 40 to 80 kilometers (figure 2.8). These features correspond to the average scale of pattern of the three physiographic domains delineated by the Coast and Cascade Ranges. Hierarchical structure at finer scales was evident within each of the three domains; the wavelet transform showed fine-scale structure grading into the larger spatial features (figures 2.9 and 2.10). The wavelet cross-covariance calculated for the visible red and near infrared bands indicated that the two bands are most closely correlated at the scale of 30 kilometers (figure 2.11).

While the data transects located along the western Cascades and the Coast Range were similar in form (figures 2.4 and 2.5), the wavelet variance showed that the spectral spatial structure were distinct (figures 2.12 and 2.13). The mid-elevation forests of the Cascades were dominated at two main scales (3 and 55 kilometers; figure 2.12). On the other hand, the Coast Range was characterised by pattern at scales less than thirty-five kilometers. The broad amplitude of the wavelet variance of the Coast Range indicated the presence of

pattern at several intermediate scales as compared with the two distinct peaks characterising the Cascades wavelet variance.

The across-scale relationship between large and small-scale features also differed between the two ranges (figures 2.14 and 2.15). Whereas the Cascade Range was characterized by a two-scale structure, the Coast Range appeared to have a nested or hierarchical structure across several scales. The Coast range showed a progression across at least three levels from the fine scale (<5 kilometers) to intermediate scaled (5-20 kilometers) and large-scale (>20 kilometers; figure 2.17). The Cascade Range data lacked the pronounced intermediate structure of the Coast Range and was confined to features less than 5 kilometers or greater than 40 kilometers (figure 2.14). These patterns were most clearly demonstrated with the calculation of the visible red and NIR wavelet cross-covariances (figures 2.16 and 2.17). The Cascades transect indicated that the two bands were significantly correlated at less than 5 kilometers and not coupled at other scales. In the case of the Coast Range, the two bands were strongly correlated across all scales up to 20 kilometers (figure 2.17).

### Multi-spectral Scanner Results

The wavelet variances calculated for the three land ownerships using MSS data indicated that the spatial patterns were somewhat similar among these locations for 1972 (figures 2.18, 2.19, and 2.20). The transect selected from private land showed the highest NIR value with a peak centred at approximately 5 kilometers (figure 2.18). The public National Forest land was characterised by an overall lower NIR value relative to the private land and dominance at one kilometer (figure 2.19). The wilderness transect also showed relatively moderate NIR values and two peaks centred at one kilometer and three kilometers (figure 2.20).

By 1988, sixteen years later, NIR values increased in all three land ownerships (figures 2.21, 2.22, and 2.23). Some of these differences may be an artifact resulting from a change in gain and offset of different satellites over the years; a comparison of the wavelet variances for the wilderness lands in 1972 and 1988 showed that while no detected clearcutting occurred along this transect between 1972 and 1988, the NIR values increased in magnitude (figures 2.20 and 2.23).

However, the change detected in the public forest and private lands was much more dramatic (figures 2.21 and 2.22). In both cases, the scale and intensity of pattern increased; the National forest transect changed from a fine scale

feature of one kilometer to a series of peaks at one, two and greater kilometers (figure 2.22). The private land increased in terms of peak magnitude centred at 5 kilometers, but also included additional structure at scales larger than 15 kilometers (figure 2.21). The wavelet transforms calculated for the public forest and private forest lands illustrates this contrast in intensity and pattern as a function of position along the transect (figures 2.24 and 2.25). Pattern in the NIR response on the private lands was dominated by fine and coarse scale features with a strong event at kilometer 10 (figure 2.24). The patterns on public forest lands was limited to finer scales (figure 2.25).

### **Thematic Mapper Analysis**

Apart from differences in the geologic histories of the eastside and westside of the Cascades, a difference in climate regimes drives much of the landscape pattern (Franklin and Dyrness, 1985). Climatically influenced patterns are evident in the pattern of the Thematic Mapper NIR and visible red response of the western Cascade and Starkey transects derived from the wavelet analysis.

The Starkey landscape was dominated by a pattern in both the visible red and NIR centred at approximately 350-400 meters (figure 2.26). Both bands track each other at this scale as indicated by calculation of the wavelet cross-

covariance (figure 2.27). Correspondence between the two bands was much less at finer scales.

The NIR band of western Cascade wavelet variance was characterised by a single peak centred at 100 meters and secondarily at several scales greater than 350 meters (figure 2.28). The visible band tracked the NIR band up to 100 meters but lost coherency at greater scales (figure 2.29). The wavelet transform for each of the two locations showed a striking difference in their hierarchical structures: while the eastside is dominated by the 350 meter pattern, the pattern of the western Cascades is much finer and relatively less distinct.

## DISCUSSION

Although the Douglas-fir forests of the Coast and mid-elevation Cascade range both belong to the Tsuga heterophylla zone, pattern analysis of spectral data suggests that these patterns are quite distinct. The mid-elevation Cascade Range transect was characterised by two distinct scales of pattern: small (3 kilometers) and large-scale (55 kilometers) while the Coast Range was dominated by patterns ranging from three to thirty-five kilometers. When examined in conjunction with topographic maps, the large-scale features of both Ranges appear to coincide with major physiographic features as drainages. However, the major difference may actually lie in the contrasting disturbance histories of the two zones in terms of wildfire and timber harvesting regimes. It has been inferred that fire has been less widespread and that clearcut areas are smaller in the Cascades, as compared with the extensive, stand replacement burns and clearcutting patterns experienced by the Coast Range over the past 150 years (Agee, 1990; Swanson and Morrison, 1990). The results from the wavelet analysis suggests that the physiographic signature has been preserved in the Cascade Range and effectively washed out or superceded by the extensive disturbances in the Coast Range. The two-scaled pattern of the Cascade Range resulting from a high contrast between small-scale aggregates of clearcutting units and presence of hardwoods superimposed

on the large-scale physiography has been overshadowed by disturbance patterns in the case of the Coast Range.

The Cascades forest pattern was dominated at two scales at the thirty meter resolution of the Thematic Mapper imagery: a fine pattern (approximately 100 meters, at scales comparable to within-stand canopy variability) and a coarse-grained pattern ( $> 350$  meters, at scales comparable to features such as aspect or clearcuts. In this instance, the within-stand variability (as inferred by the 100 meter peak) and topographic patterns or clearcuts were co-dominant. In striking contrast, the spatial pattern of the near infrared and red spectral response along the Starkey transect was dominated by scales of pattern corresponding to the topography. Variability at smaller scales also occurred but was subordinate to the strong topographically-linked patterns. The smaller scale pattern was attributed to changes in vegetation biomass as a function of aspect.

A possible explanation for the differences between the two Thematic Mapper transects may be found by comparing their respective environmental settings. The Starkey area is characterized by much steeper environmental gradients relative to the mid-elevation western Cascades. A combination of low summer precipitation, widely fluctuating temperatures, and local soil conditions in the Starkey area creates steep gradients or environmental thresholds associated with aspect and local topography. Species such as Douglas-fir, western

Hemlock and larch are sensitive to moisture availability and tend to occupy the steep canyon area which dissect the landscape (Franklin and Dyrness, 1984). Because of the relatively extreme climatic conditions in this area, subtle changes in soil type, aspect, or elevation can alter moisture conditions sufficiently to levels below a given plant species' requirement. The pattern at 50-100 meters was attributed to aspect changes; north to east facing slopes tend to be forested to the hotter south to west facing slopes.

The less distinct coupling inferred between topography and change in biomass in the Cascades transect may reflect: 1) a lower moisture or climatic gradient relative to the Starkey, or 2) a climate whose fluctuations fall well beyond a critical threshold restricting the overall for the distribution of Douglas-fir trees along the transect.

The comparison between the 1972 and 1988 MSS images provided a measure of how the landscape changes over time purely as a result of one disturbance factor: timber harvesting practices. Because of differing harvesting practices among land ownerships, the landscape change is both heterogeneous in time and space. A non-uniform distribution of cutting practices and rates will result in a landscape characterised by a non-uniform distribution of stand age and conditions.

## CONCLUSIONS

A spatial analysis based on one-dimensional transects on a complex three-dimensional surface represents serious undersampling of the landscape and potential loss of important spatial relationships. Nonetheless, the simple comparison presented here allowed the identification of landscape spatial characteristics of the western Cascades which may be investigated more fully with a later two-dimensional wavelet analysis using a combination of spectral and digital terrain data. The comparison between landscapes demonstrates that an evaluation of landscape pattern must consider both the effects of natural and human disturbance in order to assess the magnitude and direction of change.

The study represents an example of how spatial pattern analysis might be used to build hypotheses regarding mechanisms responsible for the generation of pattern in the forested landscape. While the results from the spatial analysis are only suggestive, such studies may be used to formulate hypotheses regarding patterns of vegetation as a function of moisture availability and disturbance.

Alternatively, spatial analyses based on remotely-sensed imagery may be used to build spatially-explicit models. For example, one way to evaluate the effects of varying timber practices on the landscape at the regional scale would be to model the spectral response across scales:

specifically, analyse simulated AVHRR data derived from models effected at the sub-kilometer scale for several different cutting regimes in terms of amount, rate and spatial configuration.

The strength of spatial analyses lies in three categories: 1) its ability to quantify to spatial patterns intuited by the field ecologist, 2) a means by which spatially explicit hypotheses regarding mechanisms and patterns may be proposed, and 3) a method by which landscape-scale sampling designs can be constructed. The increased accessibility of spatial data and techniques for their analysis provides a much-needed bridge between ground-level understanding and the landscape scale.

**Figure 2.1** Rectified AVHRR image of western Oregon displayed in the visible red and near-infrared bands. Superimposed blue lines correspond to the three transects selected in the study: T4= western Cascades transect (500 kilometers), T3=Coast Range transect (500 km), and O1=west to east transect across western Oregon.

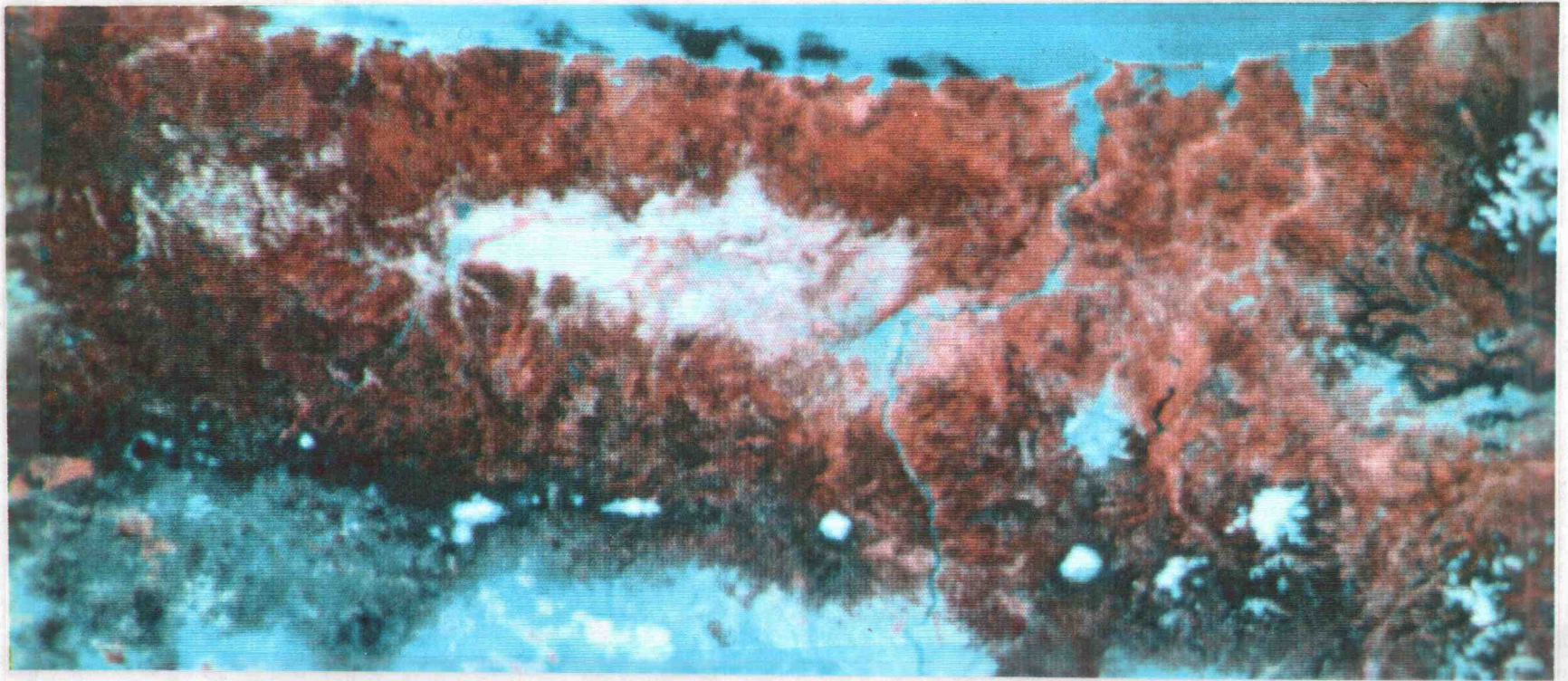
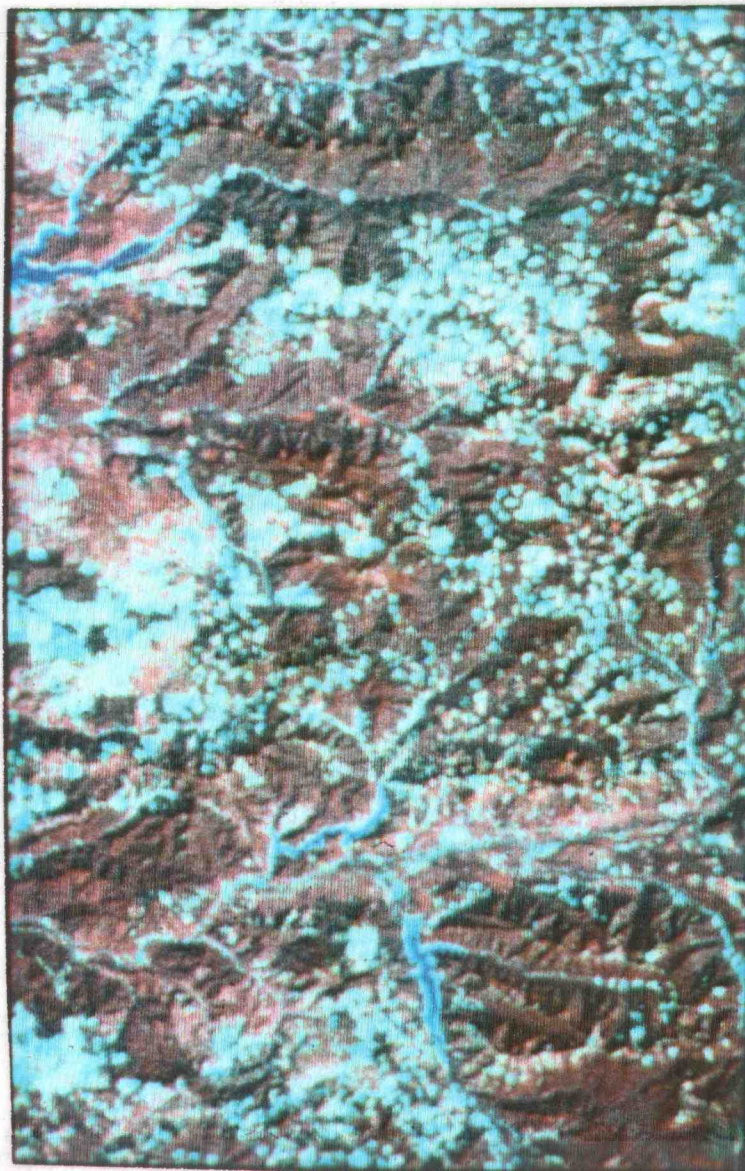


Figure 2.1



**Figure 2.2:** Rectified MSS image of an approximately 3500 km<sup>2</sup> area located in the western Cascades, Oregon. Superimposed blue lines denote the transects used in the study: P1=private land transect, P2= public land, P3=wilderness land.

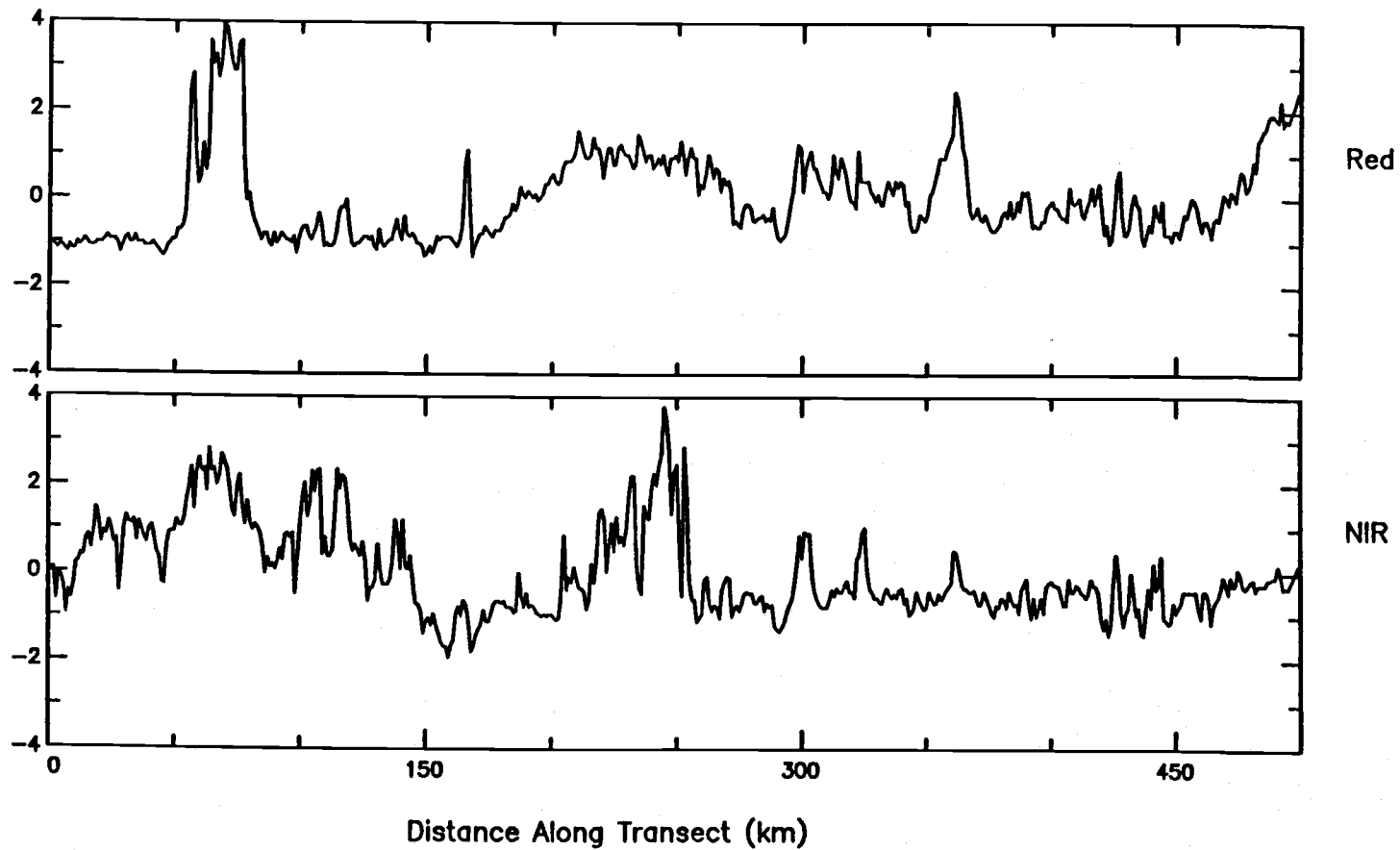
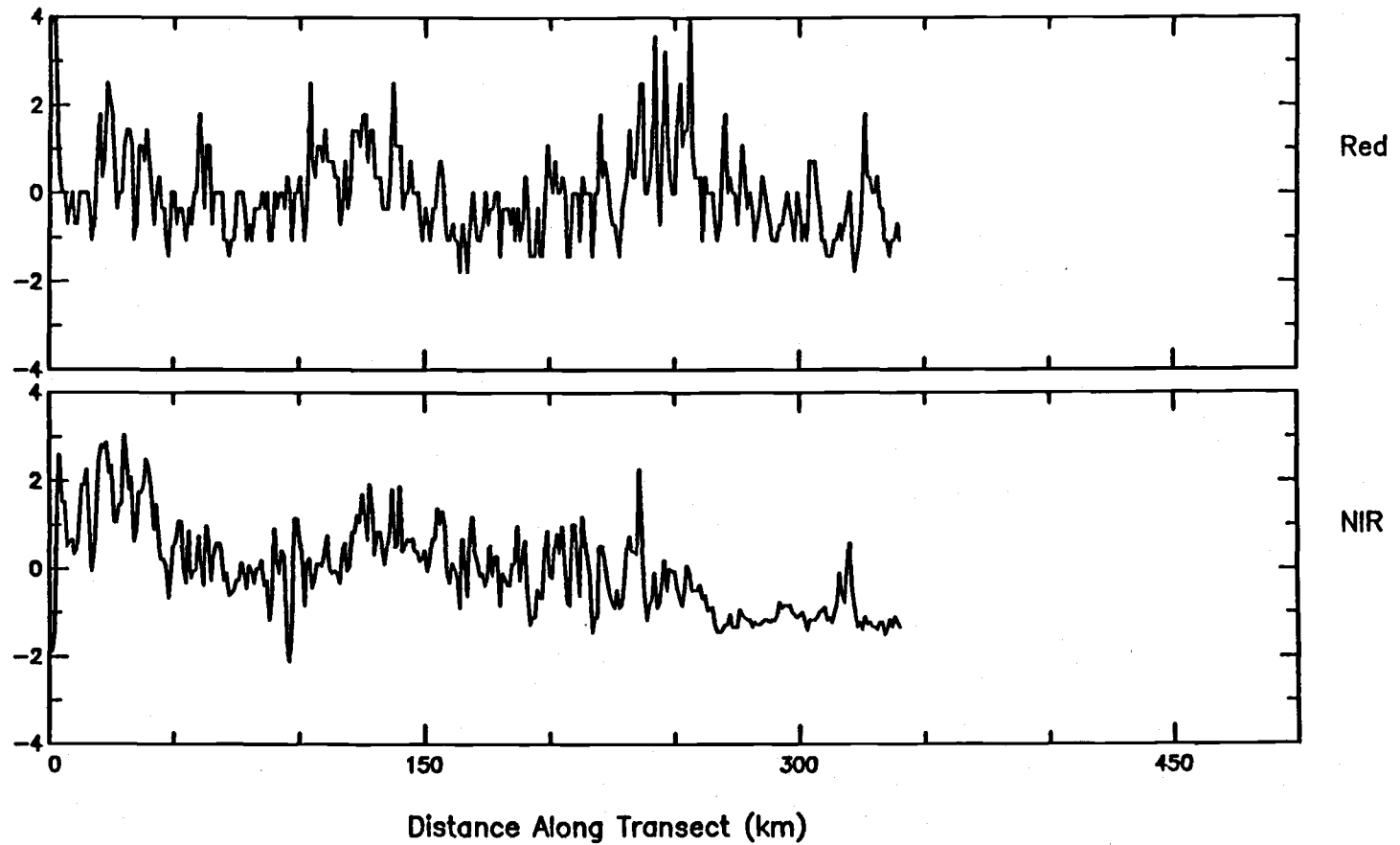


Figure 2.3 Standardized NIR and red visible AVHRR data transects of the west to east transect across Oregon (O1).



**Figure 2.4** Standardized NIR and red visible AVHRR data transects of the Cascade Range (T4).

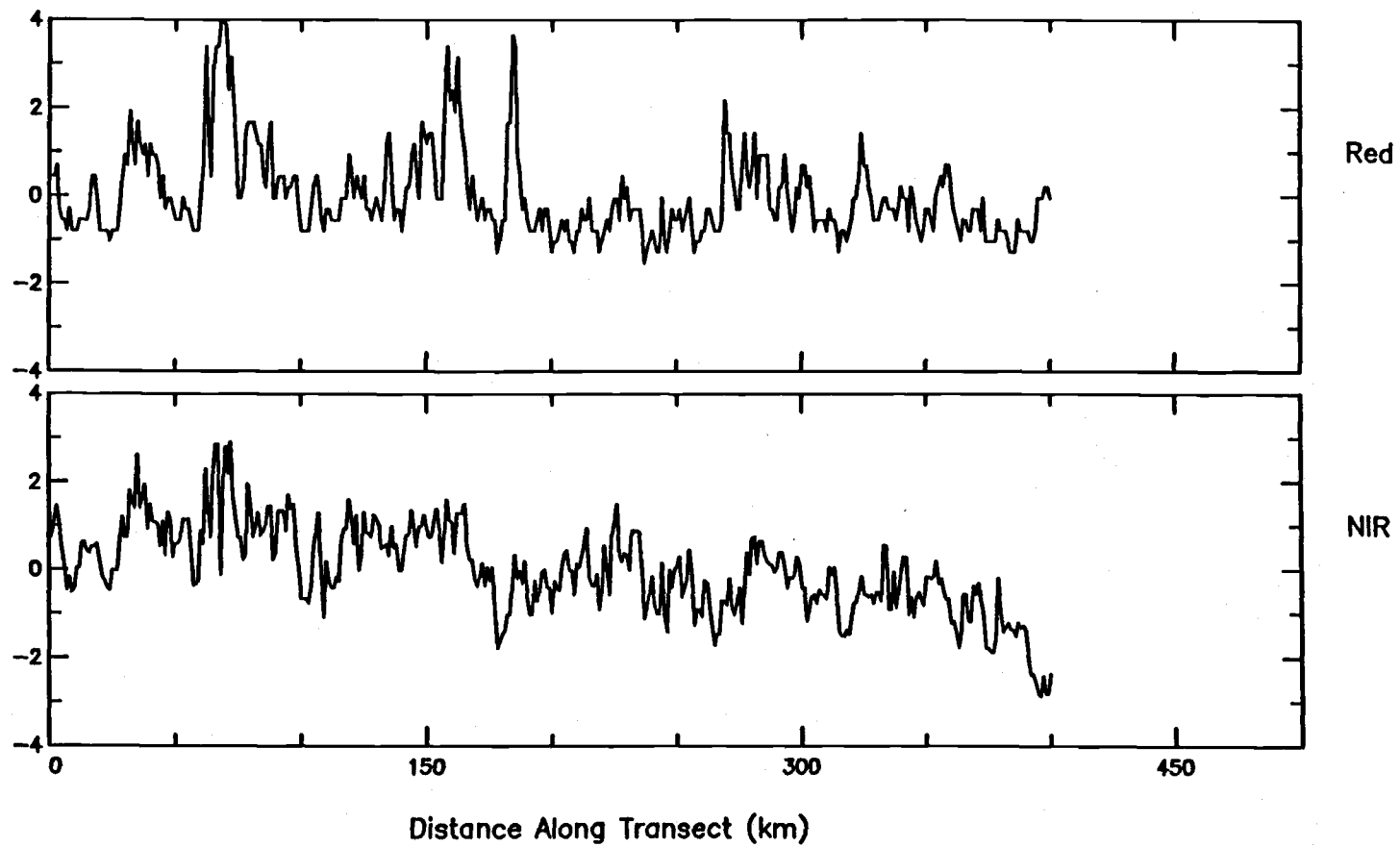
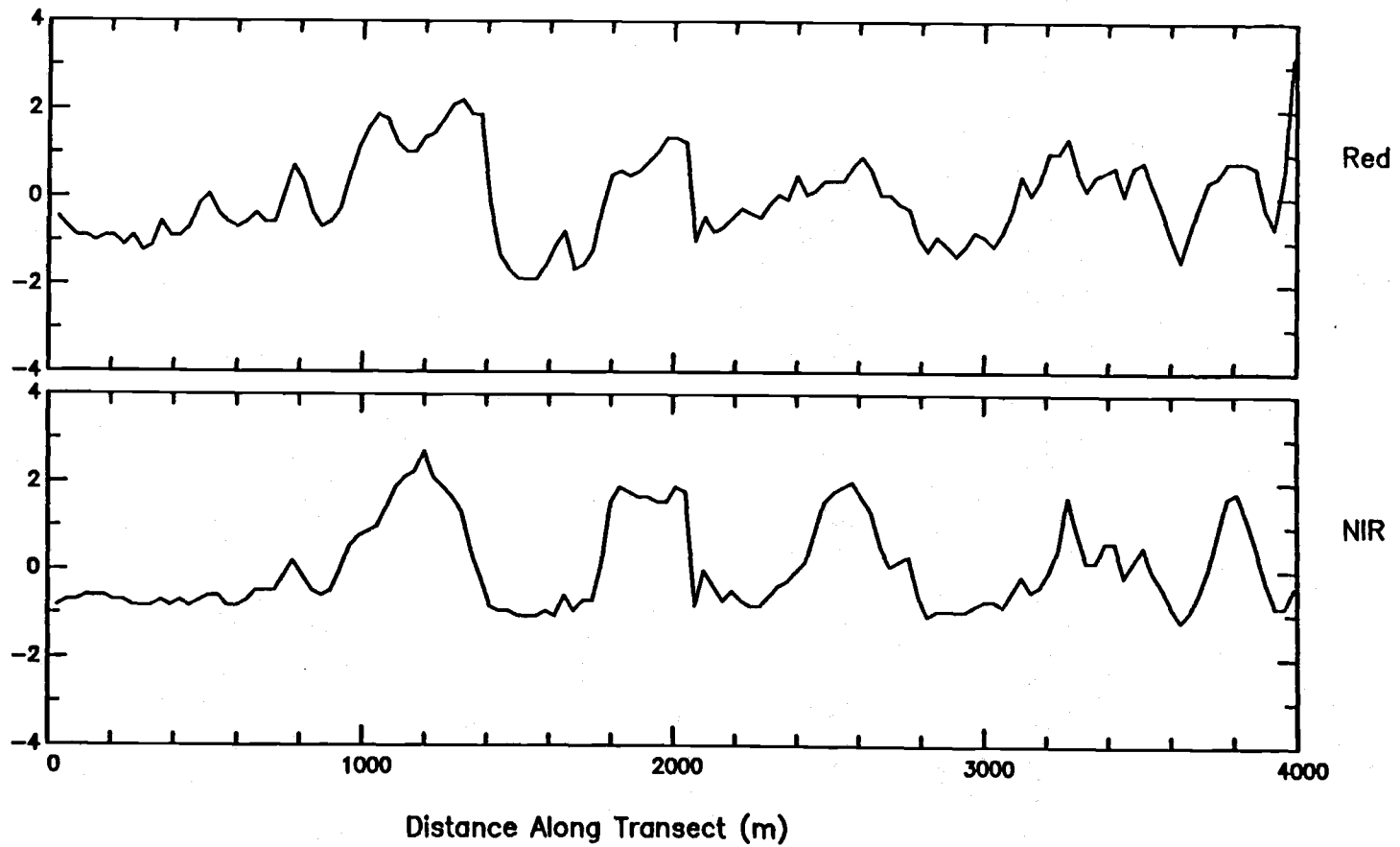
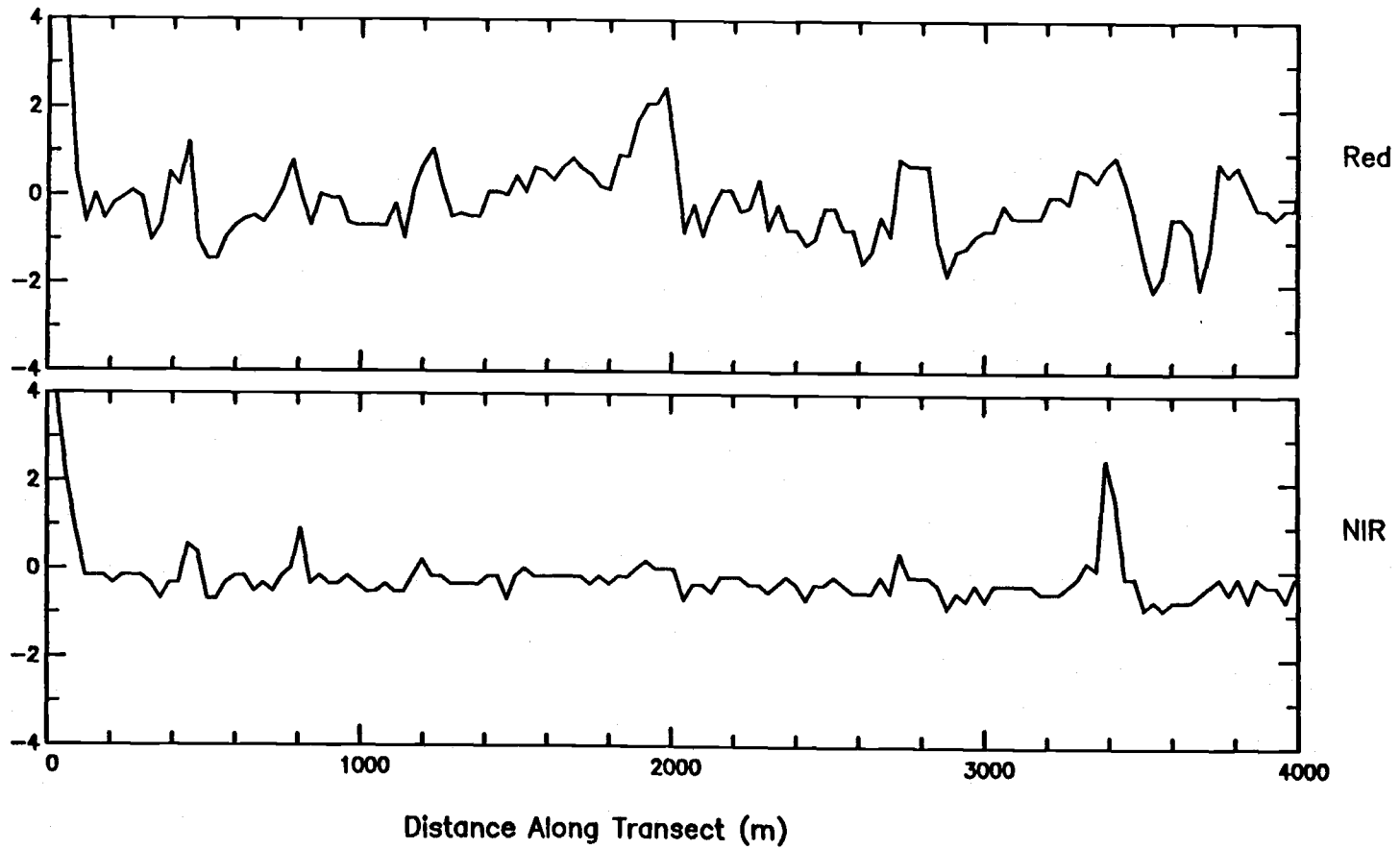


Figure 2.5 Standardized NIR and red visible AVHRR data transects of the Coast Range (T3).



**Figure 2.6** Standardized NIR and visible red TM data transects of the Starkey Experimental Forest.



**Figure 2.7** Standardized NIR TM data transect of the western Cascades Range.

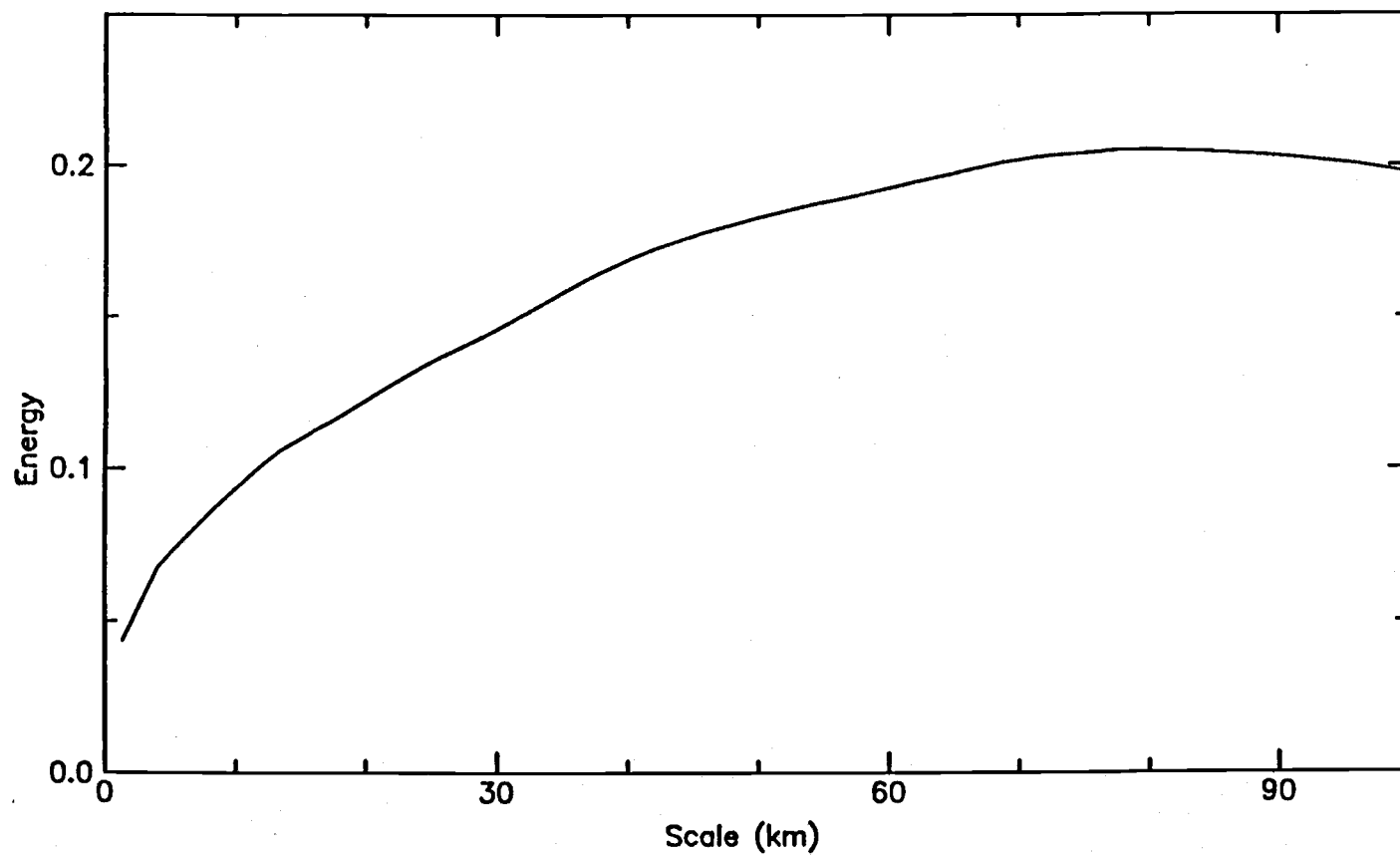


**Figure 2.8** Wavelet variance for NIR AVHRR band of the west-east transect across western Oregon (O1). y-axis corresponds to wavelet variance amplitude; x-axis corresponds to scale of pattern (km).

Figure 2.9 Wavelet transform of west-east transect (O1). y-axis corresponds to scale (km); x-axis corresponds to distance along the transect (km). Grey-scale denotes signal intensity.

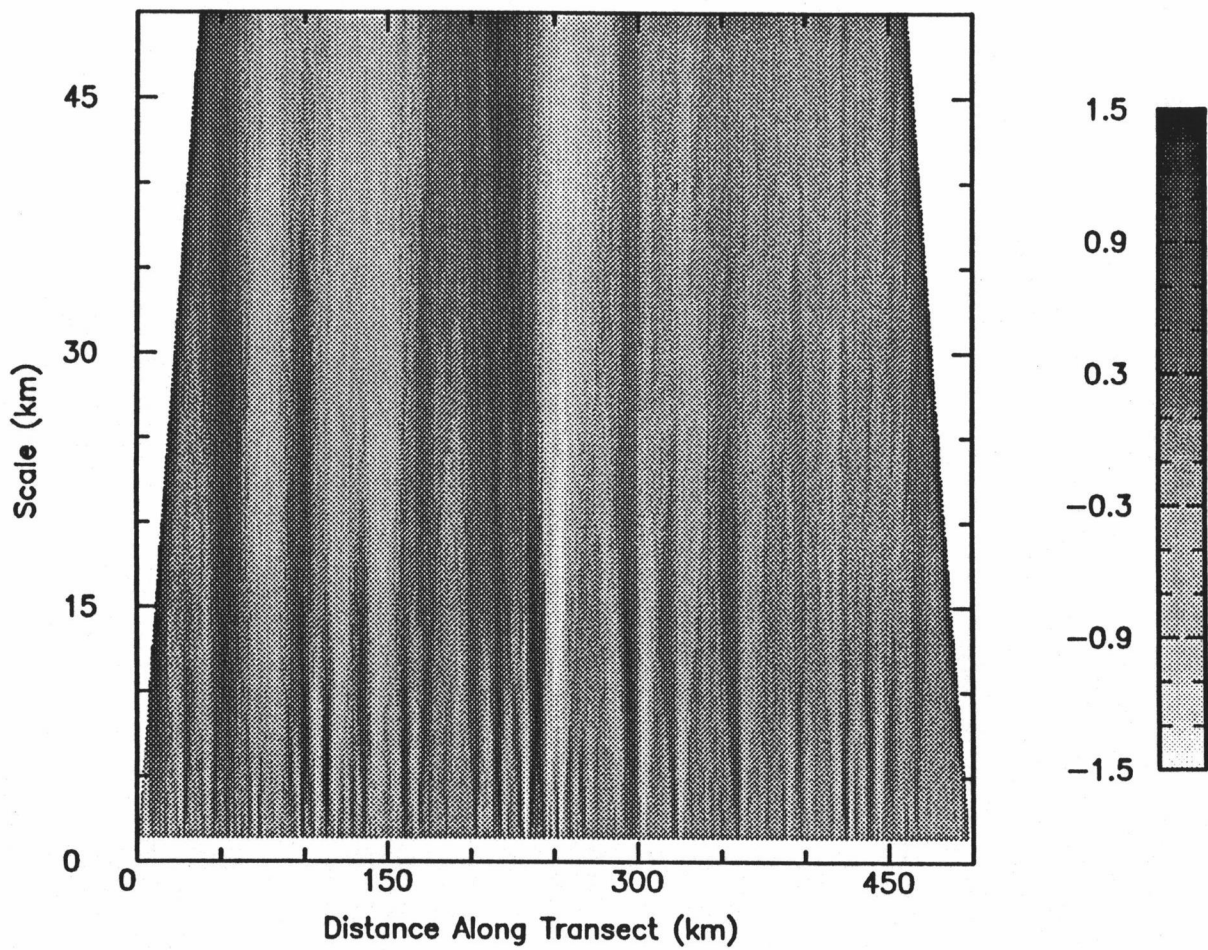


Figure 2.9

**Figure 2.10** Small-scale wavelet transform of west-east transect (O1) ranging from one to twenty kilometer scale to illustrate fine-scale structure.

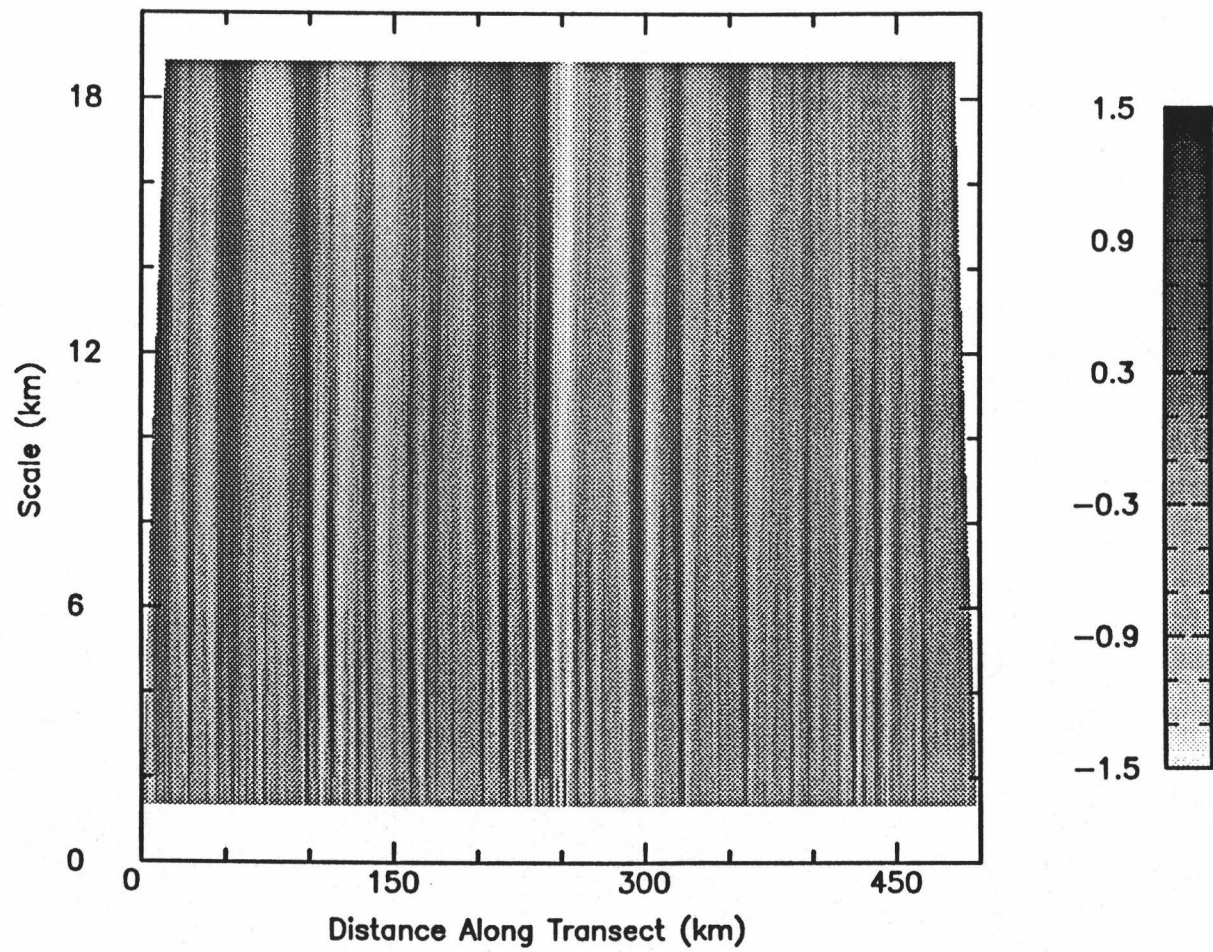


Figure 2.10

**Figure 2.11** Wavelet cross-covariance between visible red and NIR spectral bands for west-east transect (01). Dark values denote high covariance. Light values denote negative covariance. y-axis corresponds to scale of interaction (km); x-axis corresponds to lag (km).

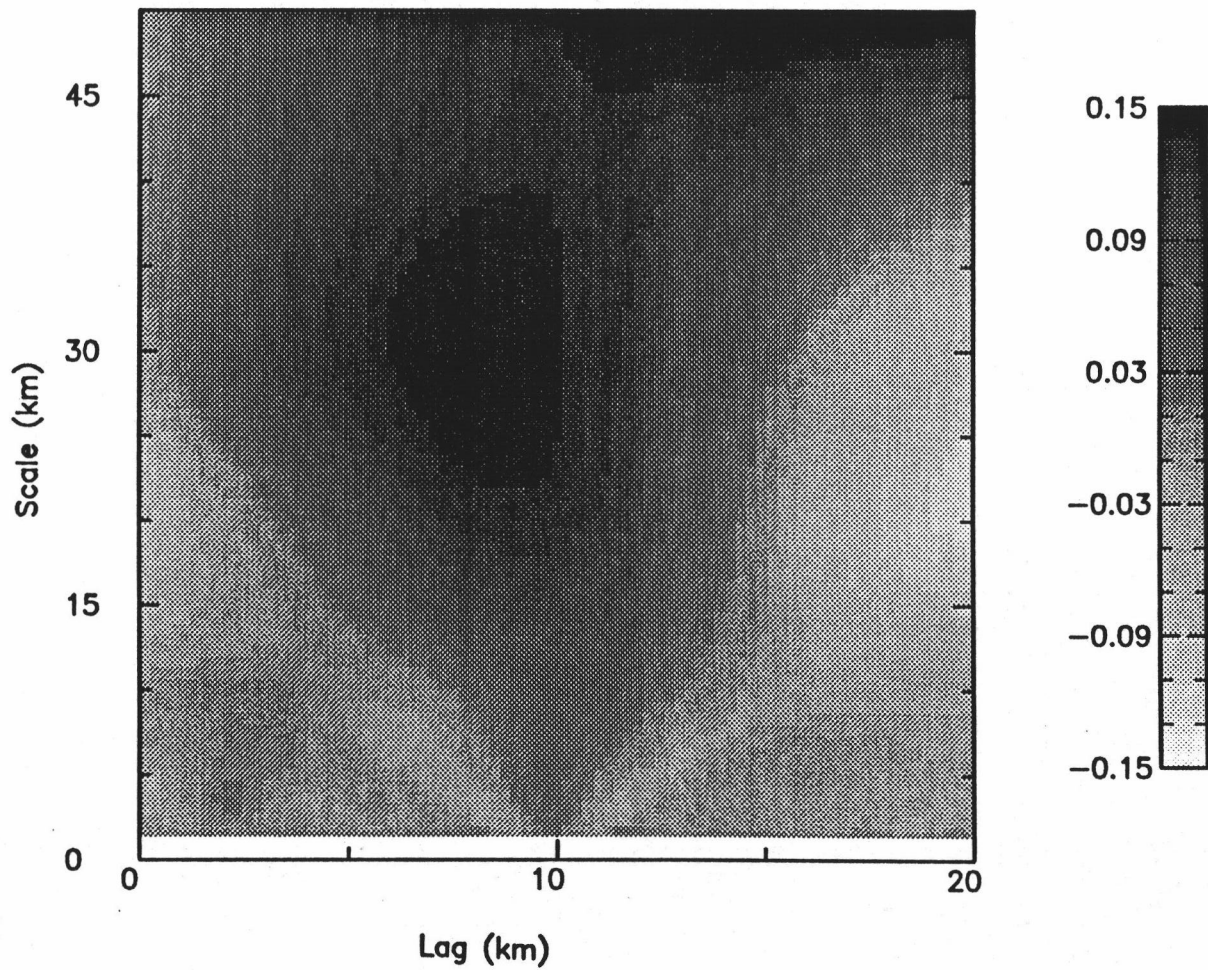


Figure 2.11

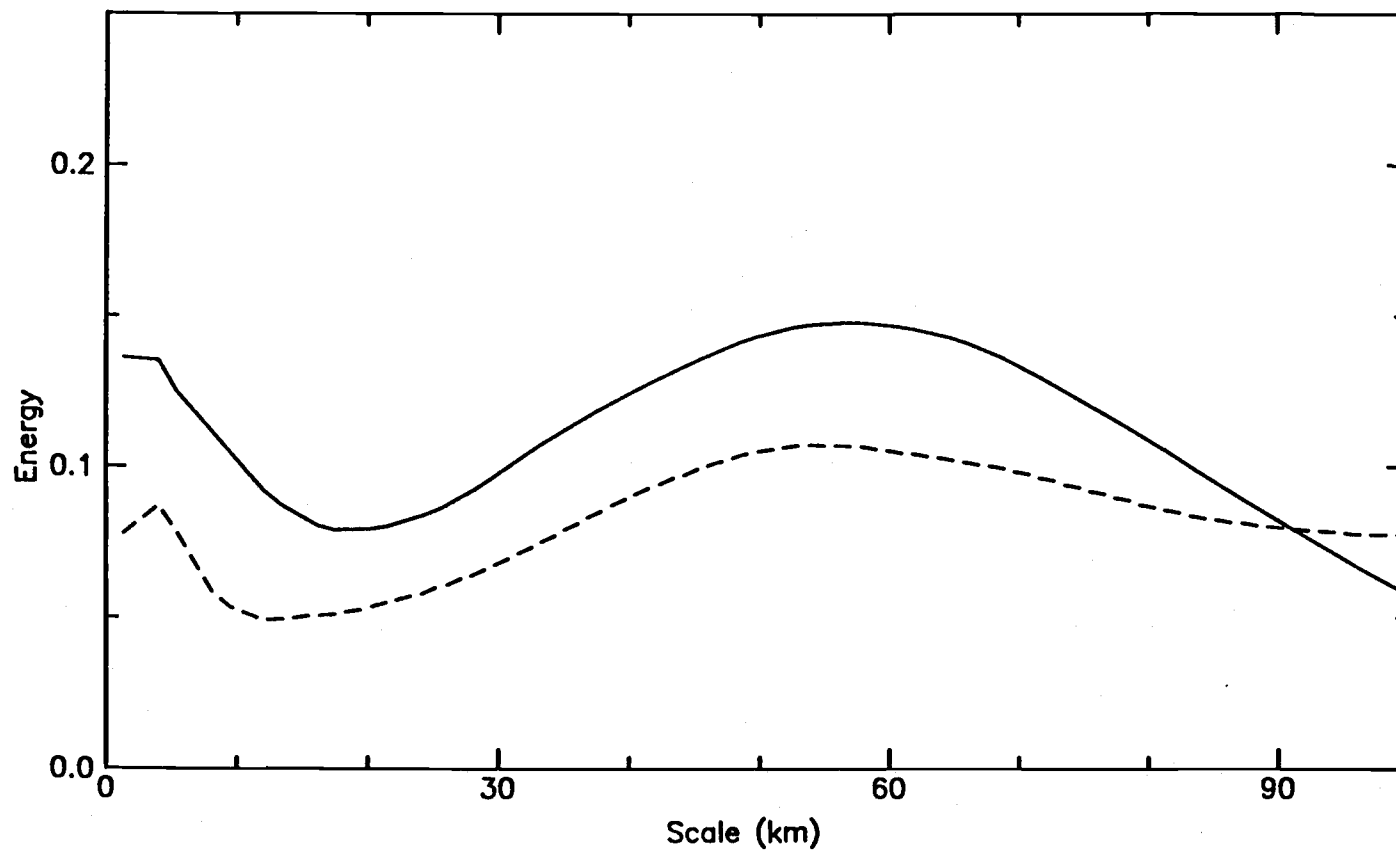


Figure 2.12 Wavelet variance for NIR and visible red AVHRR band of the western Cascades transect in western Oregon (T4).

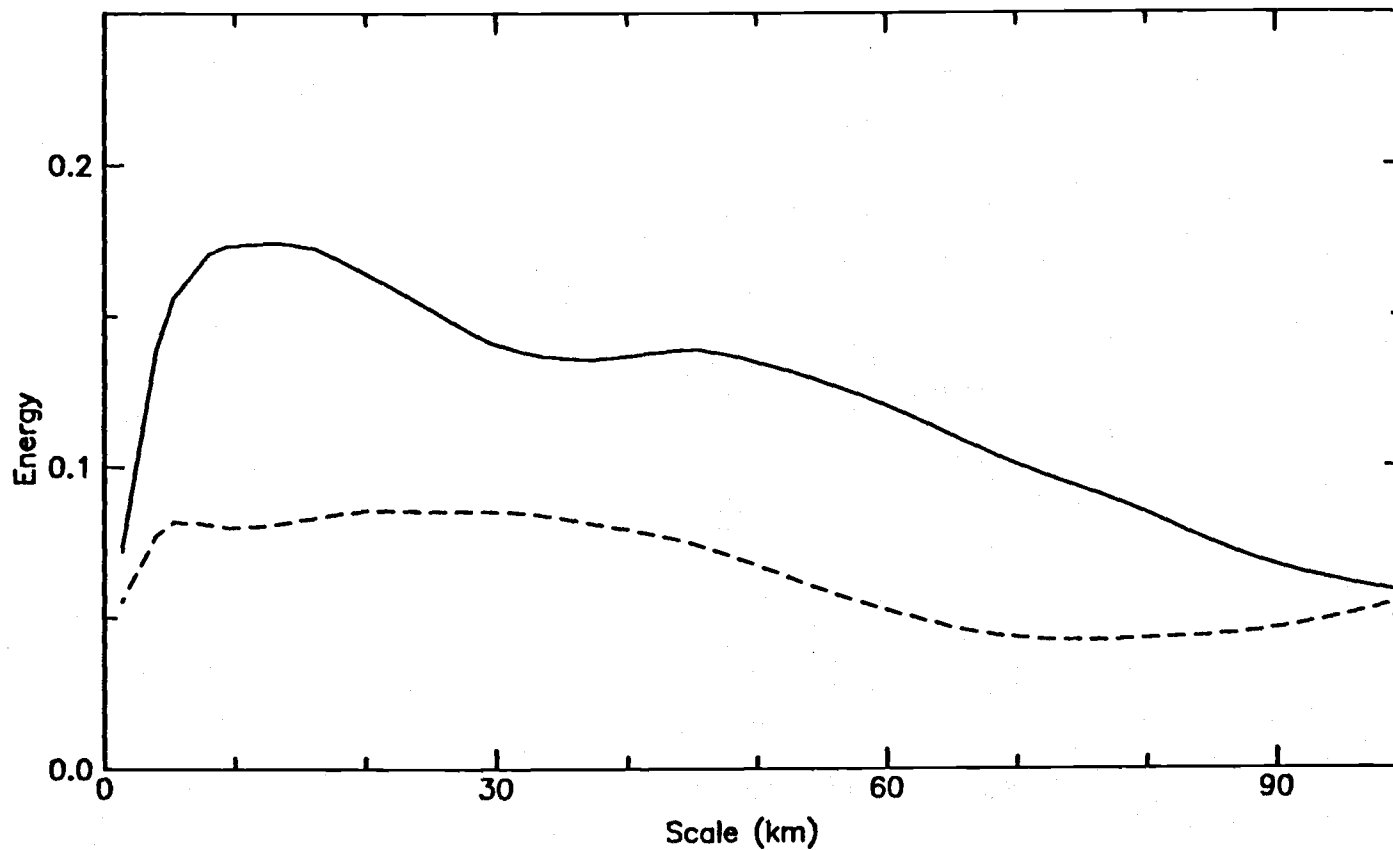
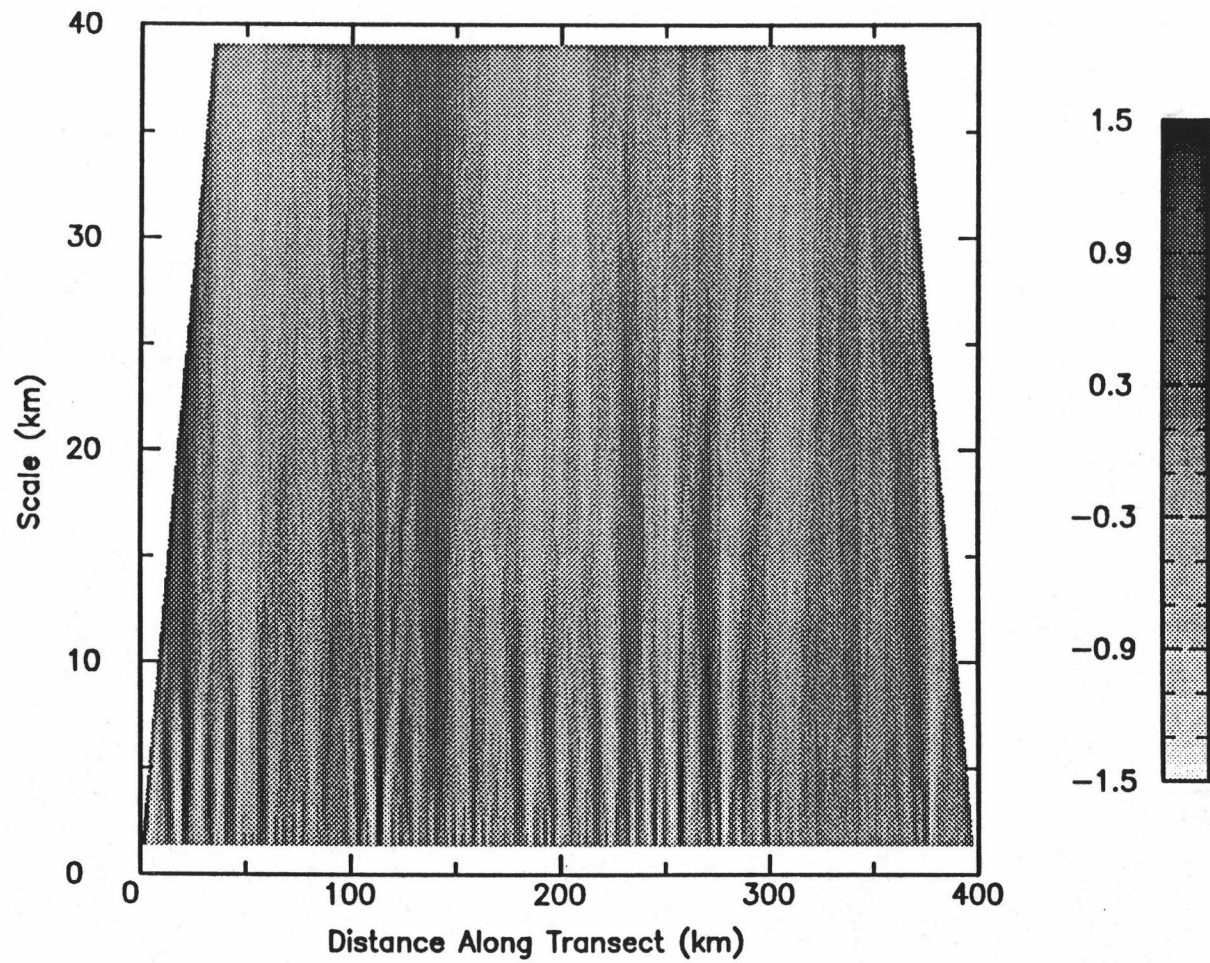


Figure 2.13 Wavelet variance for NIR and visible red AVHRR band of the Coast Range transect across western Oregon (T3).



**Figure 2.14** Wavelet transform of western Cascades transect (T4).

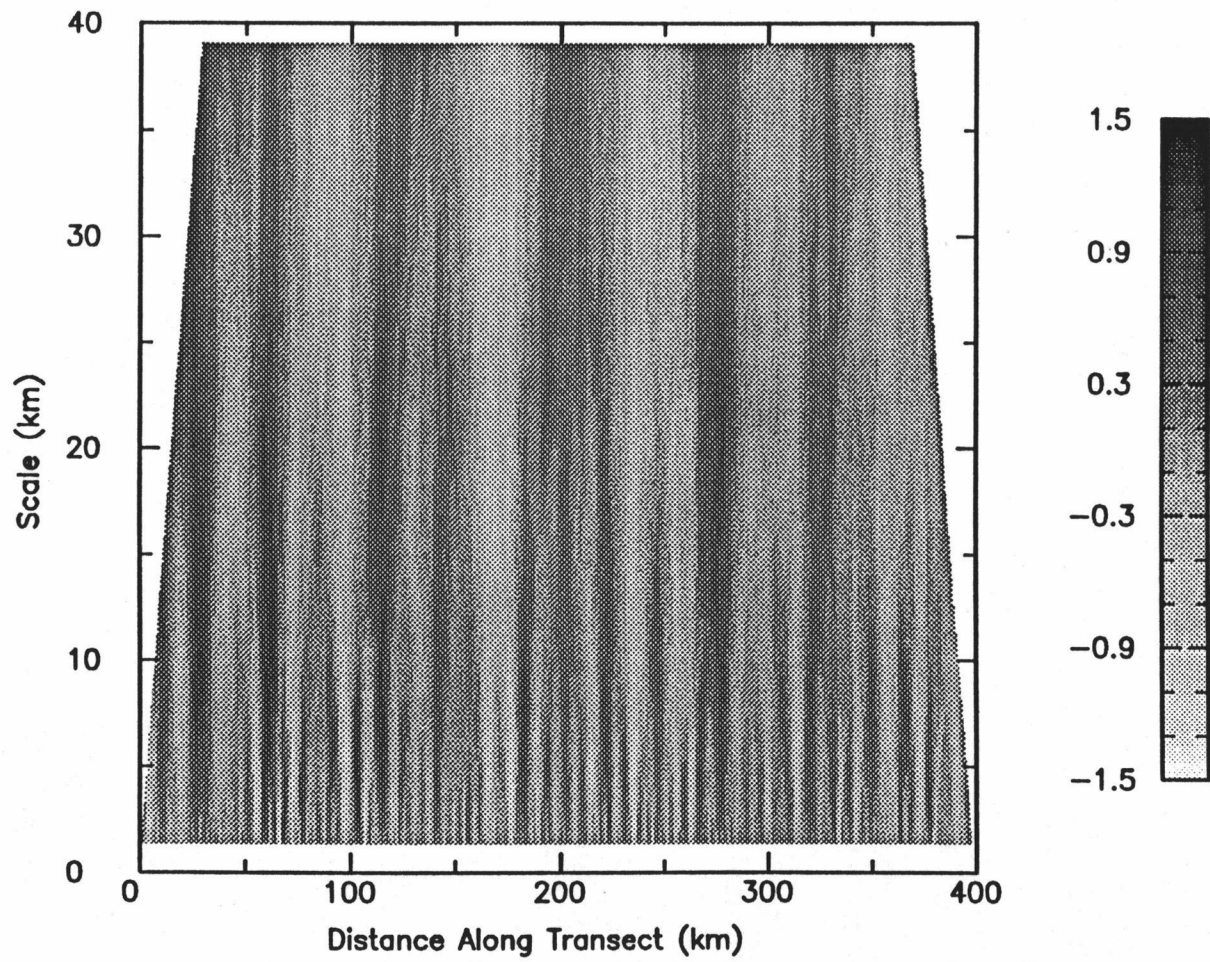
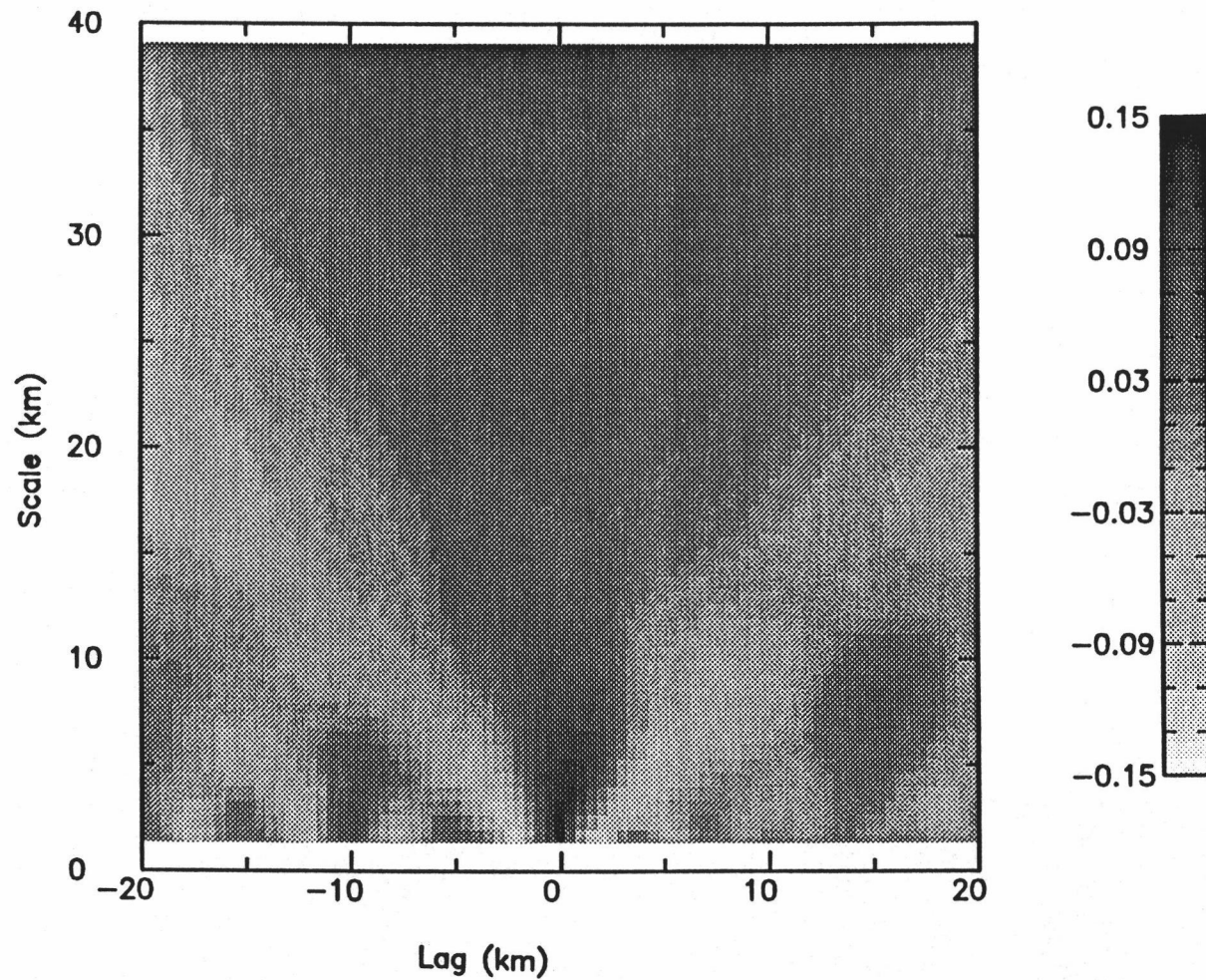
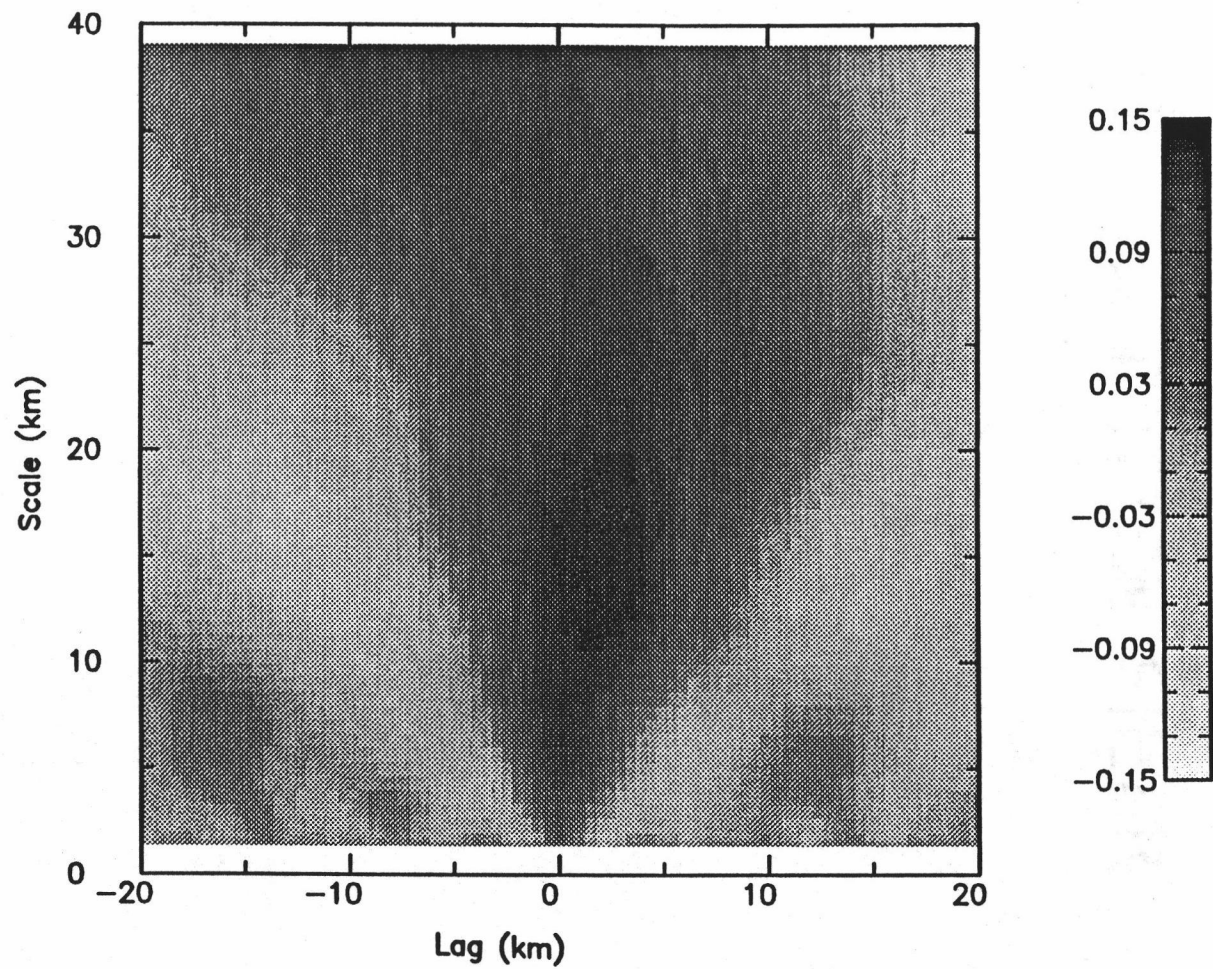


Figure 2.15 Wavelet transform of Coast Range transect (T3).



**Figure 2.16** Wavelet cross-covariance between visible red and NIR spectral bands for western Cascades transect (T4).



**Figure 2.17** Wavelet cross-covariance between visible red and NIR spectral bands for Coast Range transect (T3).

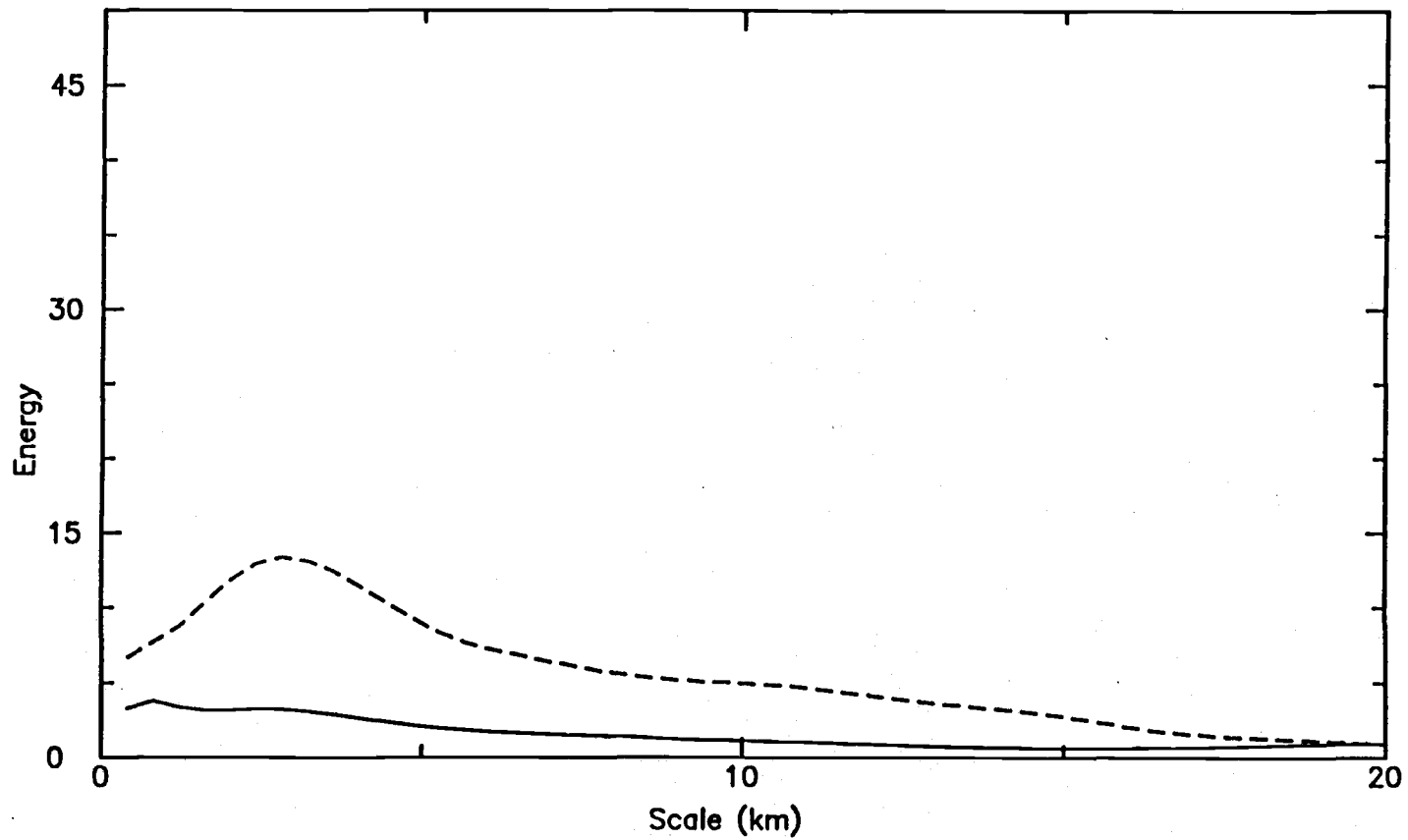


**Figure 2.18** Wavelet variance for MSS private lands transect in 1972. Visible red corresponds to solid line and NIR to the dashed line.

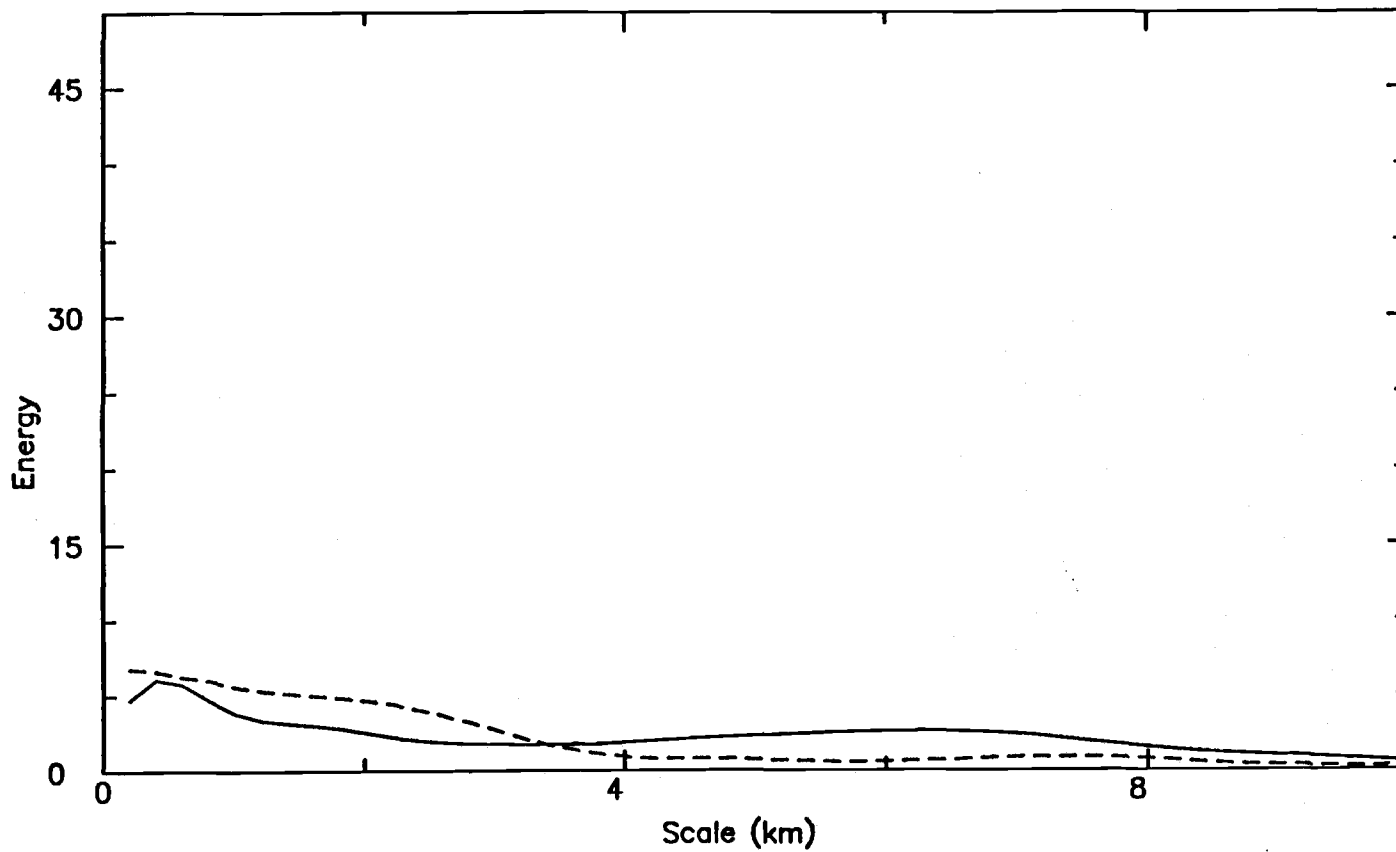


Figure 2.19 Wavelet variance for MSS public lands transect in 1972. Visible red corresponds to solid line and NIR to the dashed line.

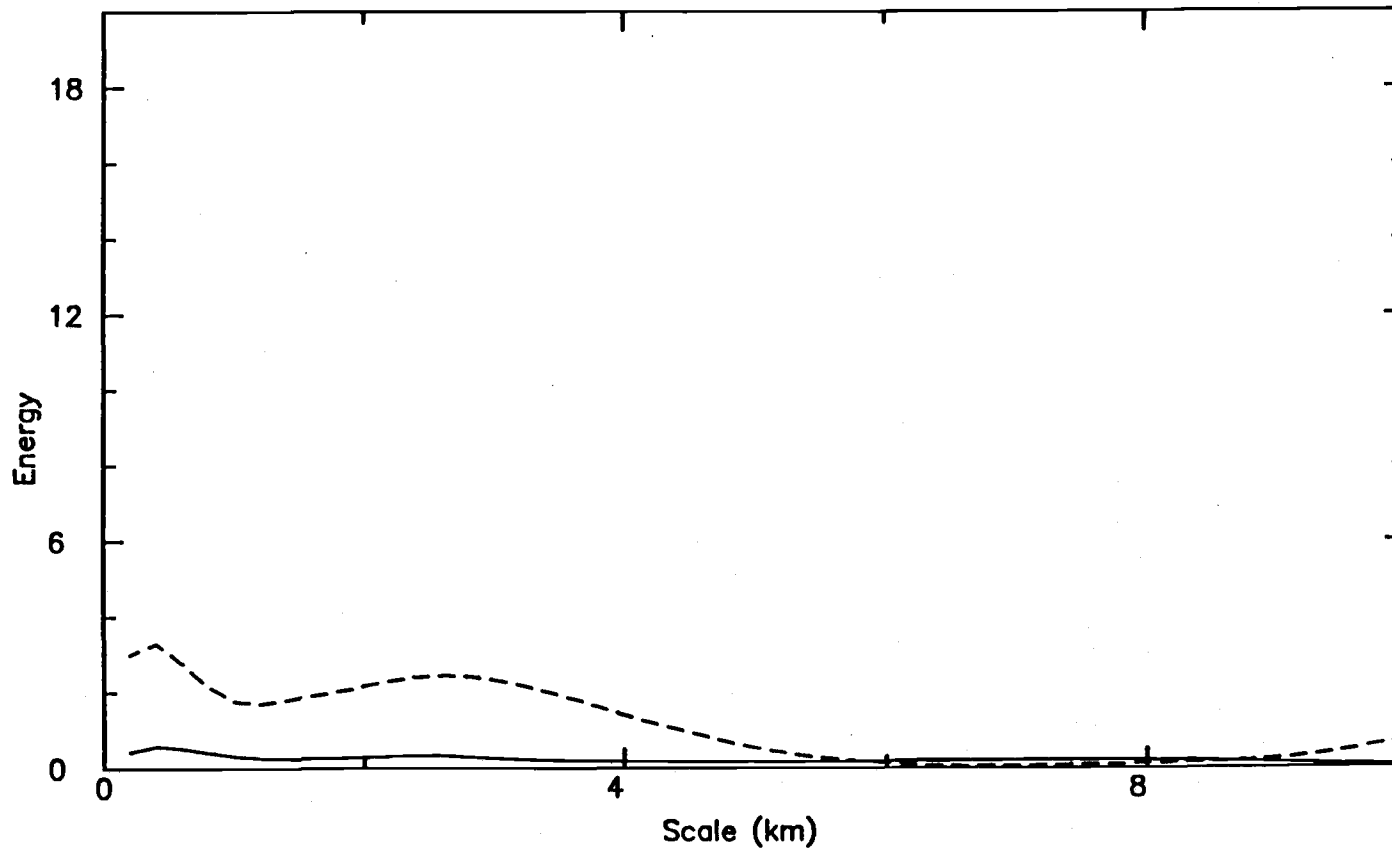
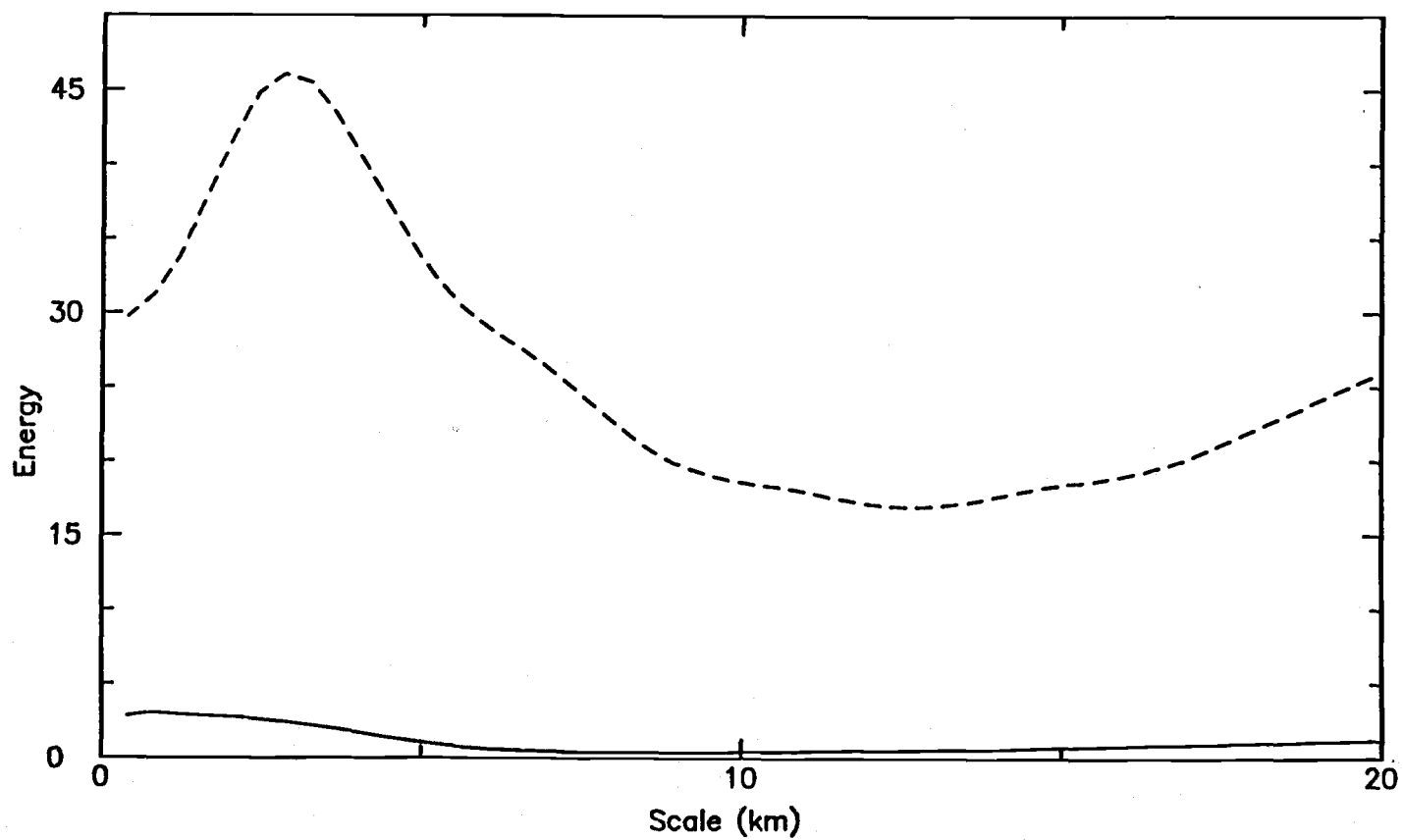


Figure 2.20 Wavelet variance for MSS wilderness lands transect in 1972. Visible red corresponds to solid line and NIR to the dashed line.



**Figure 2.21** Wavelet variance for MSS private lands transect in 1988. Visible red corresponds to solid line and NIR to the coarse dashed line.

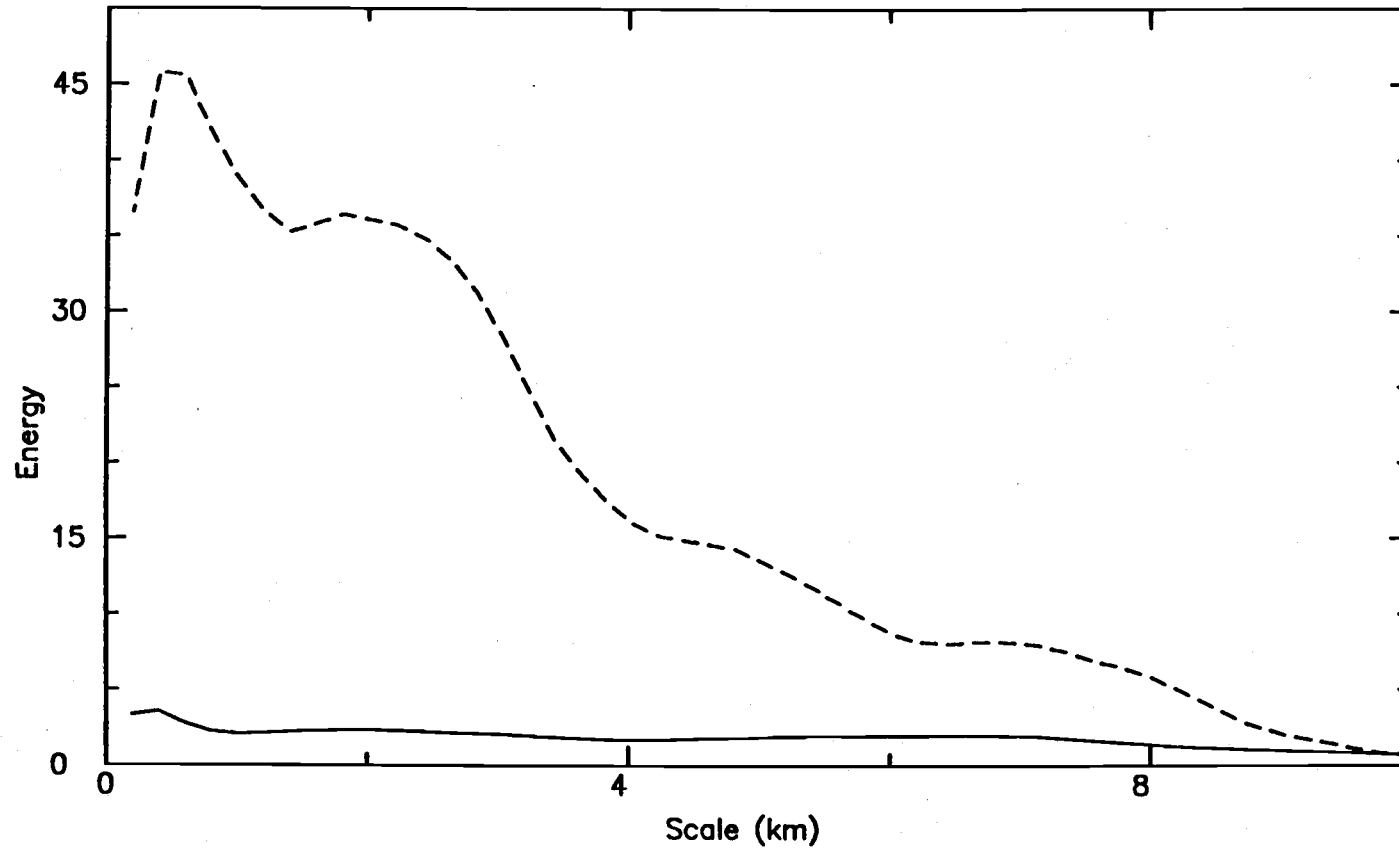


Figure 2.22 Wavelet variance for MSS public lands transect in 1988. Visible red corresponds to solid line and NIR to the dashed line.

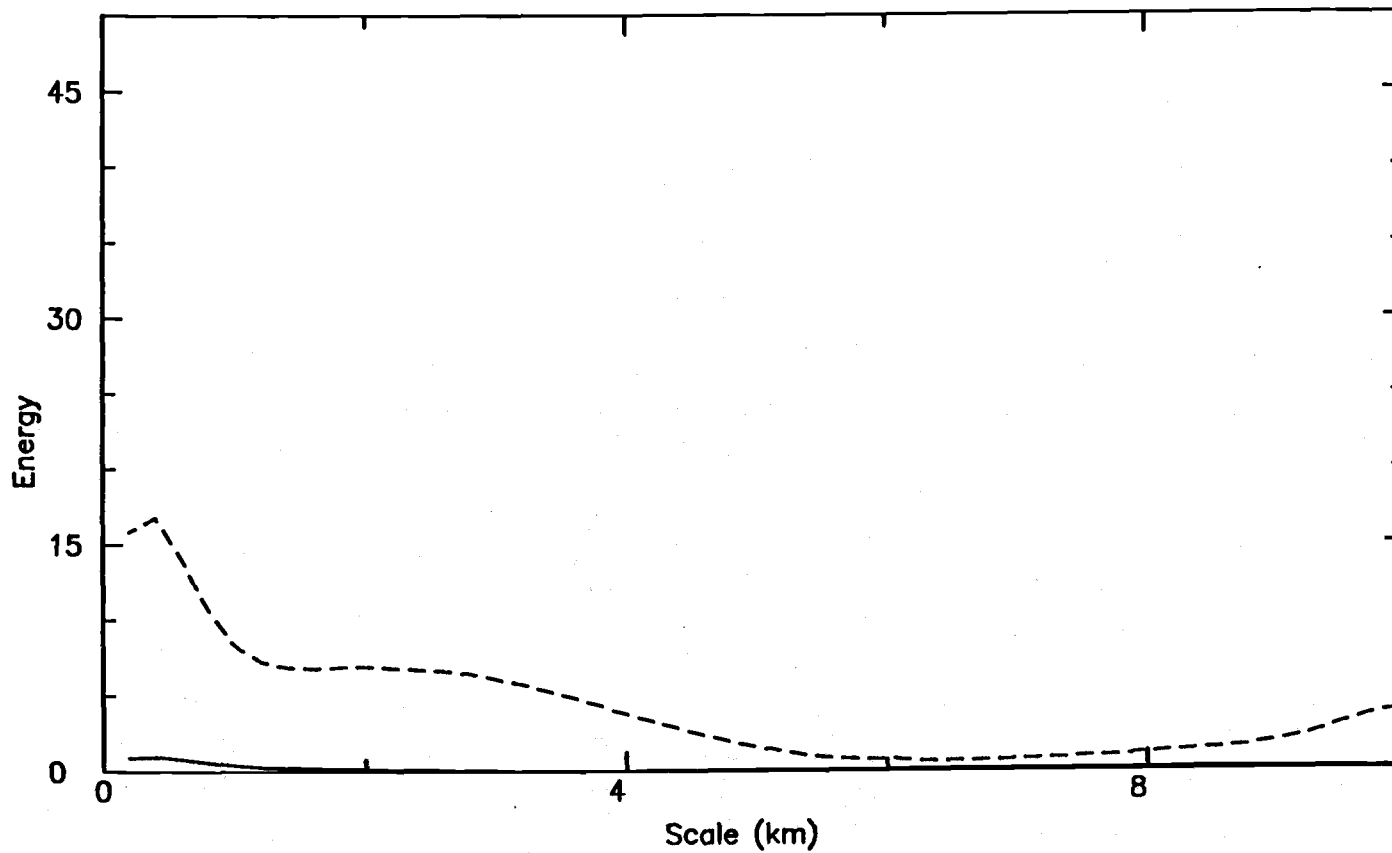
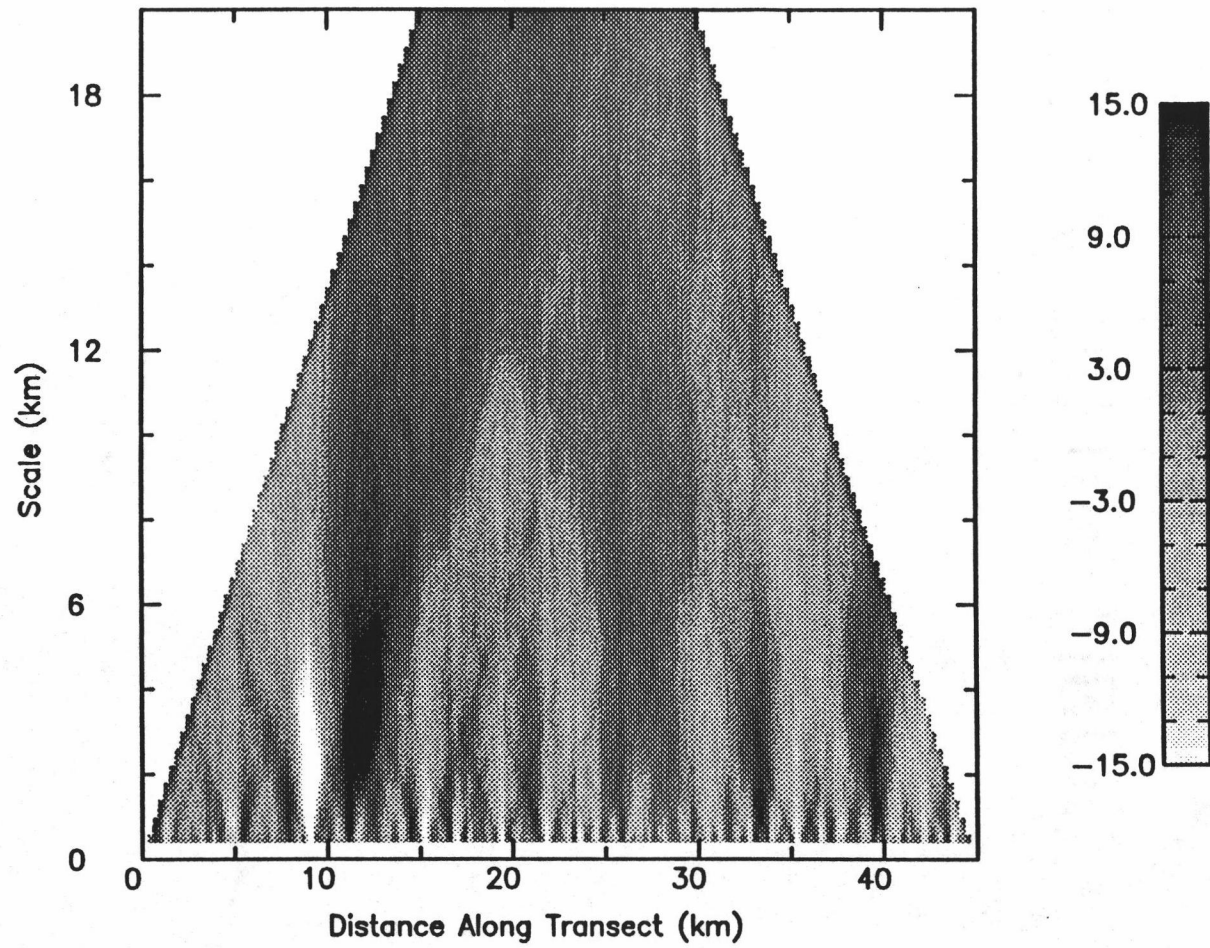
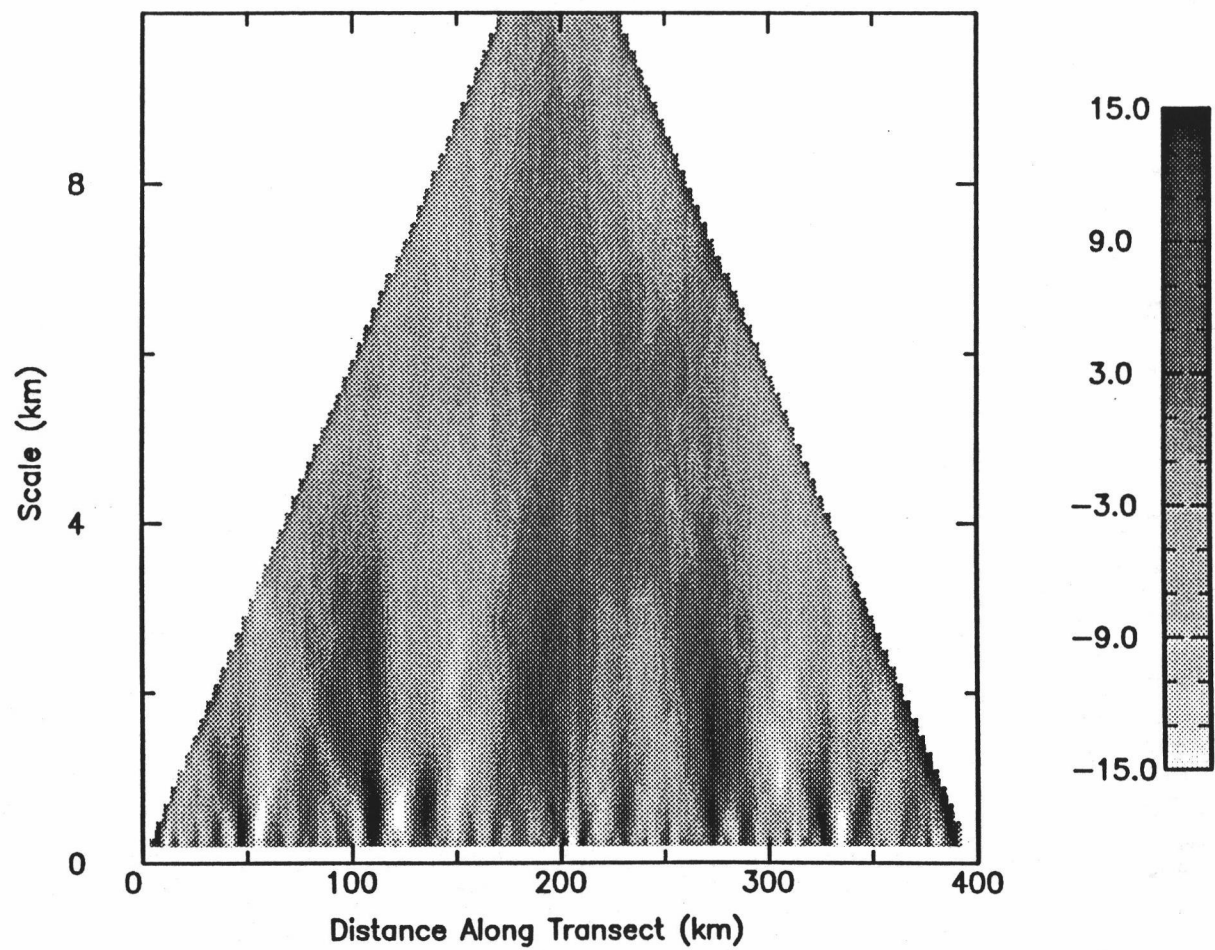


Figure 2.23 Wavelet variance for MSS wilderness lands transect in 1988. Visible red corresponds to solid line and NIR to the coarse dashed line.



**Figure 2.24:** Wavelet transform for MSS NIR transect on private lands in 1988.



**Figure 2.25** Wavelet transform for MSS NIR transect on public lands in 1988.

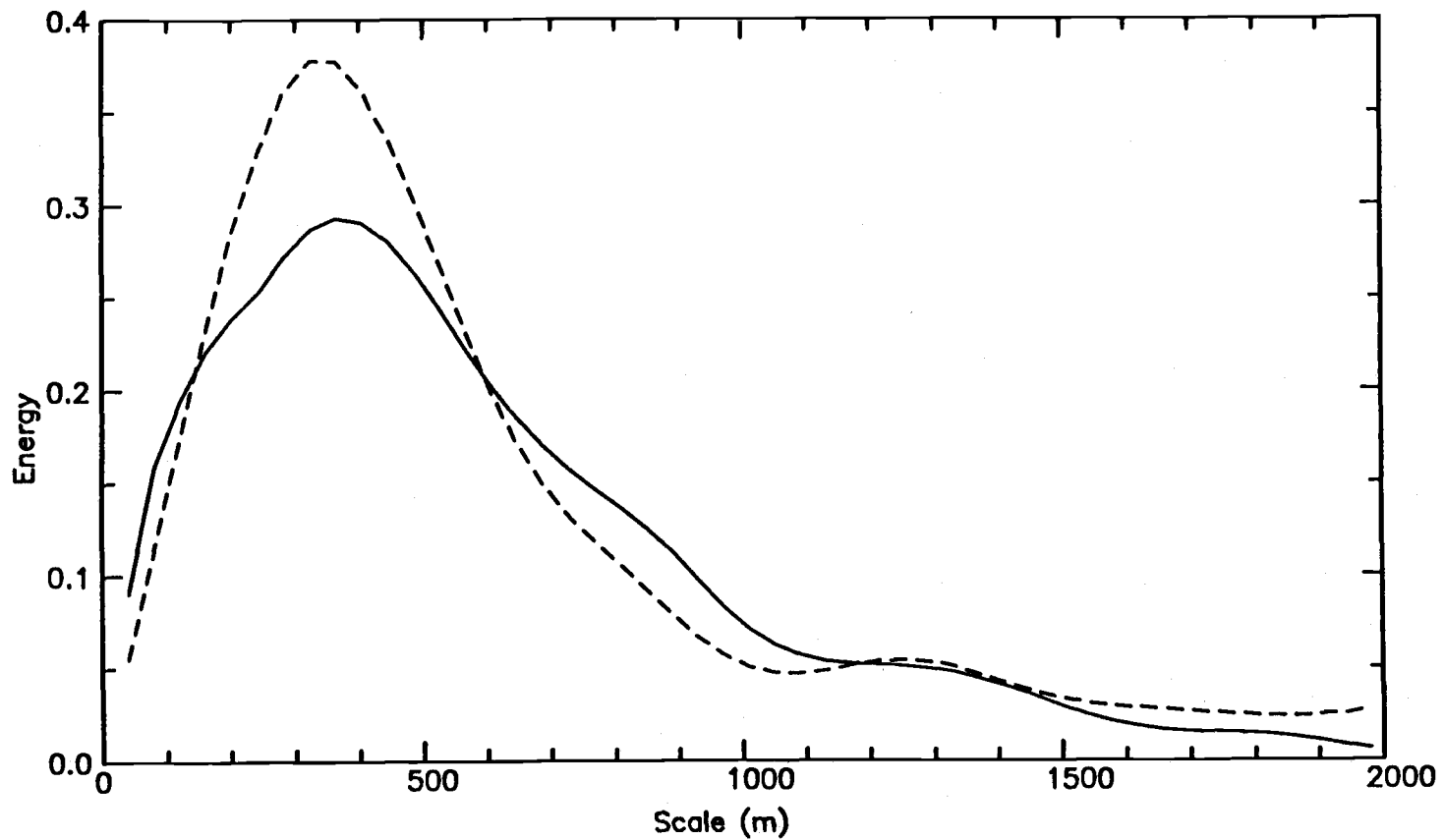


**Figure 2.26** Wavelet variance for Starkey Experimental Forest for visible red (solid line) and NIR (dashed line). Note peak centred at 350 meters.

Figure 2.27 Wavelet cross-covariance for the Starkey transect between the visible red and NIR TM bands. Notice high covariance at 350 meters.

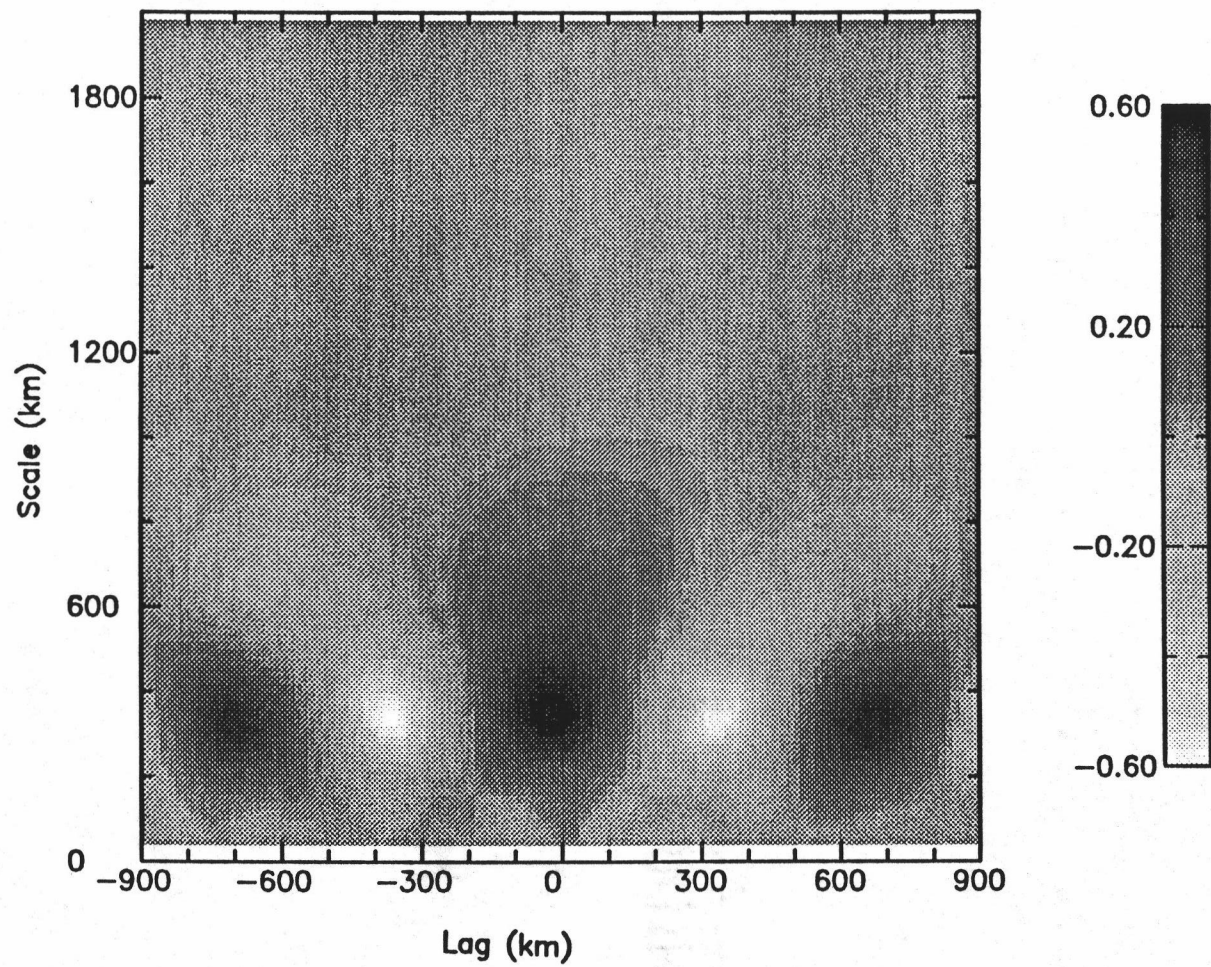


Figure 2.27

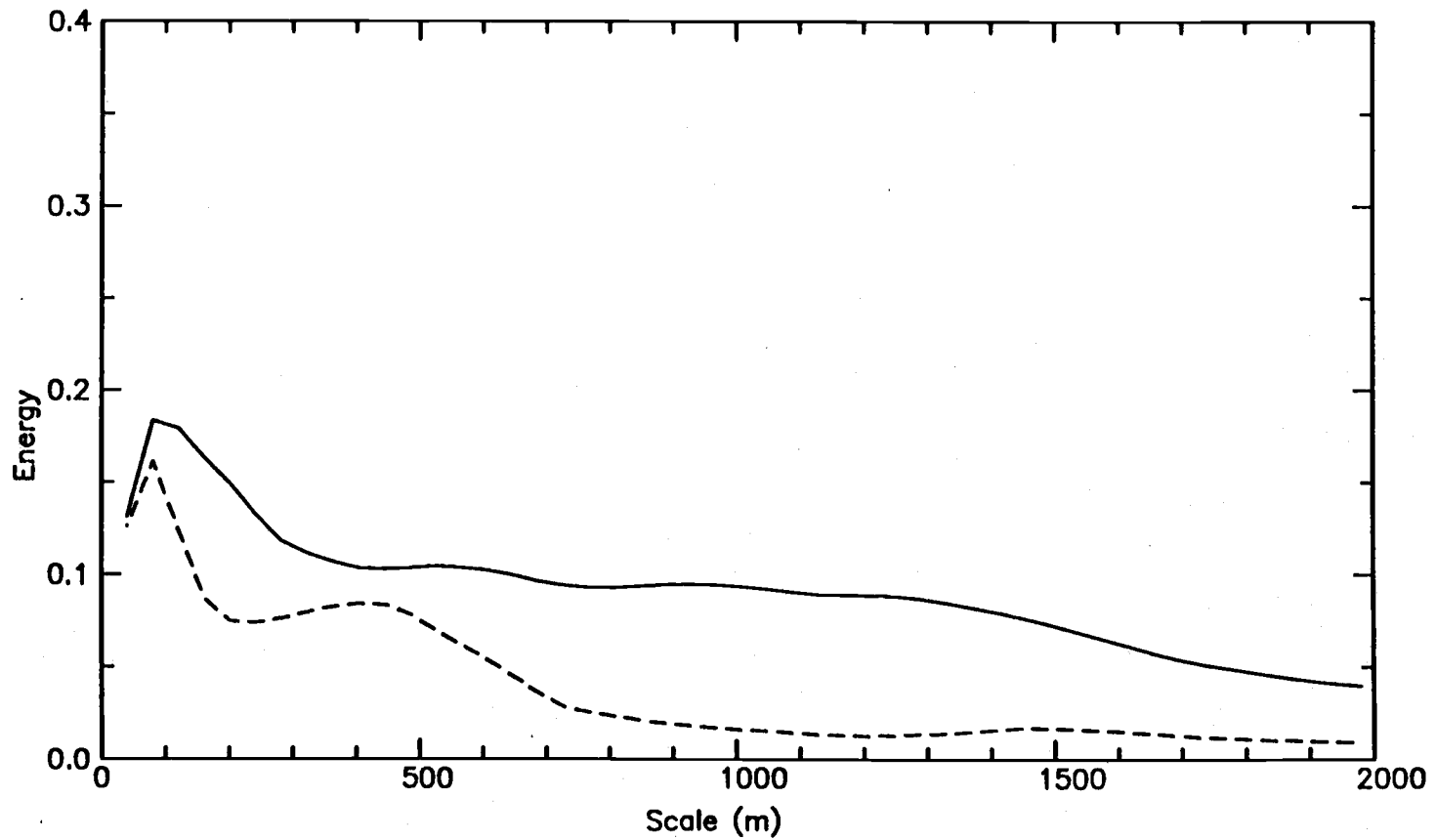


Figure 2.28 Wavelet variance for western Cascades TM transect for visible red (solid line) and NIR (dashed line). Note peaks centred at 100 meters and 350 meters.

**Figure 2.29.** Wavelet cross-covariance for the western Cascades TM transect between the visible red and NIR TM bands. Notice high covariance at the fine scale.

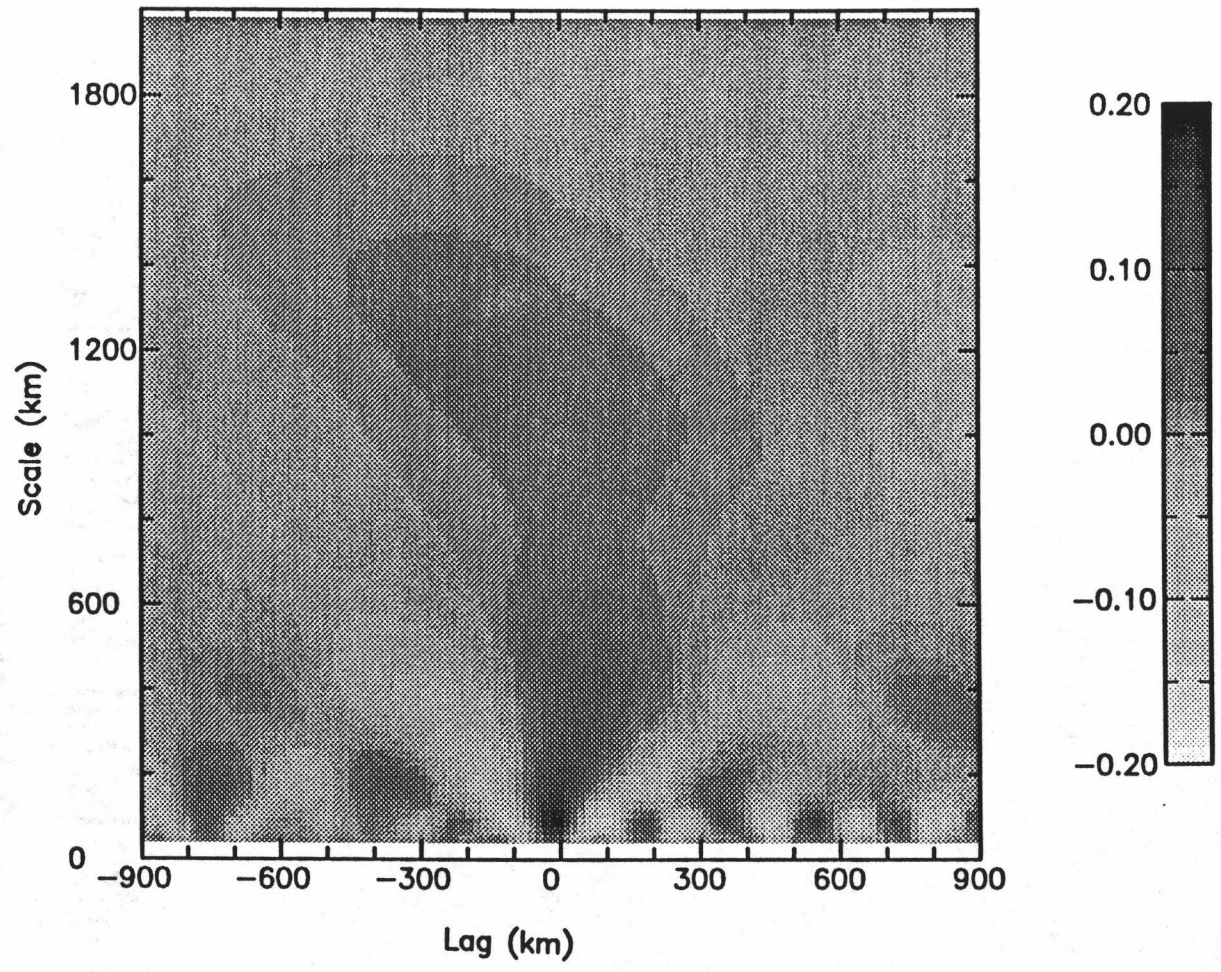


Figure 2.29

## LITERATURE CITED

- Agee, J., 1990, "The historical role of fire in the Pacific Northwest fires", in "Natural and Prescribed fires in Pacific Northwest Forests". Oregon State University Press. 317 pp.
- Baldwin, E.M., 1976, "Geology of Oregon. Kendall/Hunt Publishing Co. 147 pp.
- Barbour, M.G., J.H. Burk, and W.D. Pitts, 1980, "Terrestrial Plant Ecology". Benjamin/Cummings Pubs. , 604 pp.
- Cohen, W.B., T.A. Spies, and G.A. Bradshaw, 1990, "Semi-variograms of digital imagery for analysis of canopy structure". Remote Sensing of the Environment. vol 34. pp. 167-178.
- Curran, P., 1988, "The semi-variogram in remote sensing". Remote Sensing of the Environment. vol 24, pp. 620-628.
- Curran, P., 1980, "Multi-spectral remote sensing of vegetation amount". Progress in Physical Geography, 4(3), pp. 315-341.

- Forman, R.T.T. and M. Godron, 1986, "Landscape Ecology". John Wiley. 354 pp.
- Franklin, J.F. and C.T. Dyrness, 1984, "Natural vegetation of Oregon and Washington". Oregon State University Press. 452 pp.
- Franklin, J.F. and R.T.T. Forman, 1987, "Creating landscape patterns by cutting: ecological consequences and principles". Landscape Ecology, 1, pp. 5-18.
- Gholz, H.L., S.A. Vogel, W.P. Cropper, K. McKelvey, K.C. Ewel, R.O. Teskey, and P.J. Curran, 1991, "Dynamics of canopy structure and light interception in Pinus stands, North Florida". Ecological Monographs, 61(1), pp. 33-54.
- Harris, L.D., 1984, "The Fragmented Forest: Island biogeography theory and the preservation of biotic diversity". University of Chicago Press. 211 pp.
- Hemstrom, M.A. and S.E. Logan, 1986, "Plant association and management guide, Siulslaw National Forest". USDA Forest Service, R6-Ecol 220-1986a.

- Jupp, D. L. B., A.H. Strahler, and C.E. Woodcock, 1988, "Autocorrelation and regularization in digital images: I. Basic Theory." IEEE Transactions. Geos Remote Sens., vol. 26, pp. 463-473.
- Knipling, E.B., 1970, "Physical and physiological basis for the reflectance of visible and near-infrared radiation from vegetation", Remote Sensing of the Environment. 1: pp. 155-159.
- Levin, S.A., 1988, "Patterns, scale, and variability". Lecture Notes in Biomathematics. Springer-Verlag, pp.1-12.
- Lillesand, T.M. and R.W. Kiefer, 1987, "Remote Sensing and Image Interpretation" (second edition). John Wiley. New York.
- MacIntosh, R. P., 1985, "The background of ecology". Cambridge Studies in Ecology. 382 pp.
- Milne, B.T., 1988, "Measuring the fractal geometry of landscapes". Applied Mathematical Computing. 27, pp. 67-79.

Pielou, E.C., 1977, "Mathematical Ecology". Wiley, New York.  
214.pp.

Ripple, W.J., G.A. Bradshaw, and T.A. Spies, 1990, "Measuring  
landscape patterns in the Cascade Range of Oregon,  
U.S.A.". Biological Conservation. 57: pp.73-88.

Waring, R.H., 1989, "Ecosystems: Fluxes of matter and  
energy", in "Ecological Concepts: The contribution of  
ecology to an understanding of the natural world".,  
29th Symposium, British Ecological Society, 1988.  
Blackwell Scientific Pubs. pp. 17-41.

Yahner, R.H., 1988, "Changes in wildlife communities near  
edges". Conservation Biology. 2: pp. 333-339.

### Chapter 3

## RESOLUTION CAPABILITIES OF THE WAVELET VARIANCE IN THE ANALYSIS OF SPATIAL PATTERN

by

G.A. Bradshaw

### ABSTRACT

While the ability of the wavelet transform to preserve the relationship between scale and location in time series data has proven useful to describe multi-scale patterns, it is not clear what advantages its derived function, the wavelet variance may have to discriminate pattern. The resolution capabilities of the wavelet variance are compared to the semi-variogram and Fourier power spectra for the description of spatial or temporal data using a set of simple, one-dimensional stationary and non-stationary processes.

To facilitate comparison between methods, the expected value of the wavelet variance was derived explicitly in terms of the autocorrelation function. The three methods do not show appreciable differences for the non-periodic stationary

processes; the same scale of pattern was identified in each case. However, in contrast to the semi-variogram, the wavelet variance and power spectrum methods had the advantage of resolving periodic structure unambiguously thereby facilitating interpretation of multi-scale pattern.

Unless a sufficient difference between the scales of dominant pattern exists in the data, the wavelet variance did not demonstrate a significant advantage over power spectra. On the other hand, clarity of interpretation of the power spectrum diminishes rapidly as the form of the data features deviated from a pure sinusoidal function. In these cases, the wavelet variance appears to discriminate multi-scale pattern more clearly.

A further extension of the wavelet transform, the "wavelet cross-covariance", was introduced which effects a scale by scale comparison of pattern in multivariate data. The wavelet cross-covariance was derived from the wavelet transform and quantifies the maximum cross-covariance between two variables as a function of scale and lag. A plot of the wavelet cross-covariance identifies the scale and offset at which both variables are maximally correlated.

## INTRODUCTION

There has been an increased interest in the quantification of pattern in ecological systems over the past years. This interest is motivated by the desire to construct valid conceptual models which extend across many scales. The utility of these analyses is based on assumption that the observed spatial and temporal patterns are an expression of the sum and interactions of the processes forcing the system. The concept of spatial and temporal dependence in biological data exists implicitly in many ecological theories (e.g. competition, gap dynamics, maintenance of species diversity, and predator-prey relations; Legendre and Fortin, 1989, Pickett and White, 1985, Levin and Kerster, 1971).<sup>1</sup> The complexity of pattern resulting from the confounding factors of time, space, and interacting biotic and abiotic processes requires analyses which not only identifies but also resolves these relationships. Spatial methods must therefore quantify pattern, discriminate types of pattern, and relate hierarchical phenomena across scales. In addition, it remains not only to develop this methodology but incorporate it into the theory and analysis of ecological processes.

Significant effort has been made to develop methods which both quantify pattern and provide insight into

---

<sup>1</sup> Henceforth, the spatial domain will only be considered. Note, however, space and time are interchangeable in the present discussion.

underlying processes (e.g. Moloney et al, 1991, Dale and MacIssac, 1989; Platt and Denman, 1975). To formulate an accurate interpretation of pattern, it is essential to understand the capabilities and information that a given method provides in the detection and quantification of pattern. A myriad of techniques have been applied to a comparably diverse set of problems in spatial analysis (e.g. Greig-Smith, 1964; Ripley, 1977; Carpenter and Chaney, 1983). Included among these techniques is a separate class of methods which utilize the autocorrelation function as the basis for the description of spatial structure. These methods view the data transect as a single realization of a stochastic process where the spatial correlation is used to estimate statistical properties of the process over a range of scales. The advantage of this approach is twofold: 1) it provides information across many scales, and 2) it provides a statistical framework which can relate pattern to process and model to data with the quantification of pattern. The empirically derived autocorrelation function can also serve as a measure of the independence of the biological variable from the spatially defined abiotic environment. For example, in the case of marine systems, the power spectra of planktonic populations and ocean currents have been used to investigate a causal relationship between the biological and physical system across scales (Powell, 1987; Platt and Denman, 1975).

Variography and spectral analysis are familiar techniques which have been employed for the purpose of identifying terrestrial processes at various scales (e.g. vegetation community structure at stand level (Renshaw and Ford, 1973) and conifer forest structure at landscape levels (Cohen et al, 1990)). The wavelet transform and wavelet variance are similar techniques which have been recently used to quantify the spatial pattern of forest canopy and understorey vegetation. While these methods are frequently cited, the differences between and capabilities of different spatial methods have only been recently discussed in the ecological literature (Carpenter and Chaney, 1983; Moloney et al, 1991).

The present paper compares the wavelet variance to the semi-variogram and Fourier power spectrum in its ability to discriminate and quantify spatial pattern. The comparison is illustrated using a set of four simple, one-dimensional stationary processes after Moloney and Levin (1990) and simulated transects exhibiting a secular or non-uniform trend. To assess similarities and differences shared between autocorrelation-based methods (e.g. Fourier power spectra and the semi-variogram) and the wavelet variance, an expression of the wavelet variance was derived in terms of the autocorrelation function.

The ability of the wavelet transform to preserve scale-location information enables procedures analogous to data

filtering of non-stationary and hierarchical data without prior detrending. The effects of this property was discussed in two ways: 1) examination of the responses of power spectra and the wavelet variance to non-stationary data (e.g. data characterized by a trend), and 2) the construction of a "wavelet cross-covariance" function. The wavelet cross-covariance function introduced here quantifies the magnitude of spatial covariance between two variables and information regarding the degree to which the spatial pattern of the variables are in phase. Thus, it is possible to measure the spatial correlation of two variables even in cases where the pattern is non-uniform or non-stationary. I begin with a brief definition and description of the wavelet transform and variance followed by a comparison of spectral analysis, the semi-variogram, and the wavelet variance.

## WAVELET VARIANCE

### Calculation of the Wavelet Variance

Consider a transect composed of  $n$  points at unit intervals. The wavelet transform of this data is a series of convolutions of the data function  $f(x_i)$  where  $x_i$  is location (distance along transect) with the analysing wavelet function  $g(x)$ . In the discrete case, it is defined as:

$$\omega(a, x_j) = \frac{1}{a} \sum_{i=j-r_a}^{j+r_a} f(x_i) g\left(\frac{x_i - x_j}{a}\right) \quad (1)$$

(Daubechies, 1988), where  $r_a$  is defined to be the half-width of the analysing wavelet beyond which the product is zero,  $x_j$  is the point at which  $g(x)$  is centred, and  $a$  is the scale. The analysing wavelet may be one of several functions fulfilling certain admissibility requirements (Daubechies, 1988). The selection of a given analysing wavelet depends on the objectives of the study and physical structure of the data. For example, the Haar function, given its step function configuration, has been found to be well-suited for edge and gradient detection (Bradshaw and Spies, in review; Gamage, 1990). Three analysing wavelets are considered in the present discussion (the mexican hat, the french hat and the Haar

wavelet) as shown in figure 3.1. Because the wavelet transform is a function of both location and scale, it requires a two-dimensional display. This two-dimensional display identifies the scale and intensity of features in the data and their position along the transect; effectively, the two-dimensional display represents the decomposition of the data into discrete components of scale as a function of location along the record (figures 3.2 and 3.3). In as simple example, the pattern is comprised of a series of peaks of two scales: four and twenty meters (figure 3.2). The four-meter peaks are clustered together forming a nested structure of twenty meters wide. The wavelet transform decomposes the data into both the fine and coarser scaled components composing the overall pattern (figure 3.3).

To facilitate comparison among multiple sets of data, a second function, the wavelet variance, may be used as a means of identifying the average spatial structure in the data. The wavelet variance is derived from the wavelet transform and is equal to the average value of the squared coefficients of the transform at each scale:

$$V(a) = \frac{1}{n-2r_a} \sum_{j=1+r_a}^{n-r_a} \omega^2(a, x_j) \quad (2)$$

$j$  is limited to range between the given upper and lower bounds to insure that the wavelet will always be within the

span of the data. Although there is loss of locational information with this averaging process, the calculation of the wavelet variance provides a summary of the information contained in the wavelet transform in a fashion similar to Fourier power spectra. In contrast, the wavelet variance is a function of a variable of time or space. In particular, use of the wavelet variance facilitates the analysis of pattern between multiple sets of data. Peaks in the wavelet variance correspond to dominant scales of pattern in the signal.

Methods based on the autocorrelation function such as spectral analysis provide a theoretical framework for data analysis when  $f(x)$  is second-order stationary. Second-order stationarity implies that the mean and variance are constant across the transect and the covariance is a function of distance between points and not position (Journel and Huijbregts, 1978). The empirically derived autocorrelation function provides a concise, statistical description of the spatial structure in the data. Both the Fourier power spectra and semi-variogram may be expressed in terms of the autocorrelation function,  $\rho(r_1)$ , where  $r_1$  is the lag or distance between two points. Both the spectral density function and the semi-variogram represent an average value across spatial scale. The semi-variogram is defined as the expected value of the differences between  $Z(x+r_1)$  and  $Z(x)$ , the values of the function at  $x$  and at  $r_1$  lags away from each  $x$ , respectively:

$$\gamma(h) = E((Z(x+r_1) - Z(x))^2) \quad (3)$$

or in explicit terms of the autocovariance function,  $C(r_1)$ :

$$\gamma(r_1) = C(0) - C(r_1) \quad (4)$$

If  $C(r_1)$  is normalized using the variance,  $C(0)$  (or "sill" in the geostatistics literature (Journel and Huijbregts, 1978)), we obtain the correlogram as a function of  $\rho(r_1)$ :

$$\bar{\gamma}(r_1) = 1 - \rho(r_1) \quad (5)$$

The normalized spectral density function in the discrete form for real-valued processes is written as:

$$h(s) = \frac{\sigma^2}{2\pi} \sum_{-\infty}^{+\infty} e^{-isr_1} \rho(r_1) ds \quad (6)$$

Because the wavelet variance is composed of the squared coefficients of the wavelet transform, it is analogous to the power spectra which in itself is proportional to the squared modulus of the Fourier coefficients (Chatfield, 1989). It is possible to express the expected value of the wavelet variance in terms of the autocorrelation. Specifically, we wish to define the expected value of the wavelet variance,  $E(V(A))$ :

$$E(V(a)) = E(\omega^2(a, x_j)) \quad (7)$$

in explicit terms of the autocorrelation function. For simplicity, consider the wavelet transform (1) for a given scale,  $a$ , and assume that  $E(f(x))=0$ . Then, writing  $\hat{\omega}(a) = \hat{\omega}_a(x)$ , the transform for a single scale,  $a$ , is given by:

$$\omega_a(x_j) = \frac{1}{a} \sum_{i=j-r_a}^{j+r_a} f(x_i) g\left(\frac{x_i - x_j}{a}\right) \quad (8)$$

Substituting equations (1) and (2) into (8) we find the explicit expression for the expectation of  $V(a)$ :

$$E(V(a)) = \frac{1}{a^2(n-2r_a)} \sum_{j=1+r_a}^{n-r_a} \left( \sum_{i,k=j-r_a}^{j+r_a} g\left(\frac{x_i - x_j}{a}\right) g\left(\frac{x_k - x_j}{a}\right) F_{ik} \right)$$

where  $F_{ik} = E(f(x_i)f(x_k))$ . Because the wavelet functions  $g(x)$  are deterministic, only the expectation of the data function  $f(x)$  need be evaluated. Noting that the product of  $f(x_i)f(x_k)$  is simply the autocovariance function  $\sigma^2 C(x_i - x_k)$  and applying a change of variables, equation (9) can be simplified to the form:

$$E(V(a)) = \frac{\sigma^2}{a^2} \sum_{l=-r_a}^{+r_a} \sum_{m=-r_a}^{+r_a} g_a(l) g_a(m) \rho(l-m) \quad (10)$$

Equation (10) represents an expression for the wavelet variance comparable to both the semi-variogram and spectral density function as defined in terms of the autocorrelation function (Journel and Huijbregts, 1978; Chatfield, 1989). Before the various autocorrelation functions corresponding to a set of different stochastic processes and the varying responses of the three spatial methods to these models may be compared, it is instructive to first examine the range and magnitude of spatial information each technique identifies for a given specific scale. This analysis is most conveniently performed in the frequency domain.

#### **Calibration of the Wavelet Variance in the Frequency Domain**

The calculation of the wavelet variance and the semi-variogram may be viewed as the result of a series of filtering processes applied to the data transect. The data are first convolved with one of the three analysing wavelet functions; in the case of the semi-variogram, the equivalent "analysing function" takes the form of  $g(x) = -1$  if  $x = -0.5$ ,  $g(x) = 1$  if  $x = 0.5$ , else  $g(x) = 0$ . The sums of squares of the "convolved" data is the non-centred variance, i.e. the

wavelet variance or the semi-variogram.

Computation of these functions may also be conducted in the frequency domain for purposes of convenience as demonstrated by the common use of Fourier transforms in data processing (Bracewell, 1978). The representation of the analysing function in the frequency domain is called the "transfer function" (Priestley, 1981). The configuration of the transfer function will determine how much of the data intensity (i.e. the magnitude of the variable of interest) and period (i.e. the scale of pattern) is retained in the analysis. A difference among the responses of each spatial autocorrelation method reflects a corresponding difference in the range and amount of spectral energy spanned by their respective transfer functions. To examine the frequencies (inversely related to scale) over which each transfer function spans, the wavelet transform of equation (1) must first be defined in the frequency domain.

For a given scale,  $a$ , the wavelet transform can be written in the continuous form as:

$$\omega(x_j) = \frac{1}{a} \int_{-\infty}^{\infty} f(x) g\left(\frac{x-x_j}{a}\right) dx \quad (11)$$

By the convolution and similarity theorems, the Fourier transform of the wavelet transform is (Bracewell, 1978):

$$W_a(s) = aF(s)G(as) \quad (12)$$

where  $F(s)$  is the Fourier transform of the data function  $f(x)$ ,  $G(as)$  is the Fourier transform of the analysing wavelet  $1/a\{g(x/a)\}$ , and  $W_a(s)$  is the Fourier transform of the wavelet transform. Equation (12) simply states that the Fourier transform of the wavelet transform is equal to the product of the Fourier transforms of the data vector and the analysing wavelet. This expression relates the frequency content of the wavelet transform to that of the individual wavelet and the data. By Rayleigh's theorem (Bracewell, pp. 112, 1978) and using equation (2), the wavelet variance,  $V(a)$ , is represented in the frequency domain by:

$$V(a) = \frac{1}{n-2r_a} \int_{-\infty}^{\infty} |F(s)|^2 |G(as)|^2 ds \quad (13)$$

The transfer functions of each of the three wavelets for a scale of one and the semi-variogram are shown in figure 3.4. There are several features to note. The amplitudes and locations of the dominant peaks differ slightly among the four transfer functions. Of the three analysing wavelet functions, the mexican hat wavelet is the only transfer function with a single peak. Secondly, the rate at which the

secondary peaks damp out differs among the semi-variogram, Haar and french hat functions. These observations indicate that the bandwidth (i.e. the frequencies or scales over which the function ranges for a specified scale) and magnitude of energy each transfer function passes differs somewhat for each method.

Based on these observations alone, one might conclude that the capabilities of the various methods might not be equivalent when applied to a given set of data. However, because the absolute scaling and magnitude of the functions are somewhat arbitrary, some of the difference may be artificial. For this reason, the locations and magnitudes of the dominant peaks of the three wavelet variances were calibrated to that of the semi-variogram in the frequency domain to isolate function morphology alone. The calibration ensures that nearly the same energy is passed at the dominant bandwidth frequency for each of the four functions. As figure 3.5 shows, while the calibration procedure has minimized differences among the functions with regards to the location of the dominant peak in the transfer function, the various contributions from secondary peaks is still distinct. In particular, the magnitude of the semi-variogram transfer function does not diminish with increasing frequency as do the wavelet functions; rather, the transfer function of the semi-variogram is composed of integral peaks of the same amplitude and form.

It is instructive to observe how the transfer function changes as a function of increasing scale,  $a$ . As an example, figure 3.6 shows the transfer function of the mexican hat at successive scales of the parameter  $a$ . (The behaviour of the other two wavelets is similar to that of the mexican hat.) As  $a$  increases, the peak becomes narrower and shifts to the left including fewer high frequencies. The rate of exclusion increases more rapidly as  $a$  increases. This implies that at coarser scales of resolution, less and less of the fine-scale features of the data are included. As a result, there is a corresponding smoothing of the data in the spatial domain with increasing scale. Conversely, information contained in large-scale features is carried into finer scale. This behaviour coupled with the fact that most data will contain greater numbers of fine-scale features than large-scale features relative to transect length suggests that the resultant wavelet variance may often be strongly influenced by the signature of fine-grained features.

**COMPARISON OF THE WAVELET VARIANCE, POWER SPECTRUM,  
AND SEMI-VARIOGRAM**

**Stationary Processes**

The autocorrelation functions of four stochastic processes (additive moving average (MA), non-additive moving average (NA), autoregressive order one (AR(1)), and autoregressive harmonic (ARH)) were chosen to examine the difference in response between the three methods of spatial analysis. These specific models were chosen based on their semblance to physical and ecological processes. All four stochastic processes conform to first- and second-order stationarity.

The additive and non-additive moving average models have been adopted from Moloney and Levin (1991). The additive moving average model is used to model data such as vegetative growth where successive events are additive and accumulate in magnitude over space. Where patches overlap, the density is the sum of the contributions of the separate patches. In contrast, in the non-additive model, the presence of a patch allows overlap of successive patches but the value of overlapping patches does not exceed unity; the magnitude of patches does not increase with overlap. This model is appropriate for presence/absence vegetation cover studies. An AR(1) (or Markov process) is the extension of moving average of infinite order (Chatfield, 1989). In the AR(1) model, the

value of a given point along a transect is only dependent on the preceding value. This model has been used to describe empirically such processes as conifer cone distribution (Means, unpublished ms).

Finally, because ecological data often contains repeating structure and the objective of many analyses is to quantify the scale of the repeating pattern (e.g. Tucker et al, 1987; Cohen et al, 1991), an AR harmonic (ARH) autocorrelation function was included to assess the effects of varying degrees of periodicity on the transform response.

Figures 3.7 and 3.8 show the responses of the three wavelets, semi-variogram and power spectra to an example of an AR(1) model where the parameter has been chosen to generate a patch size of five meters. The semi-variogram as viewed as a spherical model (Journel and Huijbregts, 1977), shows a range between 5 and 6 meters. The range is defined as the scale beyond which the data are no longer correlated. It is estimated as the position along the x-axis corresponding to the point along the curve where the semi-variogram flattens (Journel and Huijbregts, 1978). Although differing slightly, all of the three wavelets show a scale of dominance lying between three and five meters. The corresponding power spectrum is shown in figure 3.8. While the power spectrum shows an inflection point around five meters, detection of this point is difficult to ascertain for the given parameter.

The example chosen to illustrate the additive moving

average model also uses five meters as the "patch" parameter. Calculation of the semi-variogram yields a range of five meters and, as shown by Moloney and Levin (1991), the power spectrum indicates the dominant peak at 5 meters (figures 3.9 and 3.10). The responses of the three wavelets are very similar for this and the case of the non-additive model (figures 3.11 and 3.12).

Figures 3.13 and 3.14 show the results for the ARH model characterized by a ten meter period. In an ARH process with parameter period of ten meters, the dominant spatial feature dimension will equal the half-period: in this case five meters. Among the wavelets, the Mexican and French hats show a distinct peak centred at five meters while the Haar peak is somewhat more diffuse centring around four meters. The power spectrum shows a peak at ten meters (the full period). The responses of these functions is much as expected considering the previous results. The noticeable deviation is the semi-variogram. Although showing a distinct peak at five meters, there is a second peak centred at 15 meters. If the scale had been carried beyond 20 meters to include higher scales in the figure, one would see a repeating peak structure in the semi-variogram at 10 meter intervals. Once again, the behaviour of the semi-variogram may be explained in terms of its transfer function. It is difficult to distinguish hierarchical or multi-scale structure from single-scale repeating structure using the semi-variogram. In contrast, the wavelet variance

and the spectral density function are able to resolve the difference between repeating, single-scale and multi-scale structure unambiguously.

Excluding the case of the ARH process, these calculations suggest that the three methods respond very similarly to stationary processes. In the case of the ARH process, the analysing wavelets and spectral density function were capable of discerning repeating structure as a single pattern scale. While the example used here was straightforward for purposes of instruction, the interpretation of a semi-variogram calculated using data comprised of measurement error coupled with aperiodic and periodic components of pattern can prove challenging (Cohen et al, 1990).

#### **Non-stationary and Non-Uniform Processes**

A collection of transect data will often coincide with an environmental gradient (e.g. elevational or moisture gradient) or encounter some degree of patchiness in a variable such as moisture. Non-uniformity in the data may reflect a change in the physical properties with location relative to the scale of detection. The term "non-uniformity" is used here to denote data which exhibit a trend or higher order pattern. In most cases, these data are non-stationary as defined above.

If trends are present in the data, most analytical techniques require detrending before the analysis may be correctly performed. The use of power spectra and the semi-variogram assume first- and second-order stationarity (Priestley, 1977; Journel and Huijbregts, 1978). Although a number of detrending schemes are available which may be applied prior to application of the spatial analysis, the trend may be difficult to discern from the features of interest. In addition, valuable information regarding the spatial relationship between multi-scale phenomena may be obscured or lost as a result.

The wavelet variance employed in conjunction with the wavelet transform has been shown to be able to detect and preserve hierarchical and non-uniform structure in the data (Argoul et al, 1989). Unlike the spectral density function and the semi-variogram, the wavelet transform and variance do not assume stationarity of the data prior to analysis. For these reasons, it may be appropriate to utilize the wavelet variance and transform in cases of obvious non-stationarity.

A transect comprised of two cosine functions of differing periods were generated (figure 3.15). The first half of the transect consists of a cosine function of period ten, while the second half of the transect consists of a cosine function of period thirty. In this case, the mean and variance are constant but the pattern is non-uniform, i.e. the period changes across the transect. Both the power

spectrum (figure 3.16) and wavelet variance (figure 3.17) are characterized by two, clearly distinguished peaks corresponding to the two scales of pattern in the data (5 and 15 meter peaks). However, the response of these methods may not always be so clear even in a simple case.

A second difference between the wavelet variance and power spectra is the flexibility of choice basis available using the wavelet and lacking in the power spectra. Fourier power spectra are limited to trigonometric functions as their basis. Thus, the analysing wavelet may be chosen based on the data structure and study objectives. For example, one may effect a decomposition of the data into a progression of components using either the mexican hat (for symmetric features) or the Haar (for asymmetric features and edges.

Figure 3.18 shows a simulated transect resembling the example in figure 3.15 with the exception that the peaks are square and have edges. As in figure 3.15, the transect is composed of two scales of pattern. However, the resultant power spectrum is quite different (figure 3.19). The power spectrum identifies the two periods in the data but contains additional information and energy at finer scales resulting from the "edges" of the peaks in the data. In contrast, the mexican hat wavelet variance distinguishes only the two dominant scales of pattern. If the main intent of such a study is to distinguish dominant scales of pattern, the wavelet variance would be a more appropriate choice in the

present example.

Figures 3.21, 3.22, and 3.23 show the response of the Fourier power spectrum, Haar, and Mexican hat wavelet variances, respectively, to a family of functions as depicted in figure 3.18 above. Five transects were generated such that the ratios between the first and second halves of the transect were 1, 2, 3, 4, and 5. (For example, a ratio of one corresponds to a transect composed entirely of cosine function of the same period, 10 meters; a ratio of two corresponds to a period of ten meters in the first half of the transect and 20 meter period in the second half of the transect, etc.). In this example, the combined effects of varying scale ratios and feature morphology are examined.

In all three cases, the resolution capabilities improve with a corresponding increase in the ratio between pattern scales. The distance between peaks in the power spectrum and the wavelet increases with increasing ratios. The Haar analysing wavelet appears to provide the clearest representation of the pattern (figure 3.23). This result might be anticipated when the morphology of the data features and the Haar wavelet are considered. Both function and feature resemble step functions. In comparison, the basis of the power spectrum and the Mexican wavelet are smooth functions.

### WAVELET CROSS-COVARIANCE

Calculation of the cross-correlation provides a measure of how related two variables are to each other in space. The wavelet cross-covariance is introduced here as a complementary method to evaluate multi-variate transect data based on the wavelet transform. An application of the wavelet cross-covariance is provided using a simple simulation and field data from a forest canopy gap and understory vegetation study.

Two cosine functions of period ten meters were generated (figure 3.24). The two functions are identical other than the fact that they are offset relative to each other by five meters. First, the wavelet cross-covariance is calculated using the wavelet transform. The wavelet transform is calculated for each variable. After these calculations, the data are reconstructed scale by scale using the wavelet transform, i.e. the wavelet transform effects a filtering of the data scale by scale. The result is a progression of filtered versions of each data transect for each scale. The wavelet cross-covariance is then calculated for the two variables scale by scale. The result is a family of values, namely the maximum cross-covariance, which are a function of scale and lag (i.e. the amount of offset between the two variables). These are plotted and interpolated as shown in figure 3.25. The covariance function was chosen over the

correlation function because it retains information about data intensity (amplitude) as well as the waveform.

The alternating dark and light areas in figure 3.26 correspond to the maximum positive and negative cross-correlation between the two cosine function. The y-axis corresponds to the scale at which the maximum cross-covariance occurs. In this case, the maximum cross-covariance occurs at ten meters at integral lags of 5 meters. Coarser scales show zero correlation.

To illustrate a further extension and application of the wavelet cross-covariance, a subset of transect data has been chosen from a larger study investigating Douglas-fir forest gap-understory dynamics. The data consist of twelve 200-meter transects along which percent canopy gap opening and understory vegetation cover were sampled at one meter intervals. The transects were chosen to represent stands from young to old growth age-classes. One of the central questions of the study has been to investigate the degree to which the spatial distribution of canopy gaps influences the spatial distribution of understory plants. One approach has been to calculate the spatial correlation of these variables.

Reconstructions of wavelet transformed transects were developed across all scales in the manner described above for canopy gap and tall shrub life-form for a young (75 year old) Douglas-fir stand and an old-growth (450-600 year) Douglas-fir stand. The canopy gap and tall shrub data for the two

stands are shown in figures 3.26 and 3.28. After each reconstruction was created in each stand (a total of two reconstructions), the cross-covariance calculated for the canopy gap reconstruction with the tall shrub variable for both stands. The maximum cross-covariance over all lags was plotted as a function of scale where scale represents the size of features in the data.

The wavelet cross-covariance for the younger stand indicates that the tall shrub and canopy-gaps are correlated at the fine (<5 meters) scales (figure 3.27). However, the correlation is strongest when the two transects are out of phase by several meters. The stand appears to lack coherence between these variables at coarser scales which might be expected in a light-limited understorey as found in younger Douglas fir stands.

In contrast, the old-growth stand shows distinct cross-covariance at the fine and coarser scales (figure 3.29). The dominant scale at which patch size of the tall shrub understorey is related to canopy gaps is much larger (averaging approximately fifteen meters) than in the case of the younger stand (less than five meters). In addition, the maximum value of the large gap-tall shrub patch size occurs at zero lag. Thus, the canopy gap-understorey relationship as represented by this example appears to be much more closely coupled compared with the young stand above.

The old-growth stand is characterized by a heterogeneous

canopy gap structure reflecting the cumulative effects of disturbance, age, and site history. The younger stand is characterized by an even canopy lacking the distinct and larger canopy openings. The canopy-gap contrast is much stronger in the older stand as a result of overlapping overstory Douglas-fir and canopy replacing hemlocks. This may create a strong contrast in the light resource "patchwork" in the understory below. The results presented appear to support the hypothesis that overstory (i.e. canopy openings) do exercise an influence over the spatial distribution of certain understory vegetation.

## CONCLUSIONS

The resolution capabilities of the wavelet transform and wavelet variance as a method of spatial analysis were compared with those of the semi-variogram and the spectral density function using a set of stationary autocorrelation functions. The wavelet variance was re-derived in terms of the autocorrelation function and calibrated to the semi-variogram in the frequency domain to facilitate comparison. Little significant differences were observed among the methods for stationary processes except in the case of the ARH autocorrelation function. Where the data are characterized by a repeating, single-scale structure, the wavelet variance and spectral density functions provide relatively unambiguous results. Interpretation of the semi-variogram in comparable circumstances appears much less straightforward.

Both the power spectrum and wavelet variance were sensitive to the ratio of the periods of the pattern characterizing the data. As the ratio increases, the resolution capabilities of both methods improves. An appropriate choice between the two methods will depend on the data feature morphology, ratio of the dominant periods, and the objectives of the study. Clarity and accuracy of interpretation of a spatial analysis will depend on these factors and determine the method or sets of methods employed.

The wavelet cross-covariance was introduced as a method to describe the spatial correlation between two variables as a function of scale offset. Results from both the simulated transect and the field-derived forest canopy data suggest that this method may provide insight in the analysis of multi-variate and hierarchical data.

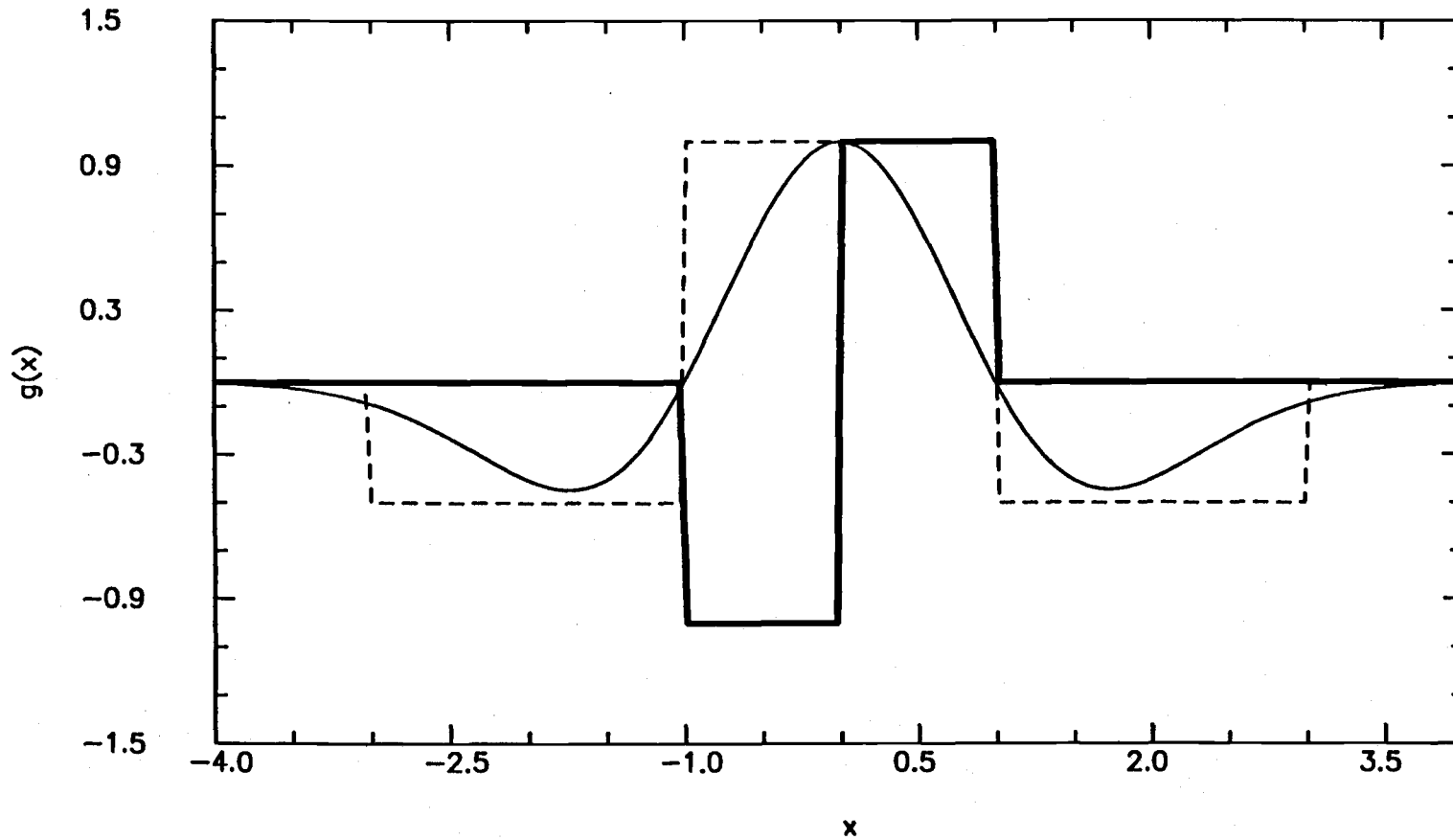


Figure 3.1 Mexican hat (solid line), Haar (heavy solid line), and french hat (dashed line) analysing wavelets.

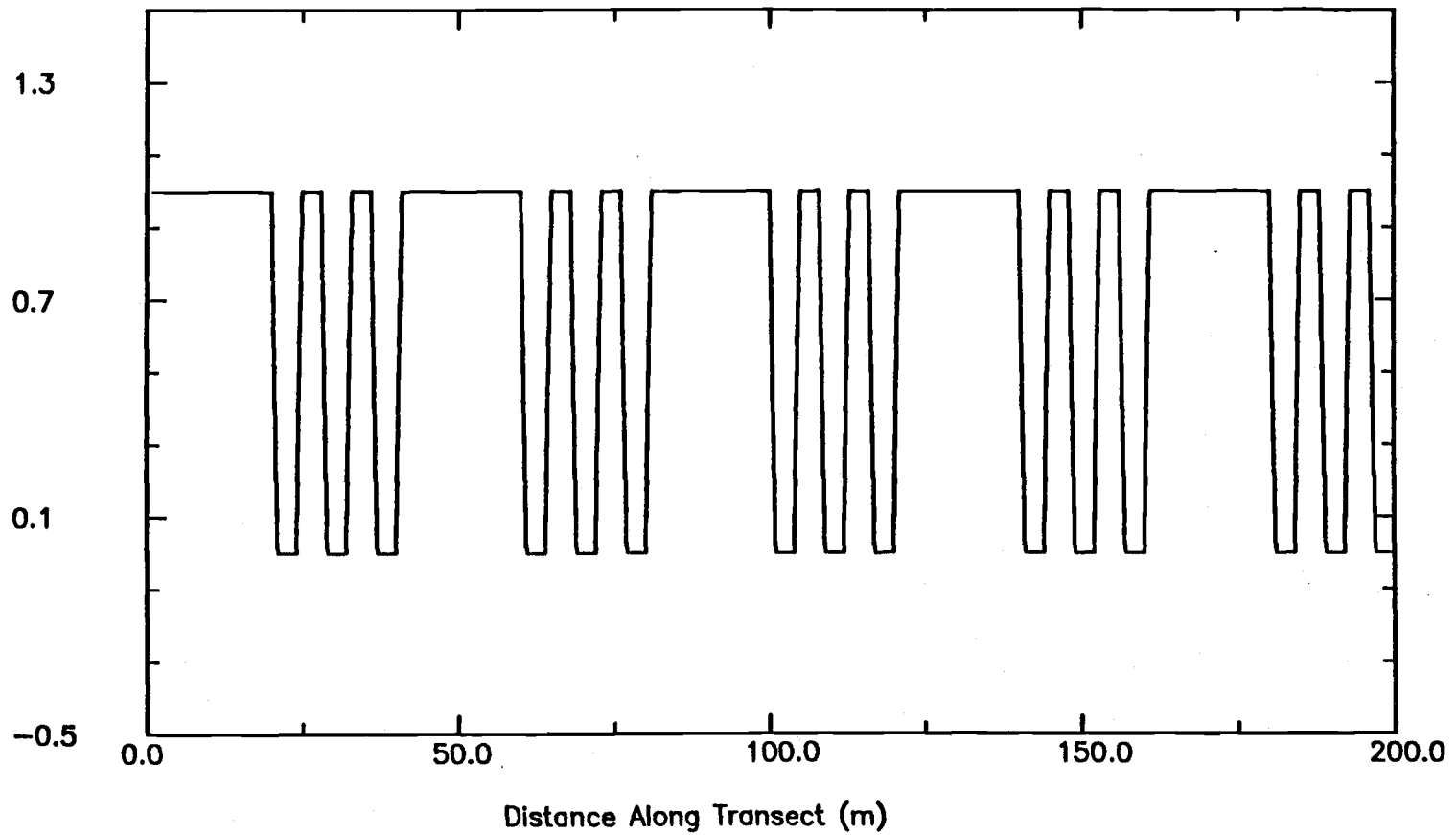
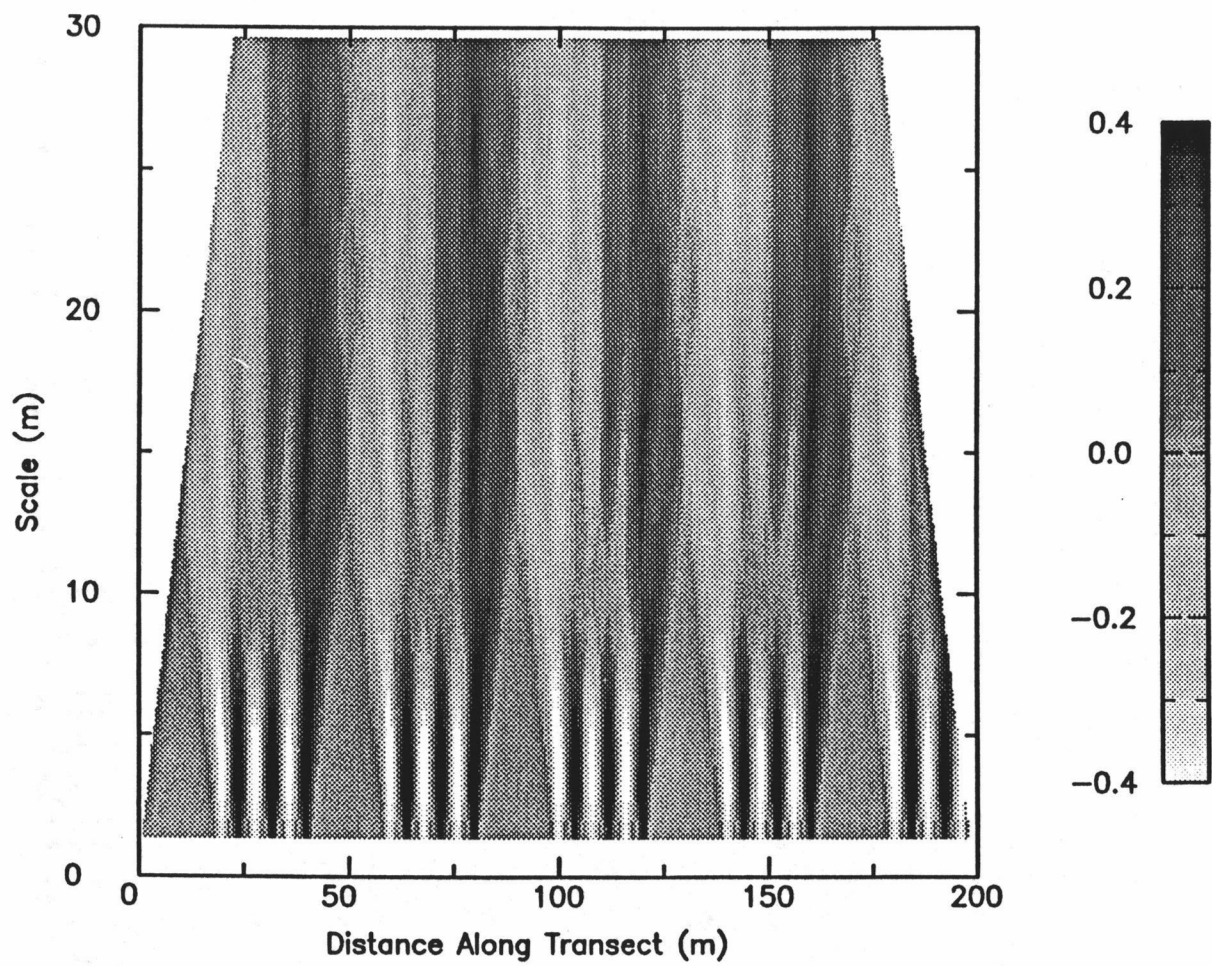


Figure 3.2 Sample data transect used in wavelet transform construction for figure 3.3.

**Figure 3.3** Wavelet transform of data transect shown in figure 3.2 calculated using the mexican hat analysing wavelet. x-axis represents distance along transect while y-axis represents scale (meters). Brightness of transform increases with increasing intensity of feature (magnitude of signal at given location and scale).



**Figure 3.3**

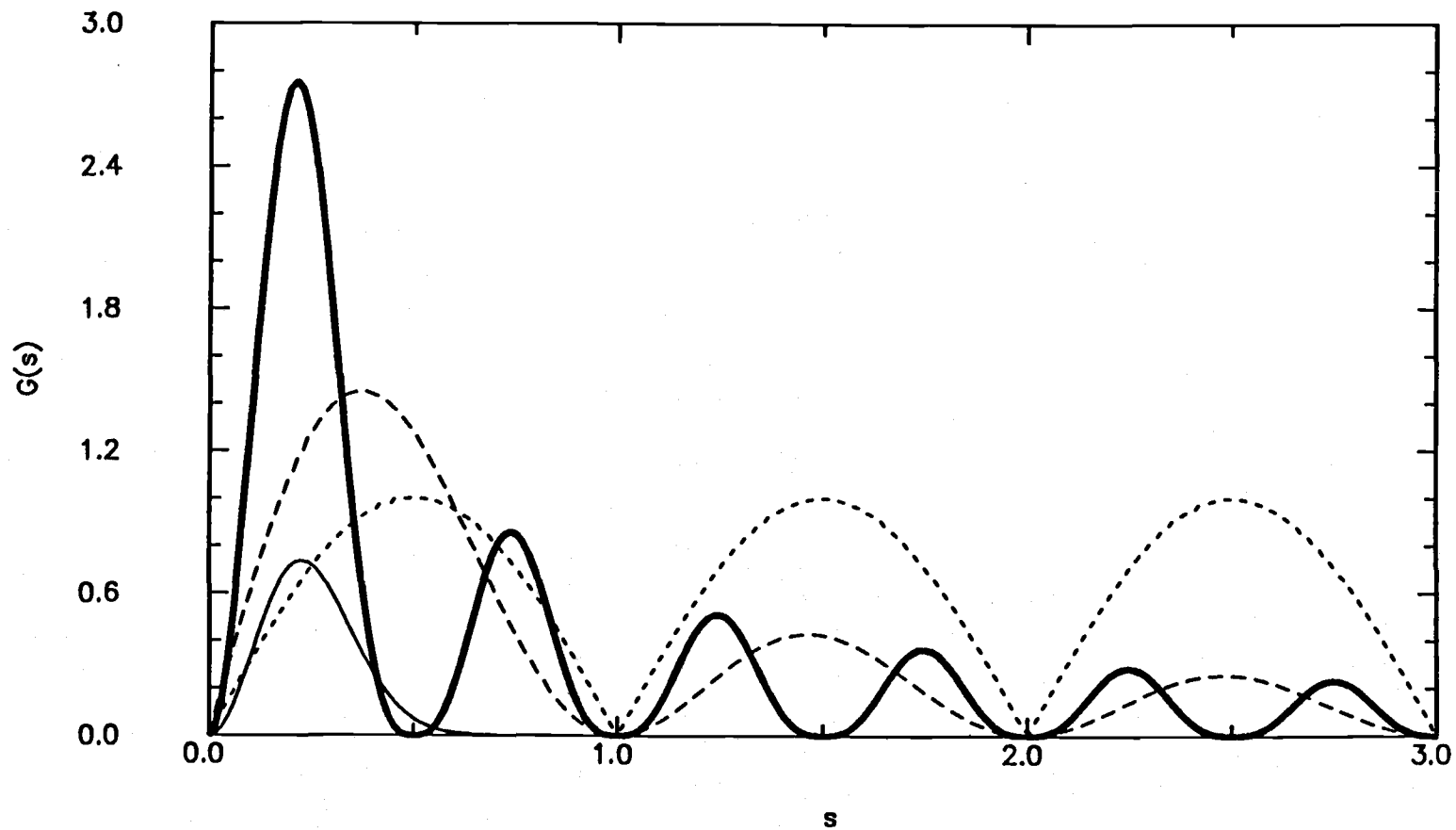


Figure 3.4 Transfer functions of mexican hat (solid line), Haar (heavy solid line), and french hat (dashed line) analysing wavelets and semi-variogram (dotted line).

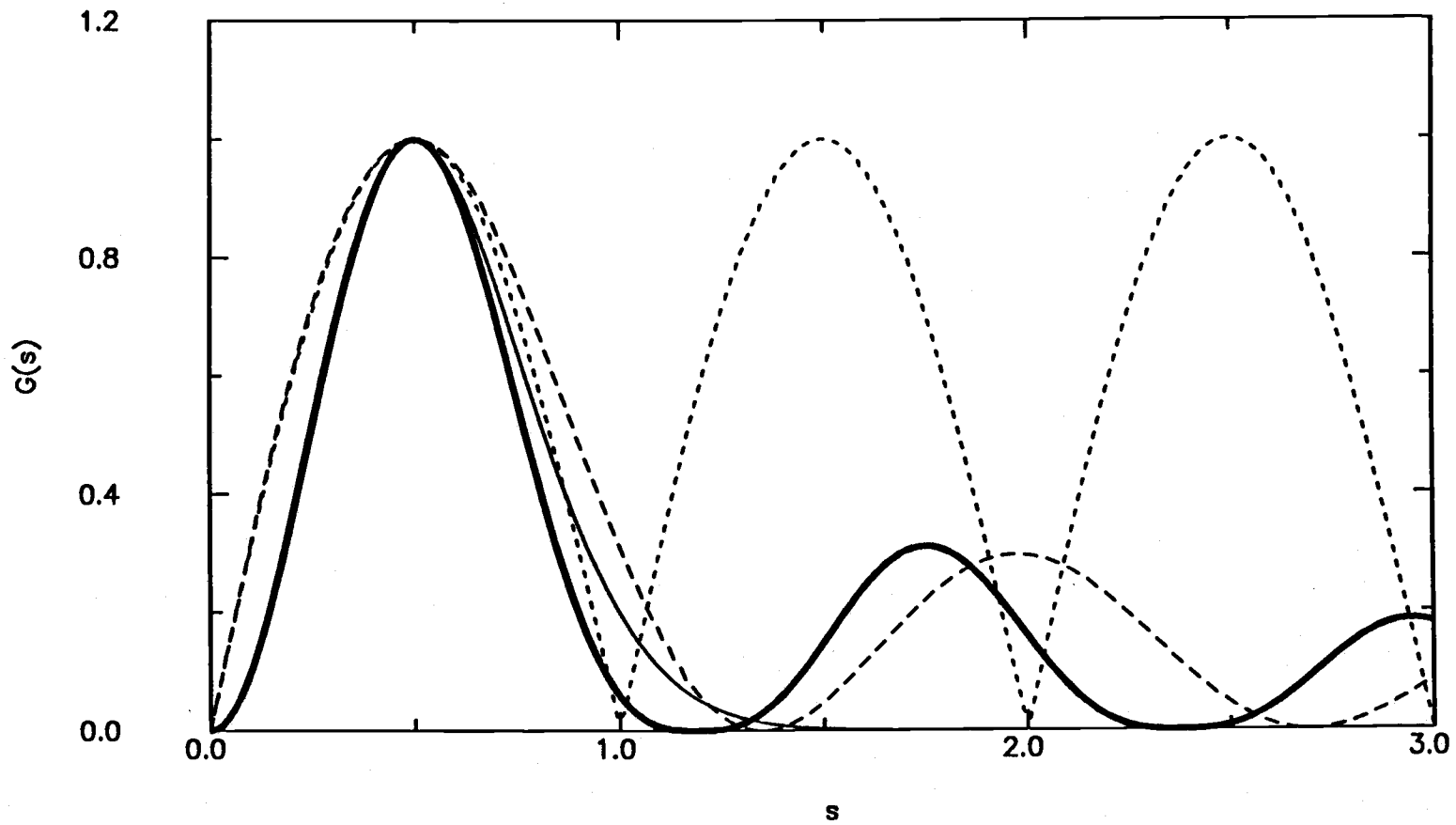
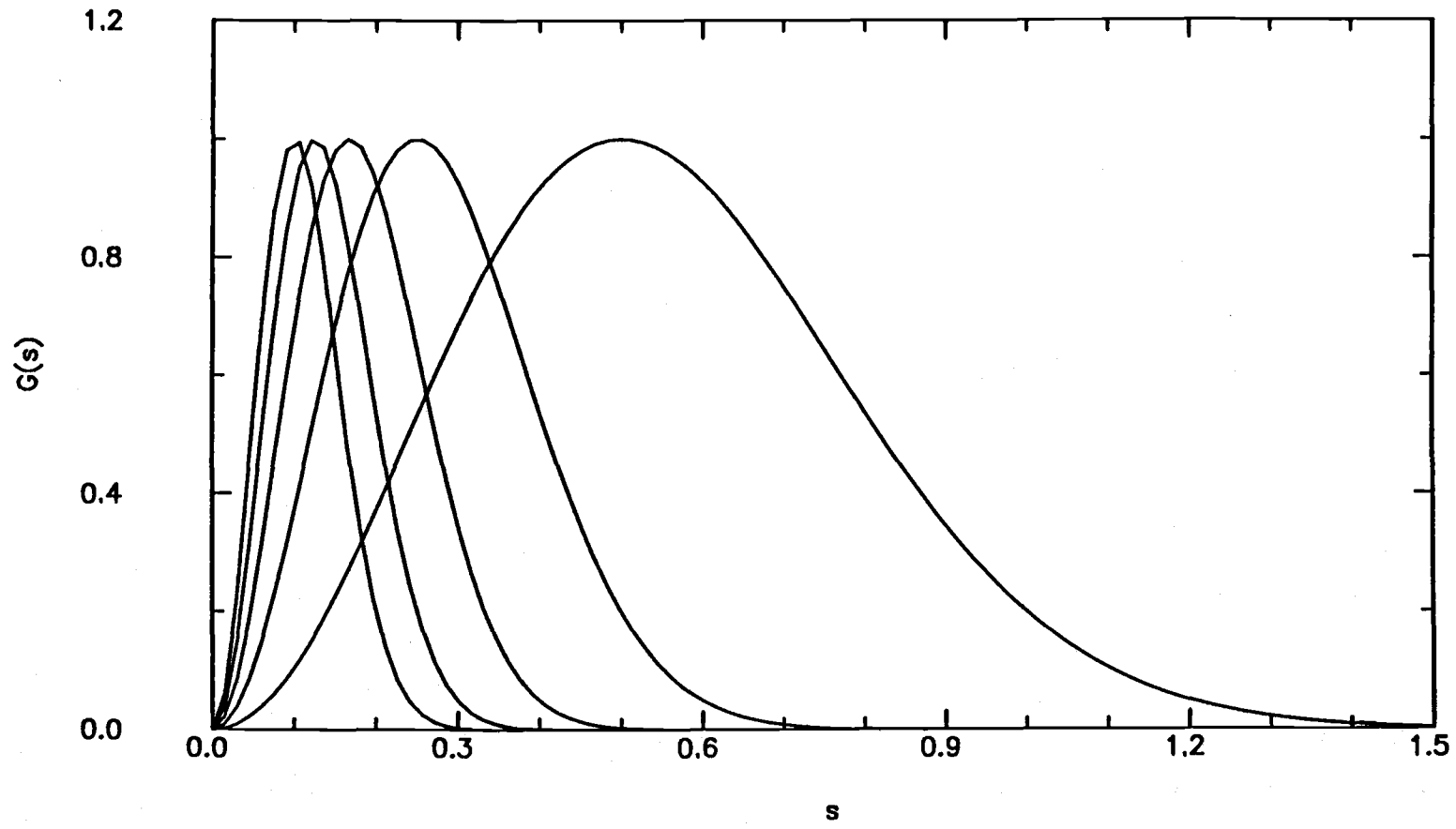


Figure 3.5 Calibrated transfer functions of figure 3.4.



**Figure 3.6** Transfer function of the mexican hat analysing function at several scales of the scaling parameter  $a$ .

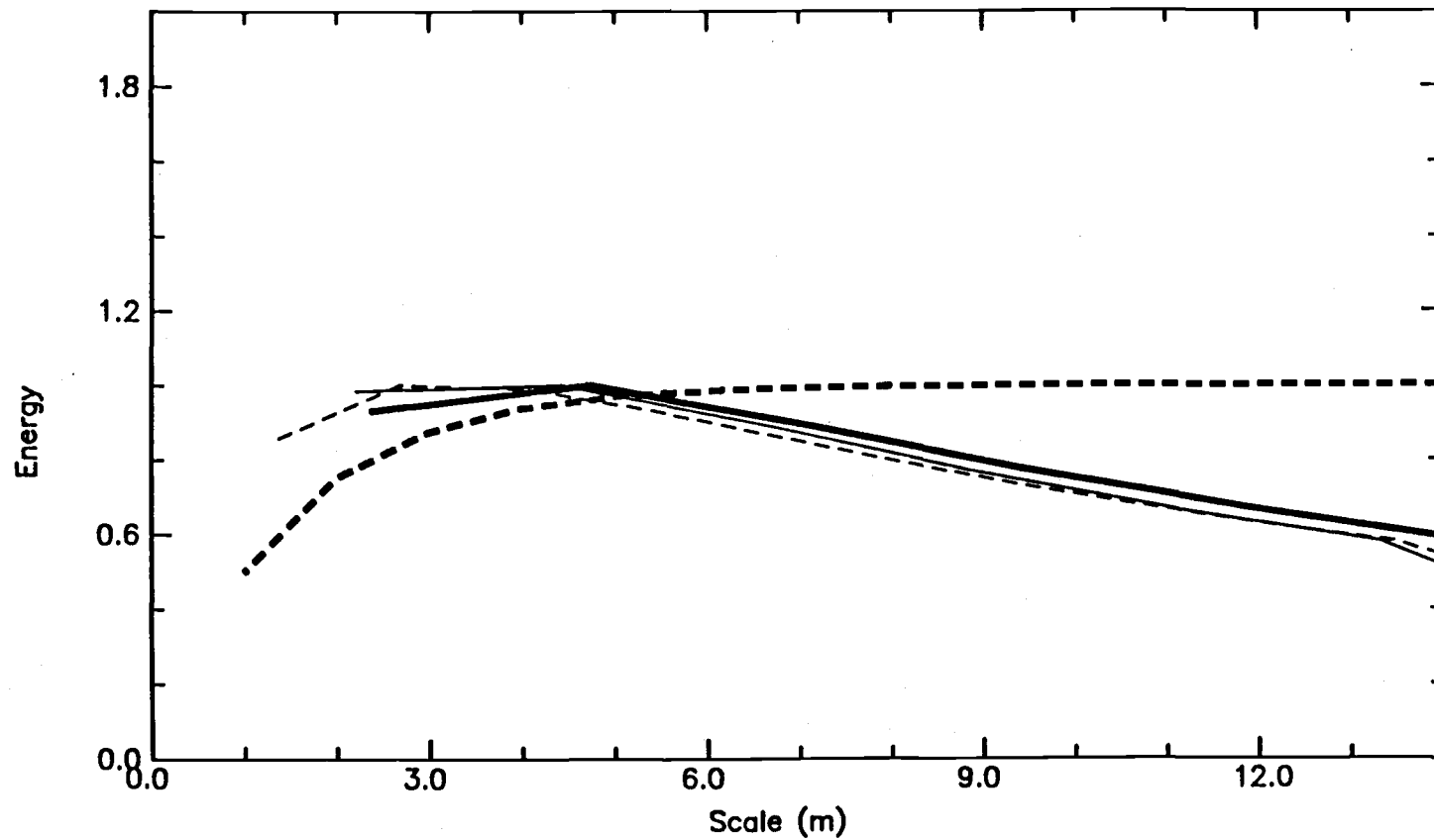


Figure 3.7 AR(1) process of parameter  $\alpha=0.5$ : wavelet variances (mexican hat (solid), Haar (heavy solid), french hat (dashed)) and semi-variogram (heavy dashed) responses.

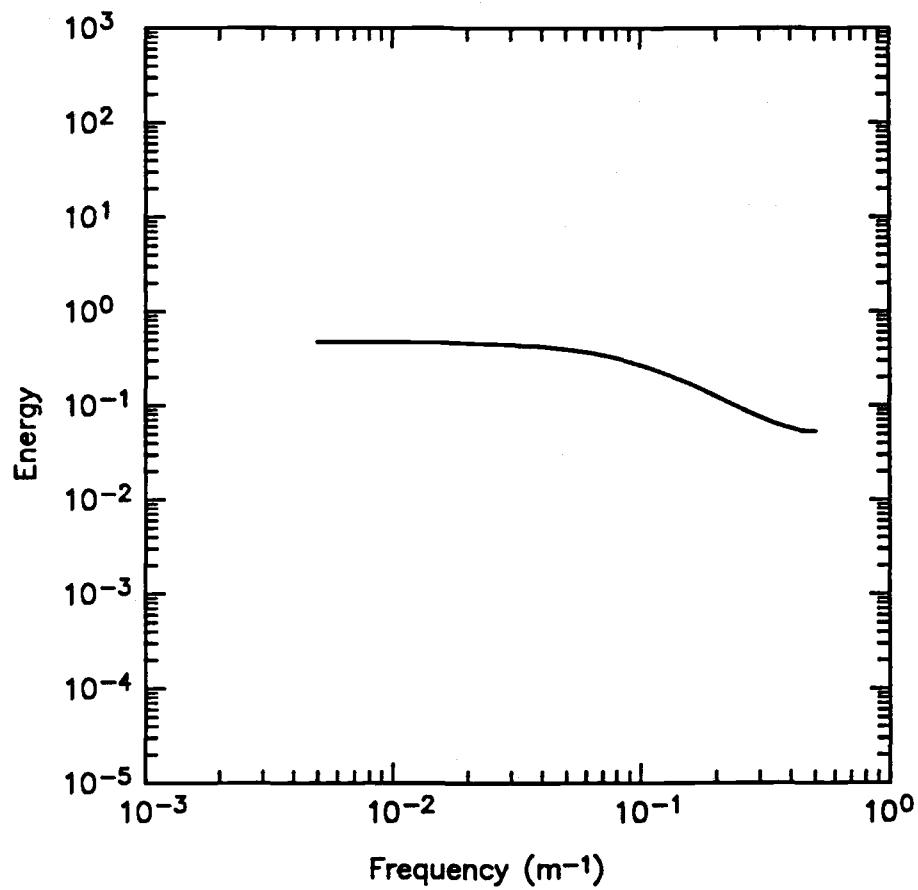


Figure 3.8 AR(1) process of parameter  $\alpha=0.5$ : power spectrum.

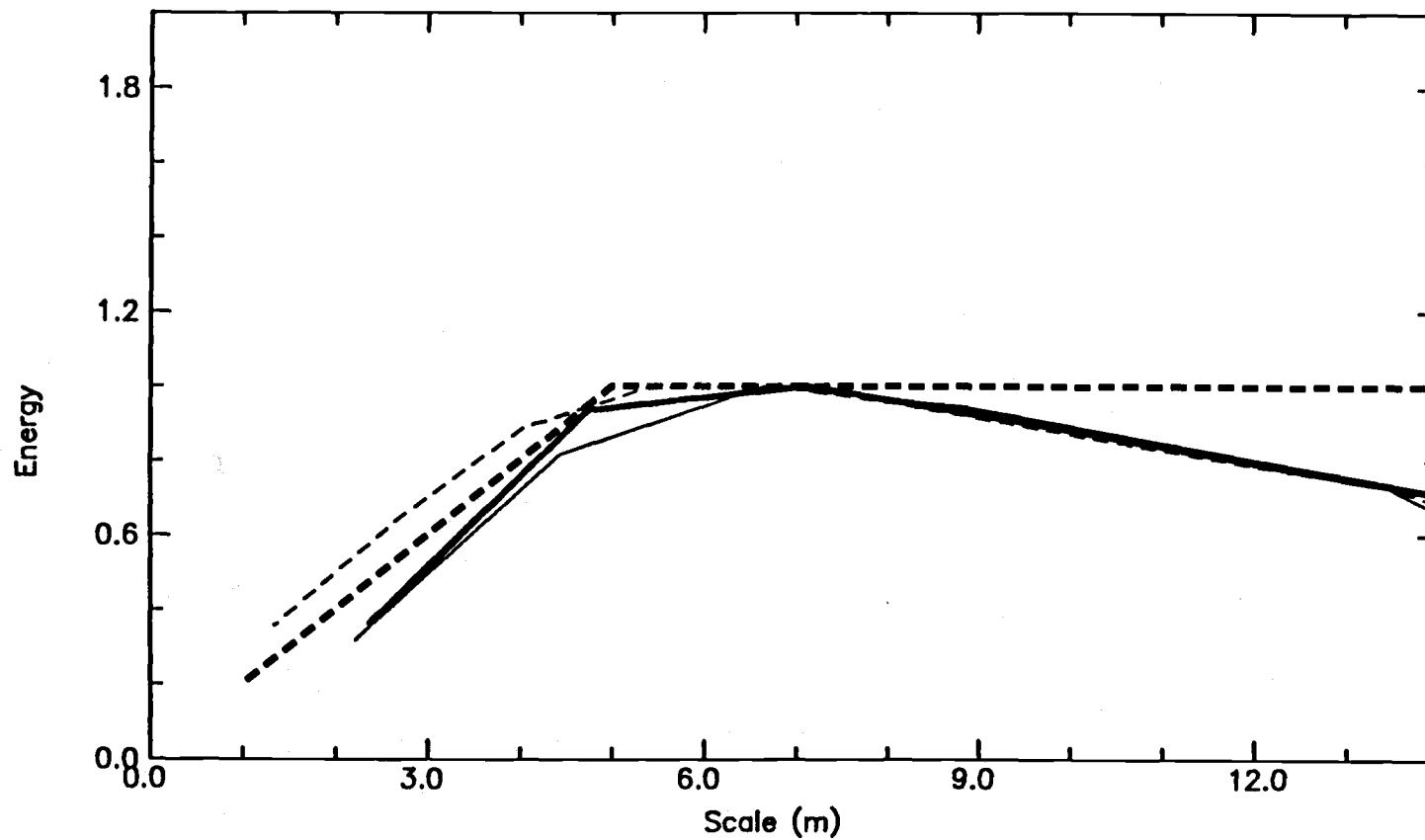


Figure 3.9 Additive moving average process of parameter  $m+1=5$ : wavelet variances (mexican hat (solid), Haar (heavy solid), french hat (dashed)) and semi-variogram (heavy dashed) responses.

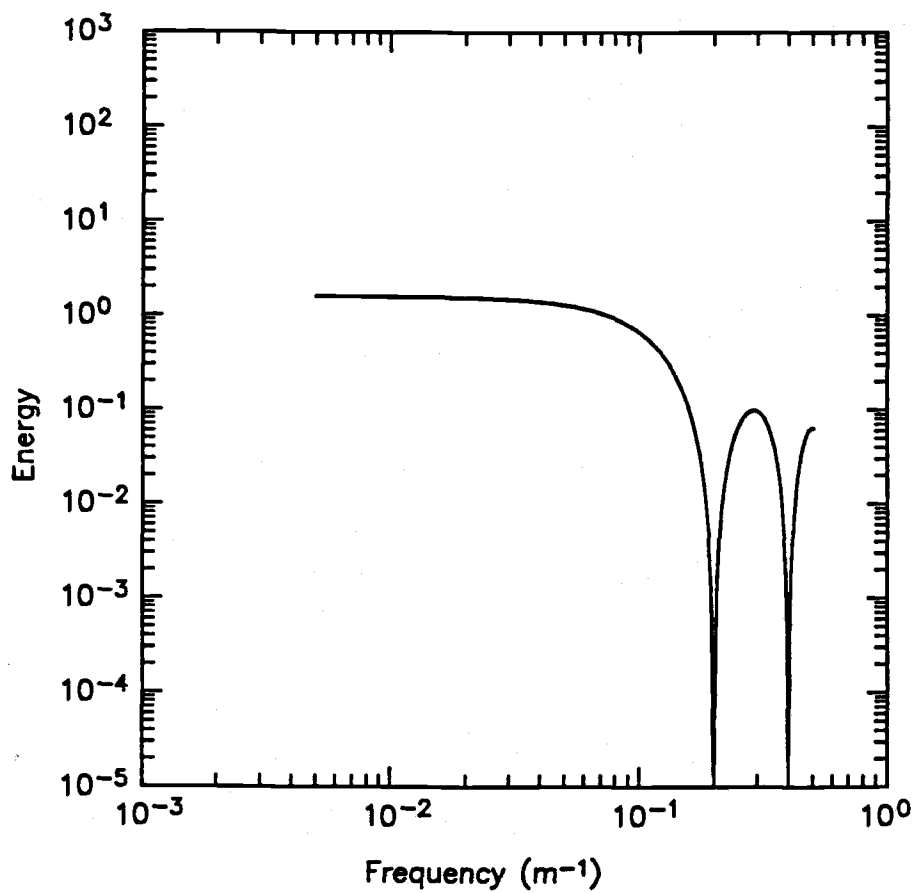
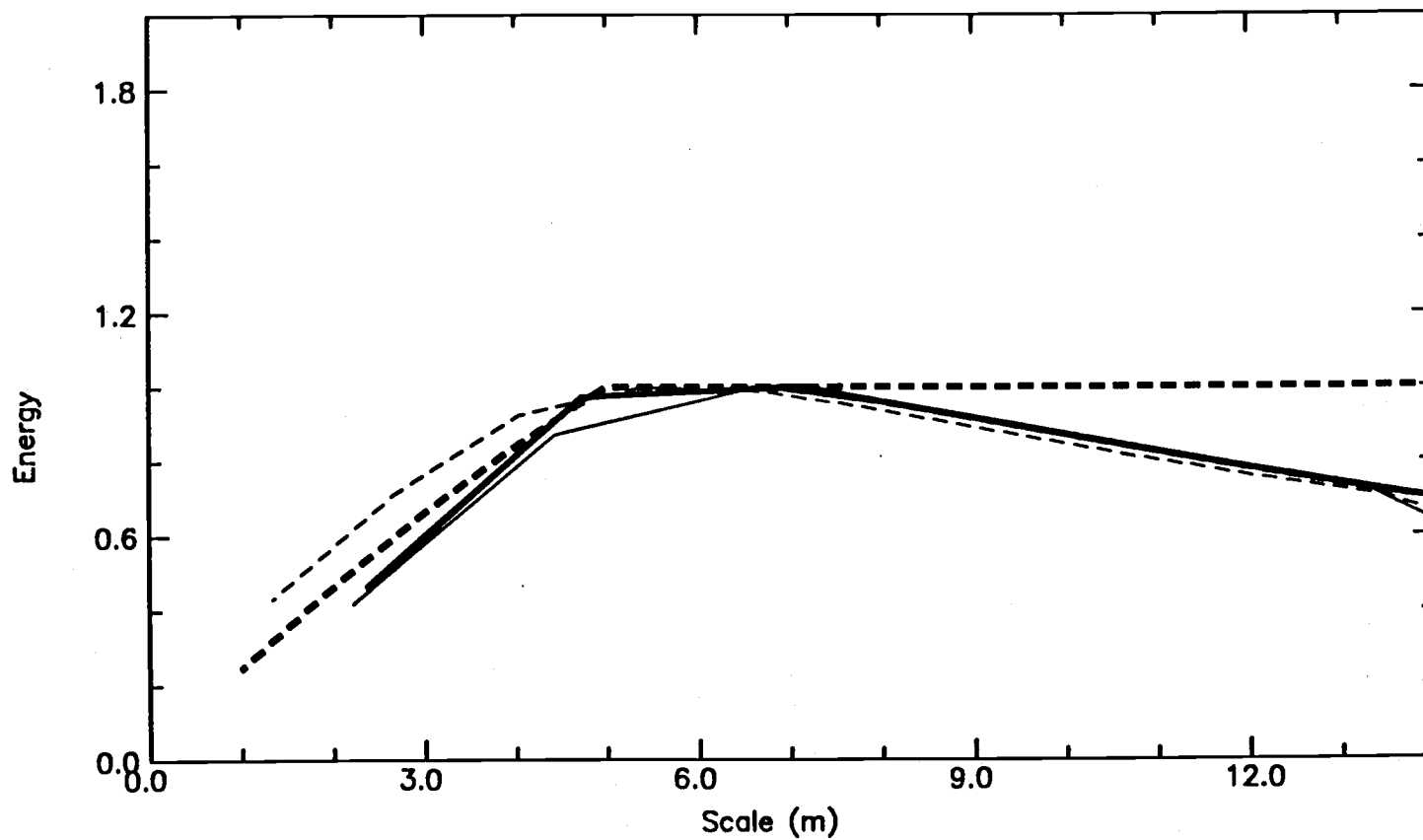


Figure 3.10 Additive moving average process of parameter  $m+1=5$ : power spectrum response.



**Figure 3.11** Non-additive moving average process of parameter  $m + 1=5$ : wavelet variances (mexican hat (solid), Haar (heavy solid), french hat (dashed)) and semi-variogram (heavy dashed) responses.

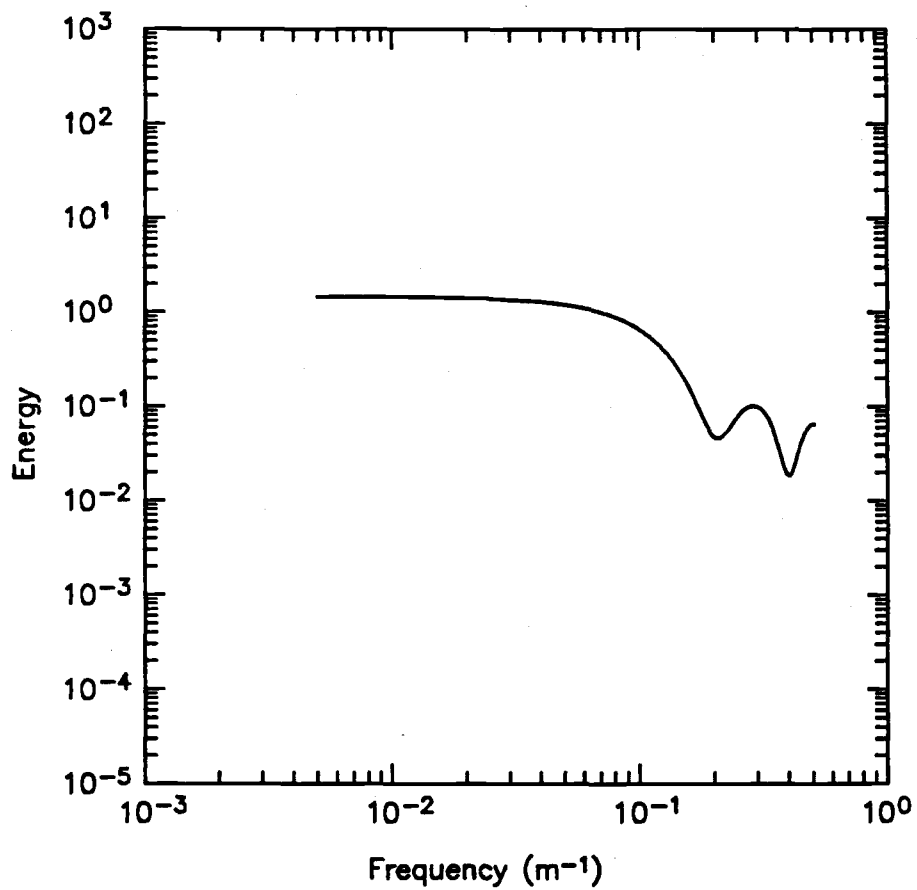
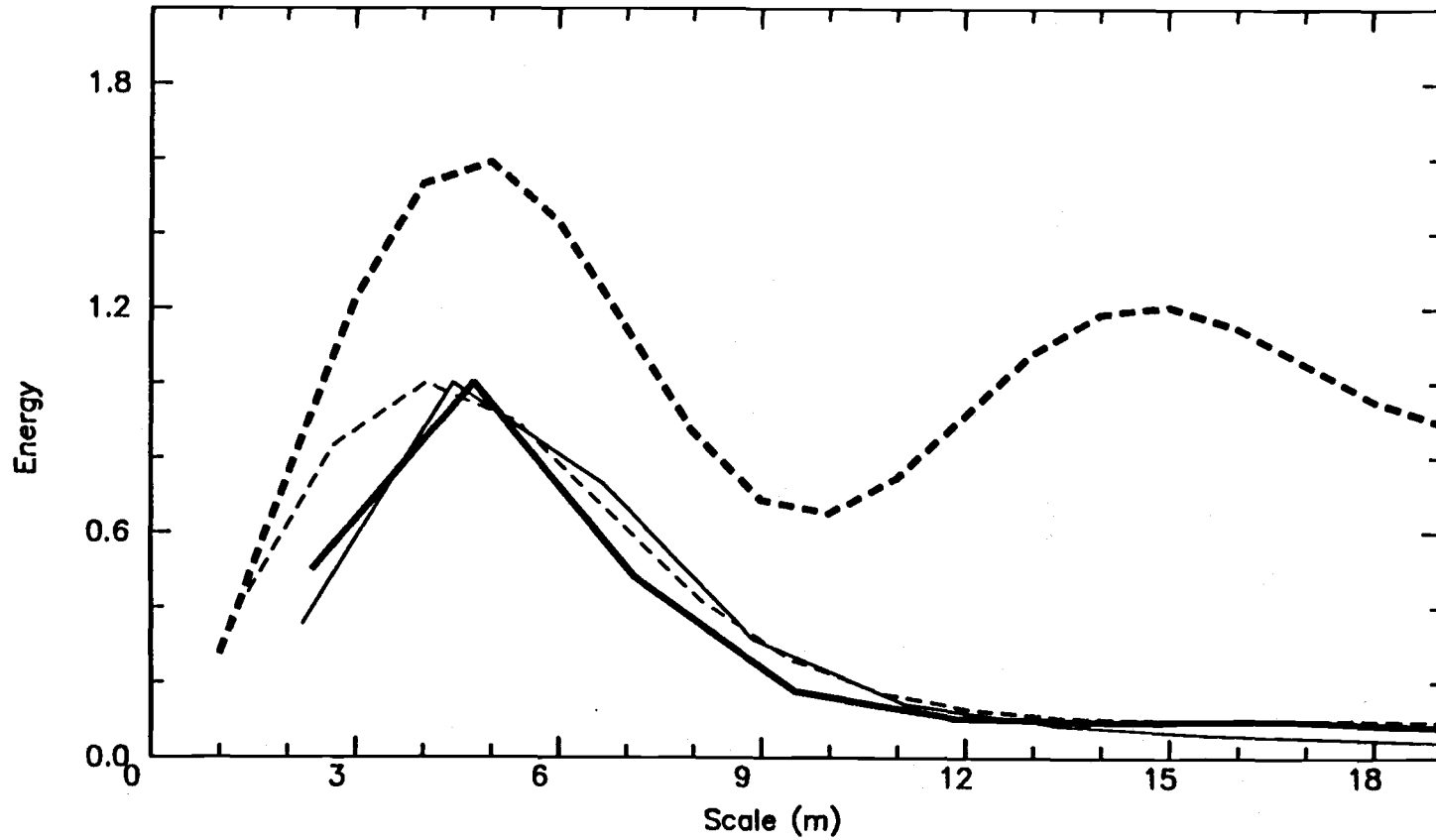


Figure 3.12 Non-additive moving average process of parameter  $m+1=5$  power spectrum.



**Figure 3.13** AR Harmonic process of parameter  $p=0.9$ , period=10 meters: wavelet variances (mexican hat (solid), Haar (heavy solid), french hat (dashed)) and semi-variogram (heavy dashed) responses.

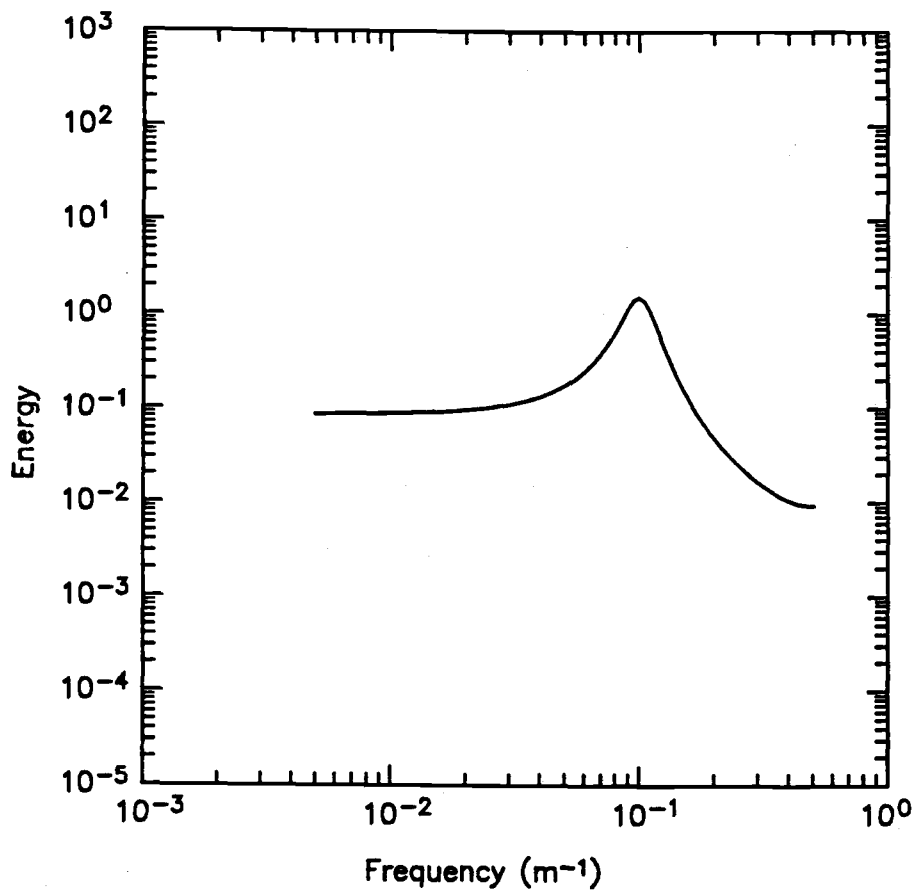
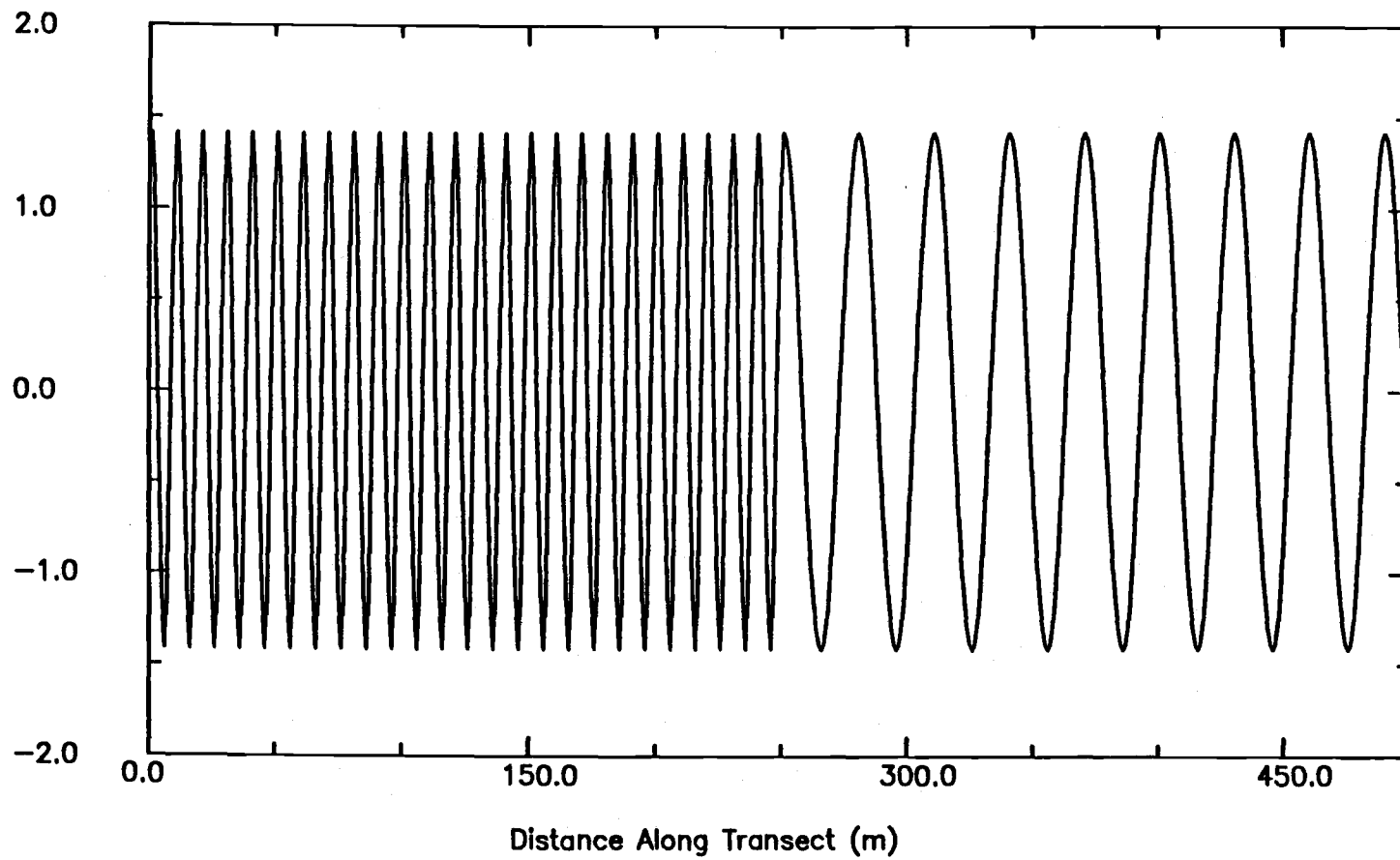


Figure 3.14 AR Harmonic process of parameter  $p=0.9$ , period=10 meters: power spectrum.



**Figure 3.15** Simulated data transect composed of two cosine functions of period 10 and 30 meters.

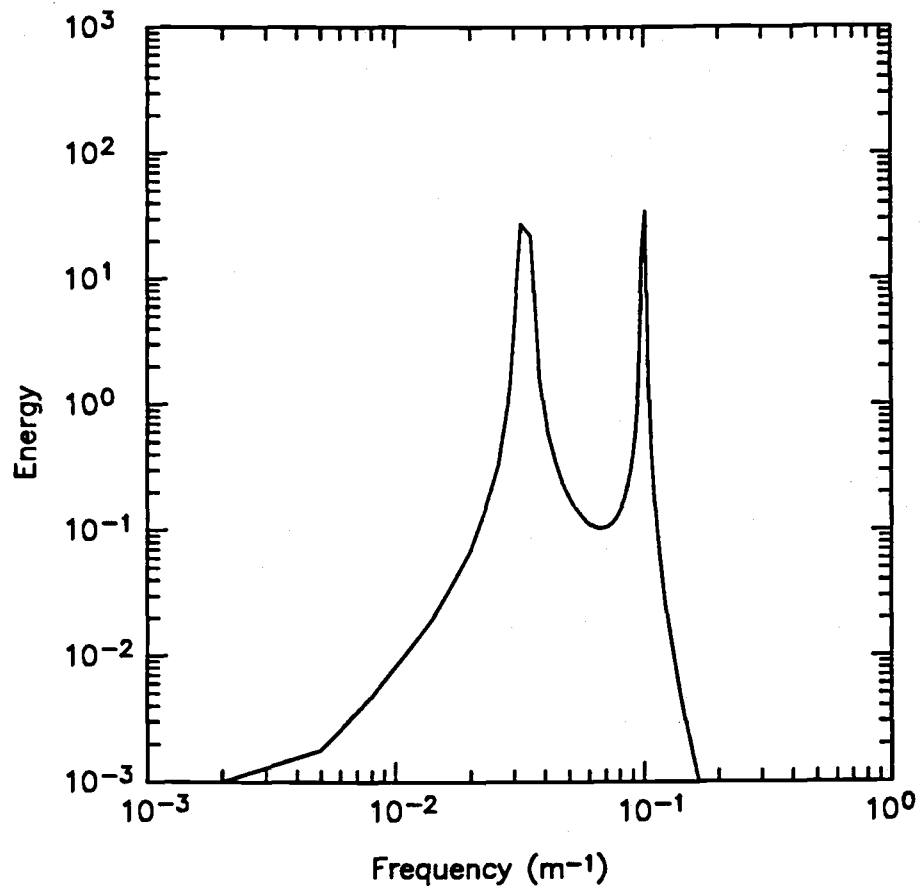


Figure 3.16 Power spectrum of transect in figure 3.15.

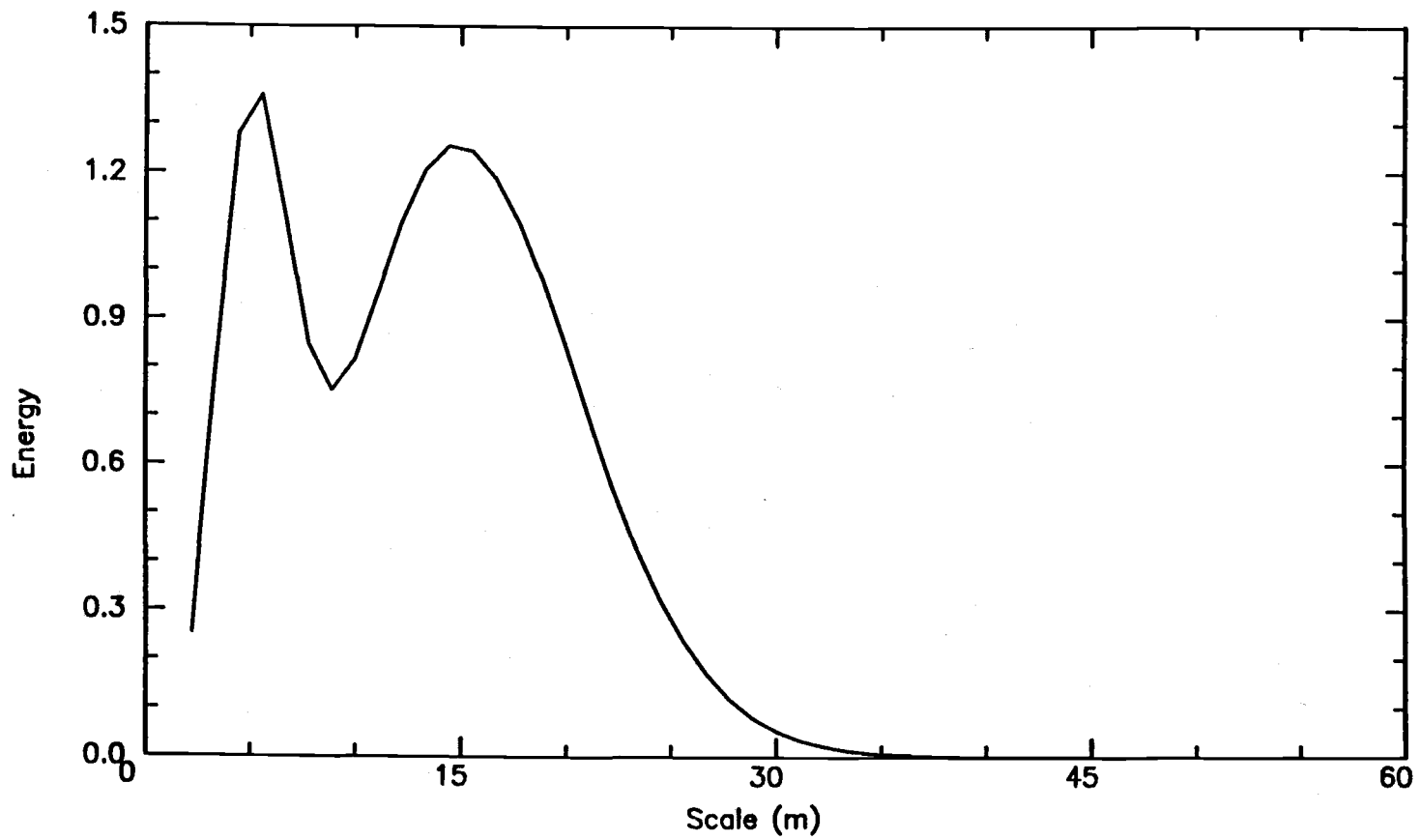
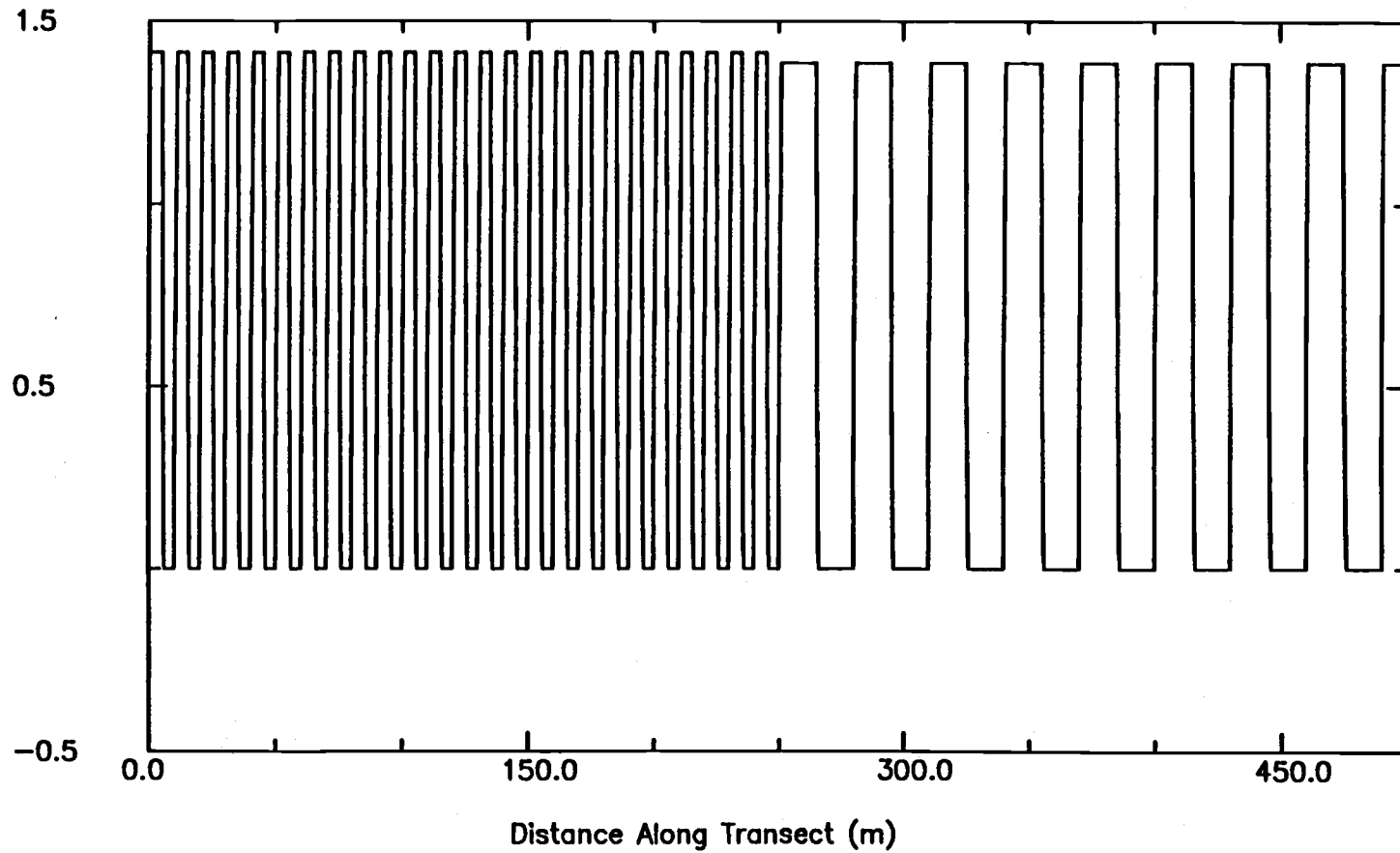


Figure 3.17 Wavelet variance for figure 3.15.



**Figure 3.18** Simulated data transect composed of two cosine functions of period 10 and 30 meters.

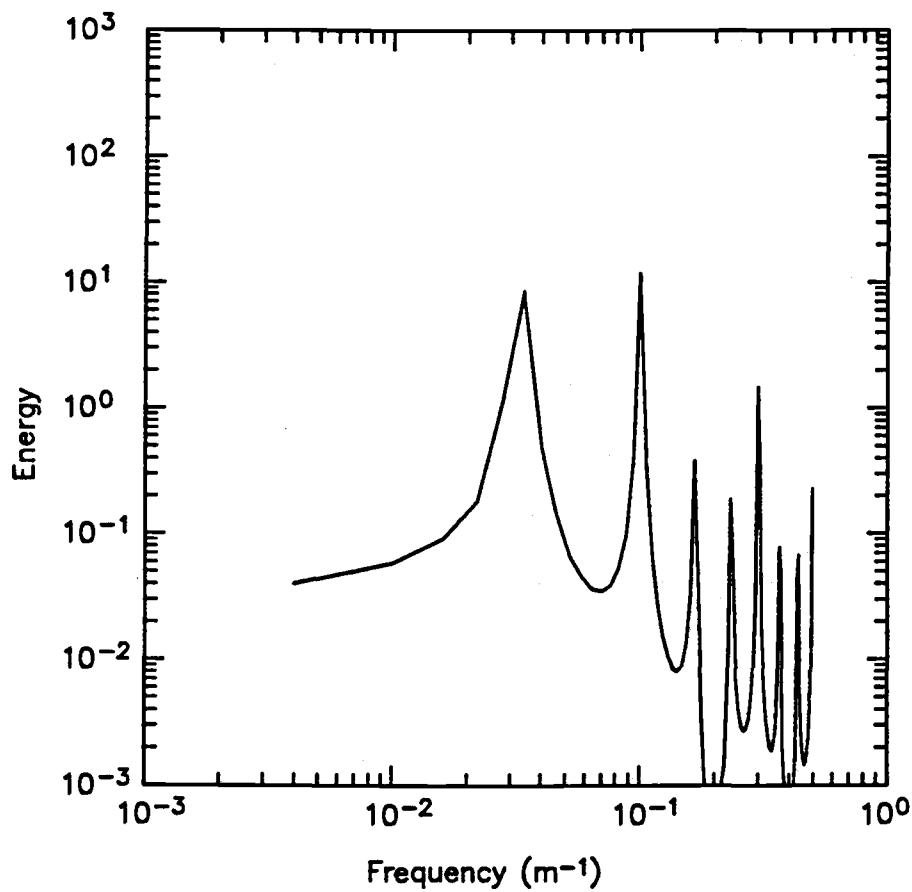


Figure 3.19 Power spectrum of transect in figure 3.18.

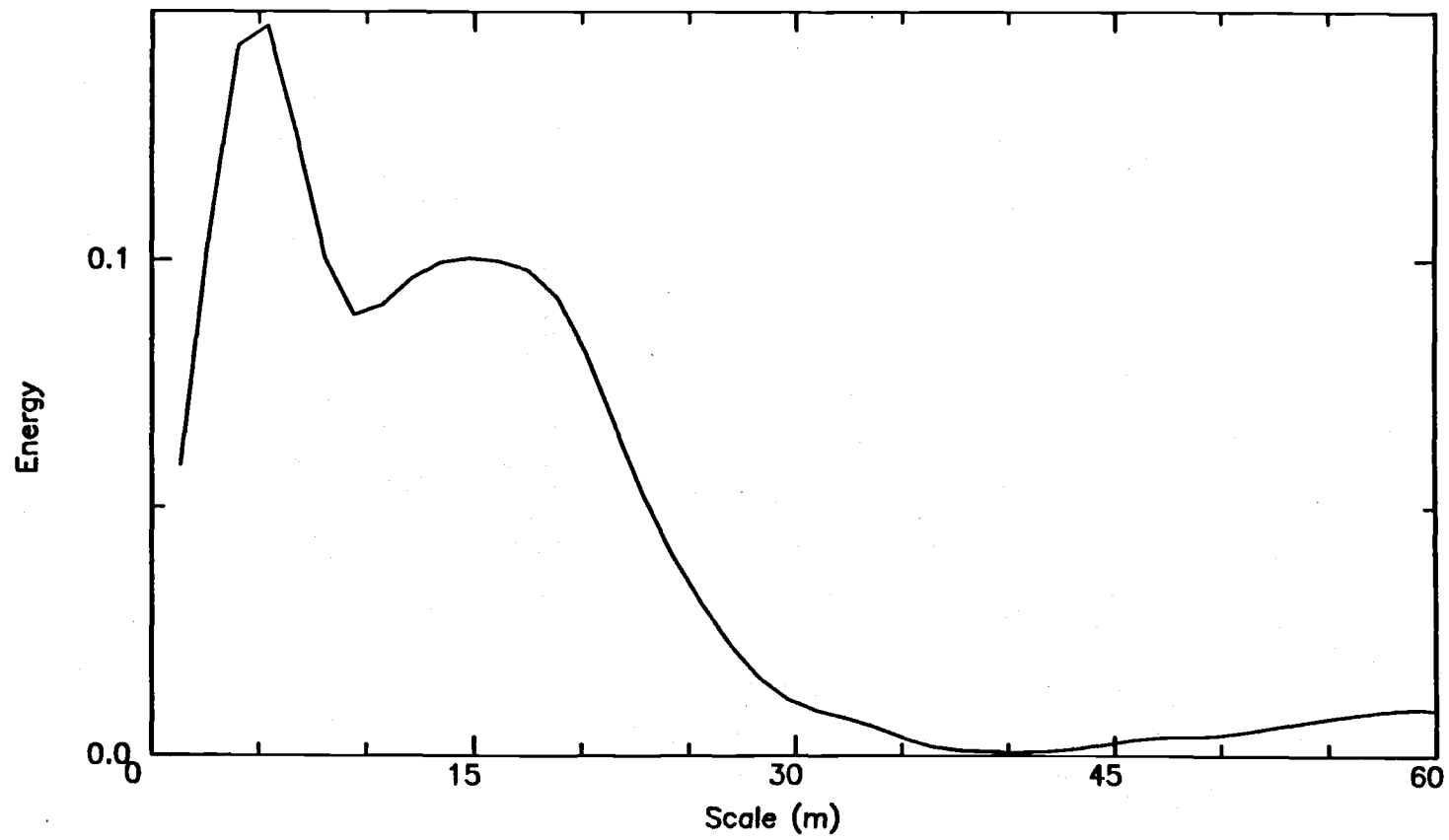


Figure 3.20 Wavelet variance for figure 3.18.

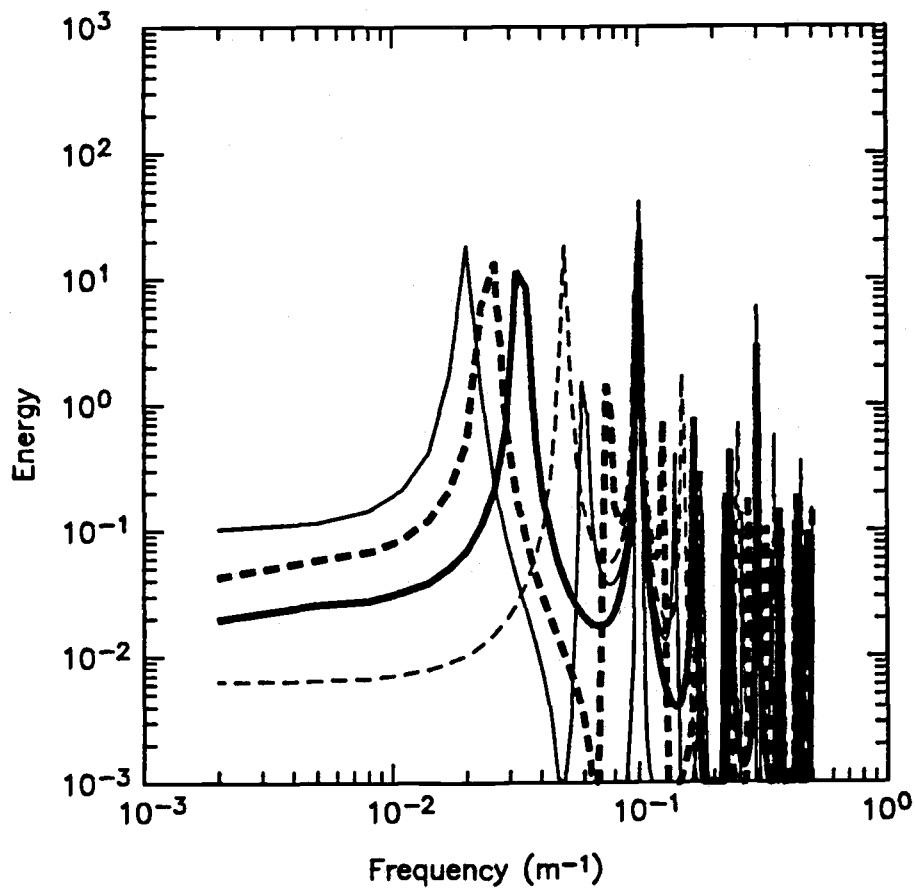


Figure 3.21 Power spectra for family of square waves of varying period ratios.: 1 (solid line), 2 (light dashed line), 3 (heavy solid line), 4 (heavy solid line).

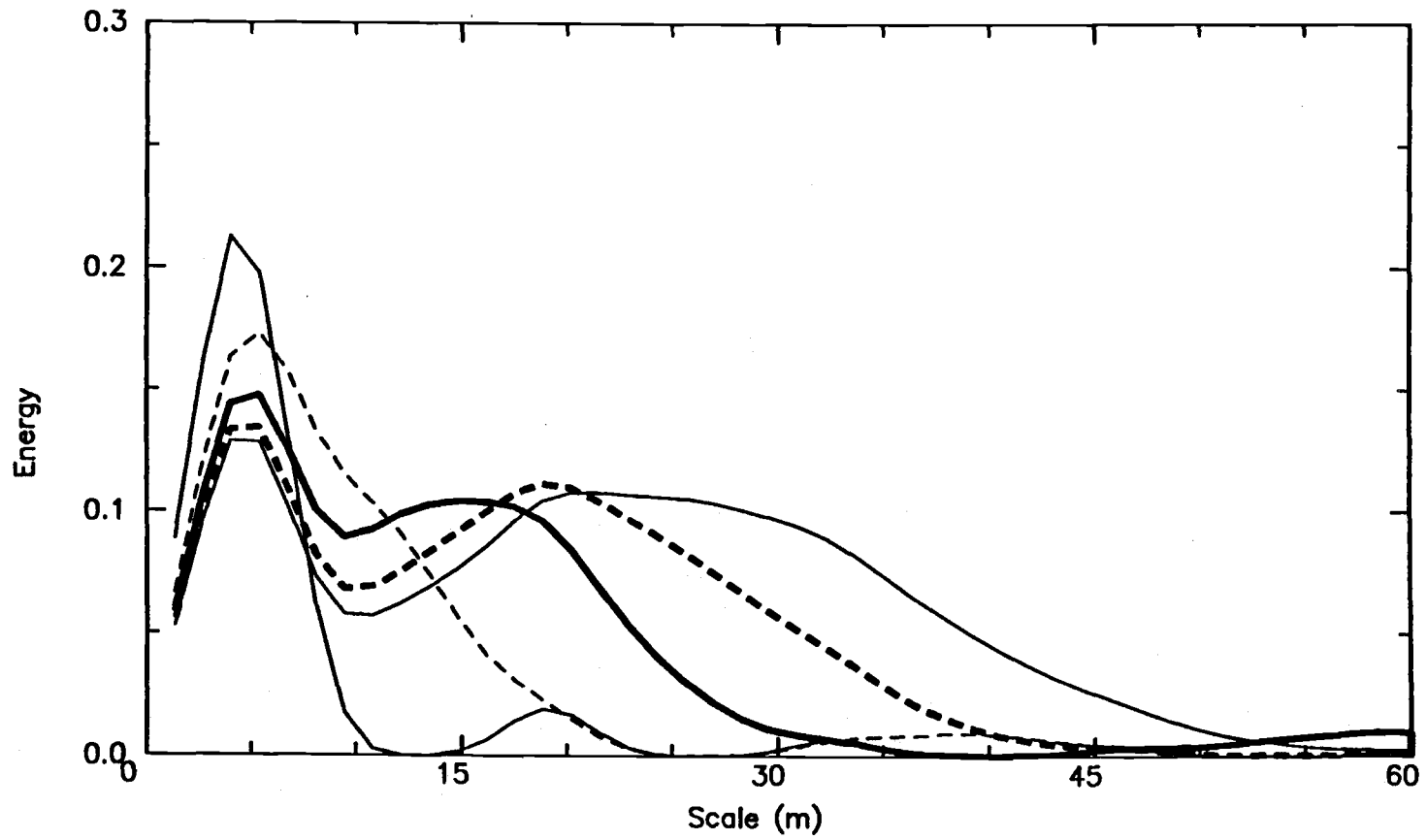


Figure 3.22 Haar wavelet variance for period ratios as described in figure 3.21 above.

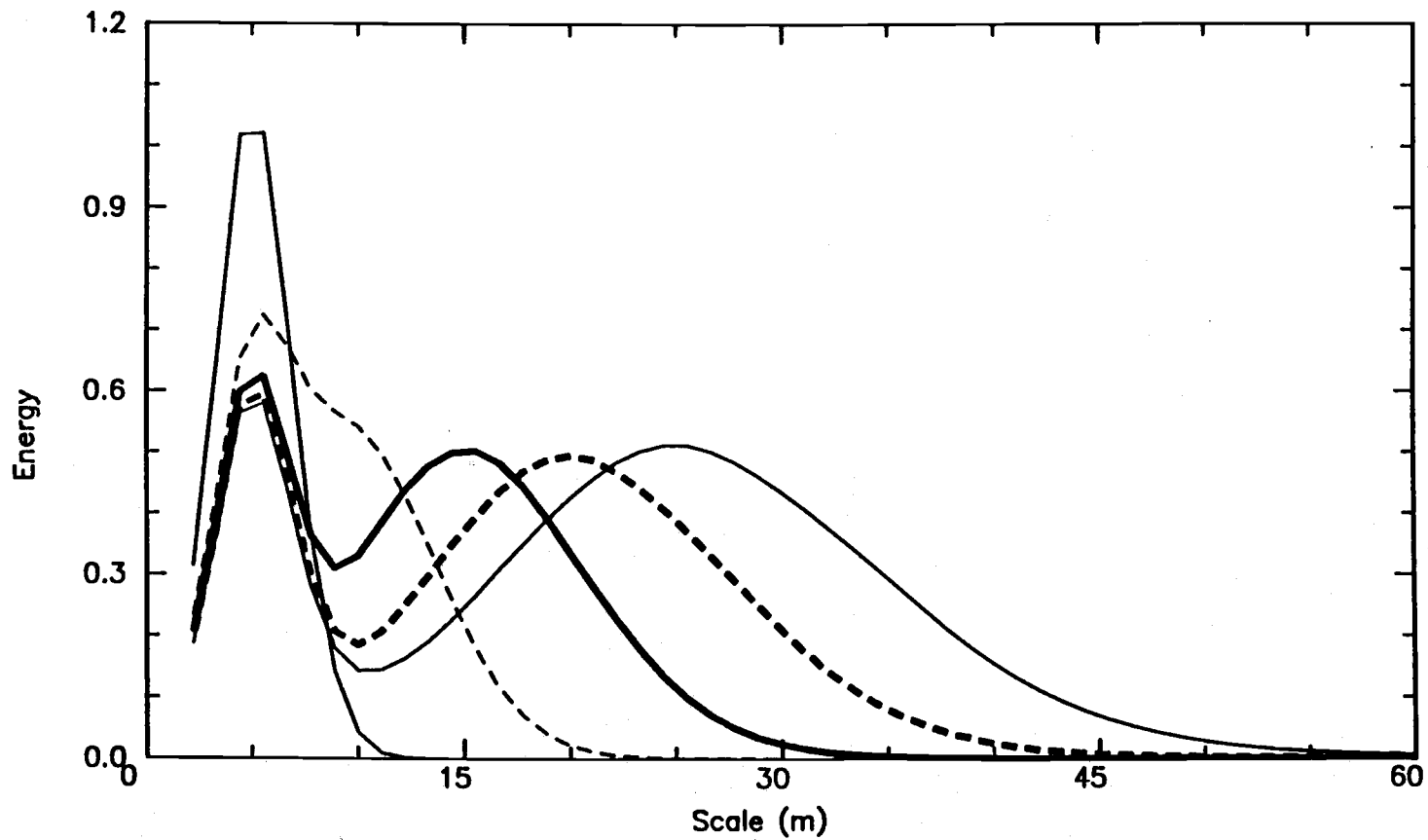
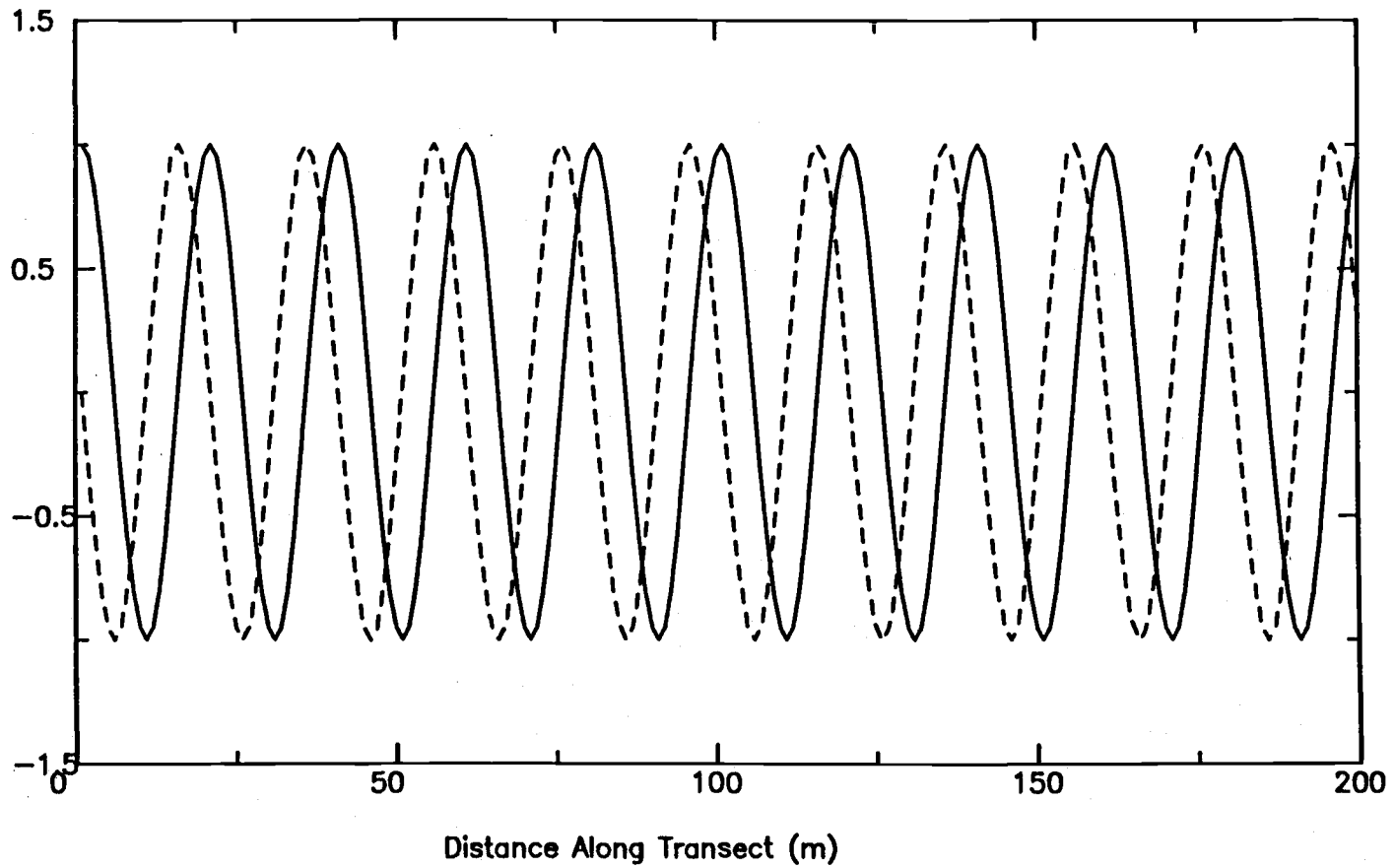


Figure 3.23 Mexican hat wavelet variance for period ratios as described in figure 3.21 above.



**Figure 3.24** Two cosine functions of period ten offset by five meters relative to each other.

Figure 3.25 Wavelet cross-covariance function for variables in figure 3.24. Grey-scale indicates correlation values. x-axis corresponds to lag (offset) between variables at which given correlation occurs. y-axis corresponds to the scale of correlation (meters).

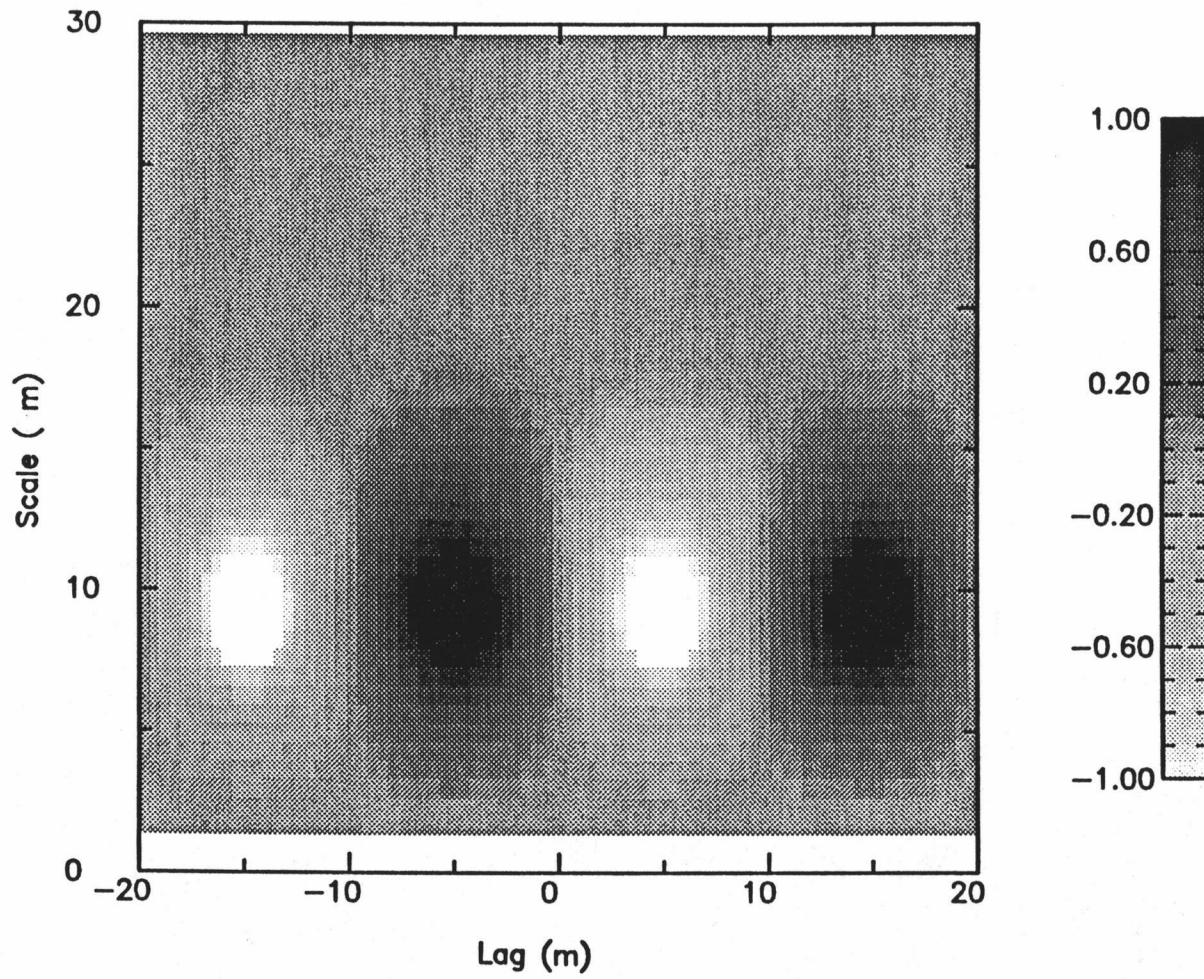


Figure 3.25

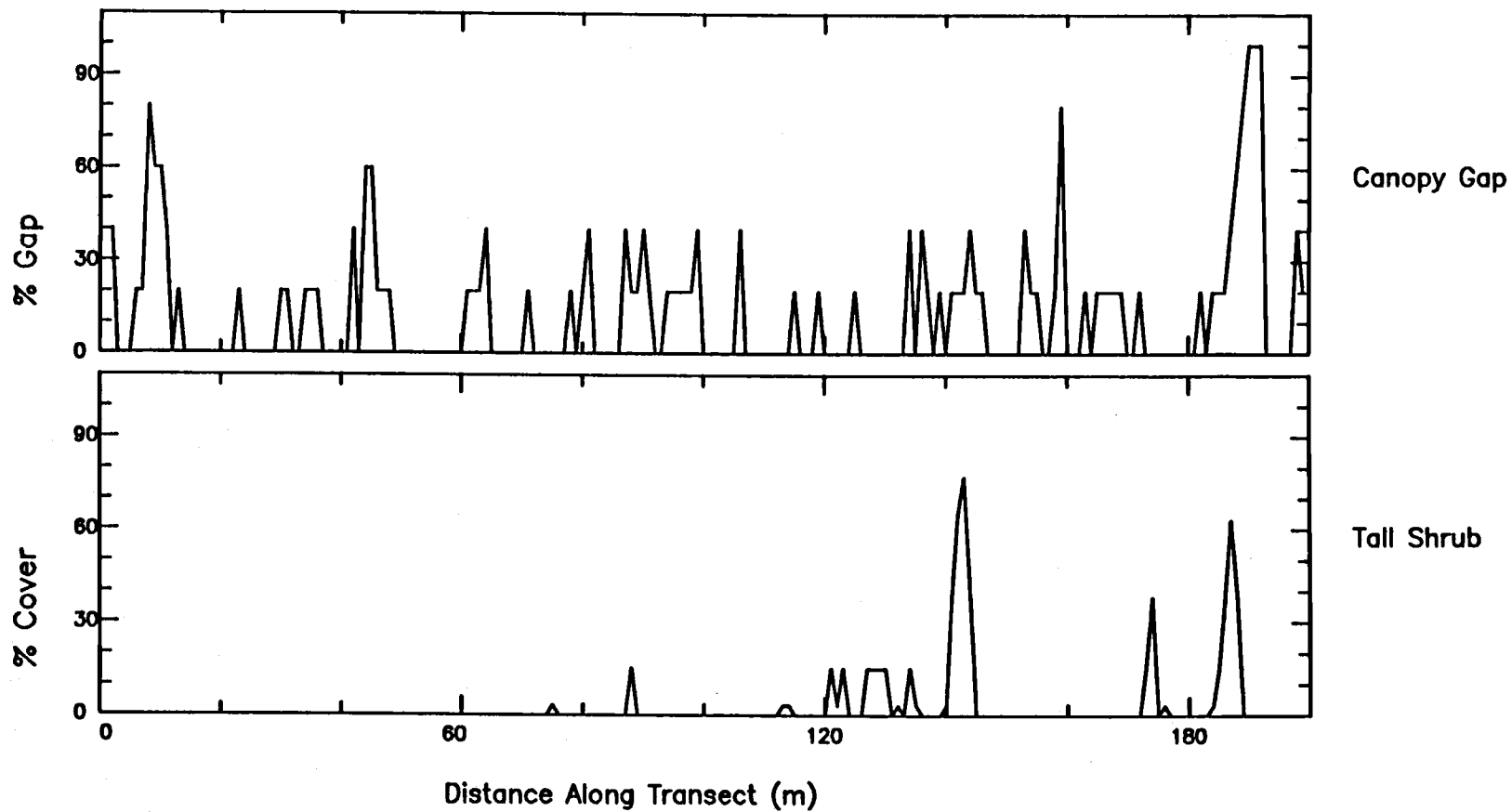
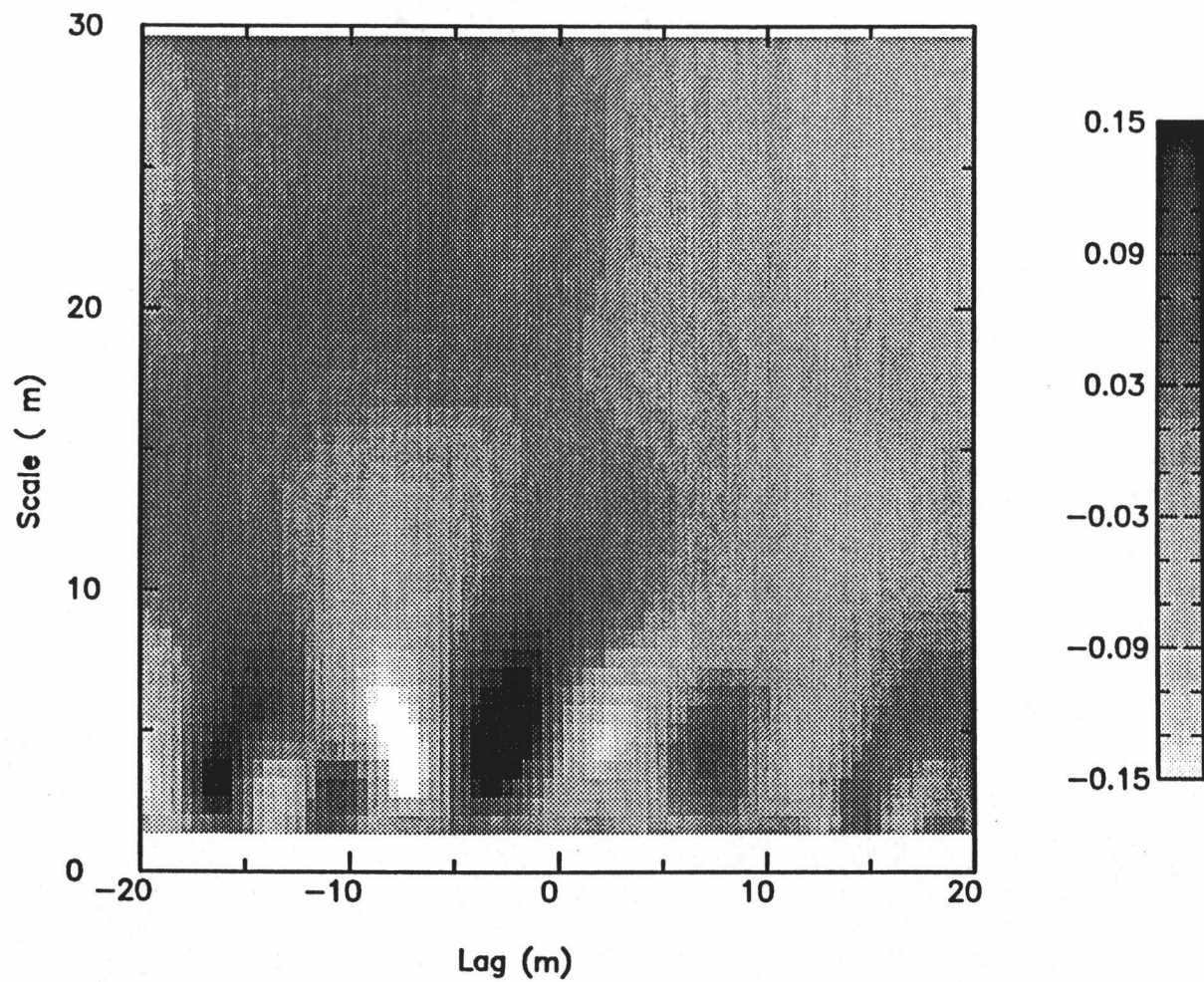


Figure 3.26 Transect of canopy gap (upper panel) and tall shrub (lower panel) data from the young Douglas-fir stand.



**Figure 3.27** Wavelet cross-covariance function for variables in figure 3.26.

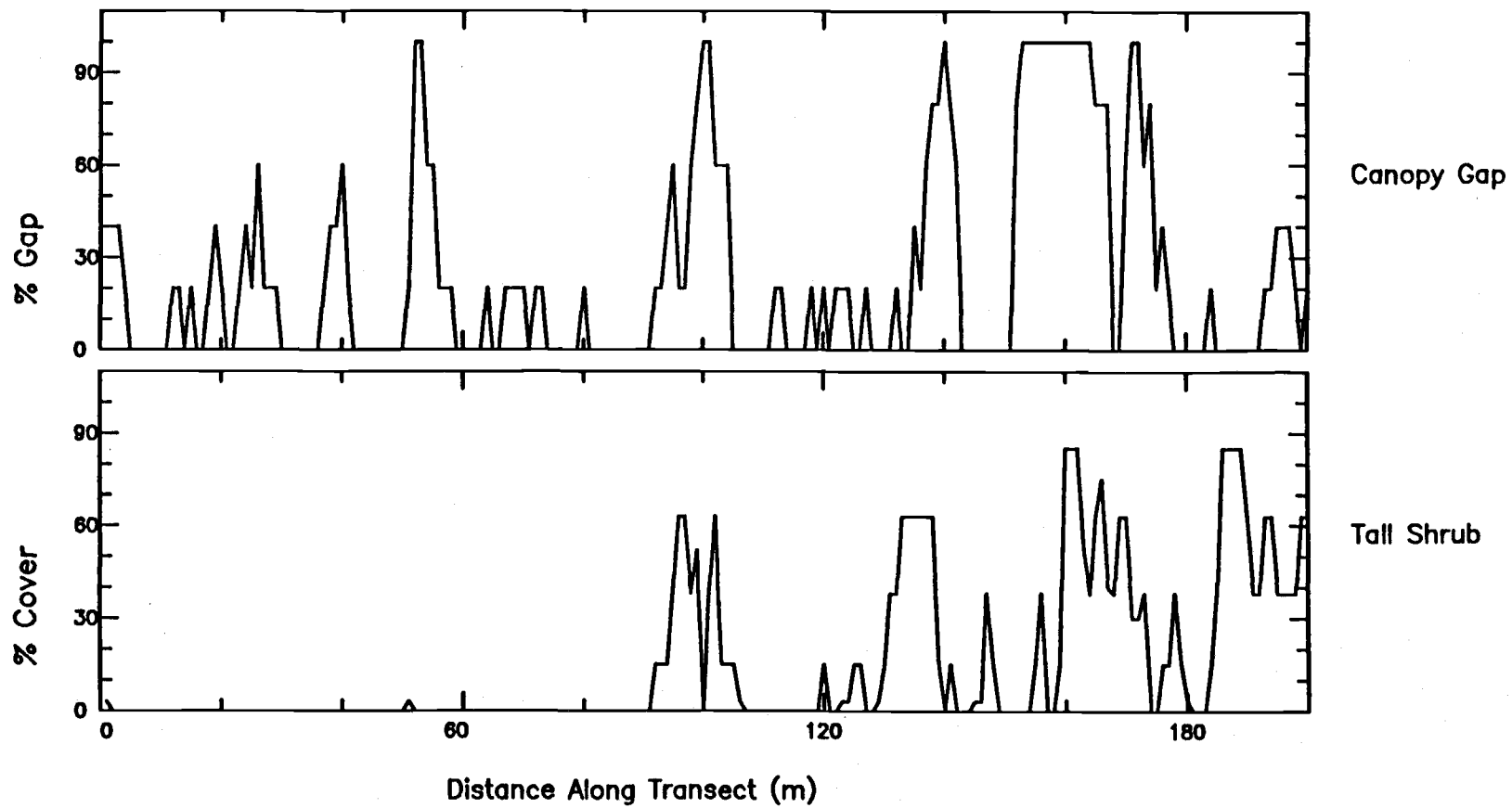
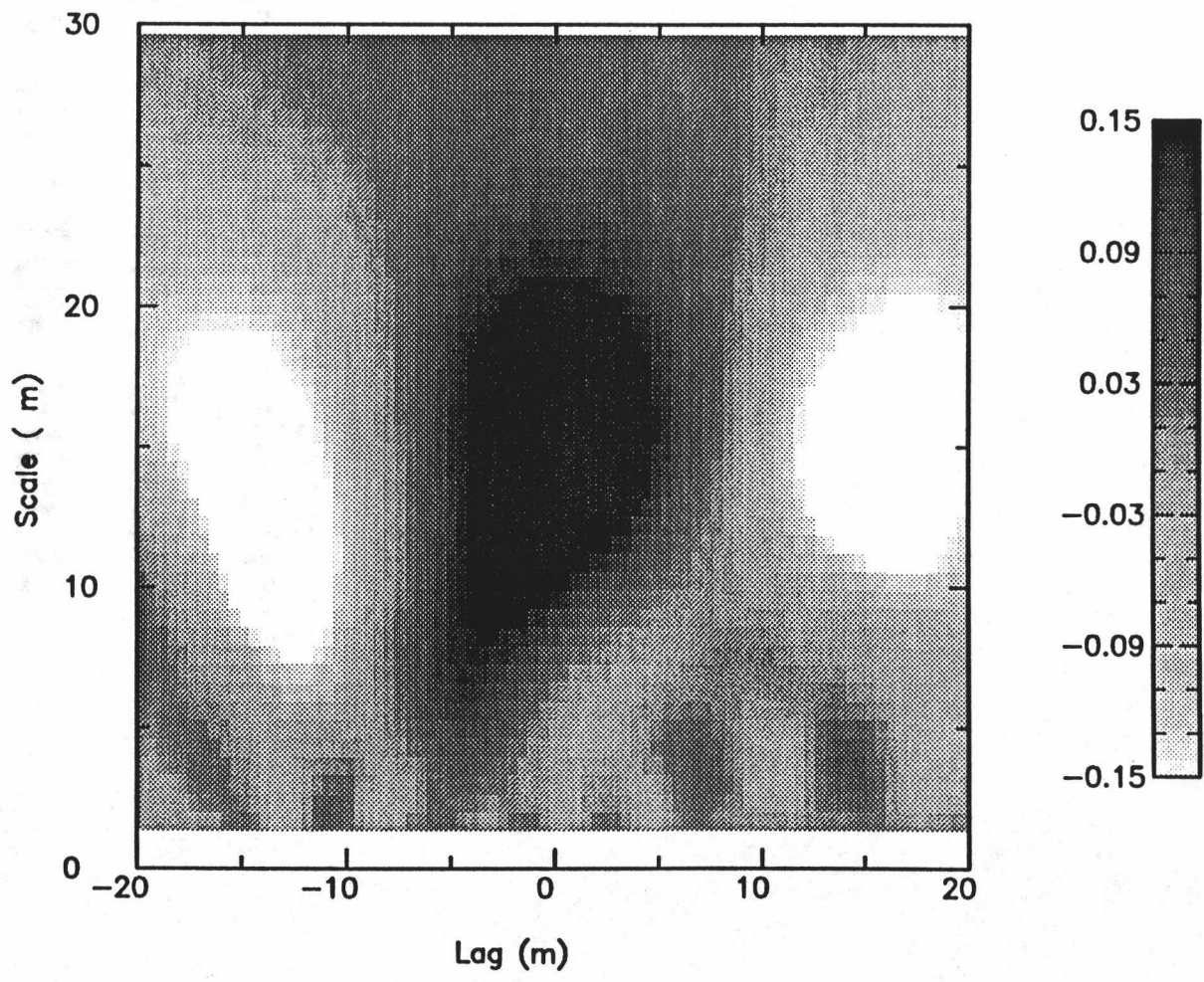


Figure 3.28 Transect of canopy gap (upper panel) and tall shrub (lower panel) data from the old-growth Douglas fir stand.



**Figure 3.29** Wavelet cross-covariance for variables in figure 3.28.

## LITERATURE CITED

- Argoul, F., A. Arneodo, G. Grasseau, Y. Gagne, E.J.  
Hopfinger, U.Frisch, 1989, "Wavelet analysis of  
turbulence reveals the multifractal nature of the  
Richardson cascade", Nature. 338: 51-53.
- Bracewell, R.N., 1978, The Fourier transform and its  
applications. McGraw Hill, New York, 444 pp.
- Carpenter, S.R. and J.E. Chaney, 1983, "Scale of pattern:  
four methods compared". Vegetatio 53: 153-160.
- Chatfield, C., 1989, "The analysis of time series: an  
introduction", 4th edition, Chapman and Hall. 241  
pp.
- Cohen, W, B., T.A. Spies and G.A. Bradshaw, 1990, "Semi-  
variograms of digital imagery of conifer canopy  
structure", Remote Sensing of the Environment.  
34: pp.167-178.
- Dale, M. R. T. and D.A. MacIssacs, 1989, "New methods for the  
analysis of spatial pattern in vegetation". Journal  
of Ecology. 77: 78-91.

- Daubechies, I, 1988, " Orthonormal bases of compactly supported wavelet. Communications of Pure and Applied Mathematics. 41: pp.909-996.
- Gamage, N.K.K., 1990, "Detection of coherent structures in shear induced turbulence using the wavelet transform methods". AMS Symposium on Turbulence and Diffusion, Roskilde, Danmark, April 1990.
- Grieg-Smith, P., 1964, "Quantitative Plant ecology". 2nd edition, Butterworth, London.
- Journel, A.G. and Ch. J. Huijbregts, 1978, Mining Geostatistics, Academic Press, 600 pp.
- Legendre, P. and M.-J. Fortin, 1989, " Spatial pattern and ecological analysis". Vegetatio 80: pp.108-138.
- Levin, D.A. and H.W. Kerster, 1971, "Neighborhood structure in plants under diverse reproductive methods". American Naturalist 105: pp. 345-354.
- Moloney, K.A., S.A. Levin, N.R. Chiariello, and L. Buttell, in review, "Pattern and Scale in a Serpentine Grassland." Moloney, K.A., A. Morin and S.A. Levin, in press, "Interpreting ecological patterns

generated through simple stochastic processes",  
Landscape Ecology.

Platt, T. and K.L. Denman, 1975, "Spectral analysis in ecology". Annual Reviews of Ecology and Systematics. 6: 189-210.

Powell, T. M., 1989, "Physical and biological scales of variability in lakes, estuaries, and the coastal ocean". in 'Perspectives in ecological theory', eds., J. Roughgarden, R.M. May, and S.A. Levin. Princeton University Press, 394 pp.

Priestley, M.B., 1981, "Spectral analysis and time series". (volumes 1 and 2), London, Academic Press.

Renshaw, E. and E.D. Ford, 1984, "The description of spatial pattern using two-dimensional spectral analysis". Vegetatio 56: 75-85.

Ripley, B.D., 1981, "Spatial Statistics". Wiley, New York.

Tucker, C.J., I. Y. Fung, C.D. Keeling, and R.H. Gammon, 1986, "Relationship between atmospheric CO<sub>2</sub> variations and a satellite-derived vegetation index". Nature. 319: pp.195-199.

## Chapter 4

**CHARACTERIZING FOREST CANOPY GAP STRUCTURE  
USING WAVELET ANALYSIS**

by

G.A. Bradshaw

and

T.A. Spies

**ABSTRACT**

The wavelet transform is introduced as a technique to identify spatial structure in transect data. Its main advantages over other methods of spatial analysis are its ability to preserve and display hierarchical information while allowing for pattern decomposition. Two applications are presented: one-dimensional simulations and a set of 200 m transect data of canopy opening measurements taken in twelve stands dominated by Pseudotsuga menziesii ranging over three developmental stages.

The calculation of the wavelet variance, derived from the transform, facilitates comparison based on dominant scale of pattern between multiple datasets such as the stands described. Results indicate that while canopy pattern trends follow stand development, small to intermediate disturbances

significantly influence canopy structure.

## INTRODUCTION

Many ecological studies use data collected along transects to examine the spatial characteristics of biotic or abiotic variables. An important objective of such studies is the quantification of the spatial and temporal pattern of the variable of interest, e.g. the structural heterogeneity of forest vegetation at the landscape and within-patch scales.

Fourier spectral analysis has been successfully applied to characterise periodic behaviour in both temporal and spatial data (Platt & Denman 1975; Ford & Renshaw 1984; Kenkel 1988). Although there are many ecological processes which resemble a sine or cosine function in structure, vegetation pattern can appear to be a mixture of periodic and aperiodic components. Such a pattern often occurs where there have been several processes at work over time (e.g. disturbance, establishment and competition) or where the dominant processes or events vary in scale (e.g. changes in topography and microclimate along a biogeographical gradient). As a result, the description of the composite signal and the identification of a specific sub-pattern can be quite difficult. Because it assumes that a periodic pattern occurs uniformly across the data, Fourier spectral analysis may not always be the most appropriate technique to detect non-uniform pattern in the data (i.e. irregular features or non-stationarity in the data; Priestley 1981). A

technique which can accommodate non-uniformity or non-stationarity in the data is desirable for application to ecological data.

A second method, related to spectral analysis, is variography. The principal tool of variography, the semi-variogram, is a graphical representation of the spatial variability of the data and is linearly related to the autocorrelation function (Journel & Huijbregts, 1977). Both are measures of spatial correlation as a function of the distance between two points. Like Fourier spectral analysis, the semi-variogram provides information on the global average of structure in the data. While it excels in the description of an average structural dimension, the semi-variogram has limited capabilities for the detection of local features deviating from the mean (Cohen, Spies and Bradshaw 1990). The interpretation of the semi-variogram becomes difficult when multi-scale structure in the data is encountered.

In this paper, we present a technique known as the wavelet transform which can be used to quantify spatial structure as a function of scale and position along a one-dimensional transect (Daubechies 1988). The wavelet transform has three main advantages over previous methods: (i) it acts as a local filter, the dimensions of which do not need to be specified a priori, (ii) the magnitude of the signal can be directly related to position along the transect, and (iii) the analysing wavelet may be chosen to suit the given data

form and study objectives. By comparison of the resultant transform at discrete spatial scales, the size, location, magnitude and number of various components of pattern along the transect can be identified. Because position is retained after the analysis, individual and sets of individual events may be related to higher-order pattern, thereby elucidating hierarchical structure. This scale-by-scale analysis is suited for the detection of local features of aperiodic data which may be overlooked by other methods such as Fourier spectral analysis. Unlike the semi-variogram and other stochastically based methods, the wavelet transform does not require stationarity of the data. (A data set may be considered non-stationary if the statistical properties of the data change with location; for example, in the case where the mean changes with distance along the transect.) Because it preserves locational information while effecting a scale-by-scale decomposition of the data into separate spatial components, the wavelet transform may serve as a useful addition to the more commonly used spatial methods such as Fourier spectral analysis, autocorrelation function analysis, and variography.

A quantity derived from wavelet analysis, the wavelet variance, is discussed as a means by which the dominant mean scales (i.e. patch size or scale of features) of the data are determined. The efficacy of the wavelet transform employed for the purposes of spatial discrimination is illustrated

with two simulated transects and canopy gap data collected from twelve coniferous forest stands located in the Cascade Mountains of Oregon and Washington, U.S.A.

## WAVELET ANALYSIS

### Wavelet Transform

The wavelet transform is a collection of convolutions of the data function,  $f(x_i)$ , (where  $x_i$  is distance along the transect) with a windowing function (or "wavelet")  $g(x/a)$  for a given range of scales,  $a$ , centred at locations  $x_j$  along the transect. It is defined in the discrete case as:

$$W(a, x_j) = \frac{1}{a} \sum_{i=1}^n f(x_i) g\left(\frac{x_i - x_j}{a}\right)$$

One may visualize the analysing wavelet as a window of a fixed dimension,  $a$ , which moves along the data transect as  $x_j$  varies. When the wavelet encounters a feature in the data with a like shape and dimension, the absolute value of the transform is high. There are several possible choices for the wavelet function given that certain admissibility requirements are met (Daubechies, Grossman & Meyer 1986; Mallat 1988). Two analysing wavelets are considered here: the Mexican Hat and the Haar (Daubechies 1988). The Mexican Hat function has been chosen such that the range of the function spans  $[-4, 4]$  when  $a$  is taken to equal one and  $g(x)$  is centred at zero (Figure 4.1):

$$g(x) = \frac{2}{\sqrt{3}} \pi^{-\frac{1}{4}} (1-4x^2) \exp\left(-\frac{4x^2}{2}\right)$$

The Mexican Hat function is an appropriate function to use for revealing patterns in the data characterized by peak and trough events that have symmetric shapes similar to the Mexican Hat wavelet. In contrast, the Haar analysing wavelet, given its semblance to a step function has been found useful in the detection of edges and gradients (Figure 4.1; Gamage 1990). As illustrated below in the first example, each wavelet will provide a slightly different perspective on the data. The appropriate choice of the specific wavelet will, therefore, depend on several factors: the structure of the data, the goals of the analysis, and computational considerations.

### **Simulated Example**

A simple example was simulated to illustrate the type of information the wavelet transform may provide for the analysis of transect data. A canopy transect characterized by a series of 10-m gaps was generated (Figure 4.2). The transect represents a schematic simplification of forest canopy-gap structure where the function  $f(x_i)$  corresponds to percent canopy opening and  $x_i$  are points along the transect at

1-m intervals. In this example, the forest canopy is composed of 10-m wide patches of relatively open gaps alternating with relatively closed, 10-meter wide closed canopy segments superimposed onto a step-function. While the overall "gap" structure remains consistent across the transect, the data are non-stationary, i.e. the mean is not constant due to the step-function trend. The first half of the data is centred at 5 % gap opening while the second half of the data is translated and centred at 25 % gap opening. This difference in gap intensities between the first and second halves of the data might represent the result of a non-uniform disturbance which has affected only one portion of the transect. Thus, the overall pattern can be viewed as the sum of two scales of pattern resulting from two separate processes.

The wavelet transform calculated from the simulated transect data using the Haar wavelet detects the periodic pattern (Figure 4.3). The 10-m half-period is evinced by the regular series of alternating white (troughs) and grey (peaks) features along the transect centred at the scale of 10 m. The presence of the step-function trend is reflected in the dark, diffuse band centred at 100 m. The extreme values of the transform occurs at 10 meters, i.e. the approximate width of the "canopy gaps". Note that  $W(a, x_j)$  is calculated only for a certain portion of the transect at each scale. This truncation is performed so that the wavelet transform is calculated only at points where the span of the analysing

wavelet is contained within the range of the data. The length of transect available for analysis decreases with a corresponding increase in the size of the analysing wavelet and scale.

The transform is also calculated using the Mexican Hat for the same transect shown in Fig. 4.2 (Figure 4.4). The Mexican Hat transform of the simulated data is similar to the Haar transform with the exception of the response to the step-function trend. The Mexican Hat detects the asymmetry of the "step" as reflected in the juxtaposition of a white to dark grey band. A second difference between the two transforms is that the length of the transect resolved by the Mexican Hat is less than that of the Haar wavelet; the Mexican Hat requires a greater span for a given scale than that of the Haar. This loss in resolution of larger features may be quite significant at times and thereby influence the choice of analysing wavelet.

### **Wavelet Variance**

Because the wavelet transform is a function of both scale and location, the interpretation of the resultant two-dimensional transform may be quite difficult for complex patterns. One way to facilitate analysis and comparison between data sets is to calculate the wavelet variance function:

$$V(a) = \frac{1}{n} \sum_{j=1}^n W^2(a, x_j)$$

where  $n$  is defined as the length of the data vector (Gamage 1990). The wavelet variance is simply the average of the squares of the wavelet coefficients at every point along the transect for a given scale,  $a$ . The variance is a function of the scale, number and relative magnitudes of the features comprising the data. Higher values of the variance at a given scale reflect the presence of a greater number of peaks and/or greater intensity of the signal at the given scale. In this case, the intensity is proportional to percent canopy opening. Scales where large values of wavelet variance are centred correspond to scales in the data which strongly dominate the overall pattern.

If a transect characterized by two scales of nested pattern is generated (i.e. individual 4-m wide peaks cluster to form larger 20-m events alternating with solid 20-m wide peaks; Figure 4.5), a more complex wavelet transform results (Figure 4.6). The transform preserves both the nested and simple structure in the data; the wavelet transform locally identifies the single 4-meter wide peaks within a larger 20-m wide event. This appears in the wavelet transform as a series of small, single events arrayed across the transect lying directly beneath the larger-scaled 20-meter peaks on the wavelet transform. This wavelet transform has the appearance

of nested folds. The hierarchical structure is more easily observed if the figure is viewed nearly parallel to the plane of the page.

The wavelet variance of the multi-scale pattern shows two distinct peaks centered at 4 and 16 m (Figure 4.7). The broad peak centred at 16-m reflects the cluster of smaller peaks and the wide, solid peaks. The dispersed character of the peaks is the result of the differences in the forms of the analysing wavelets from the sinusoidal data function. It is instructive to compare the wavelet variance with the transform to discern the two types of wide larger-scale peaks. We now extend the discussion to a more complex set of data composed of periodic and aperiodic components, namely forest canopy gap data, and examine the utility of the wavelet transform in distinguishing forest canopy structure as measured by gap distribution and size.

### APPLICATION TO FOREST TRANSECTS

The spatial pattern of canopy density in forests reflects the disturbance and developmental history of the stand and acts as an important control over growth and establishment in the understorey. The pattern of canopy density is frequently simplified into a classification of canopy gaps and non-gaps, where both the presence and size of gaps are considered to be ecologically important features of the stand. Most gap studies set minimum gap sizes and do not characterize variations in densities of the "closed" portions of the canopies between the gaps. The gap paradigm has been criticized because it ignores variations in the density of non-gap canopy areas which may be important to understory response (Lieberman, Lieberman, and Peralta 1989). A more objective view of the canopy density pattern of a forest requires a systematic sampling scheme with fine spatial and canopy density resolution.

Wavelet analysis was performed on canopy density measurements taken along twelve 200-m transects to characterise spatial patterns of canopy density in relation to stand age and structure. While any study based on a one-dimensional analysis of a two- or three-dimensional pattern is intrinsically weak, the use of transects allowed a greater number of stands to be sampled; decreased dimensionality offered sampling of four stands per age class.

## Study Sites

Transects selected from three broad age classes of Pseudotsuga menziesii (Mirb.) Franco (Douglas fir) and Tsuga heterophylla (Raf.) Sarg. (western hemlock) stands in the western Cascade Range of Oregon and Washington, U.S.A. were established. Canopy opening measurements were taken at 1 m intervals along 200 m transects in four stands from each of the following dominant tree age classes: young (< 80 years), mature (80-200 years), and old growth (> 200 years). The twelve stands are denoted O1, O2, O3 and O4, in the case of the four old-growth stands, M1, M2, M3 and M4, for the mature stands, and Y1, Y2, Y3 and Y4 for the young stands.

The stands were selected to be representative of the range of stand conditions observed in a regional study of forest development and structure (Table 4.1; Spies & Franklin, 1990). Within each stand, an area of similar slope, aspect, topography and soils was identified and a single transect was sampled along the slope contours from a randomly selected starting point. Data on percentage canopy opening were obtained at 1-m intervals along the transect using a moosehorn with bubble levels (Mueller-Dombois & Ellenberg 1974). Percent closure classes from 0% (closed canopy) to 100% (gap) were recorded in 20% increments. Gaps are defined as any part of the canopy at least 1 m wide where the measured value (percent canopy opening) is positive.

## Wavelet Analysis

Three stands were chosen for detailed discussion to illustrate how canopy gap patterns were extracted from the data using wavelet analysis. The three stands represent the spectrum of canopy patterns and types found in the analysis. Stand Y1 is fairly typical of many young stands with dense, uniform canopies; canopy closure is continuous and punctuated with small (2-6 m) areas of low density (predominantly < 40% opening) canopy gaps (Figure 4.8). The corresponding wavelet transform shows three faint clusters of gaps of low amplitudes centered at 40, 90, and 150 meters (Figure 4.9). The wavelet variance is low in amplitude across all scales with the greatest contribution from gaps < 5 meters in size (Figure 4.10). Thus, according to the wavelet analysis, the stand canopy is characterised by low intensity gaps (where intensity corresponds to the percentage canopy opening) and lacks distinct gap structure at all scales except diffuse gaps < 5 m in diameter.

In contrast, a transect through an old-growth stand (stand O1) shows a canopy comprised of several sizes of gaps ranging from 2 to 30 m in size (Figure 4.11). These gaps are greater than 60% open on average. The gaps cluster in two main groups centered at 40 and 110 m with two minor groups at 50 and 120 m (Figure 4.12). These clusters are most easily perceived when the transform is viewed near-parallel to the

plane of the page. Overall, the amplitude of the transform is much greater than that of the younger, more homogeneous canopy (Figs. 4a and 4b). The variety of gap sizes is reflected by high wavelet variance values across a broad range of scales between 5 and 30 m (Figure 4.13).

A third transect sampled from a second young stand (Y4) illustrates the signature of disturbance on canopy gap structure (Figure 4.14). The combination of pre-crown closure, patchy disturbance and areas of thin soils have increased the contrast in the canopy structure. This stand lacks the very large-sized gaps of the old-growth stand described above and is instead dominated by low intensity, 1-2 m wide and high intensity 5-10 m wide gaps (Figure 4.15). The wavelet variance shows a strong contribution from features 1-7 meters in scale as evidenced by the peak centered at 5 m (Figure 4.16). The wavelet variance is distributed evenly at scales >10 m. While visual inspection of the transect data suggests two dominant gap sizes, a double peak is lacking in the corresponding wavelet variance. Although the 1-2 m diameter gaps form a strong component of the canopy structure (as evidenced by the high variance value), their intensity is low (i.e. the percentage canopy opening is 20% on average) relative to the intensity of the larger gaps. In contrast, the majority of larger gaps (> 60% open) caused by disturbance or site conditions dominate the wavelet variance.

The wavelet variance is a measure of the contribution of pattern at each given scale to the overall pattern. In the present context, a high wavelet variance at a given scale indicates either a large number and/or very open gaps of a given width. The presence of peaks in the wavelet variance indicates dominance of a feature at the given scale. For instance, the single strong peak in Figure 4.16 reflects the strong dominance of gaps ranging from 4 to 6 m in size. A non-zero variance at greater scales reflects the contribution of other gap sizes to the signal. Canopy transects characterized by broad, high wavelet variance or the presence of two or more peaks indicates the presence of gaps across several scales relative to stand dimension (e.g. Figure 4.13). On the other hand, a low variance and/or lack of distinct peaks in the wavelet variance indicate a stand marked by a canopy lacking a multi-scale gap pattern (e.g. Figure 4.11).

#### **Canopy Patterns Along a Chronosequence**

The wavelet variance of the twelve transects representing twelve stands from three forest age classes were calculated (Figure 4.17). Trends of canopy pattern among age-classes are present, although variation within age-classes is high. Old-growth stands (stands O1-O4) tended to have higher wavelet variance amplitudes and pattern at several scales. In

general, the young stands (stands Y1-Y4) tended to have wavelet variances of lower amplitudes and finer pattern. The mature stands (stands M1-M4) exhibited characteristics intermediate to both old-growth and young stands depending on their individual histories.

The wavelet variances can be classified into four general groups based on their curvilinear form. The wavelet variances of the Group I (O1, O2, O3 and M3), have peaks in the range 5 to 30 m and are high in amplitude either across several scales (O1) or dominated by two strong peaks (O1, O2). These stands have large gaps and a diverse canopy structure as a result of their advanced stage of development. Stand M3, an older mature stand, has experienced mortality from a root rot (Phellinus weirii) and bark beetles in the last 20 years. These conditions have created the relatively intense and larger scale of gaps rendering its gap signature more similar to the canopy structure of the old-growth stands (O1, O2 and O3).

Group II (Y1, Y2, M2 and M4) is characterised by low intensity (diffuse) gaps of fairly small size (<8 m). These stands have relatively closed, homogeneous canopies that are typical of many young and mature Pseudotsuga menziesii/Tsuga heterophylla. Competition mortality, most often affecting single, relatively small canopy trees, has been the primary form of tree death in these stands. Small gaps between crowns may result from branch abrasion of adjacent swaying crowns or

as the result of the death of intermediate and suppressed canopy trees. The low intensity gaps of these stands are areas of thin crowns or crown fringes that are incompletely covered by branches and leaves.

Group III (Y3 and Y4) exhibits the highest wavelet variance of any of the stands at the scale of two meters. The wavelet variance of stand Y4 has a single, strong peak at 5 m. While stand Y3 has a peak at 4 m, it is less dominant than the second peak at 12 m. The canopies of both these stands are characterized by numerous small, but moderately open gaps. The canopy of stand Y4 is still in the process of closing in in some portions with small gaps formed by relatively open crowns and spaces between adjacent tree crowns (Table 1). Stand Y3 is also a young with small pockets of Phellinus weirii that are expanding within the stand in addition to the smaller gaps.

The two remaining stands comprising Group IV (O4 and M1) each have a wavelet variance distinct from any of Groups I-III. Stand O4 has a dominant peak in the range 8-12 m, similar to the Group I, but lacks the higher scale patterns found in their wavelet variances. This young old-growth stand retains a high density of large, canopy Douglas-firs and western hemlocks. The canopy has not yet been broken-up by gaps formed by the death of the larger canopy trees or groups of trees: a condition typical of many old-growth stands (Spies, Franklin and Klopsch 1990). The wavelet variance of

stand M1 (a 140-year-old stand) suggests the canopy pattern is characterised by moderately intense gaps at scales  $>6$  m. These gaps may represent areas of low-density canopy where crowns are sparse and small spaces occur between crowns.

The canopy wavelet variances of the twelve stands reveal that gaps occur across a wide range of intensities and scales. In many cases, the stands were characterised by very small gaps or by relatively large, low intensity gaps. These types of gaps can be considered as the canopy background for large more intense gaps which are the focus of most gap studies. The relative importance of large, intense gaps to understorey dynamics may be determined in part by the context of the canopy, its characteristic scales and intensities of openings. In this sense, canopies should not be viewed as "swiss cheese" (Lieberman, Lieberman, and Peralta 1989), but rather as complex structures of variable densities and patch sizes which are not only a function of the processes of stand development, but also disturbance history and local site conditions.

## CONCLUSIONS

Changes in heterogeneity and pattern with scale are common to many ecological systems. Differences in scale-heterogeneity relationships can be used to characterise ecological systems and provide insight into processes that determine pattern at the stand and landscape scales. There are three main applications for which spatial methods may be used in such studies: i) the description and characterization of spatial pattern, ii) testing and confirmation of hypotheses regarding spatial pattern, and iii) exploration and discovery of new information. The objectives of the study and the properties of the data will determine the most appropriate method of analysis. We have attempted to illustrate the utility of the wavelet transform as an additional method for the use of pattern analysis and quantification. The wavelet transform has the ability to expand transect data into constituent multi-scale components while preserving location along the transect. The graphical representation of this spatial decomposition of the data allows for the examination of hierarchical pattern and non-uniform structure.

A variant of the wavelet transform, the wavelet variance, quantifies the contribution of each signal component at a given scale to the overall pattern and facilitates comparison between multiple data sets. The wavelet variance is a useful

method to compare two or more sets of data to characterise relative differences and similarities of scales of pattern. Because the wavelet variance is both proportional to the number and intensity of a feature of a given scale, a peak in the wavelet variance may indicate either a large number of low intensity gaps and/or the presence of a number of high intensity (very open) gaps. For this reason, it is important to examine the original data transect and wavelet transform to identify the source of the peak. The combination of the wavelet variance and transform can be used to detect non-stationarity in the data and identify domains of relative spatial homogeneity.

As with other techniques such as spectral analysis, the resolution capabilities of the wavelet transform are limited by the transect length and sampling density. Longer transects relative to resolution scale are needed for a more complete description of the hierarchical structure of the data. This restriction is important to bear in mind during the formulation of sampling designs. For longer transects at a given spacing of the data, the graphical display of the wavelet transform allows resolution of the transect into distinct sub-domains based on pattern scale and frequency.

We have illustrated the capabilities of the wavelet transform to describe forest canopy structure using gap data. The wavelet transform was able to discriminate different canopy gap structures between stands based on gap size and

intensity. While it is acknowledged that a one-dimensional analysis of an intrinsically complex, three-dimensional phenomenon, i.e. gap structure, may be simplistic, certain patterns and trends emerged consistent with the ecology. Using this limited set of data, canopy gap structure was inferred to be generally correlated with stand age. Deviations from the general trend can be directly linked to events in stand history and site conditions. We have found that the wavelet transform is an effective technique for the analysis of spatial phenomena. It is a method which has numerous potential applications particularly in studies of landscape ecology where several scales of pattern may be present.

**Table 4.1** Description of canopy structure of the twelve Psuedotsuga stands.

Table 4.1

Stand Number	Stand Age (years)	Stand Condition
Y1	75	Uniform PSME & TSHE <sup>1</sup> canopy, no evidence of disease
Y2	70	Thin PSME canopy, windthrow mounds and thin soil
Y3	75	Uniform PSME canopy with large root rot pockets
Y4	43	PSME <sup>2</sup> canopy still closing, patchy disturbance and high site variability
M1	130-140	Homogeneous canopy of predominantly PSME with some TSHE
M2	130-140	Mixed PSME and TSHE canopy, moderate levels of root rot and canopy openings
M3	145	Porous PSME canopy resulting from bark beetles and disease, no hemlock
M4	160	Closed, TSHE-dominant canopy
O1	400-600	PSME canopy over multi-age TSHE and THPL <sup>3</sup>
O2	400-600	Distinct, two-layer canopy of PSME and TSHE
O3	350-500	Canopy composed of PSME over TSHE, low productivity site with many openings, no evidence of disease or recent fire
O4	250-275	Intact, uniform PSME and TSHE canopy

<sup>1</sup>TSHE - Tsuga heterophylla (Raf.) Sarg.

<sup>2</sup>PSME - Pseudotsuga menziesii (Mirb.) Franco

<sup>3</sup>THPL - Thuja plicata Donn.

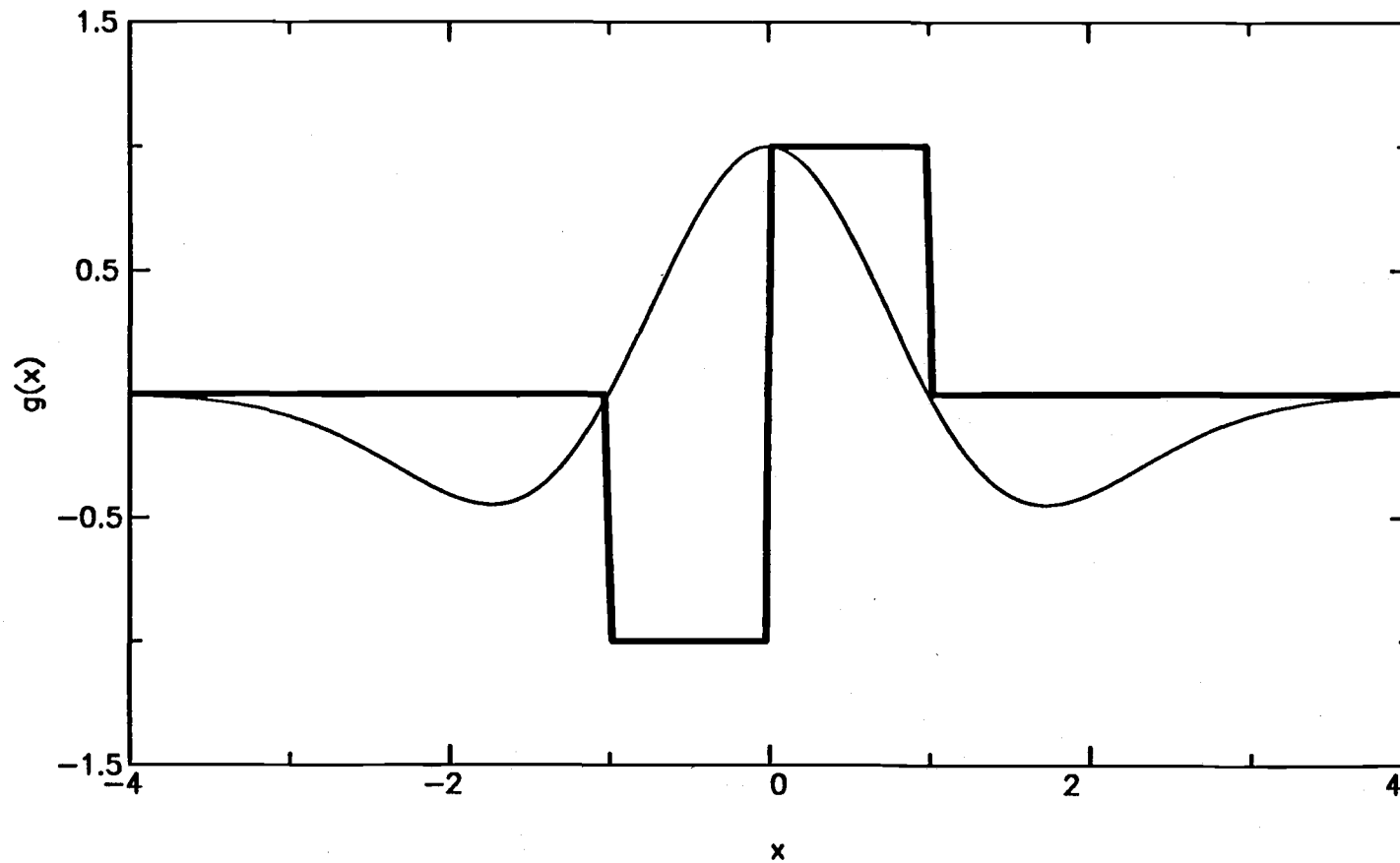


**Figure 4.1** The mexican hat (solid line) and Haar (heavy solid line) analysing wavelets used in the simulation and empirical analyses.

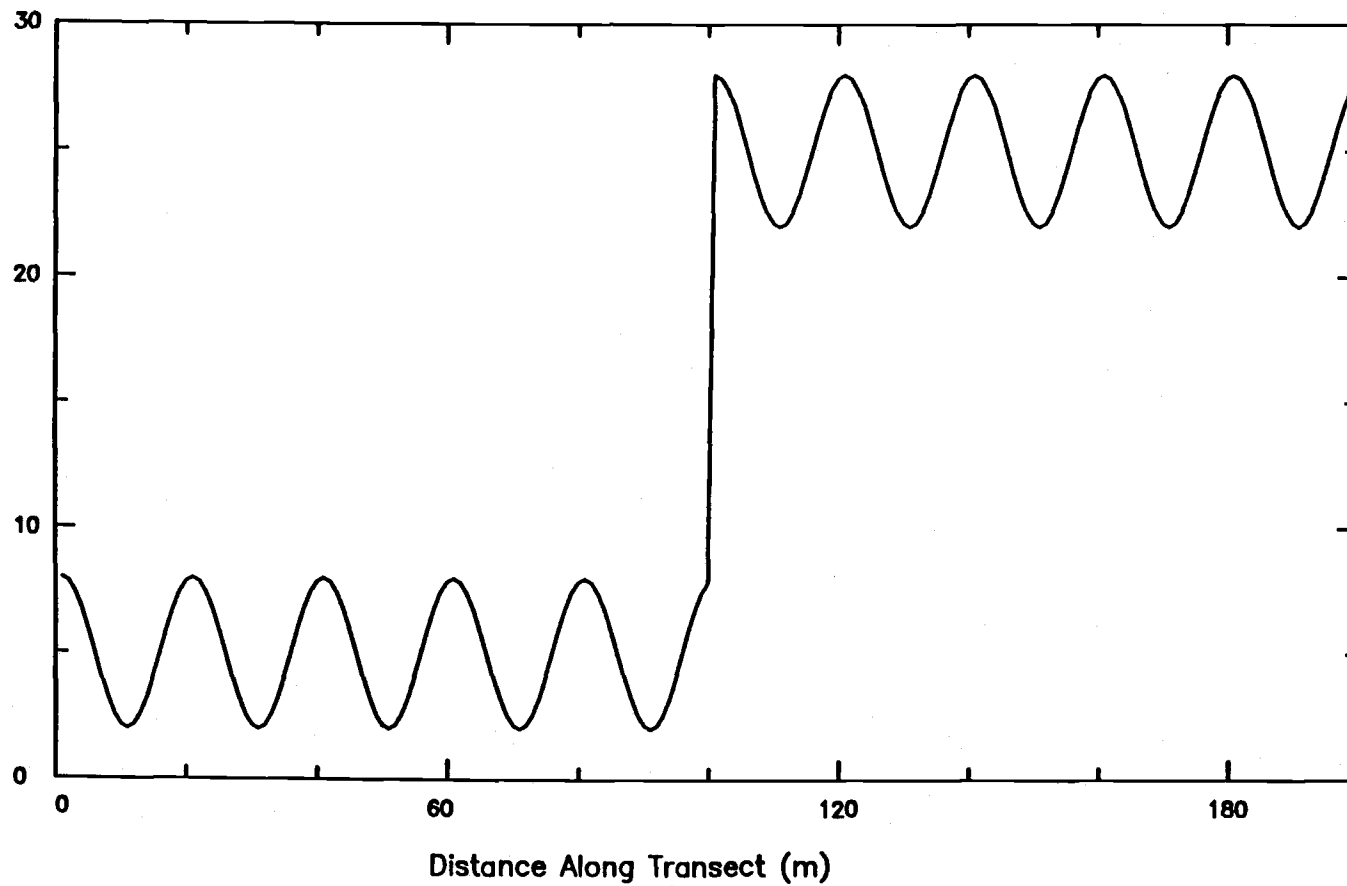


Figure 4.2 Simulated forest canopy-gap transect of simple pattern.

**Figure 4.3** Haar wavelet transform for data in figure 4.2. Grey-scale indicates values of wavelet transform. y-axis corresponds to scale (m); x-axis corresponds to distance along transect (m). Viewing the figure nearly-parallel to plane of the page emphasises the transform structure.

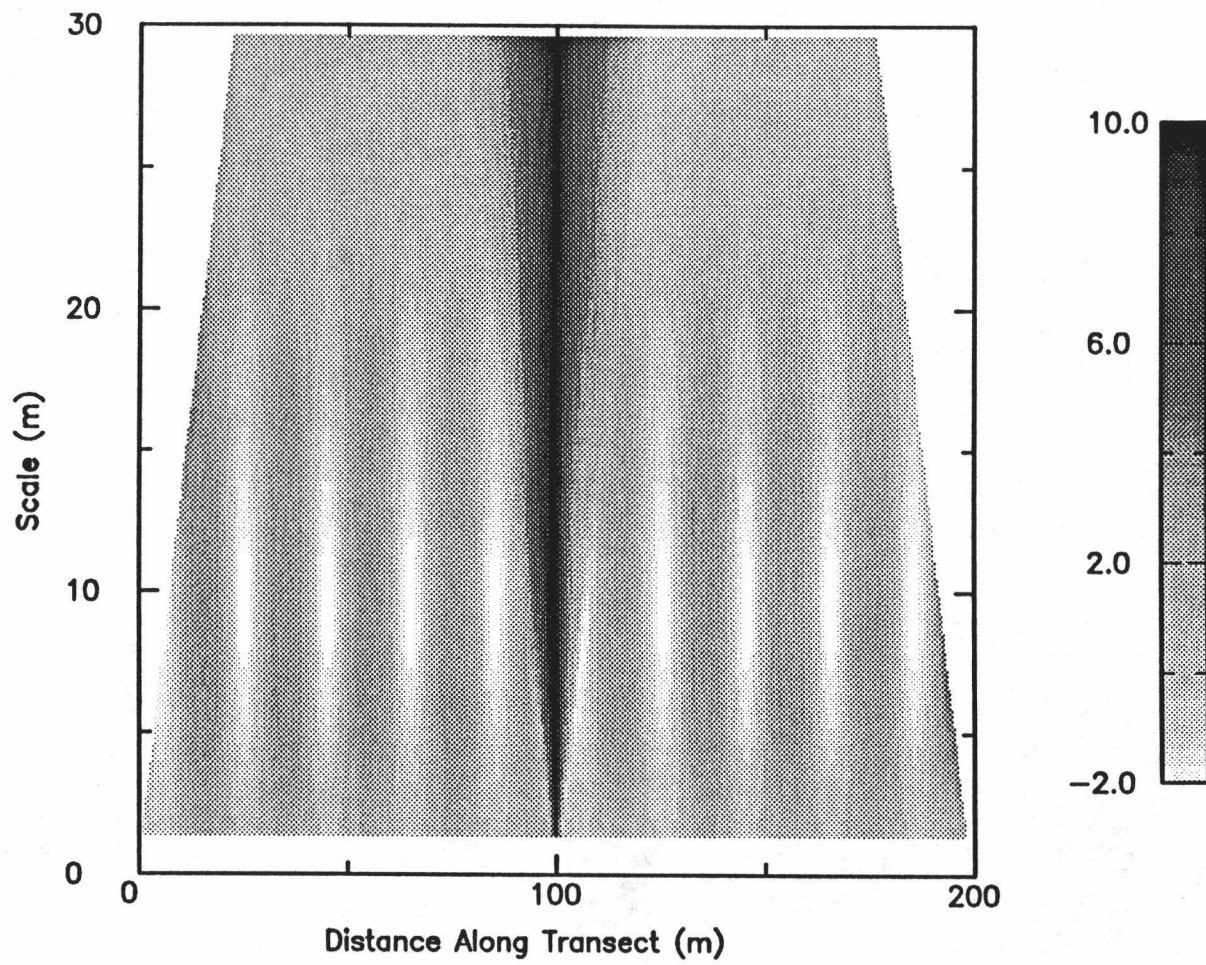
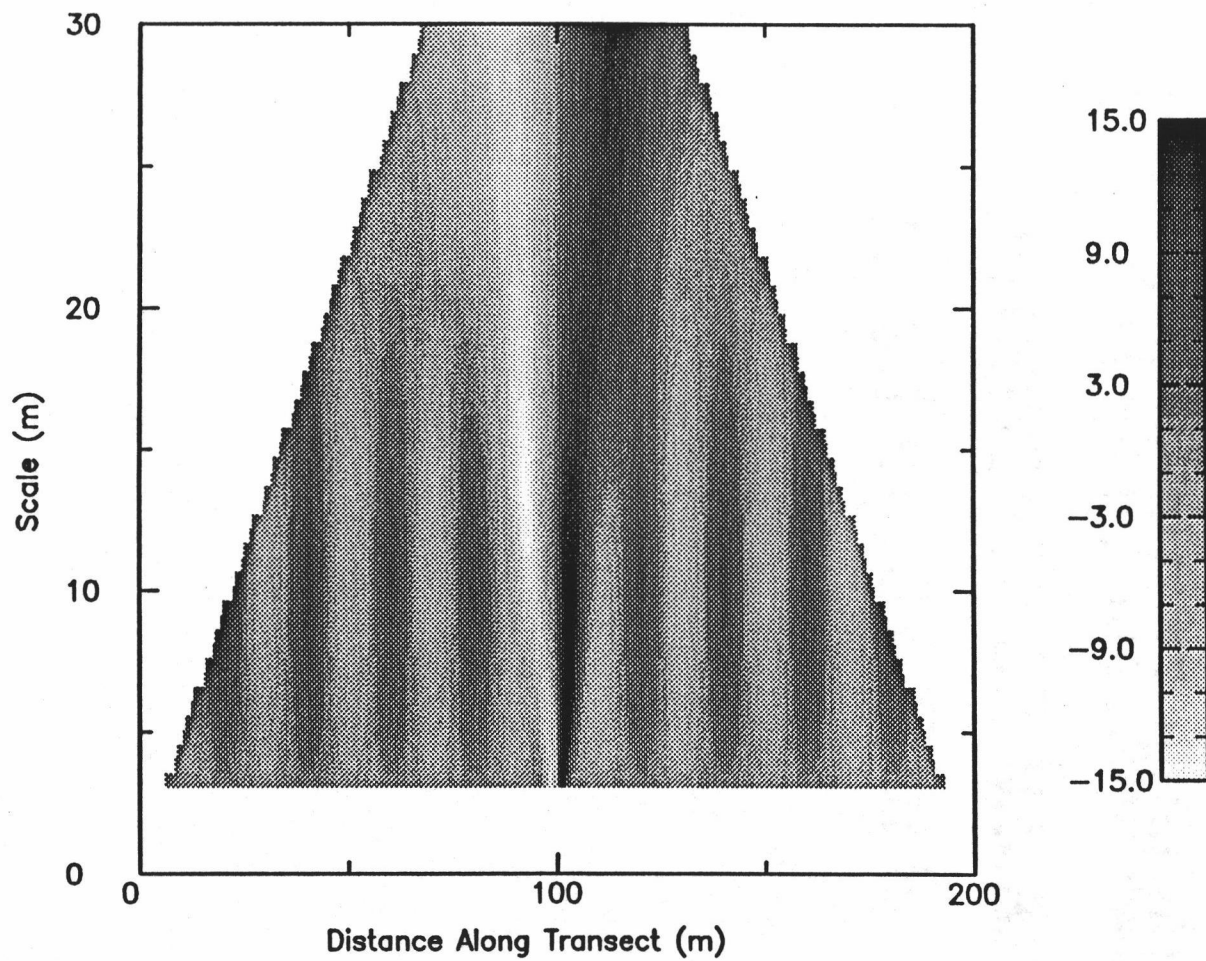
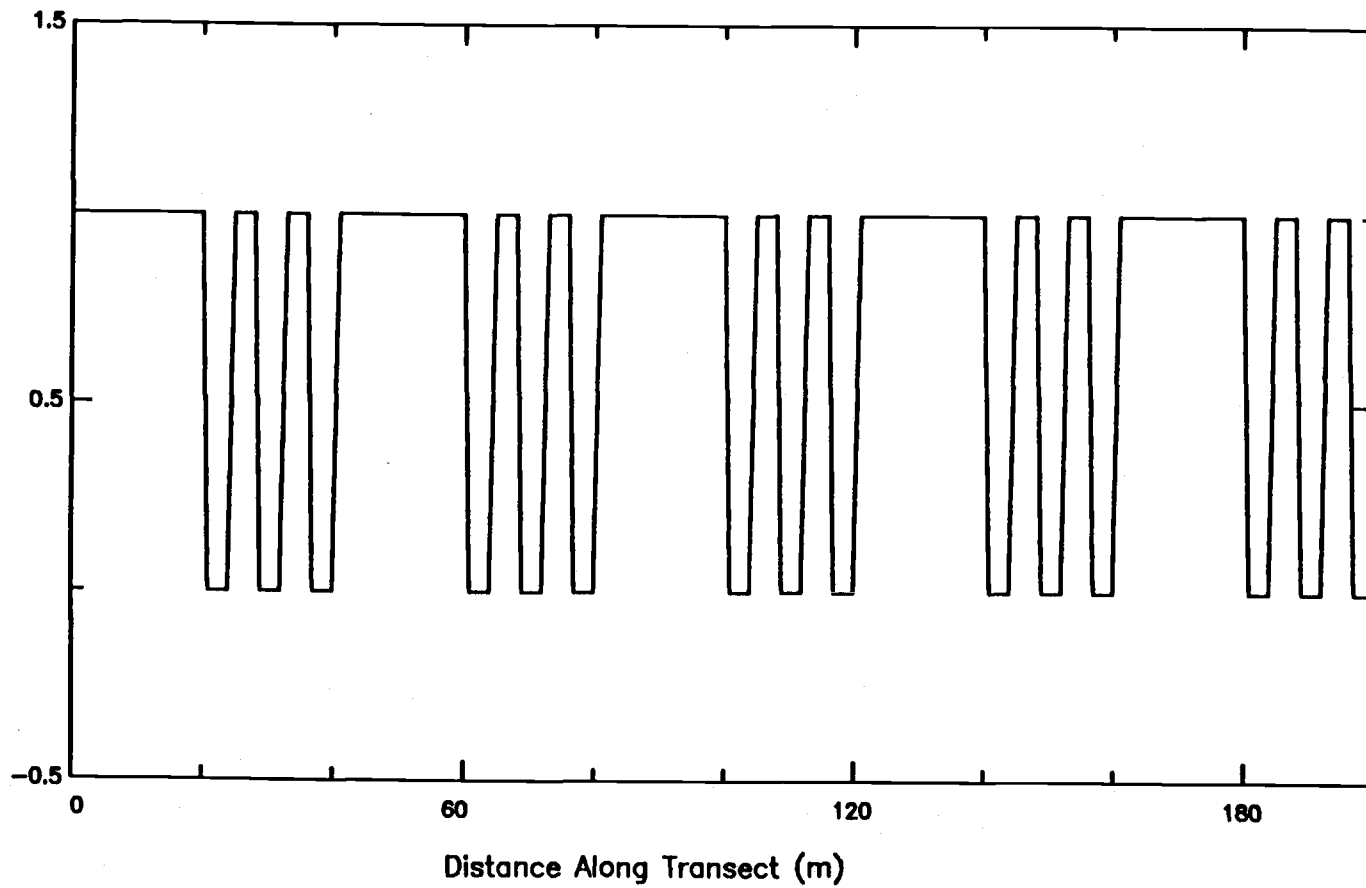


Figure 4.3



**Figure 4.4** Mexican hat wavelet transform for data in figure 4.2.



**Figure 4.5** Simulated forest canopy transect of nested, two-scale pattern.

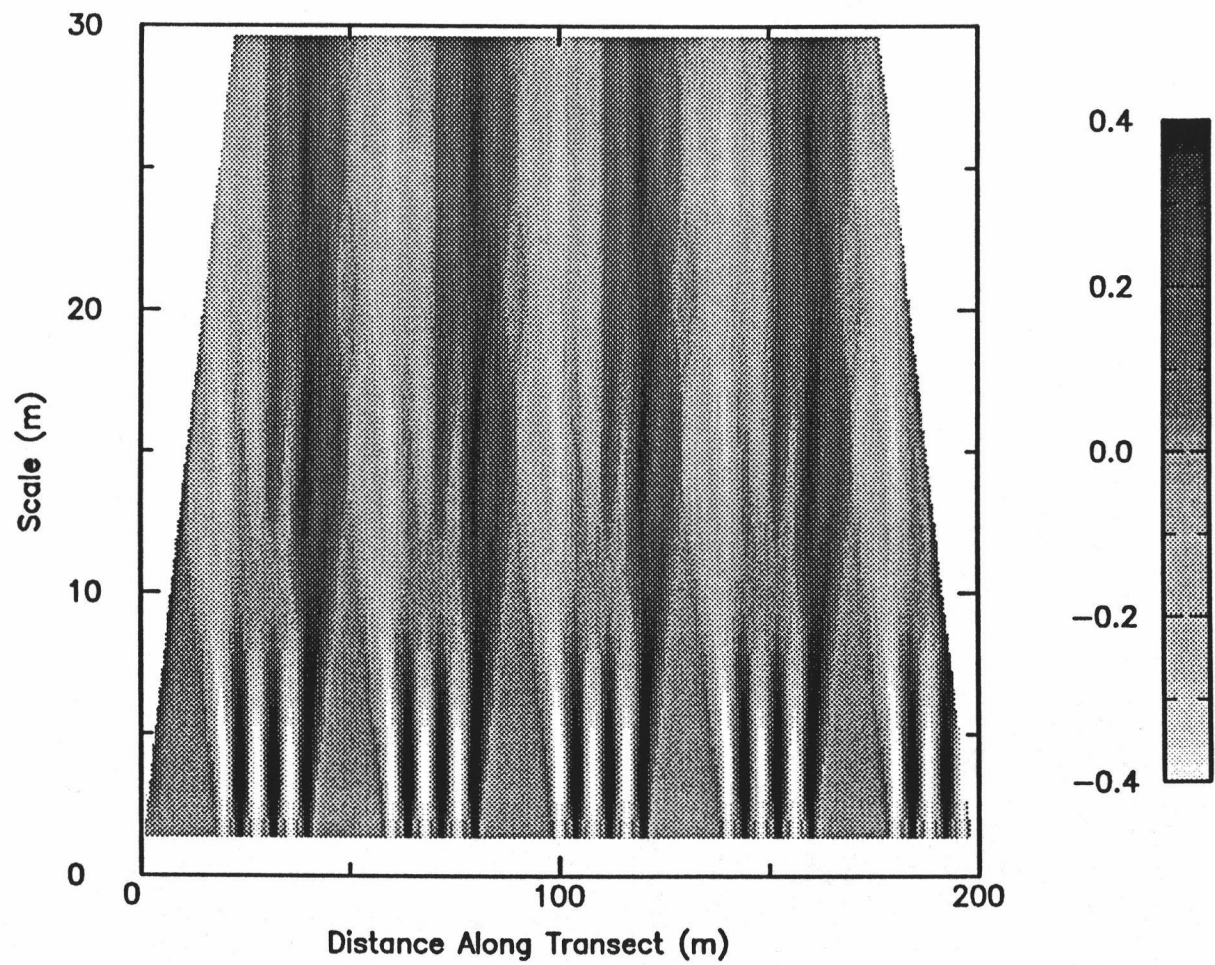


**Figure 4.6** Wavelet transform of data in figure 4.6.

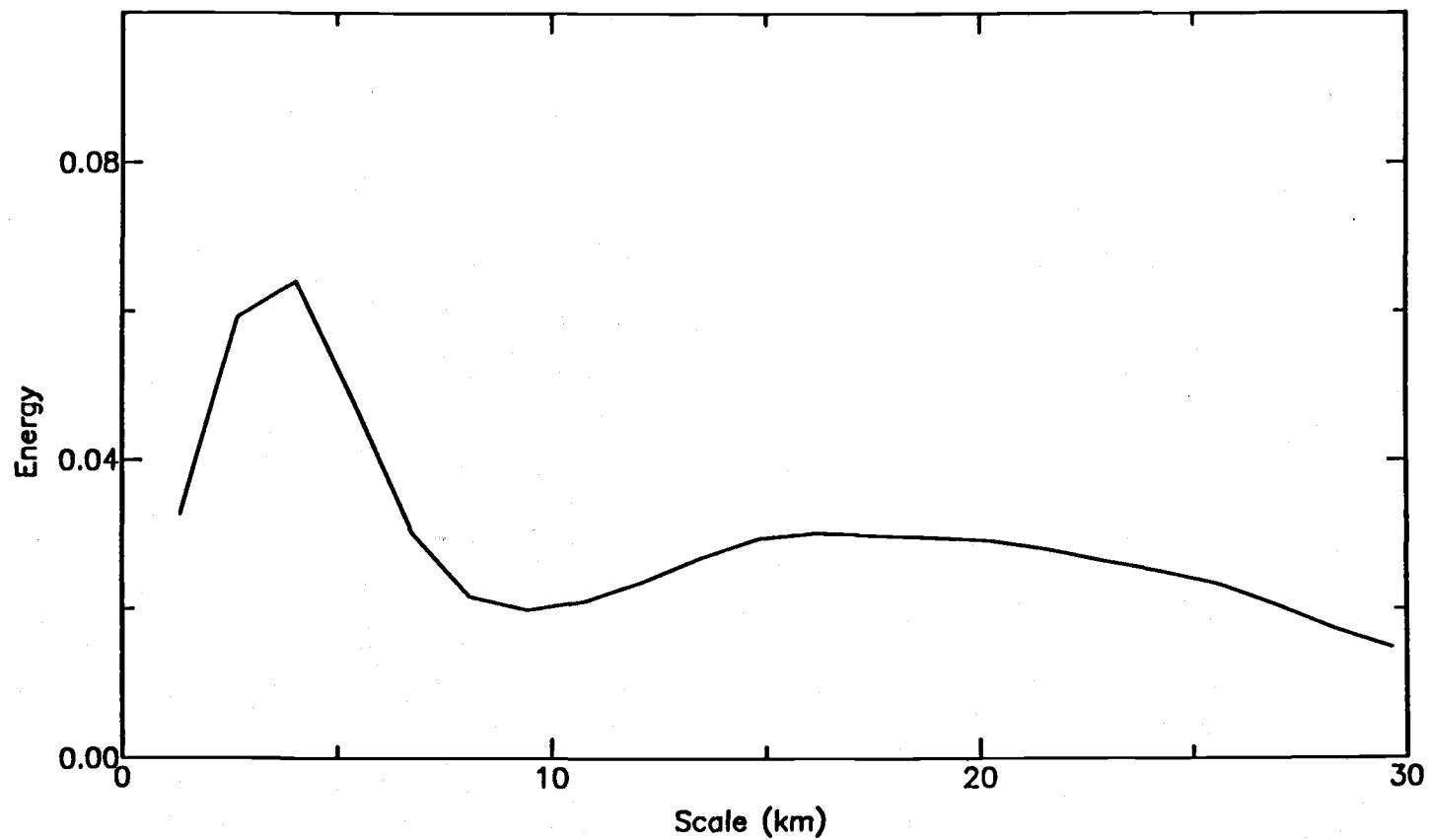


Figure 4.7 Wavelet variance of the nested, two-scale transect in figure 4.5.

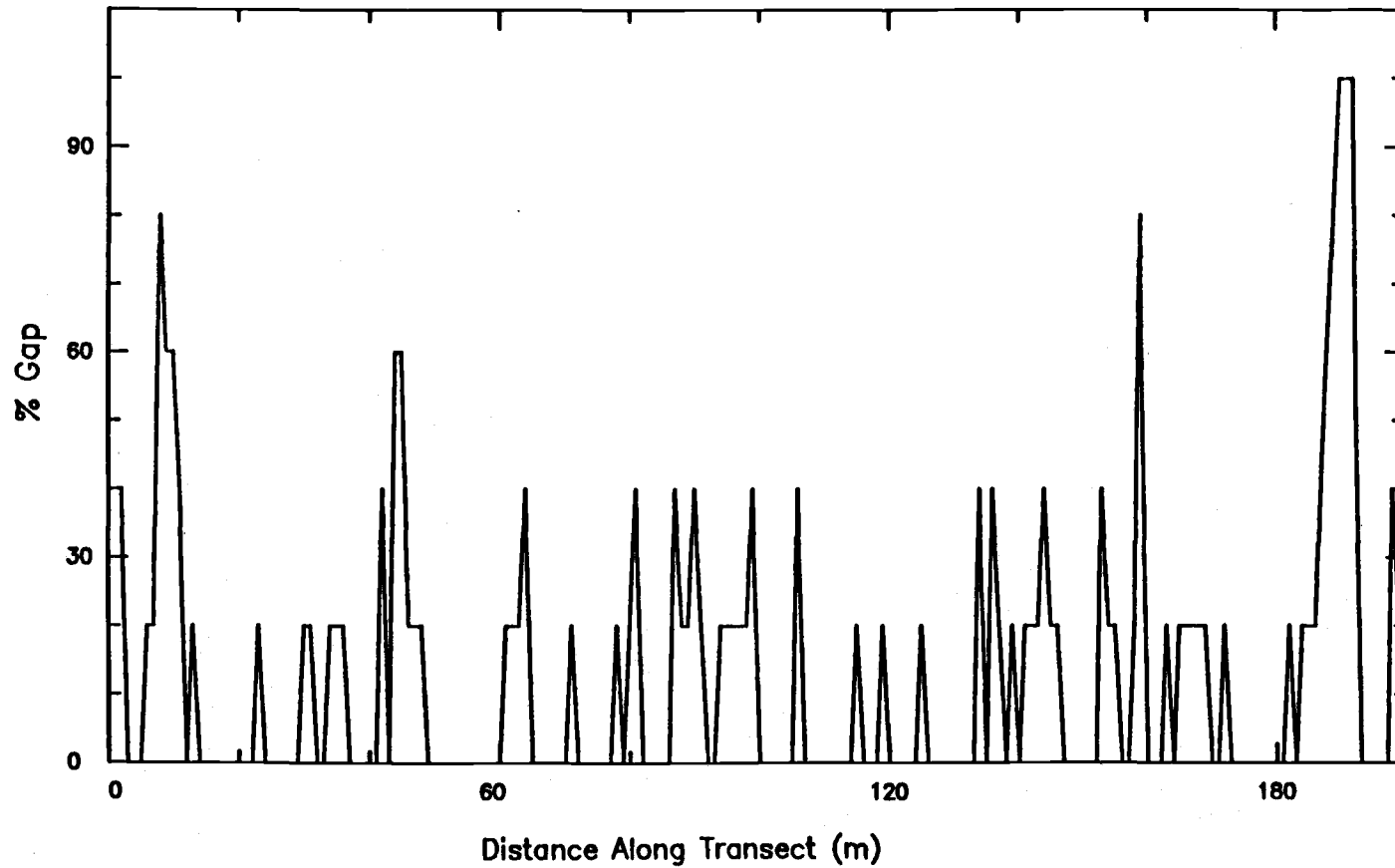


Figure 4.8 Data transect of forest canopy gap of a young stand (Y1).

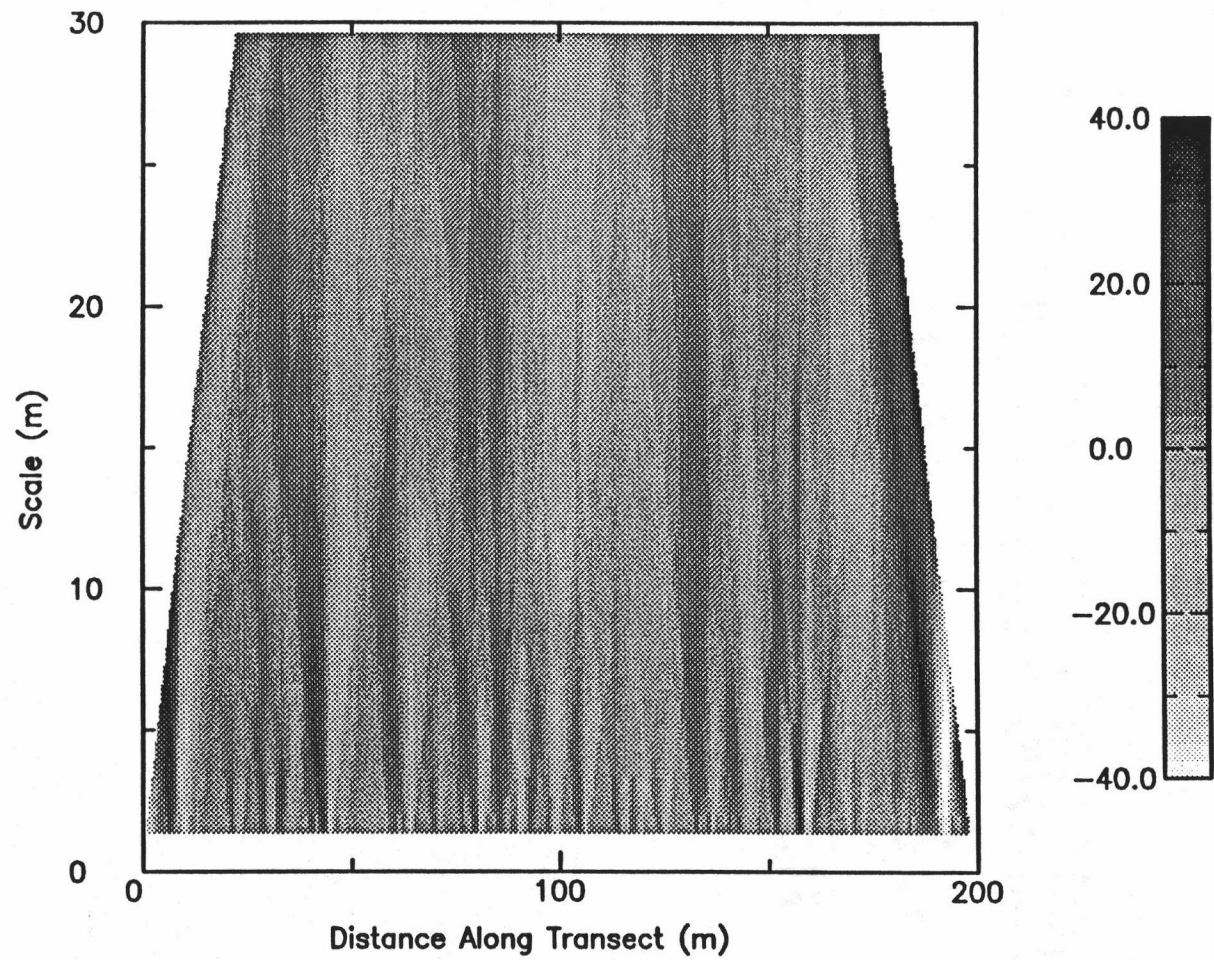


Figure 4.9 Wavelet transform of canopy gap data of young stand (Y1) shown in figure 4.8.

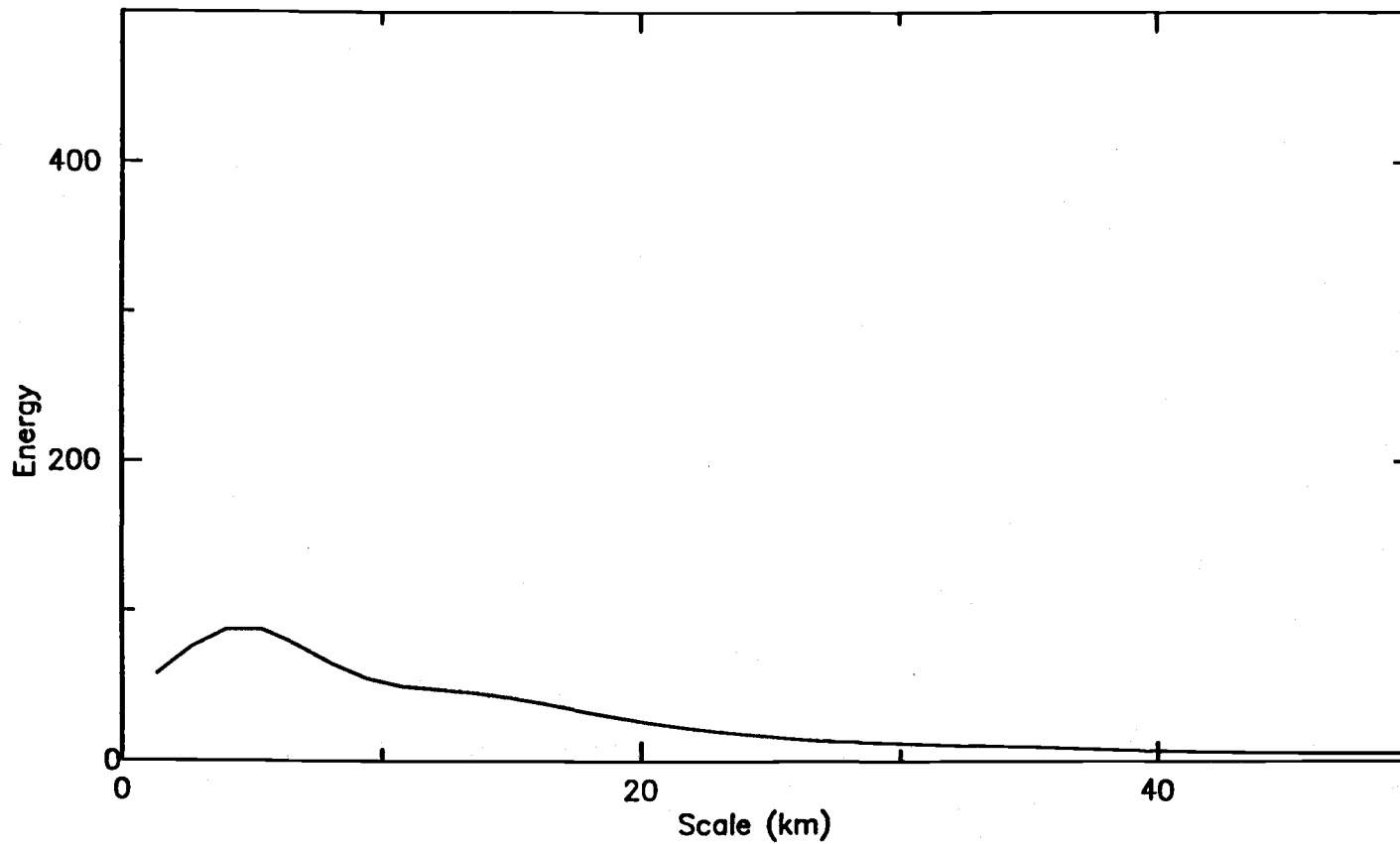


Figure 4.10 Wavelet variance of canopy gap data of young stand (Y1) shown in figure 4.8.

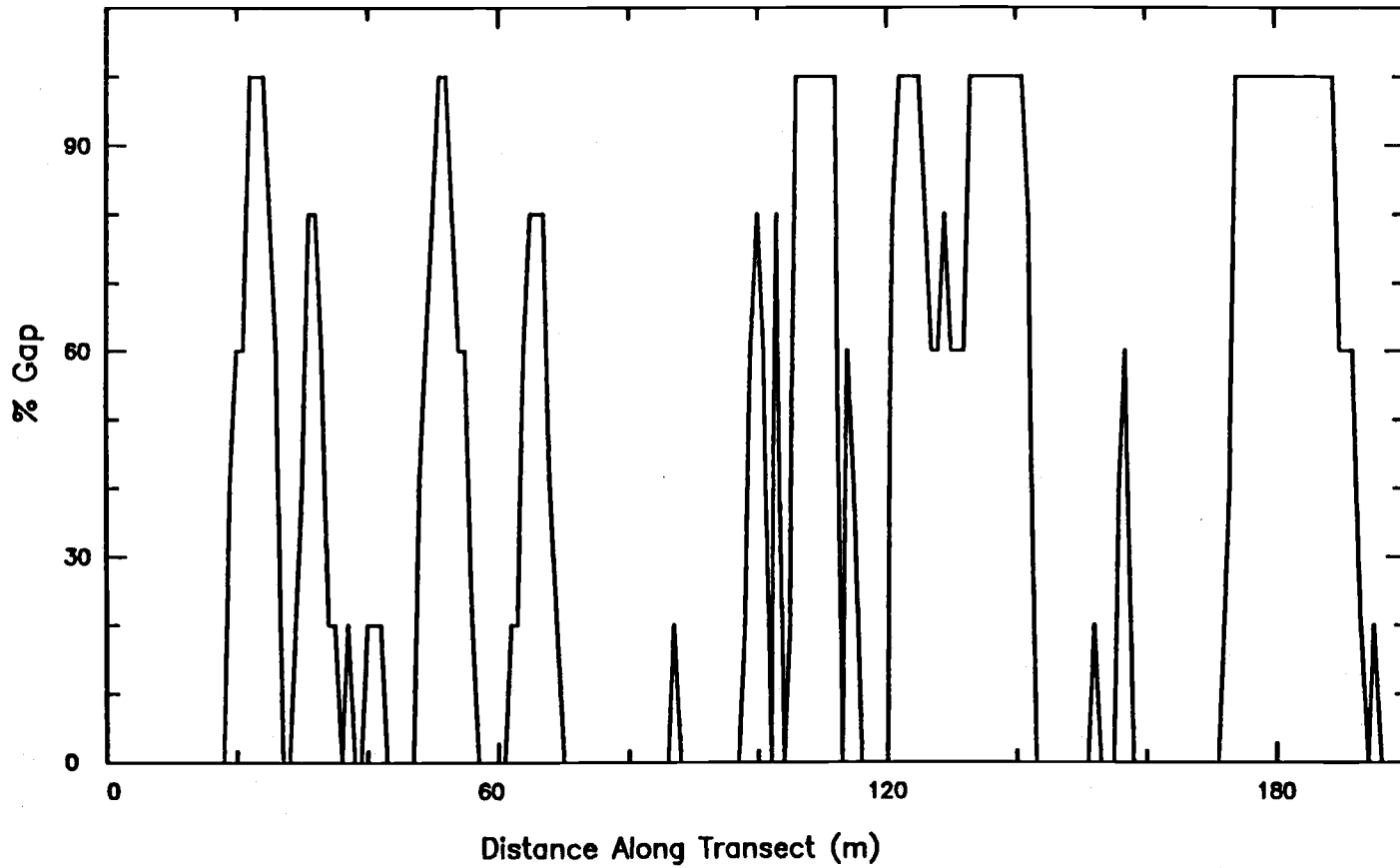


Figure 4.11 Data transect of forest canopy gaps of an old-growth stand (O1).

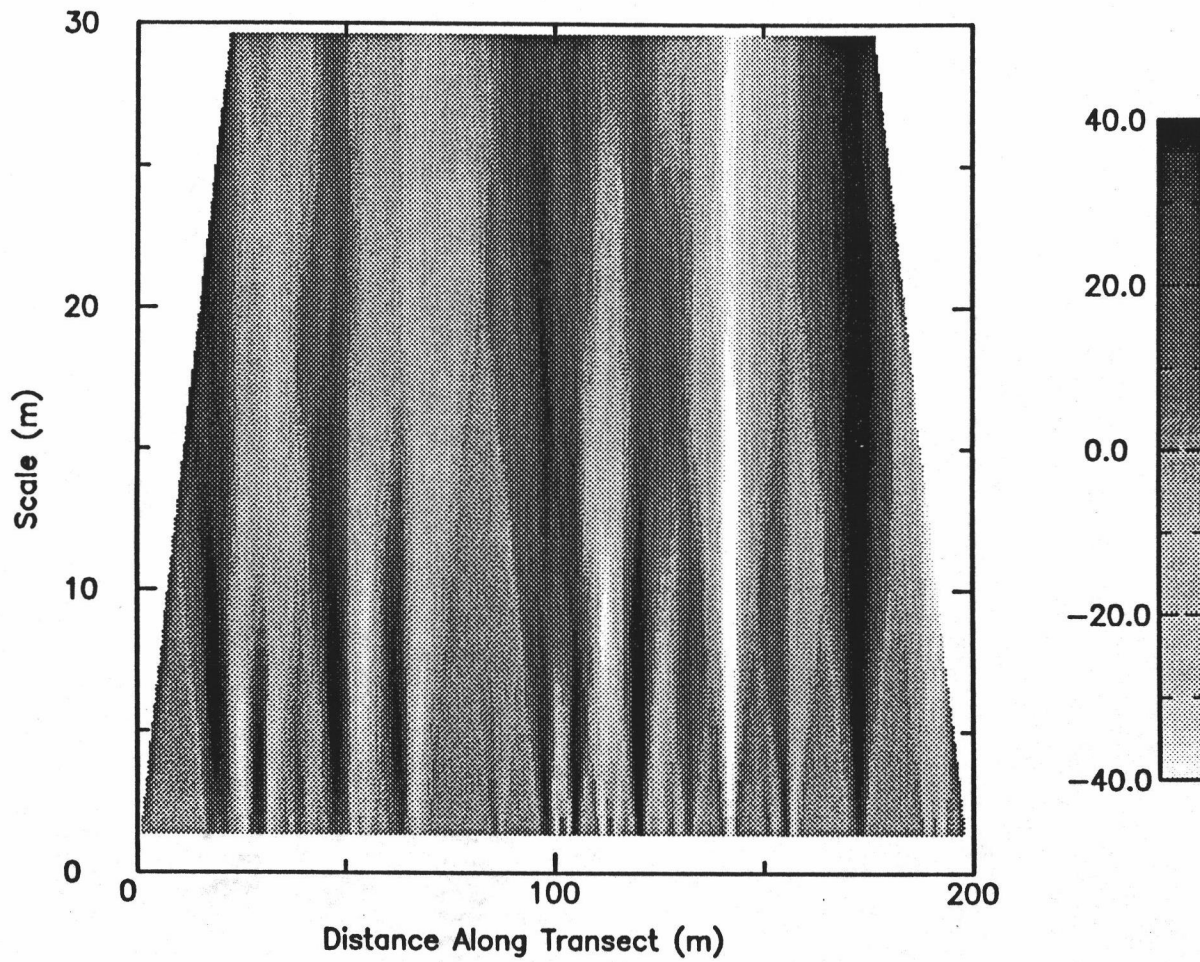


Figure 4.12 Wavelet transform of canopy gap data of old growth stand (O1) shown in figure 4.11.

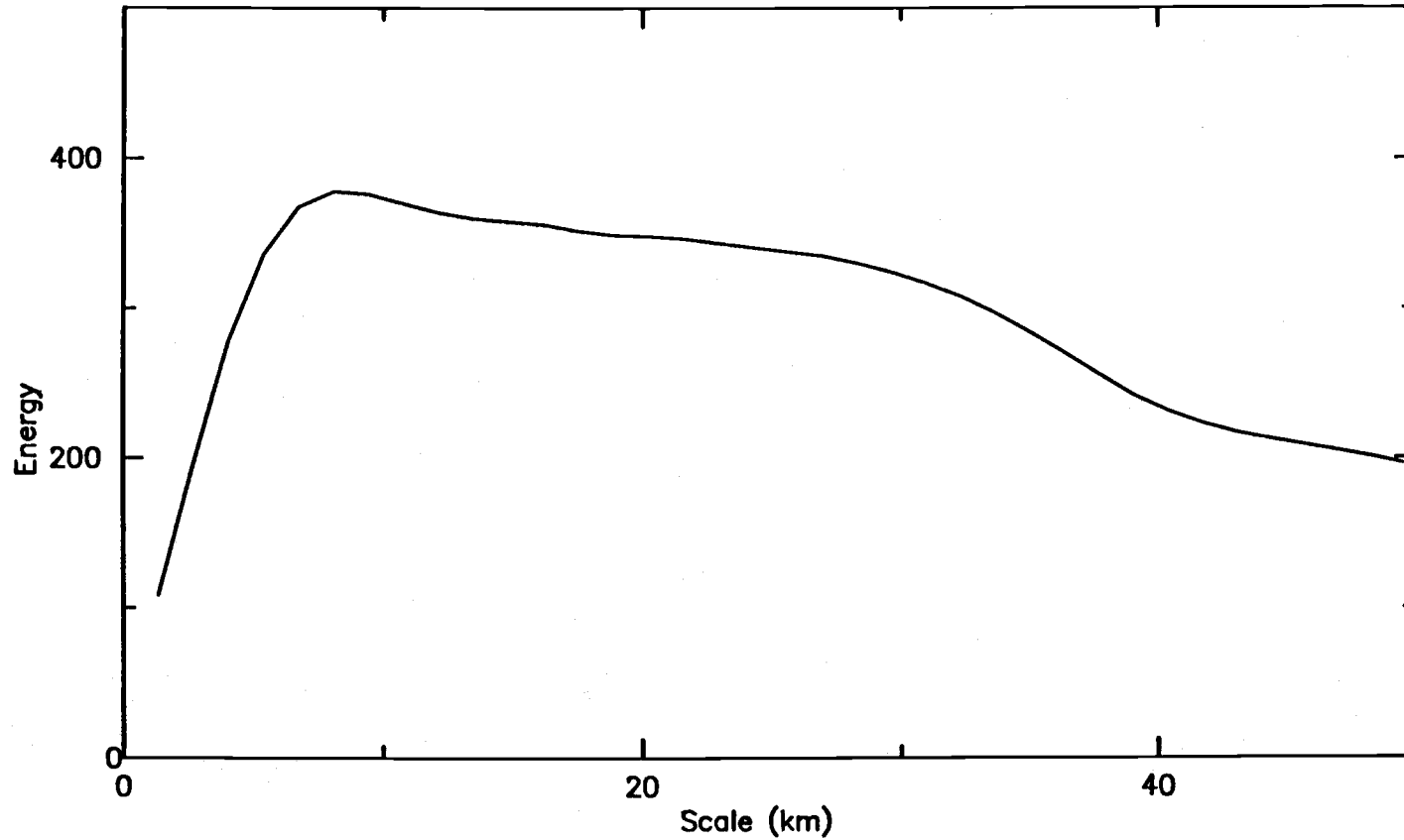


Figure 4.13 Wavelet variance of canopy gap data of old growth stand (O1) shown in figure 4.11.

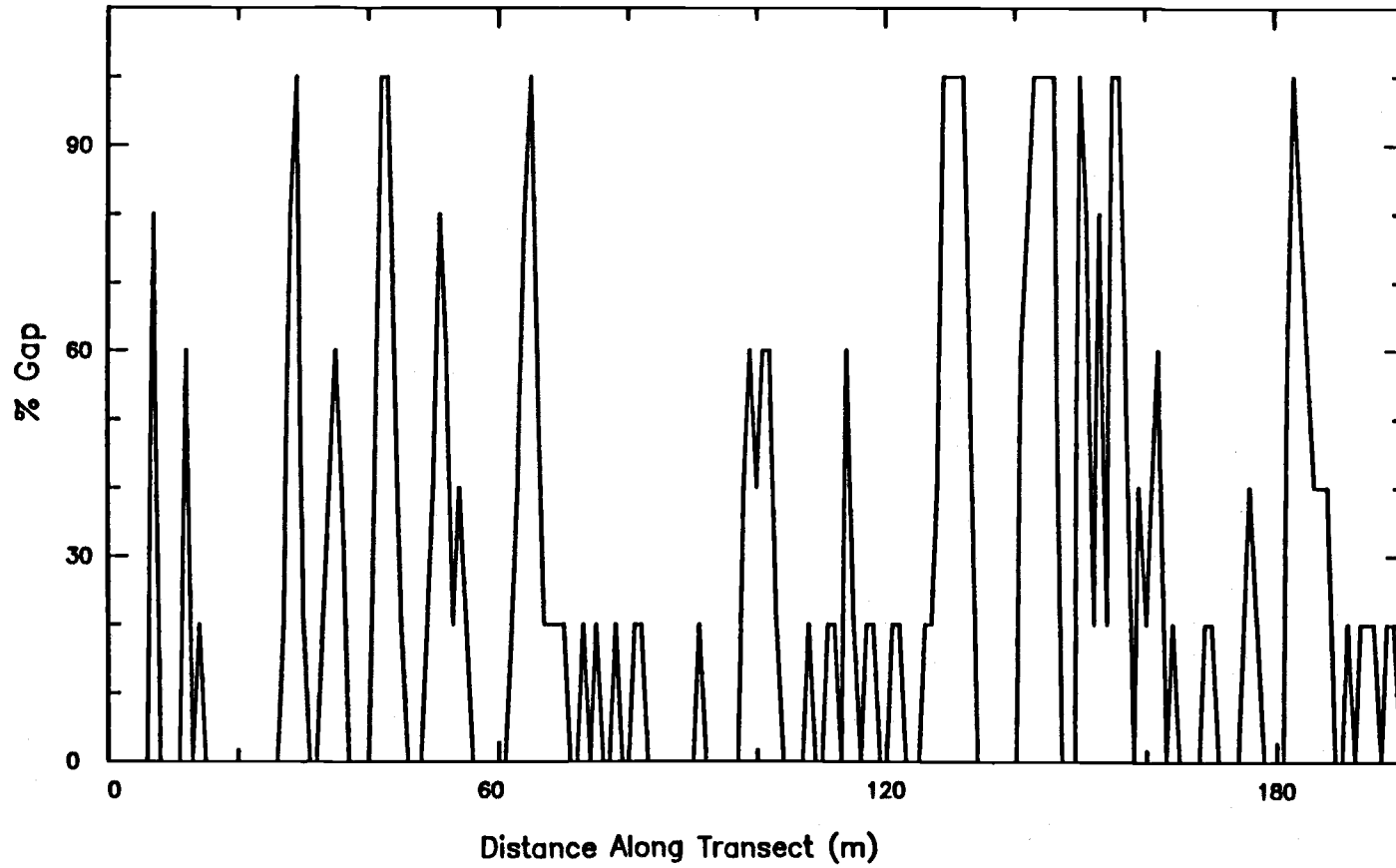
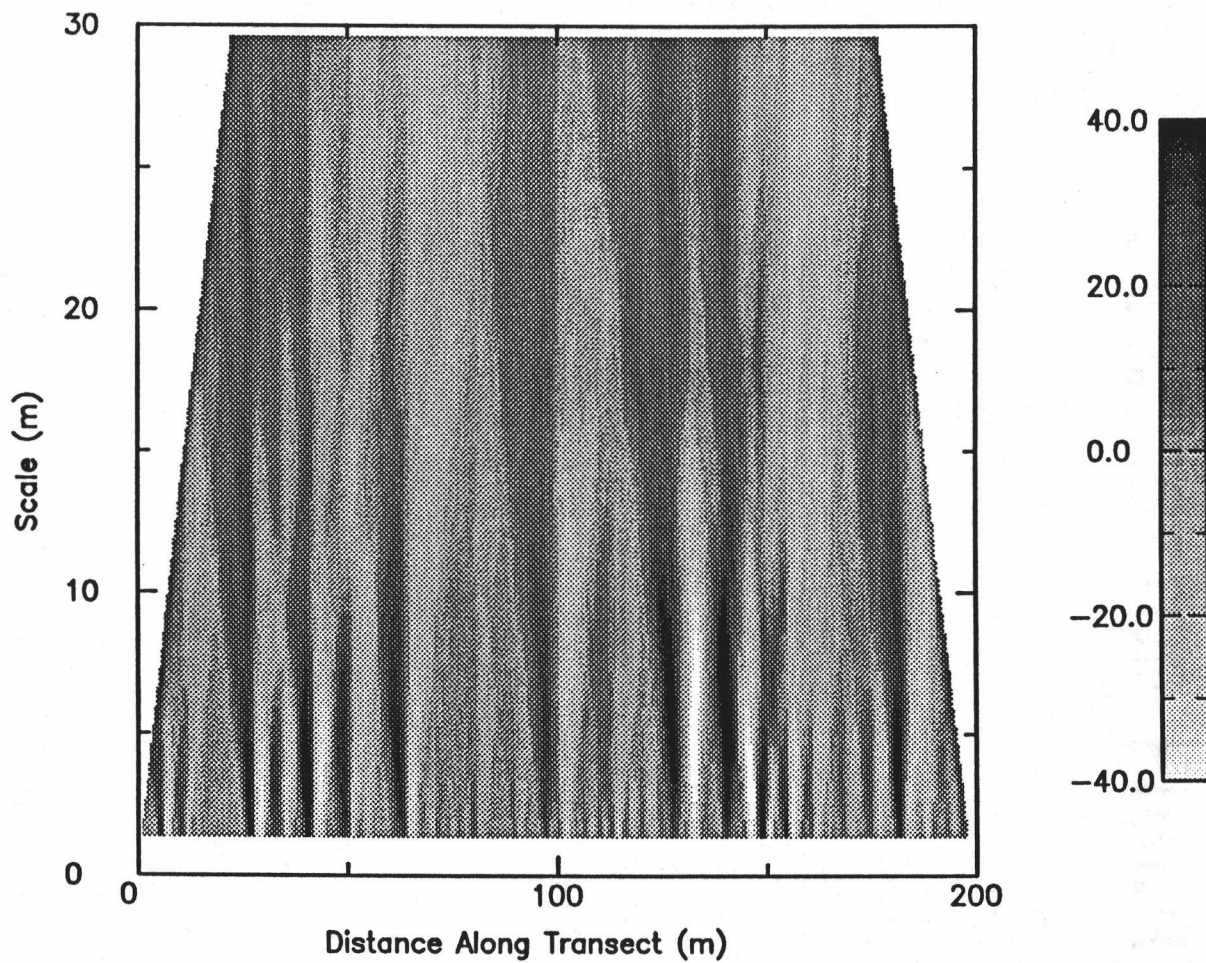


Figure 4.14 Data transect of forest canopy gaps of a second young stand (Y4).



**Figure 4.15** Wavelet transform of canopy gap data of second young stand (Y4) shown in figure 4.14.

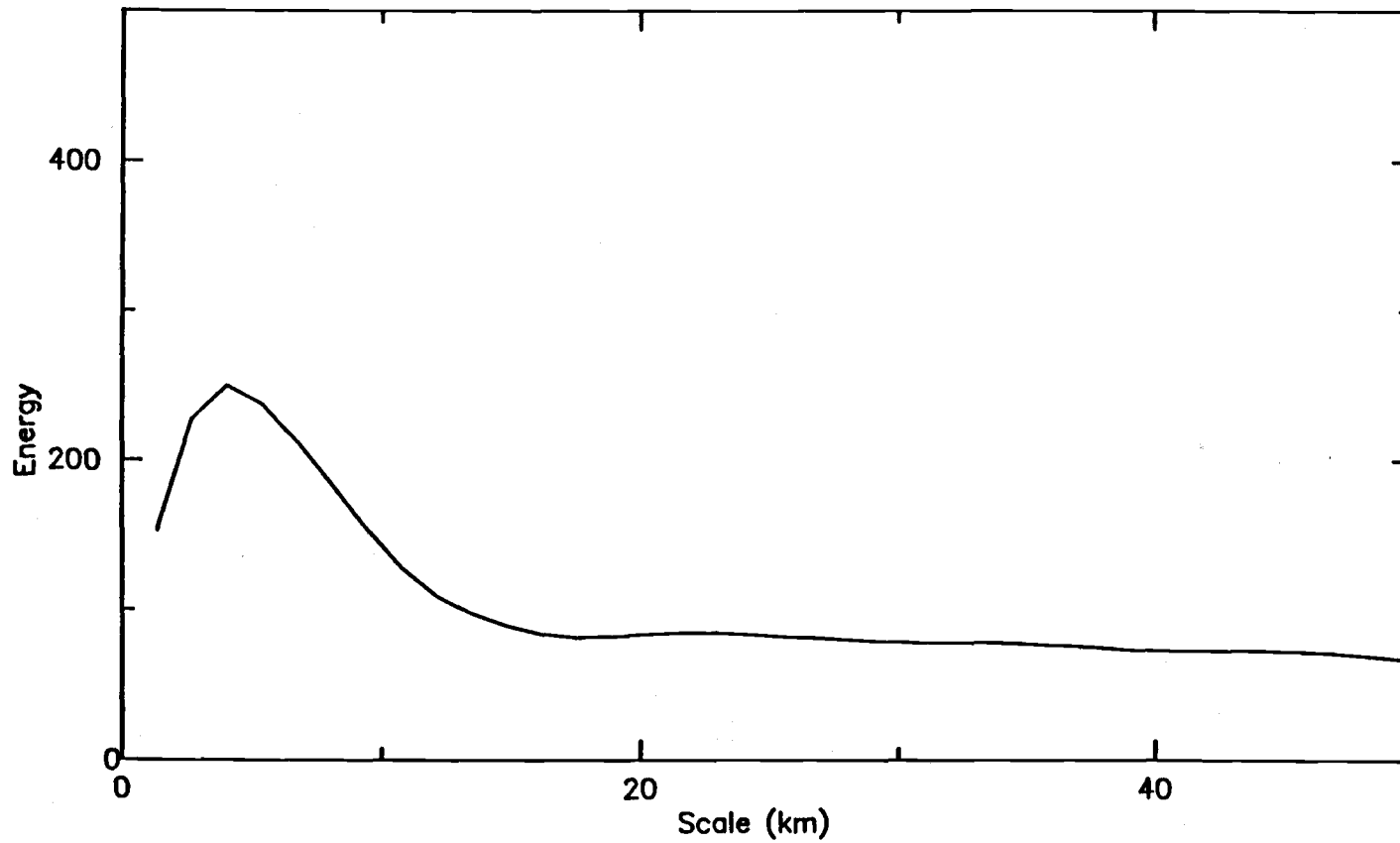


Figure 4.16 Wavelet variance of canopy gap data of second young stand (Y4) shown in figure 4.14.

**Figure 4.17** Composite plot of wavelet variances calculated for canopy gap transects established in twelve Pseudotsuga menziesii stands representing three age classes: young, mature, and old growth. The twelve wavelet variances are grouped according to group I (multi-scale, open gaps (5-30 m)), heavy dashed lines to group II (small (<8 m), diffuse gaps), light dashed lines to group III (small to moderately sized (4-15 m), open gaps), and heavy solid lines to group IV (moderately sized, diffuse gaps).

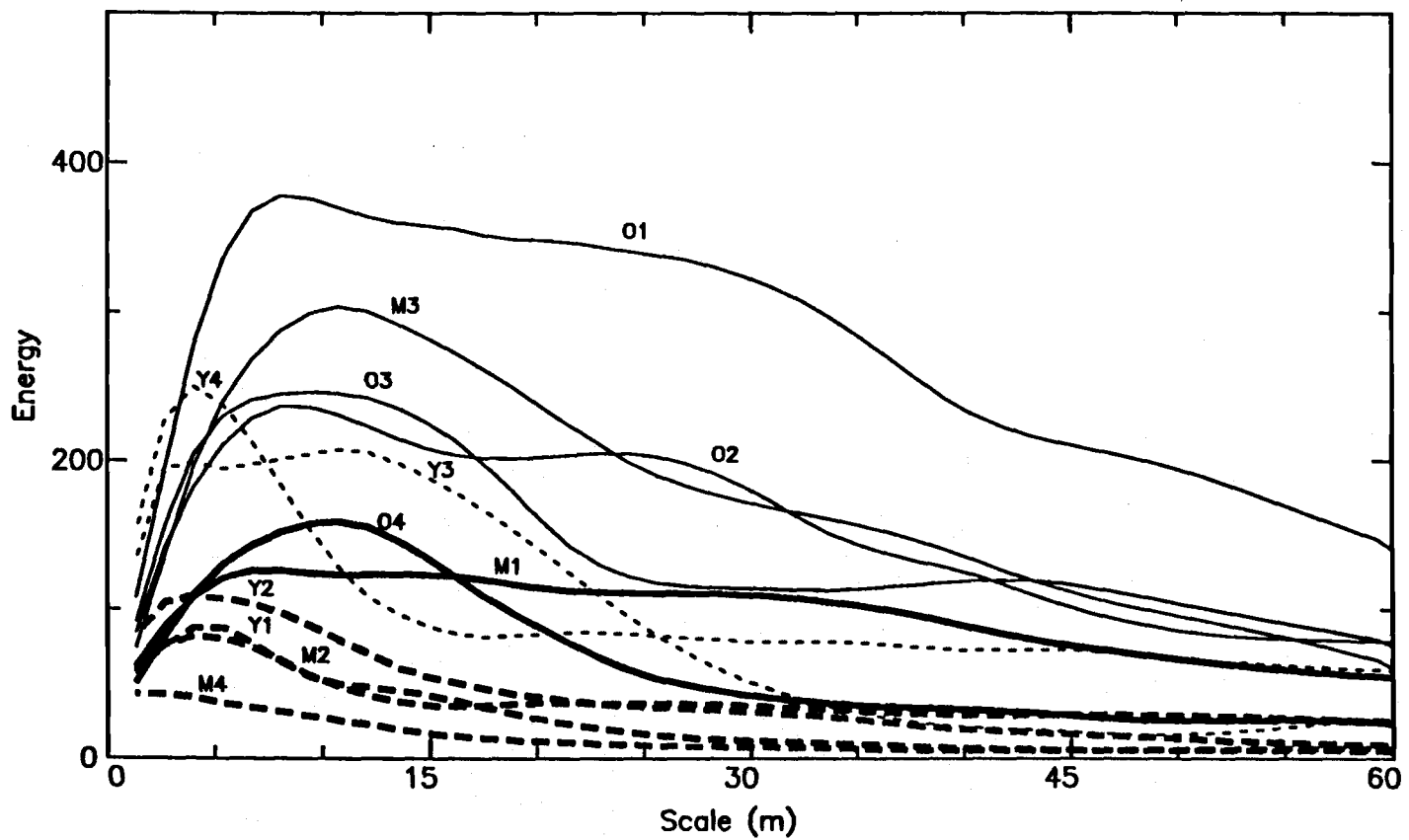


Figure 4.17

## LITERATURE CITED

- Cohen, W.B., T.A., and G.A. Bradshaw (1990). Using semi-variograms of serial videography for analysis of conifer canopy structure. *Remote Sensing of the Environment*, 34, 167-178.
- Daubechies, I. (1988). Orthonormal bases of compactly supported wavelets. *Communications on Pure and Applied Mathematics*, 41, 909-996.
- Daubechies, I., Grossman, A. & Meyer, Y.J. (1986). Painless non-orthogonal expansions. *Journal of Mathematical Physics*, 27, 1271-1283.
- Ford, E.D. & Renshaw, E. (1984). The interpretation of process from pattern using two-dimensional spectral analysis. *Vegetatio* 56, 113-123.
- Gamage, N.K.K. (1990). Detection of coherent structures in shear induced turbulence using wavelet transform methods. *American Mathematical Society Symposium on Turbulence and Diffusion*, Roskilde, Danmark.
- Journel, A.G. & Huijbregts, C. (1977). *Mining Geostatistics*, Academic Press, 617 pp.

- Kenkel, N.C. (1988). Spectral Analysis of hummock-hollow pattern in a weakly minerotrophic mire. *Vegetatio* 78, 45-52.
- Lieberman, M., Lieberman, D. & Peralta, R. (1989). Forests are not just swiss-cheese: canopy stereogeometry of non-gaps in tropical forests. *Ecology*, 70(3), 550-552.
- Mallat, S.G. (1988). Review of multi-frequency channel decompositions of images and wavelet models. Robotics report no. 178, Courant Institute of Mathematical Sciences, New York University, New York.
- Mueller-Dombois, D. and Ellenberg, H. (1974). *Aims and Methods of Vegetation Ecology*. John Wiley and Sons, New York. 546 pp.
- Platt, T, & Denman, K.L. (1975). Spectral analysis in ecology. *Annals of Ecological Systems* 6, 189-210.
- Priestley, M.B. (1981) *Spectral Analysis and Time Series*. Academic Press, 890 pp.
- Spies, T. A. & Franklin, J.F. (1990). The structure of natural young, mature, and old-growth forests in

Washington and Oregon. in Old Growth Symposium GTR,  
1989.

Spies, T. A., Franklin, J.F. & Klopsch, M. (1990). Canopy  
gaps in Douglas-fir forest of the Cascade Mountains.  
Canadian Journal of Forest Research 20, 649-659.

Turner, S.J., O'Neill, R.V., Conley, W., Conley, M. &  
Humphries, H. (1991). Pattern and Scale: statistics  
for landscape ecology. in M.G. Turner & R.H. Gardner,  
editors, "Quantitative Methods & Landscape Ecology".  
Springer Verlag.

## Chapter 5

SPATIALLY CORRELATED PATTERNS BETWEEN UNDERSTORY  
VEGETATION AND AGE-RELATED GAP STRUCTURE  
IN DOUGLAS-FIR FORESTS

by

G.A. Bradshaw

**ABSTRACT**

Transects from twelve Douglas-fir stands located in the Pacific Northwest representing three broad age classes: young (40-75 years), mature (80-200 years), and old growth (> 200 years), were used to identify trends in vegetation life-form cover across stand age classes and spatial relationships between overstorey gap structure and understorey vegetation. With the exception of herbs and hemlock seedlings, distinct trends between stand age and amounts of understorey life-form cover were not observed; variability within age classes dominated across age trends.

Calculation of the wavelet cross-covariance function allowed for the identification of certain spatial correlations between understorey vegetation and two resource variables: canopy gap structure and total woody debris. Consideration of the spatial information derived from wavelet

analysis revealed that the spatial distributions of the overstorey and understorey did reflect stand age. On average, herb, low shrub, tall shrub, and hemlock seedling patch size generally increased with stand age. Deviations from these correlation trends were identified with differences in the abundance of overstorey hemlock and allogenicly derived disturbance gaps. These results illustrate the importance of including spatial information and system heterogeneity in analysis of forest systems.

## INTRODUCTION

The view of plant community succession has traditionally been viewed from a purely floristically based (i.e. autogenic) perspective or one which emphasises environmental (i.e. allogenic) factors. More recent approaches have been developed which obviate the necessity to choose between these two schools of thought (Connell and Slatyer (1977); Oliver, (1982), Waring and Schlesinger, (1983)). These analyses focus on the various mechanisms governing plant community dynamics (e.g. mechanisms based on plant life-histories such as facilitation, tolerance, and inhibition). While much of forest community development may be determined by knowledge of the life-histories of the species present and environmental site factors, the type and history of disturbance plays an important role in the determination of a given succession pathway (Halpern, 1989). Natural disturbances ranging from the landscape scale (e.g. fire) to within-stand scale (e.g. single to several tree windthrow) are now recognized as critical factors in the development of community structure and composition (Halpern, 1989; Spies and Franklin, 1990). Succession is no longer regarded as a monotonic progression of species toward the climax community, but instead mediated by a series of complex interactions between plants species and their environment at many different temporal and spatial scales.

From the functional or ecosystem approach, disturbances result in re-allocation of resources within the stand (Vitousek, 1985). For example, in the Douglas fir forests of the western Cascades, Oregon, disturbance events such as single-tree windthrow and root rot often characterise many forest stands (Spies et al, 1988; Spies and Franklin, 1990). Differences in canopy structure among stands result from a combination of varying crown and gap sizes which in turn are related to stand development and disturbance history. The formation of canopy gaps allows light to reach the forest floor thereby shifting the moisture and temperate resource from the overstorey tree to the previously shaded area below. Similarly, fallen tree boles increase moisture availability along the forest floor. These nurse logs function as germination "hotspots" for overstorey tree seedlings.

Small-scale disturbance events increase canopy and forest floor substrate heterogeneity creating a mosaic of micro-environments throughout the stand in response to newly available "patches" of light, moisture and nutrient resources. Although certain trends in species' distribution and abundances may be recognizable, much variability at the single to several tree scales is influenced by local disturbance events. As a result, forest understorey conditions reflect changes effected by stand maturation processes and allogenic disturbance events.

While much attention has focused on overstorey species

and their response to disturbance, the role and form of understorey vegetation through succession in Douglas fir forests has only recently been studied (Zamoro, 1981; Halpern and Franklin, 1990). The forest understorey plants of Douglas-fir forests in the Pacific Northwest are chiefly responsible for providing ecosystem diversity in an otherwise plant species-poor system (Alaback and Herman, 1988). The form and abundance of understorey vegetation in Douglas-fir forests of the western Cascades play an important role in succession. For example, overstory seedling establishment and survivorship may either be promoted or inhibited depending on the amount and type of understory species present. These plants provide the lateral and vertical structural diversity requisite for wildlife cover and forage. Architecture of the understorey may also affect the spread and intensity of forest fires by creating a fuel ladder from surface to crown (Agee, 1989). Because shrubs and herbs are involved in forest nutrient cycling and productivity, they may have both a positive (facilitation) and negative (competition) influence on overstory seedling establishment and survivorship.

Field experiments (Halpern and Franklin, 1990; Alaback, 1981; Zamoro, 1981) generally concur with traditional models of physiognomic change through succession; appearance and dominance in the understorey vegetation follow a sequential replacement of life-form of increasing stature, e.g. low-growing herb species are followed by low and tall shrubs with

eventual dominance and replacement by overstorey saplings (Zamoro, 1981). While this description may predict general trends in forest physiognomy through succession, it does not account for significant variability observed in the field nor does it predict the effects of allogenic disturbance on understorey distributions. In a field study of *Picea/Tsuga* forests in Alaska, Alaback (1981) observed that while certain trends in the distributions of understorey plants with forest age classes were apparent, factors such as canopy density and overstorey foliar biomass played an equally important role in understorey vegetation composition and structure.

The present paper examines the relationship of understorey community vegetation structure to stand age and structure using twelve transects of canopy and understorey cover measurements from three broad age classes of Douglas fir (*Pseudotsuga menziesii*)/western hemlock (*Tsuga heterophylla*) stands located in the western Cascades of Oregon and Washington. These data were used to assess understorey vegetation cover and spatial patterns as a function of stand age-class. Because of the limited number of transects (i.e. four transects per age group) and the fact that inferences regarding a stand were based on a single transect, certain assumptions were made.

## Assumptions

The main assumption underlying the analysis was that the observed composition and structure of the forest stands sampled reflected present physical conditions. Furthermore, in the absence of disturbance or legacies left from disturbance, canopy gaps were assumed to increase in amount with age as observed (Chapter 4). Deviations from this trend (e.g. the presence of sizeable gaps in a young stand) were inferred as evidence of local disturbance (Bradshaw and Spies, in press). Gaps inferred to result from disease, fire, or insect predation are referred as allogenuically derived disturbance gaps as opposed to canopy structure resulting from autogenic processes such as tree competition and thinning.

Amounts of understorey vegetation cover was viewed as a response variable susceptible to microclimatic and edaphic factors (i.e. light and moisture availability). Specifically, canopy gaps and substrate woody debris were used as two independent "resource" variables representing light and seed bed moisture availability, respectively. The magnitude of the spatial correlation between a resource variable (e.g. canopy gap) and a response variable (e.g. herb cover) was used to infer a causal relationship.

## STUDY AREA

The study area lies primarily in the Tsuga Heterophylla vegetation zone with majority of tree species consisting of Douglas-fir (Pseudotsuga menziesii), western hemlock (Tsuga heterophylla), and western redcedar (Thuja plicata) in the western Cascades of Oregon and Washington (Franklin and Dyrness, 1984). Douglas-fir is the seral dominant species at elevations below 1000 meters. Western hemlock typically occurs as a codominant species eventually replacing Douglas-fir or occasionally occurring as an seral species.

Transects from twelve Douglas fir stands representing three age-classes (young (40-75 years), mature (80-200 years) and old growth (> 200 years) were established. Percent vegetation cover (Daubenmire, 1968) representing four life-form classes (i.e. tall shrubs, low shrubs, herbs, and hemlock seedlings), total woody debris abundance, and canopy gap measurements were taken at one meter intervals along 200 meter transects in four stands from each of the three age classes (field data collected by T.A. Spies). The life-form class "tall shrub" included species such as Rhododendron (Rhododendron macrophyllum) and vine maple (Acer circinatum). "Low shrubs" included species such as Oregon grape (Berberis nervosa). Hemlock regeneration "seedlings" included seedlings and saplings less than 5 centimeters dbh (diameter breast height).

Percent vegetation cover was measured in twenty percent increments ranging from 0 to 100 percent. Thus, each data "point" was in actuality an area of one meter squared. The stands were selected to minimize differences between slope, aspect, topography, and soils. Each transect was started from a randomly chosen point running parallel to slope contours. Canopy gap estimates were made using a modified moosehorn Mueller-Dombois and Ellenberg, 1974). The data transects of the six variables (herb, low shrub, tall shrub, hemlock seedling, canopy gap and woody debris) are shown in Figure 5.1-5.6)

## METHODS

Analysis of variance was performed on each of the variables independently to test for differences in the amounts of the overall percent cover for each variable between age-classes. Prior to calculation the data were transformed using a modified logit transformation to render the data normal in distribution:

$$y = \ln\left(\frac{z+0.1}{\alpha-(z+1)}\right)$$

where  $y$  is the transformed value of datum  $z$  and  $\alpha$  is equal to 101.

Wavelet analysis was performed to quantify the overall amount of canopy gap, total woody debris, and understory vegetation cover per stand. The wavelet variance for each life-form and resource variable was calculated to estimate the overall cover and average patch size of each of the six variables per stand. The total wavelet variance, equal to the wavelet variance integrated across scales, was used as an estimate of the total cover in the stand. Greater areas under the function correspond to greater percent cover. Conversely, shallow functions corresponded to low abundances. The scale at which the maximum wavelet variance occurred was used to infer the dominant patch of the variable. Several resultant wavelet

variances were characterized by more than one peak or a very broad peak indicating the presence of multi-scale phenomena. In these cases, the peak at the larger scale was chosen to represent the average patch size.

Additionally, each stand was ranked per age group according to the total cover of total woody debris, percent gap cover, and amount of western hemlock present in the overstorey (Table 5.1). The relative amounts of woody debris cover were used to infer potential seedbed sites for the seedlings. Increased canopy gap opening was used to infer increased availability of light to the understorey below. Estimates of the total woody debris and canopy gap cover amounts was obtained from the calculation of the wavelet variance as discussed. Overstorey hemlock abundances were estimated qualitatively from field observations. Stands with overstorey hemlock were used to infer a more dense canopy (as compared with pure Douglas-fir).

The second part of the wavelet analysis, the wavelet cross-covariance, was performed to identify and quantify the spatial relationships between local resource availability (estimated by canopy gap and substrate total woody debris) and the four physiognomic understory classes (herb, low shrub, tall shrub, and hemlock seedlings). This function provides a measure of the spatial correlation between two variables as a function of scale and lag. The lag is defined as the amount in spatial offset in meters between the

correlated pair of variables. The lag at which the maximum correlation occurs provides a measure of the degree to which gap structure (or woody debris) and understory vegetation distribution were linked in each stand. For example, a high correlation at a given scale at zero lag indicated that patches of vegetation occurred coincident with the projection of the canopy gaps of the same scale. A lack of correlation at zero-lag or a high value at a non-zero lag indicated that the two variables were not closely coupled in space, e.g. the occurrence of understorey life-form patches were not coincident with the overlying canopy gaps. In this case, the lack of spatial correlation would be inferred as an absence of a causal relationship or a reflection of offset effects. The results of the analysis were used to infer light and moisture patterns by identifying the correlation between canopy gap and total woody debris with understorey physiognomic classes.

## RESULTS

### Trends in Vegetation and Resource Cover

Excluding the herb vegetation class and woody debris abundances, no statistically significant differences between age-classes were found in the four understory vegetation classes using a nested ANOVA scheme (Table 5.2). The variability within individual age classes was much greater than differences between age classes.

Overall cover amounts did not increase systematically with stand age with the exception of herb and hemlock seedling cover as estimated by total wavelet variance (Table 5.3). Herb cover was generally low relative to other life-form classes (Figure 5.7) increasing with stand age (Figure 5.8), and decreasing with increased abundance of hemlock in the canopy (Table 5.1). Average herb patch size increased with stand age (Figure 5.9). O1 was characterized by very large patches (20 meters) of herbs while other stands were generally dominated by patches less than 10 meters (Figure 5.7).

Hemlock seedling cover showed a gradual increase with stand age (Figure 5.10) and woody debris cover (Figure 5.11) but no positive relationship with canopy gap opening (Figure 5.12). Stands with high levels of woody debris generally had greater levels of hemlock seedling cover (M1 and M2; Figures

5.13 and 5.14). Hemlock seedling patch size also increased with stand age (Figure 5.15) although woody debris patch size did not change (Figure 5.16). Woody debris cover did not show a systematic relationship with age (Figure 5.17). High values characterized young stands and mature stands dropping to low to moderate levels in old growth stands (Figure 5.13).

Neither low shrubs nor tall shrubs showed a positive trend similar to herbs in terms of total cover (Figures 5.18 and 5.19) or patch size (Figures 5.20 and 5.21). Tall shrub cover showed a sensitivity to the presence of canopy gaps (Figure 5.22) and overstorey hemlock (Figure 5.23 and Table 5.1). Tall shrub cover was higher in young and mature stands characterized by moderate to large-sized (5-15 meter diameter) gaps (Y3, M1, M3; Figure 5.24); percent cover was lower in stands with a closed canopy or overstorey hemlock (Table 5.1). Young (Y1), even-canopied older (O4) or hemlock dominated (M4) stands had low amounts of tall shrub understorey (Figures 5.24, Tables 5.1 and 5.3). The three oldest old-growth stands (O1, O2, O3) all had moderate amounts of tall shrubs found in patch sizes ranging from 5-20 meters.

Low shrub cover increased with canopy gap opening as estimated from total wavelet variance (Figure 5.25). Generally speaking, mature stands (M2, M3, M4) were characterized by low to moderate abundances of low shrubs of small (< 8 meters) patch sizes (Figure 5.26). The older old-

growth stands (O1, O2, O3) grouped together having moderate to high abundances of low shrubs of moderate (<15 meters in stands O2 and O3) to large (8-20 meters in stand O1) patches. Both O1 and O3 are characterised by two distinct low shrub patch sizes (Figure 5.26). Y1-Y4 range over a spectrum of abundances and patch sizes.

Canopy gap size and total opening as measured by the total wavelet variance generally showed an increase with age (Figures 5.27 and 5.28). However, gap size and intensity (i.e. degree of openness) decreased with the presence of hemlock in the overstory (M4) and the lack of recent exogenous disturbance (Y1, M2, O4). Older stands (O1 and O2) were characterized by distinct multi-scale gaps as indicated by high broad peaks in the wavelet variance (Figure 5.24).

#### **Spatial Correlation Between Canopy Gap and Understory Vegetation**

Wavelet cross-covariance analysis revealed that understorey vegetation spatial patterns were generally correlated with age-related gap structure; as canopy gap size increased with stand age, the patch size of the understory life-forms also increased. Figures 5.29, 5.30, and 5.31 illustrate such a progression from a young (Y1) to mature (M3) to an old-growth stand (O1) in the case of gap and low shrub patterns. Young stands were generally characterized by

fine structure of vegetation patches corresponding to the fine-scale gaps in the overstory. For example, small, low shrub patches (<4 meters) occurred coincident with overstory canopy gaps of similar scale in a stand characterised by a continuous even canopy (figure 5.29). Patch sizes of the understory vegetation tended to increase and correlate with moderately sized gaps (5-10 meters) in mature stands (figure 5.30) and large gaps and patches (20 meters) in old growth stands (Figure 5.31). A young, heterogeneous 43 year old stand (Y4) characterised by patchy disturbance history and variable site conditions yielded a correlation between tall shrubs and gap structure at a larger patch size (5-8 meters; Figure 5.32) as compared to another young, single-aged stand with a uniform canopy and lack of non-uniform disturbance history (Y1; Figure 5.33).

Older (400-600 years), more recently disturbed old growth stands (O1 and O2) often showed a strong correlation between understory vegetation patches and canopy gap at two distinct scales. For example, hemlock seedlings and canopy gap structure were correlated in patches of 5 meters in diameter and again at 25 meters in stand 120 at zero lag (Figure 5.34). This multi-scalar pattern suggests that the hemlock seedlings may respond to gaps formed by gap forming processes occurring at least two distinct scales (e.g. single versus multiple tree mortality).

Understory vegetation and seedling distributions also

followed the spatial distribution of substrate woody debris. The scales at which understory vegetation and woody debris were correlated differed from the scales at which canopy gap-vegetation patterns were correlated. For example, Figure 5.35 shows the cross-covariance for the hemlock seedlings and substrate woody debris for stand O1 described above. Although both figures 5.34 and 5.35 show two scales of correlation, their individual patch sizes differ. Hemlock seedlings and woody debris were correlated at smaller scales ( $< 3$  meters) and again at 18 meters while canopy gap and hemlock seedlings were correlated at 5 and 25 meters. A comparison of the two figures suggests that the distribution of hemlock seedlings in the understory is a composite pattern of patches related to both woody debris distributions at one set of scales and canopy gap distribution at another.

Similar correlations were not found in all cases. For example, stand M1, a mature 130 year old stand, was characterized by high abundances of woody debris and seedlings. The spatial correlation between these two variables was high, occurring in patch sizes of 9 meters at zero lag (Figure 5.36). In contrast, the canopy gap structure and seedling spatial distributions were not as closely coupled; maximum correlation occurs in patches of 8 meters but 5 meters out of phase as evidenced by non-zero lag offset (Figure 5.37). These results suggest that while seedling establishment is coupled to patterns of woody debris, the

hemlock seedling-canopy gap relationship is less explicit in this mature stand. In other cases such as mature stand M3, no spatially correlated structure is observed (Figure 5.38).

## CONCLUSIONS

A description of the patterns of understory vegetation in Douglas-fir forests was approached in two ways, by: 1) an investigation of the relationship between understory vegetation abundances and stand age excluding spatial relationships, and 2) an examination of understory spatial patterns and stand age. With the exception of herbs and woody debris, strong trends between canopy gap structure and understory life-form cover were not observed. Based on statistical assessment of the abundance of vegetation cover as a function of stand age alone, there was no marked pattern in understory physiognomy through succession.

These preliminary results suggested that local disturbance and site history modified local resource availability trends sufficiently to override age-related patterns in community structure. A second conclusion was that the use of life-form classes as a variable may have obscured age-related community patterns. Species comprising a given life-form class (e.g. tall shrubs such as *Rhododendron* and vine maple) may have very different life-histories and autecologies; life-form classification does not distinguish between individual reproductive strategies which may be very important in patch formation and development.

However, when the spatial relationships between the overstory gap structure and understory vegetation were

considered and quantified using the wavelet cross-covariance, canopy structure trends were revealed. In many instances, understorey vegetation was spatially linked to overstorey gap structure. The dominant patch size of tall shrubs, low shrubs, and herbs were showed a strong tendency to be positively correlated with overstorey gap structure. Young stands were characterized by small patches of vegetation cover that were spatially coincident with the fine-scale gap structure in the forest overstorey. In older stands characterized by two or more dominant gap sizes, patches of tall shrubs and herbs also tended to aggregate in patches of corresponding gap sizes.

The roughly linear increase in herb abundance with stand age and corresponding correlation with increased canopy gap size suggests that light availability may be an important determinant in herb establishment and survivorship. However, the explanation is likely to be more complicated as examination of the herb and canopy patterns in mature stand M3 suggests. While this stand was characterized by a porous canopy resulting from disease pockets, no corresponding response in the herb vegetation was observed. There are at least two possible explanations based on the hypothesis of light availability as a controlling resource. One possible explanation is that the high abundance of low and tall shrubs attenuates incoming light to levels physiologically comparable to those under the closed canopy. Thus, the light

gradient detected at the height of the herb layer does not vary across the closed canopy-gap interface and no distinct spatial correlation between gap and herb emerges. The presence of understory litter may physically block the establishment and growth of lower-statured plants. Calculation of the (negative) spatial correlation between understory vegetation classes would be a useful measure to assess the amount of interaction between the two physiognomic classes. A second possibility is that the time elapsed since disturbance has been insufficient to impress the gap "signature" on the herb cover below. Again, further analysis is required to evaluate these hypotheses.

Consideration of factors such as the presence of overstory hemlock and woody debris abundance also helped to elucidate deviations from age-related patterns. Stands with a high abundance of woody debris were characterized by a correspondingly high abundance of hemlock seedlings in the understory if the stands were mature or older. Young, even-canopied stands such as stand Y1 with high levels of woody debris had low to moderate amounts of hemlock seedlings. A possible explanation for the absence of strong spatial correlation between these younger stands is that there has been insufficient space and light or moisture available for seedlings to establish.

Tall shrub abundances generally increased with gap intensity and size. A decrease in the abundance of tall

shrubs, low shrubs, and gap size was associated with overstory western hemlock. This relationship has been found in other ecosystems as well (Beatty (1984)). The higher leaf area of hemlocks (c.f. Douglas fir; Oliver and Larson, 1990), increases light attenuation through the canopy thereby decreasing the amount of light available for photosynthesis (Waring and Schlesinger, 1985). In contrast to hemlock seedlings, tall shrubs generally showed a stronger correlation with areas of moderate to high light availability in the understory. There may be several explanations for this relationship: 1) certain more tolerant tall shrubs may have persisted after a disturbance such as fire which killed the less fire-tolerant hemlock seedlings and prevented seedling re-establishment, 2) light availability under the canopy is sufficient for hemlock seedlings, 3) tall shrub distribution is responding to a covariate of canopy gap structure.

As discussed in the introduction, the pattern and development of the understory vegetation plays an important role in several ways. An ability to predict patterns in the understory community could also be used to aid in the identification of stand age, structure, and condition by satellite. Because shrub reflectances can differ substantially from their conifer overstories, their presence and distribution may alter the spectral signature of the stand. An understanding of the spatial relationships between understory vegetation and disturbance versus age-related gap

structures may further refine detection and classification accuracy.

A comparison of the understory spatial patterns associated with canopy gap and woody debris distributions indicated that the observed understory vegetation distributions represent the result of a complex pattern of interacting resource variables at differing temporal and spatial scales. The degree to which a given vegetation life-form was coupled to a given resource variable changed with both stand age and site history resulting in a mosaic of vegetation patches changing through time and space as resource patterns shift with stand development.

The wavelet cross-variance was presented as an alternative method for the identification of understory-canopy gap relationships as a function of varying stand age and structure. A spatial-explicit method was chosen in response to the inability of classical statistical measures to detect patterns intuited and observed in the field. The wavelet cross-covariance was used to substantiate ecological hypotheses by quantifying these relationships. The increased use of spatial methods reflects the skepticism of the reliability of traditional significance tests as indicators of the presence of trends in ecological data (Yoccoz, 1991). As in any study, the choice of method will be determined by the study objectives and data structure.

**Table 5.1** Total woody debris, canopy gap, and overstorey hemlock of each stand ranked by overall amount of cover. Woody debris and canopy gap estimates were obtained using the wvalet variance. Overstorey hemlock represents a qualitative estimate based on field observations. Y1-Y4 are youn stands, M1-M4 are mature stands, and O1-O4 are old growth stands.

Table 5.1

<u>YOUNG</u>				
HEMLOCK				
Low	-----			High
Y3	Y2	Y1	Y4	
CANOPY GAP				
Low	-----			High
Y1	Y2	Y3	Y4	
TOTAL WOODY DEBRIS				
Low	-----			High
Y1	Y3	Y1	Y2	
<u>MATURE</u>				
HEMLOCK				
Low	-----			High
M3	M1	M2	M4	
CANOPY GAP				
Low	-----			High
M4	M2	M1	M3	
TOTAL WOODY DEBRIS				
Low	-----			High
M4	M3	M1	M2	
<u>Old GROWTH</u>				
HEMLOCK				
Low	-----			High
04	03	01	02	
CANOPY GAP				
Low	-----			High
04	03	02	01	
TOTAL WOODY DEBRIS				
Low	-----			High
04	03	02	01	

**Table 5.2** The mean, maximum, minimum, and interquartile range for each variable according to age class (O=old, M=Mature, and Y=young). Summary statistics are in transformed units; low values of percent cover are negative, high values of percent cover are positive. Results of nested ANOVA performed on each variable are included (Sig=Significance level  $Pr>F=0.0001$  at 0.05).

Table 5.2

VARIABLE		Mean	IQR	Min, Max	Sig
Gap	O	-3.0	-6.8, 0.5	-6.8, 6.0	No
	M	-3.8	-6.7, 0.5	-6.8, 6.0	
	Y	-3.4	-6.7, 0.5	-6.8, 6.0	
Tall Shrub	O	-5.4	-7.3, -2.4	-7.3, 1.4	No
	M	-5.3	-7.3, -2.2	-7.3, 1.2	
	Y	-5.3	-7.3, -2.4	-7.3, 1.1	
Low Shrub	O	-3.5	-4.0, -0.7	-7.4, 1.0	No
	M	-3.0	-4.0, -0.7	-7.4, 0.8	
	Y	-2.1	-2.3, 1.2	-7.4, 1.2	
Reg. Tree	O	-5.4	-7.1, -2.4	-7.1, 0.5	No
	M	-5.4	-7.1, -2.6	-7.1, 0.7	
	Y	-5.7	-7.1, -2.5	-7.1, 1.2	
Herbs	O	-2.8	-7.0, -1.8	-7.0, 1.5	Yes
	M	-4.5	-7.0, -3.5	-7.0, 0.5	
	Y	-5.8	-7.0, -3.5	-7.0, -1.5	
W. Debris	O	-3.5	-6.0, -2.0	-7.0, 1.5	Yes
	M	-2.0	-6.2, -2.5	-7.0, 0.6	
	Y	-3.2	-5.3, -3.0	-7.0, 1.0	

**Table 5.3** Total wavelet variance for twelve Pseudotsuga stands (%<sup>2</sup> cover) by variable. Y1-Y4=young stand, M1-M4=mature stand, O1-O4=old growth stand.

Table 5.3

<i>Stand Number</i>	<i>Herb</i>	<i>Low Shrubs</i>	<i>Tall Shrubs</i>	<i>Hemlock Seedlings</i>	<i>Canopy Gap</i>	<i>Total Woody Debris</i>
Y1	8	1011	423	2497	1092	4538
Y2	11	3384	5707	1667	1777	5349
Y3	17	4569	7876	1355	3908	4273
Y4	24	3931	2995	874	4356	2523
M1	544	3369	7526	6321	4298	5456
M2	507	2176	2176	7316	1726	6973
M3	70	2435	6096	2	7670	4119
M4	41	1699	343	2660	597	693
O1	2074	2436	4653	6556	12242	4361
O2	808	2407	2446	2120	6897	2784
O3	208	4733	2753	2735	6407	2330
O4	1244	154	2828	2121	2919	1790

Figure 5.1 Transect data for young stand Y1. Canopy gap measured in percent canopy opening.

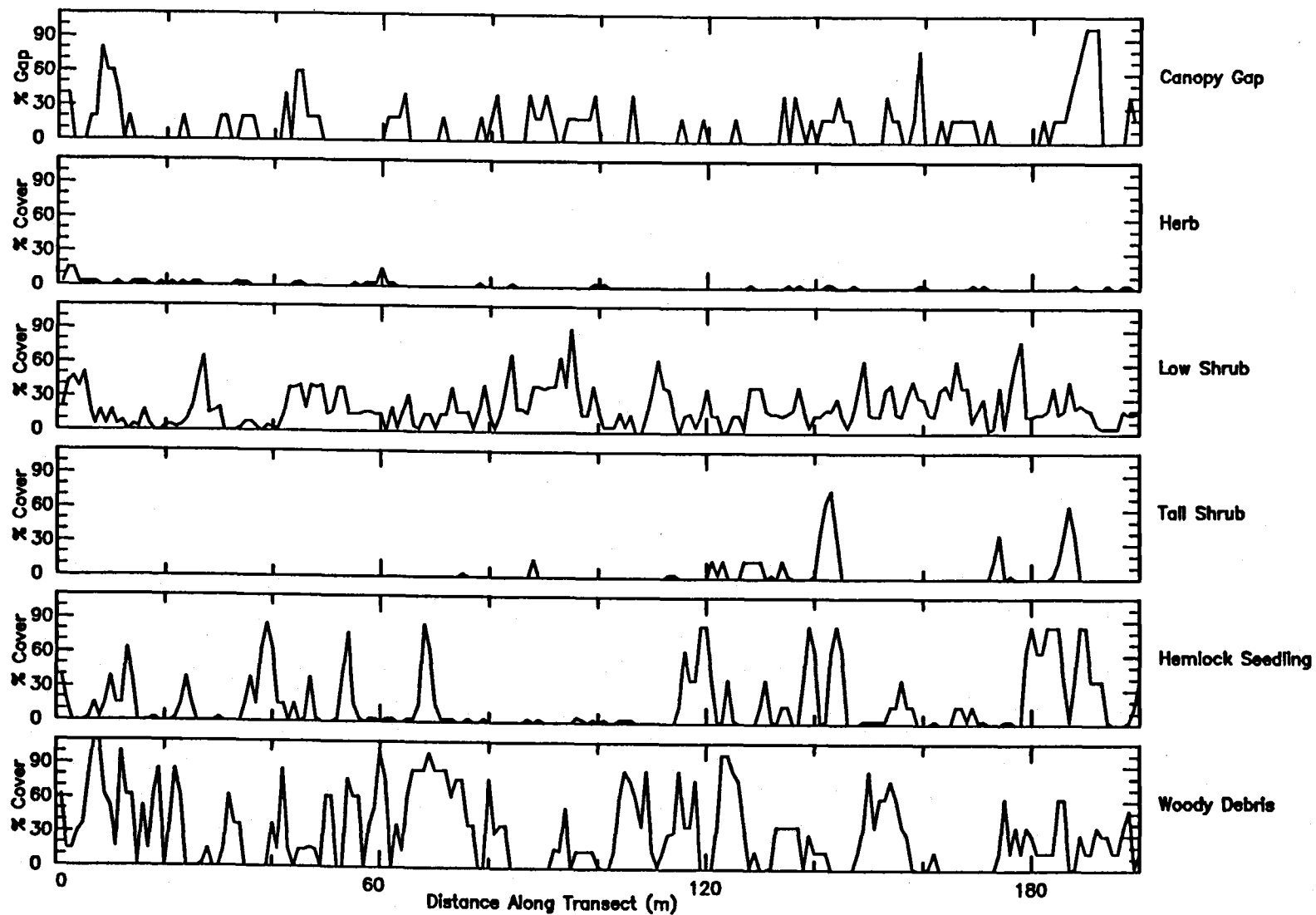


Figure 5.1

**Figure 5.2** Transect data for mature stand M1. Canopy gap measured in percent canopy opening.

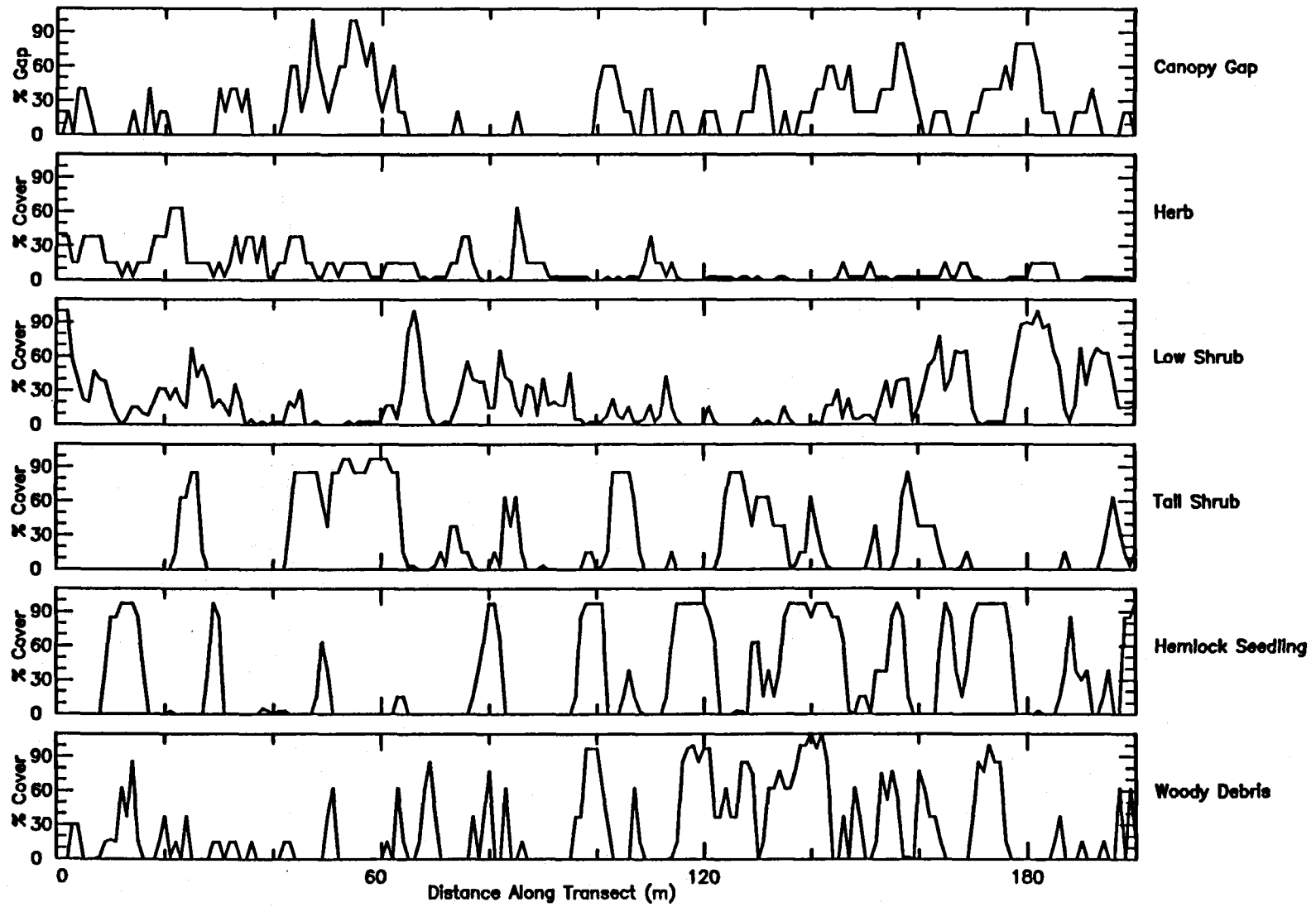


Figure 5.2

**Figure 5.3** Transect data for old growth stand 01. Canopy gap measured in percent canopy opening.

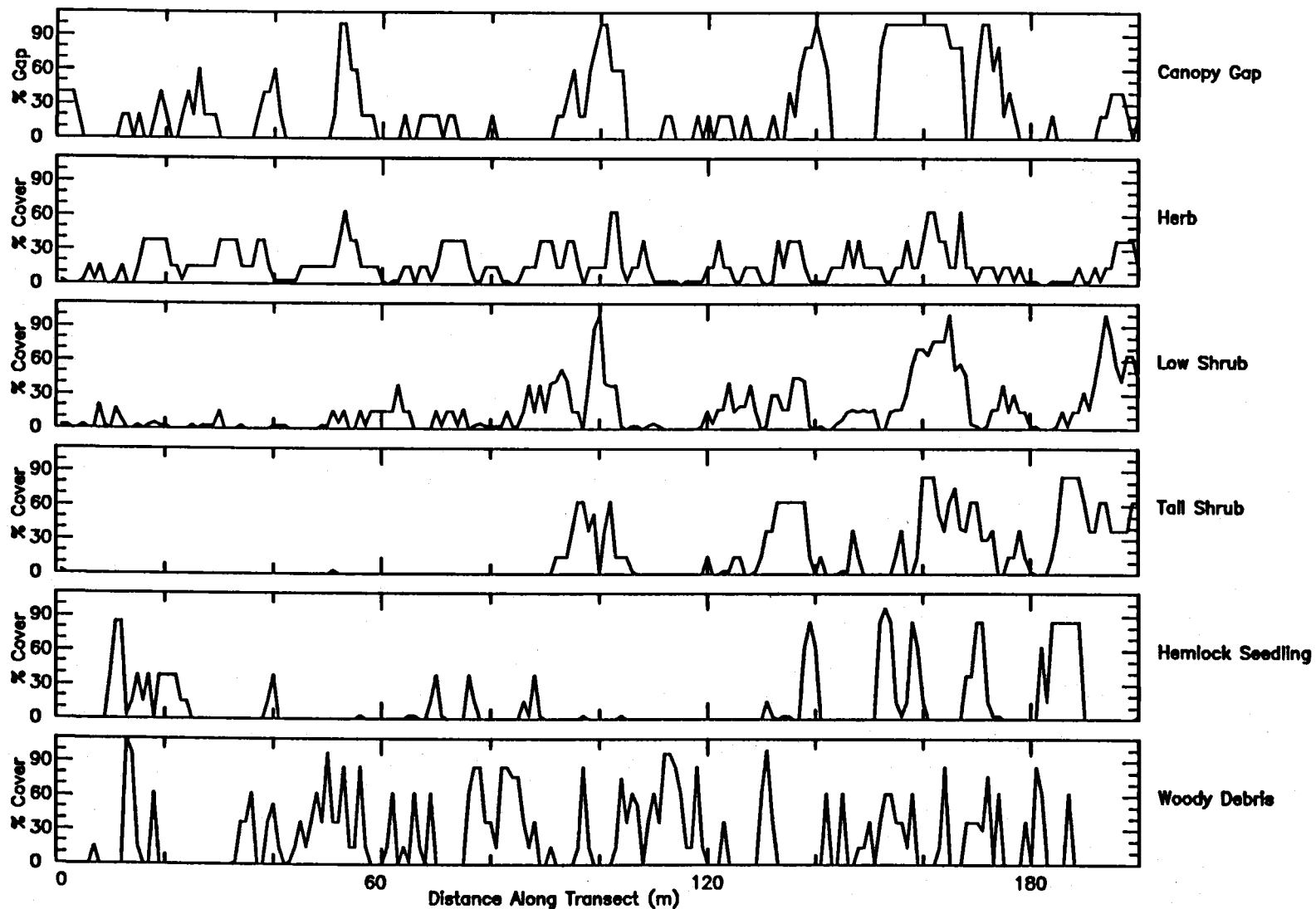


Figure 5.3

**Figure 5.4** Transect data for young stand Y4. Canopy gap measured in percent canopy opening.

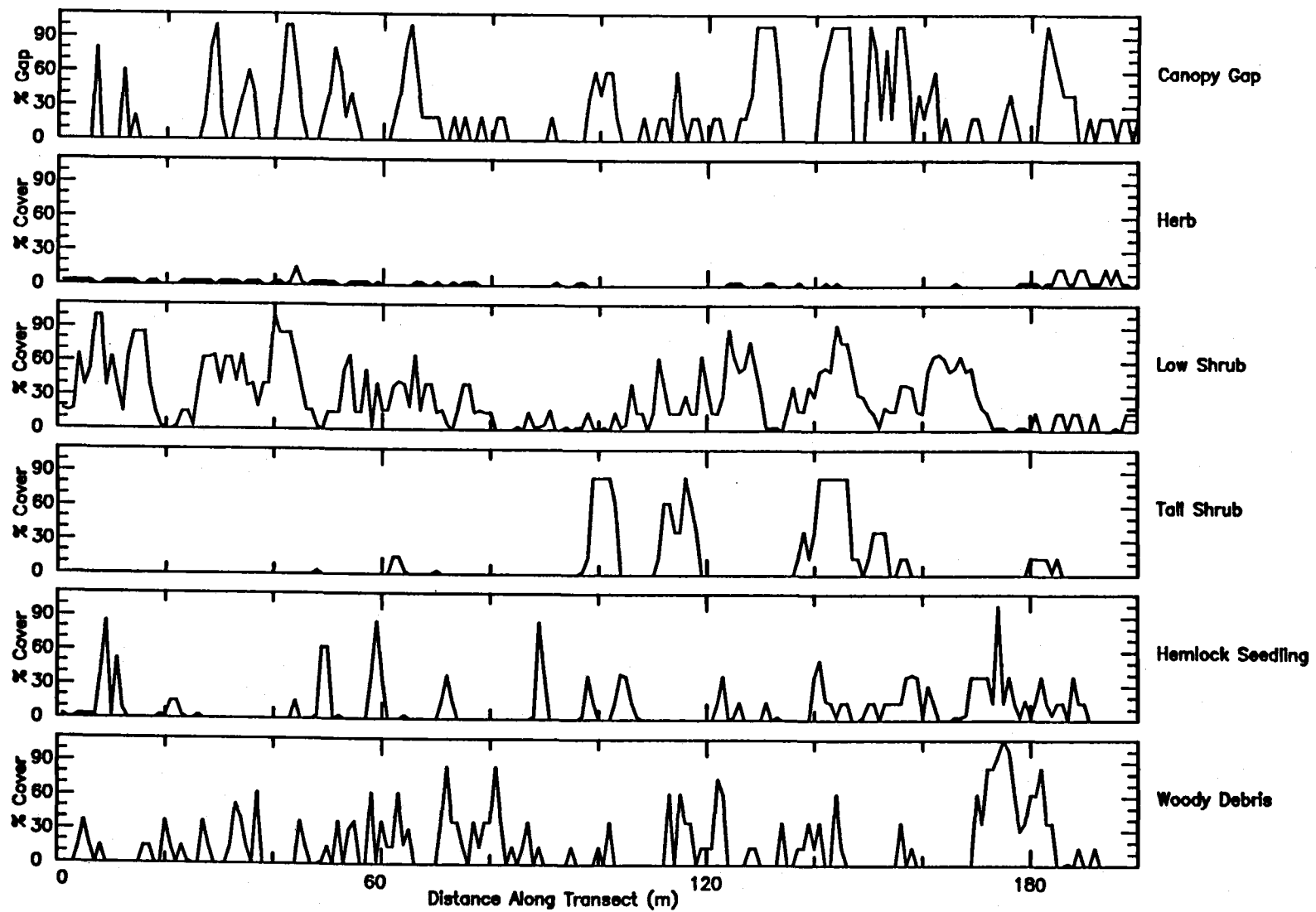


Figure 5.4

**Figure 5.5** Transect data for mature stand M3. Canopy gap measured in percent canopy opening.

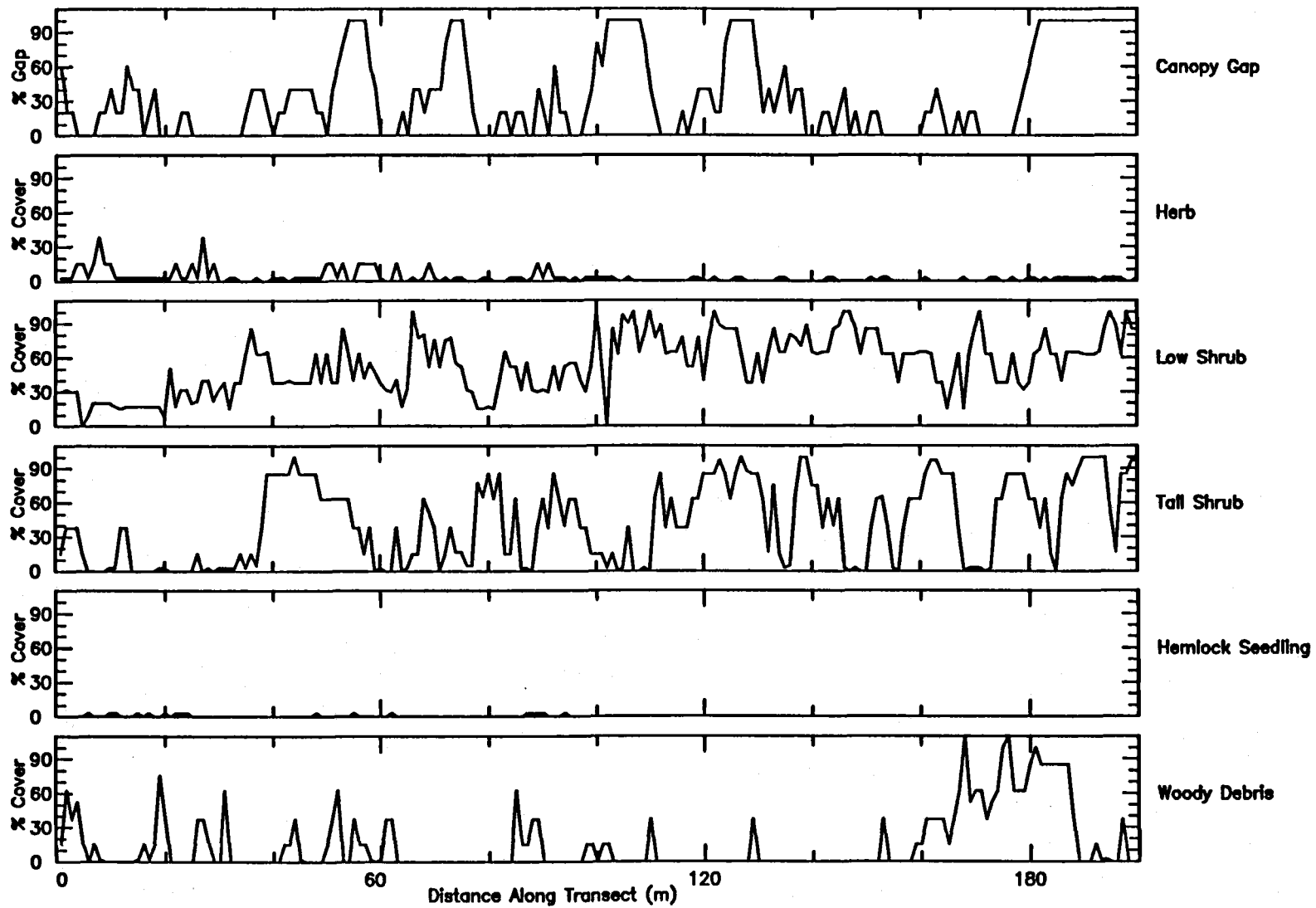


Figure 5.5

**Figure 5.6** Transect data for old growth stand O2. Canopy gap measured in percent canopy opening.

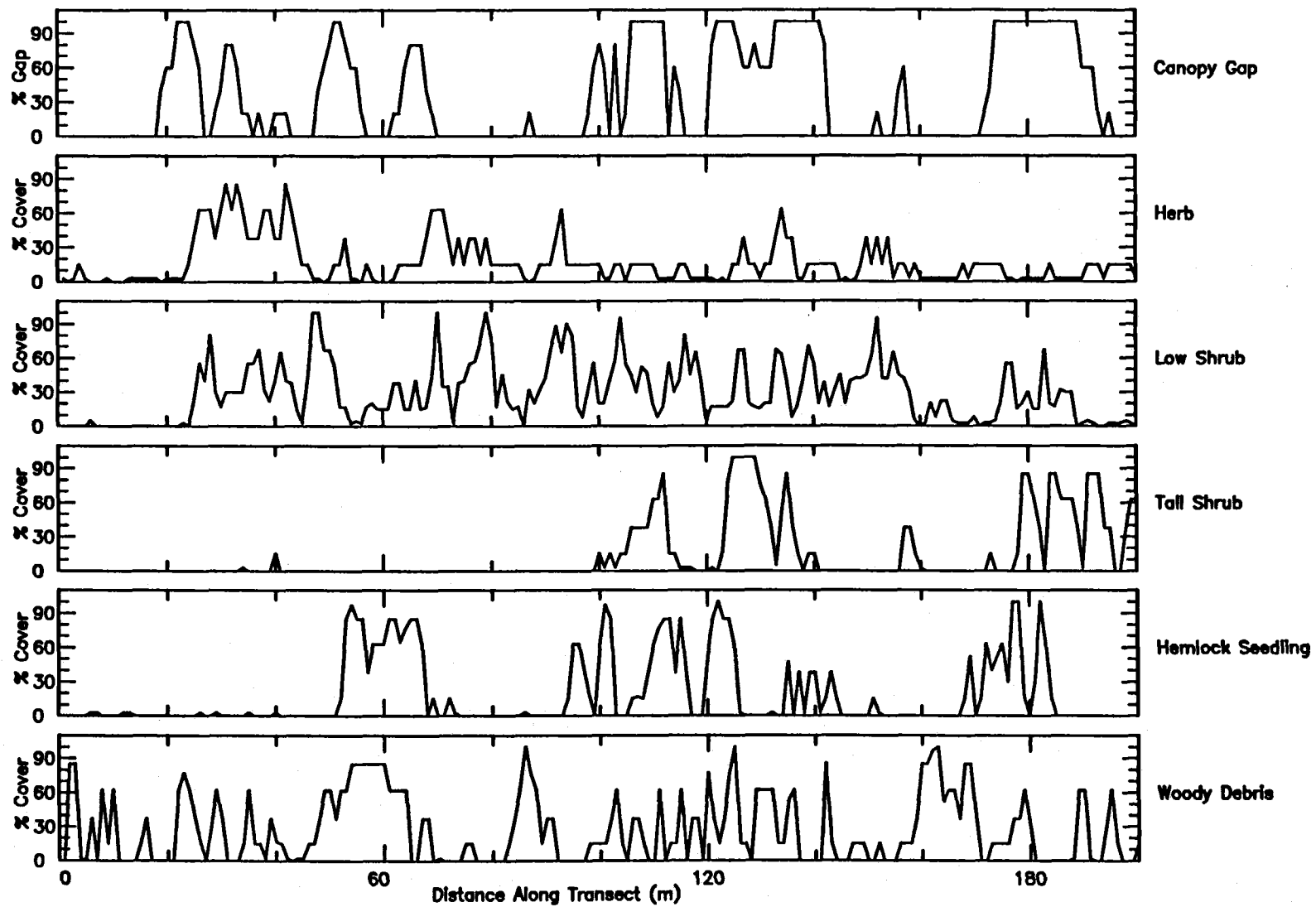


Figure 5.6

**Figure 5.7** Wavelet variance for herb cover in all twelve stands. x-axis corresponds to scale of patch size; y-axis corresponds to the magnitude of the wavelet variance at a given patch size. Y1-Y4=young stands (dashed lines), M1-M4=mature stands (solid lines), O1-O4=old growth stands (heavy solid lines).

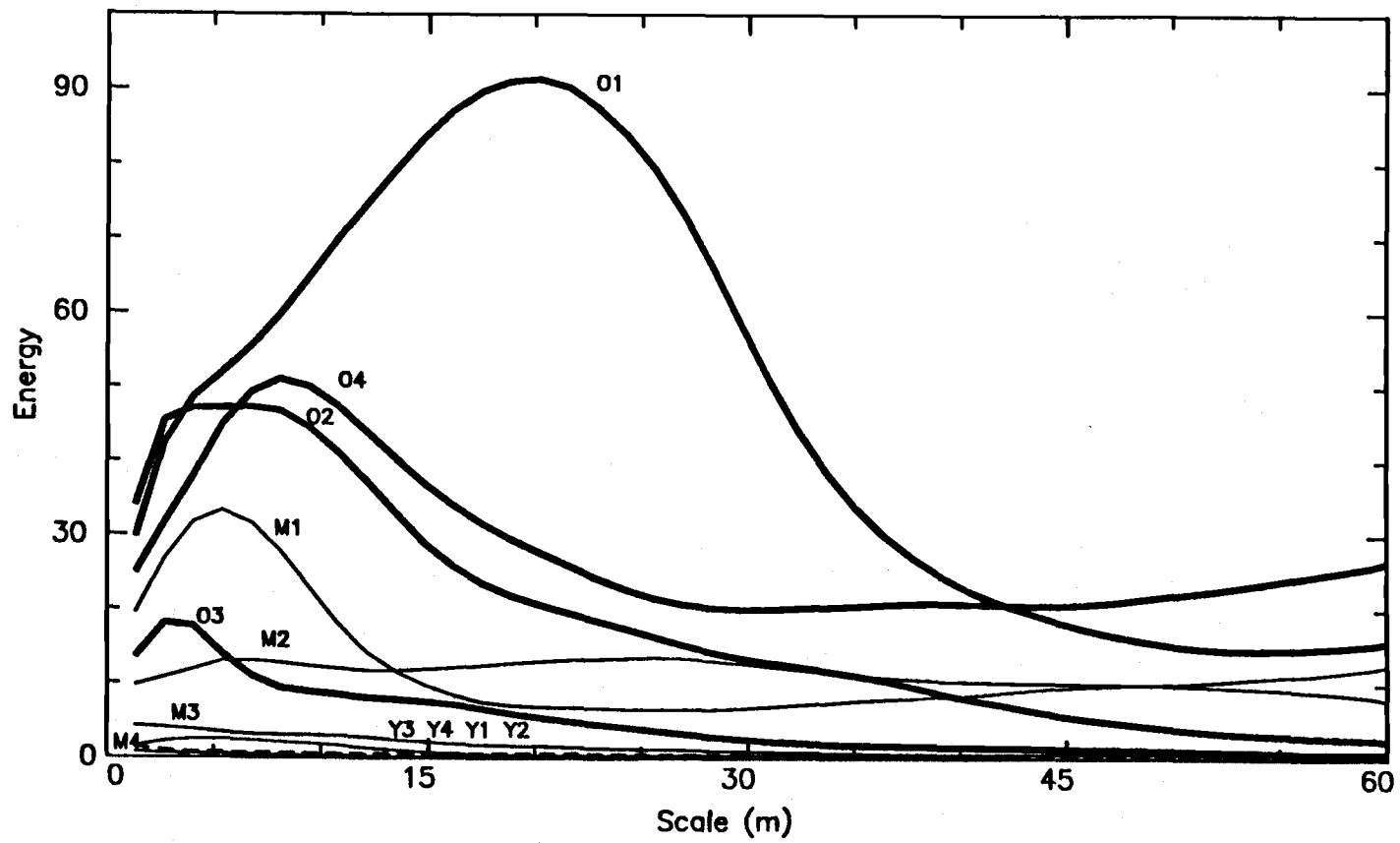
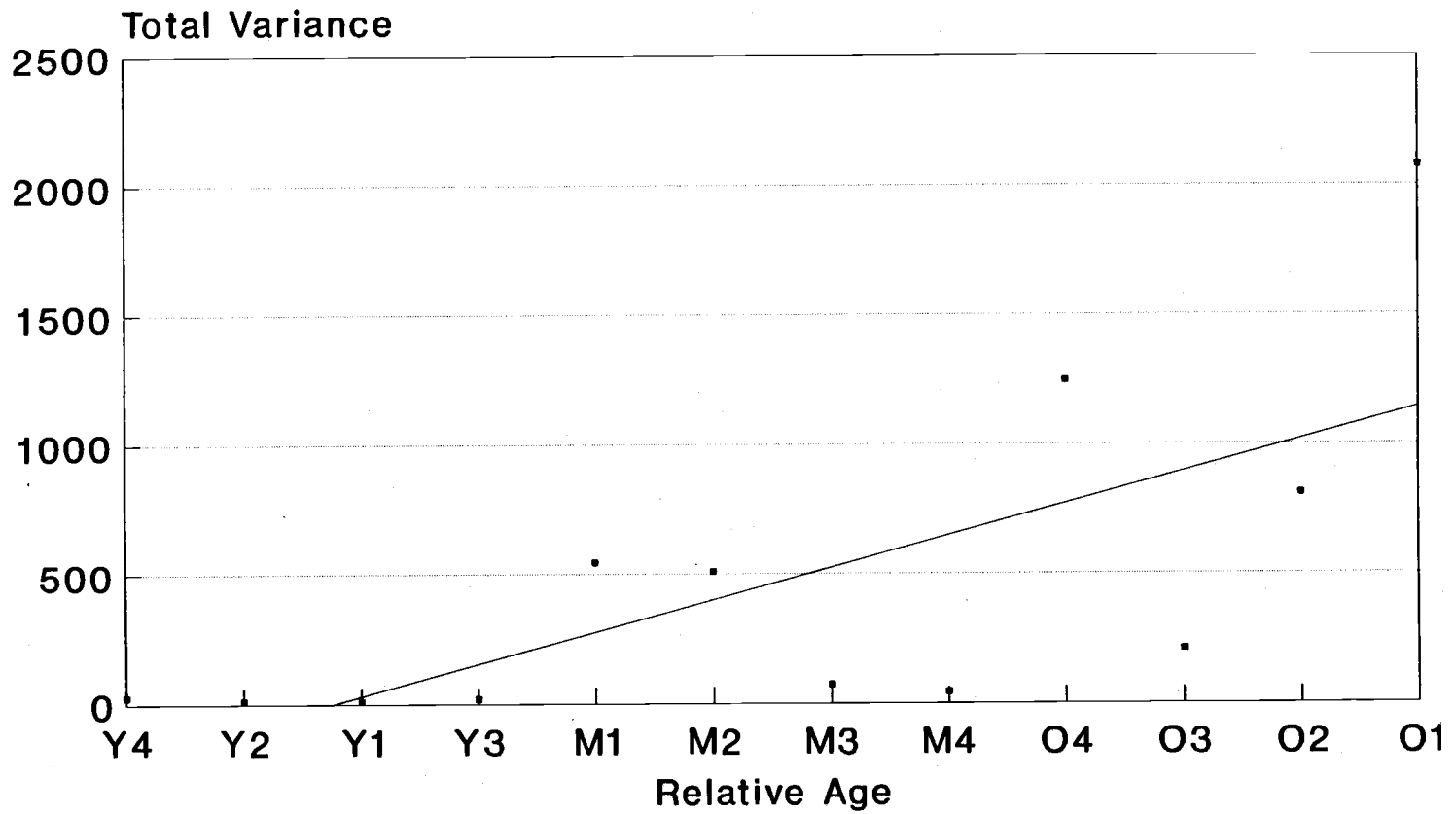
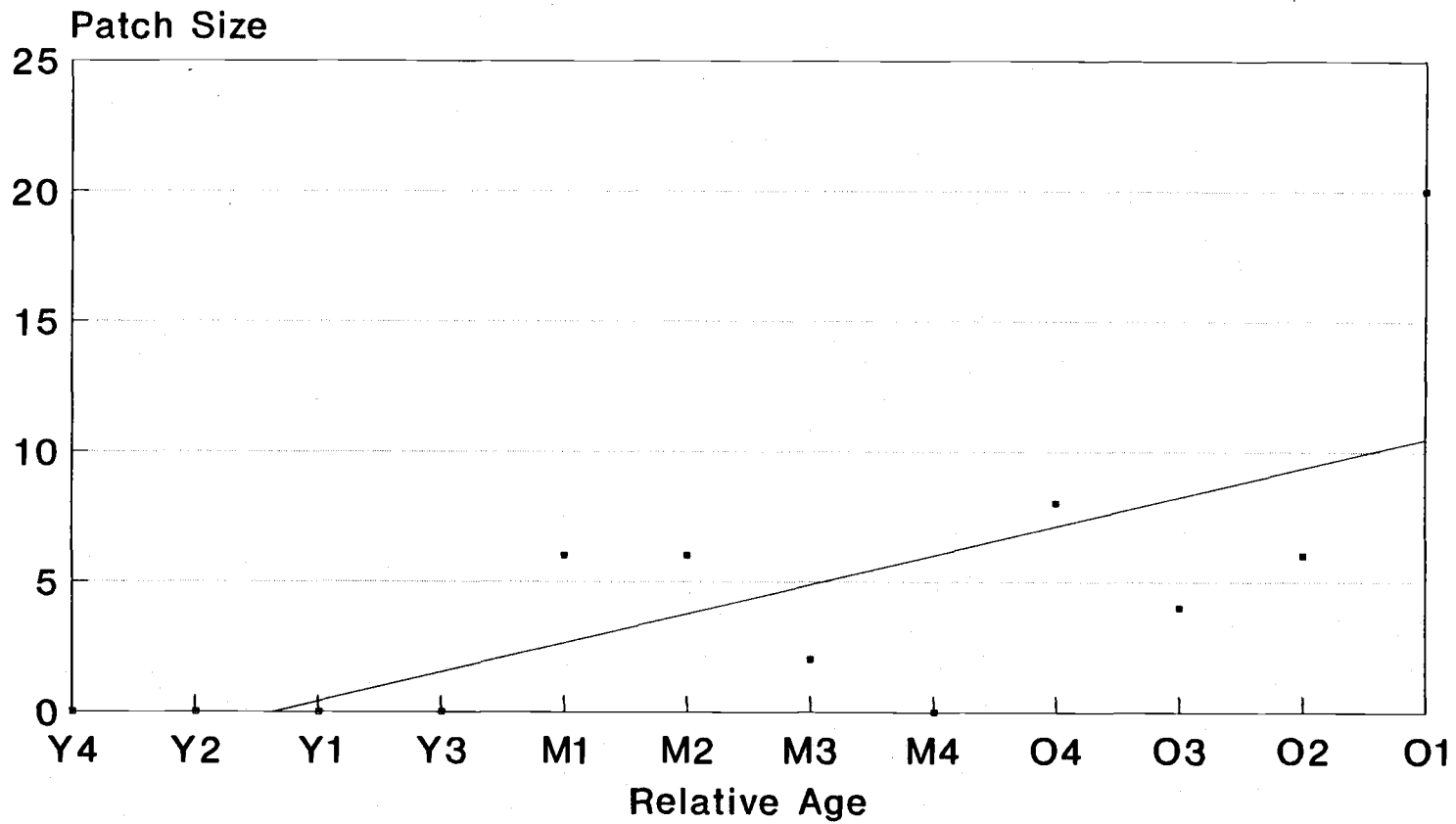


Figure 5.7



**Figure 5.8** Total wavelet variance for herb class as a function of stand age. Total wavelet variance is in units of (%<sup>2</sup> cover).



**Figure 5.9** Scale at which maximum wavelet variance occurs in meters (average patch size) as a function of relative stand age for herb class.

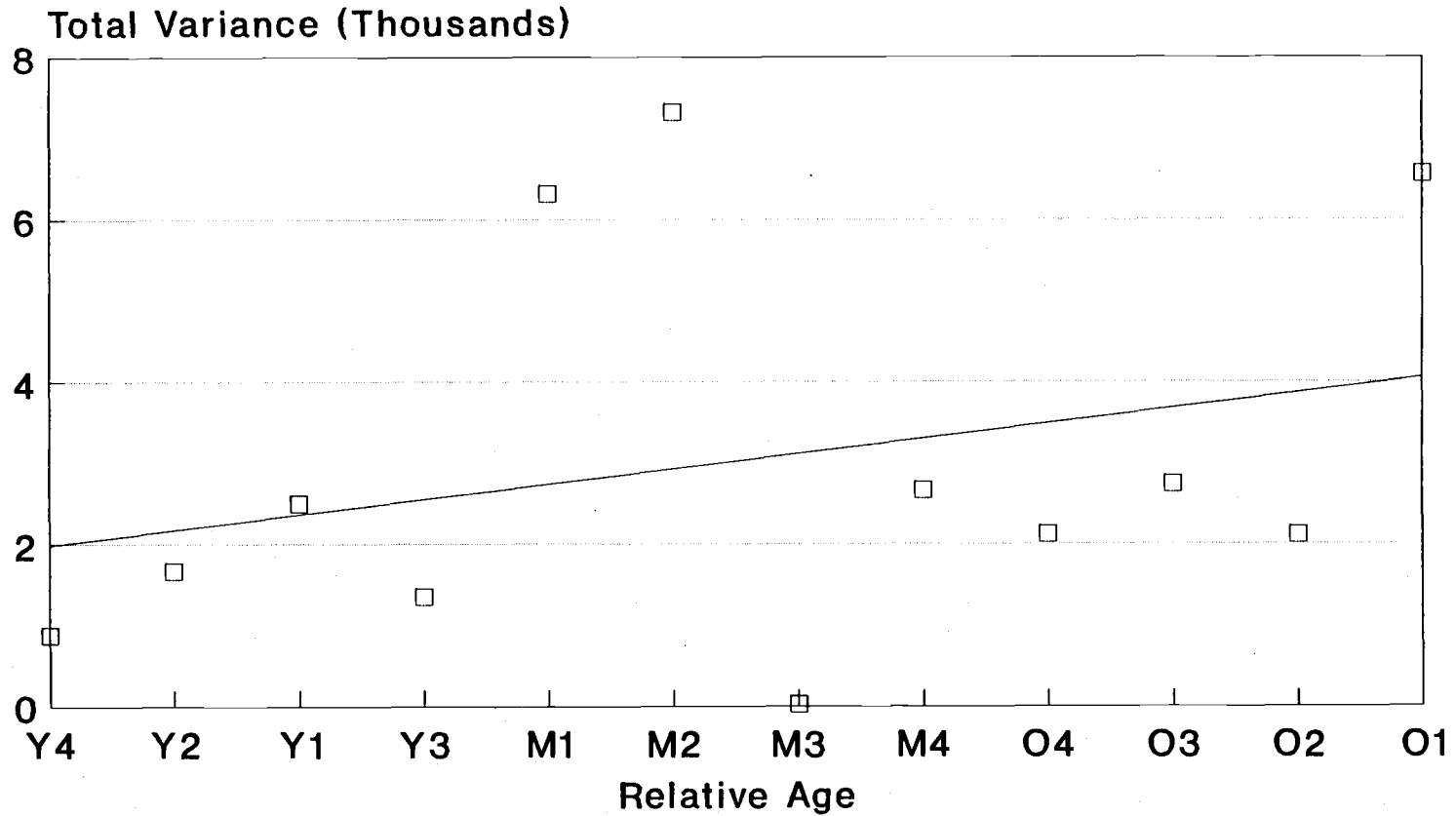


**Figure 5.10** Total wavelet variance for hemlock seedling class as a function of stand age. Total wavelet variance is in units of (%<sup>2</sup> cover).

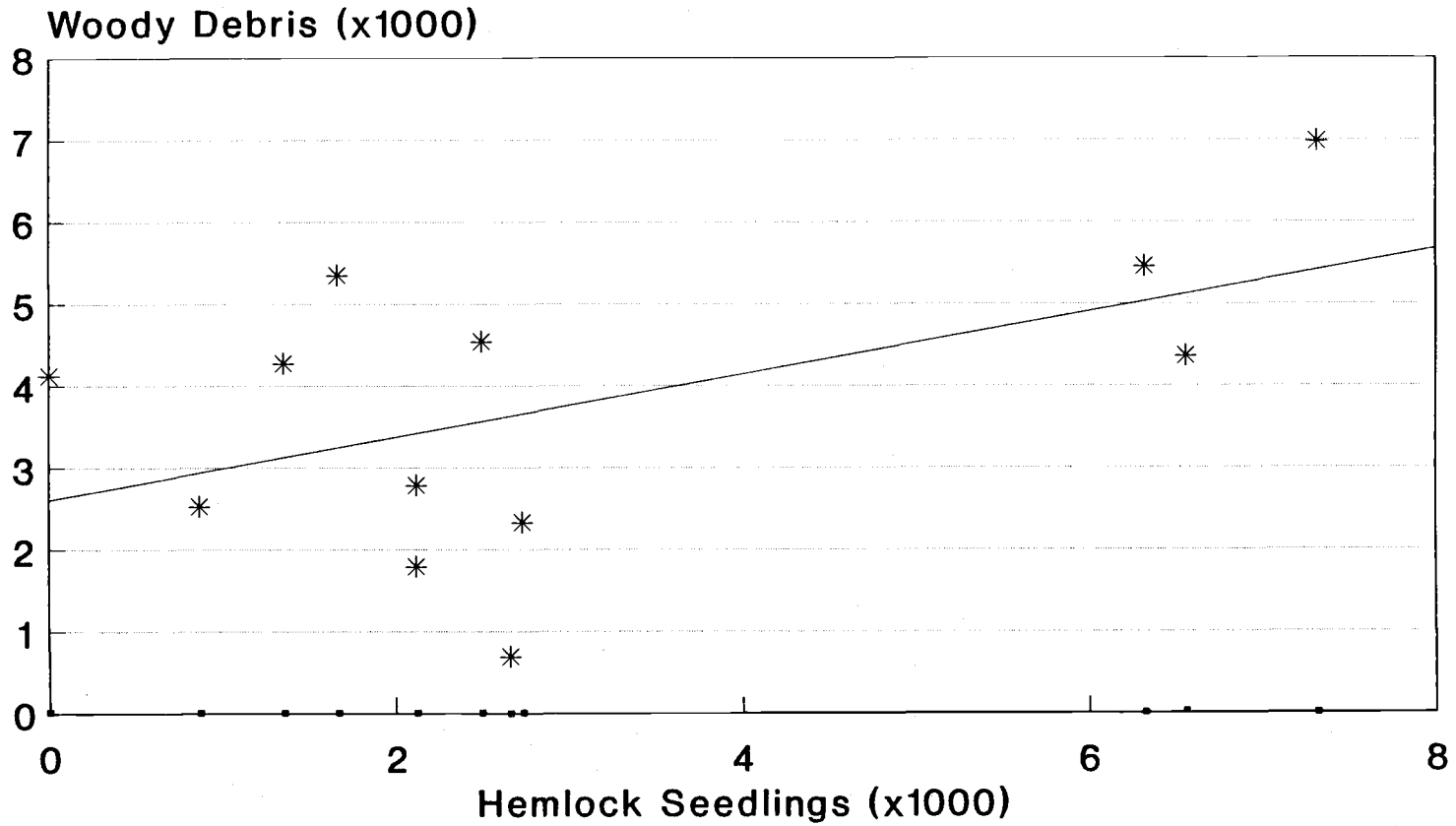


Figure 5.11 Total wavelet variance of woody debris cover versus total wavelet variance of hemlock seedling ( $\%^2$ ).

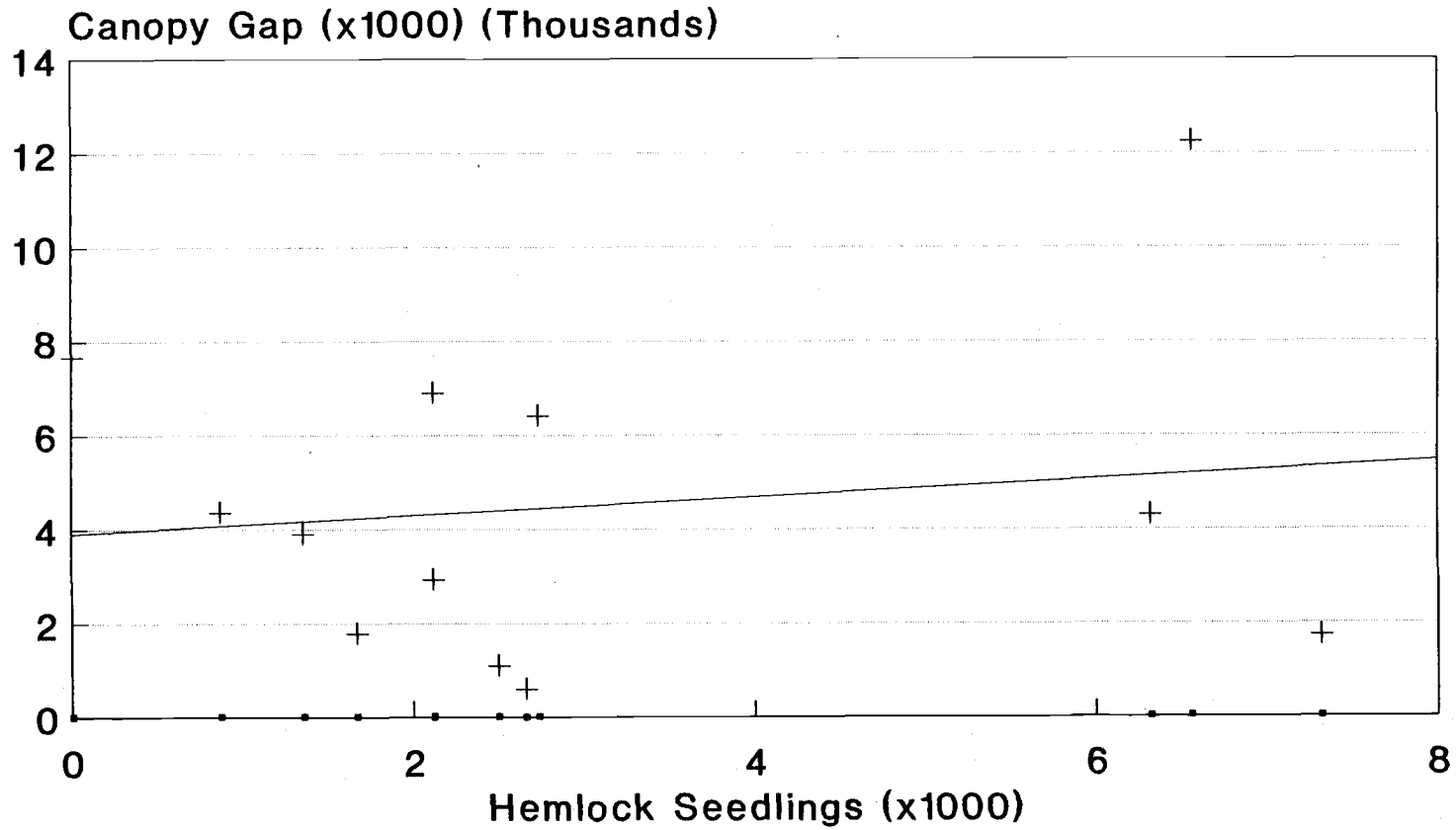


Figure 5.12 Total wavelet variance of canopy gap cover versus total wavelet variance of hemlock seedling (%<sup>2</sup>).

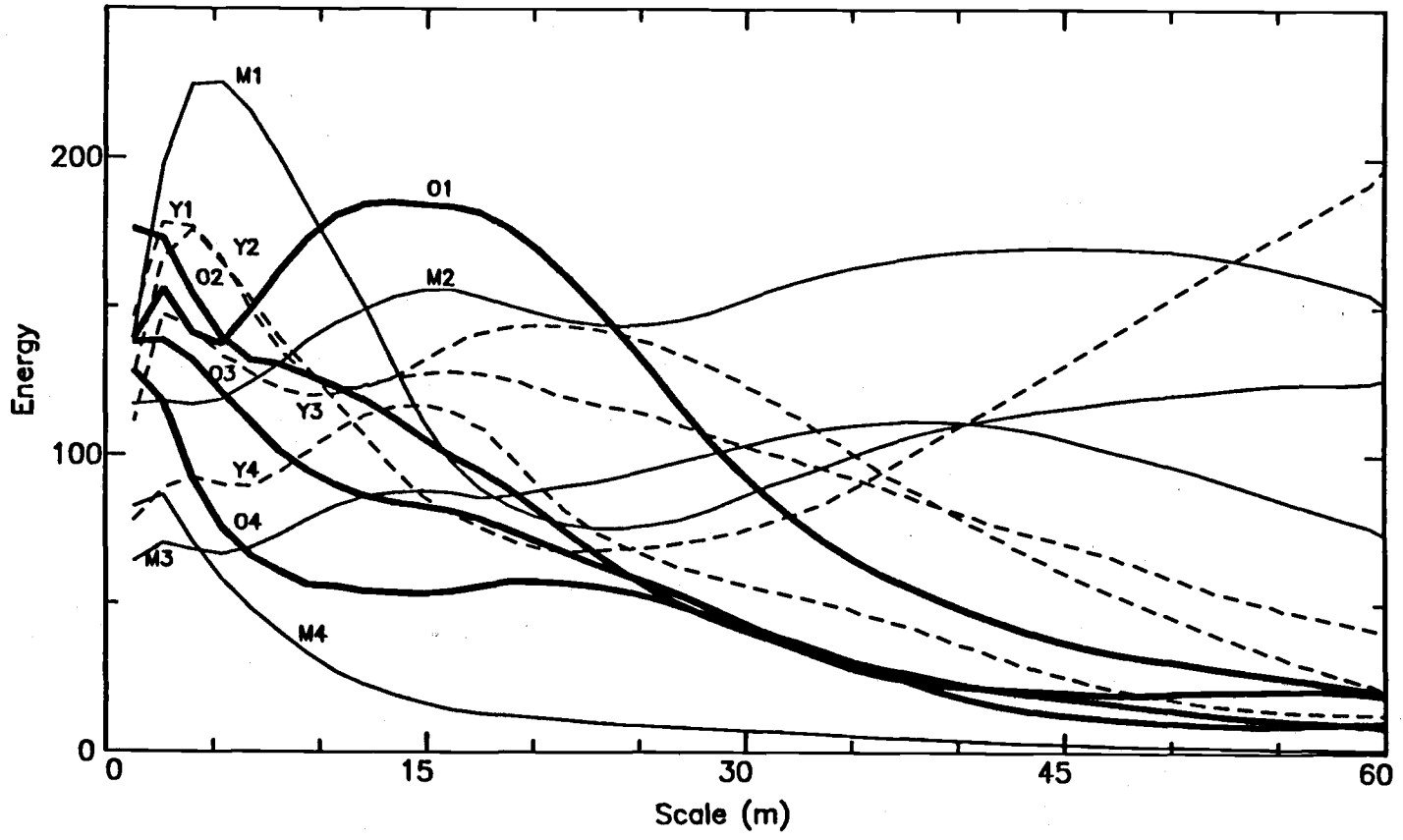


Figure 5.13 Wavelet variance for woody debris in all twelve stands.

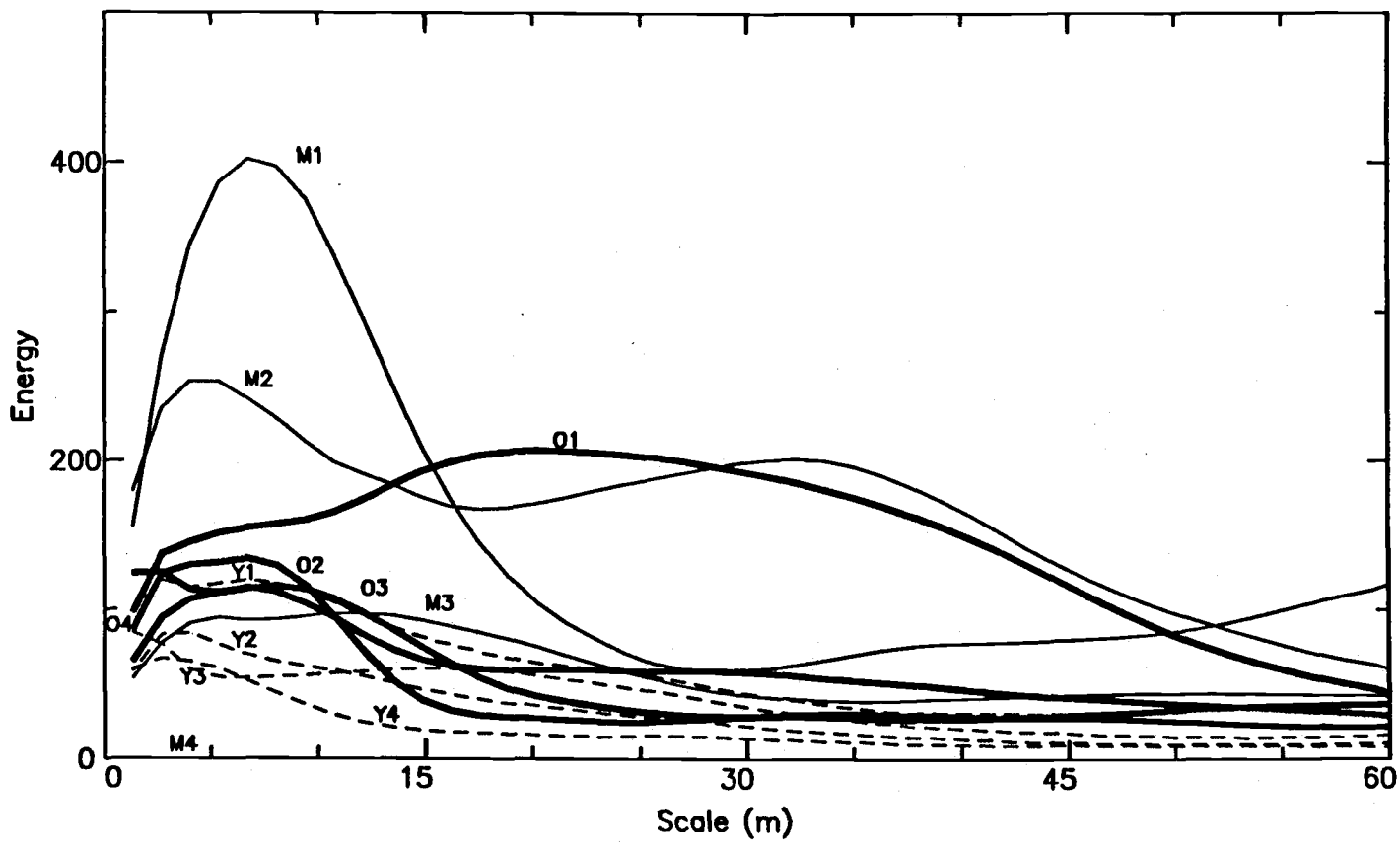
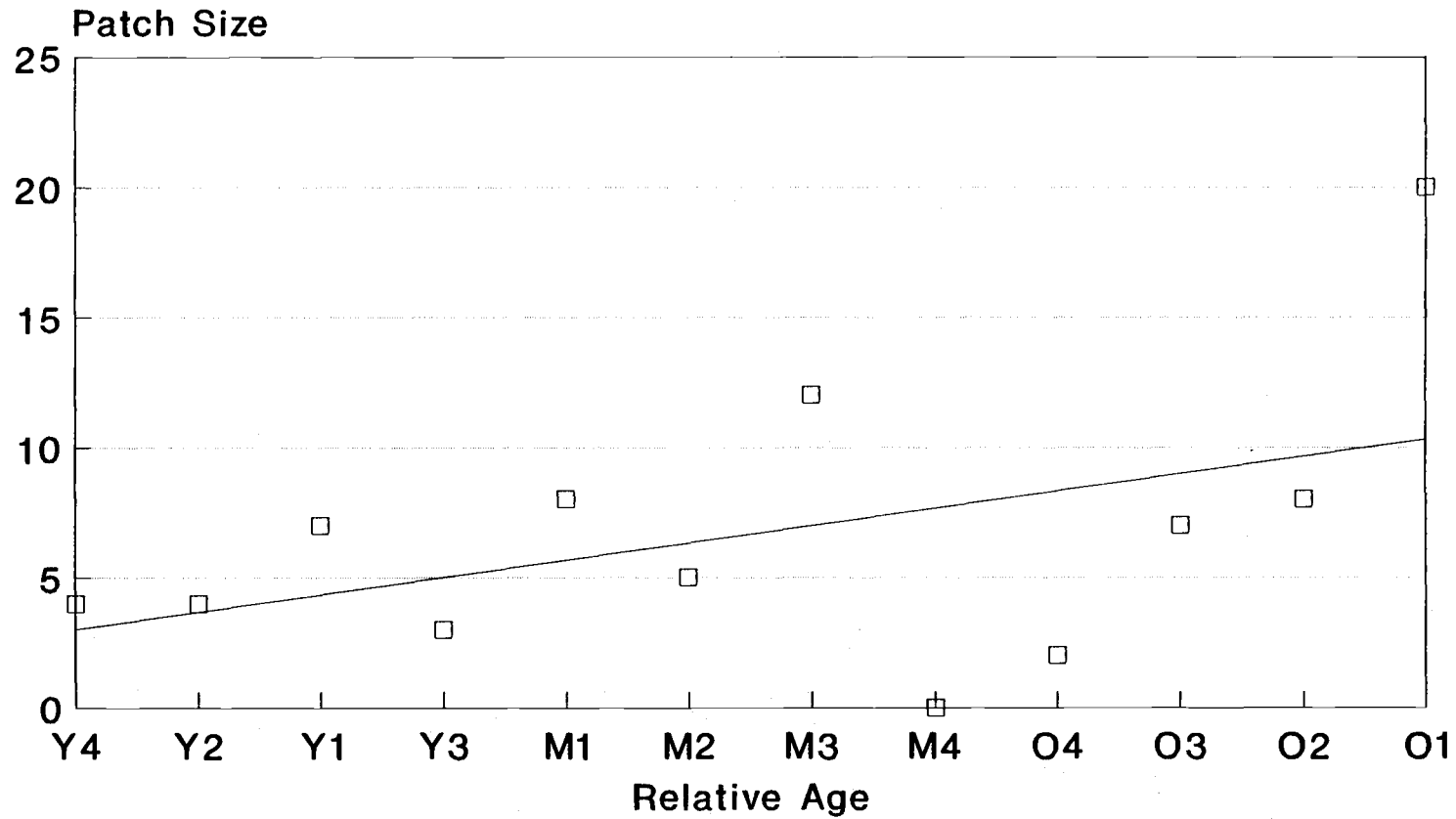
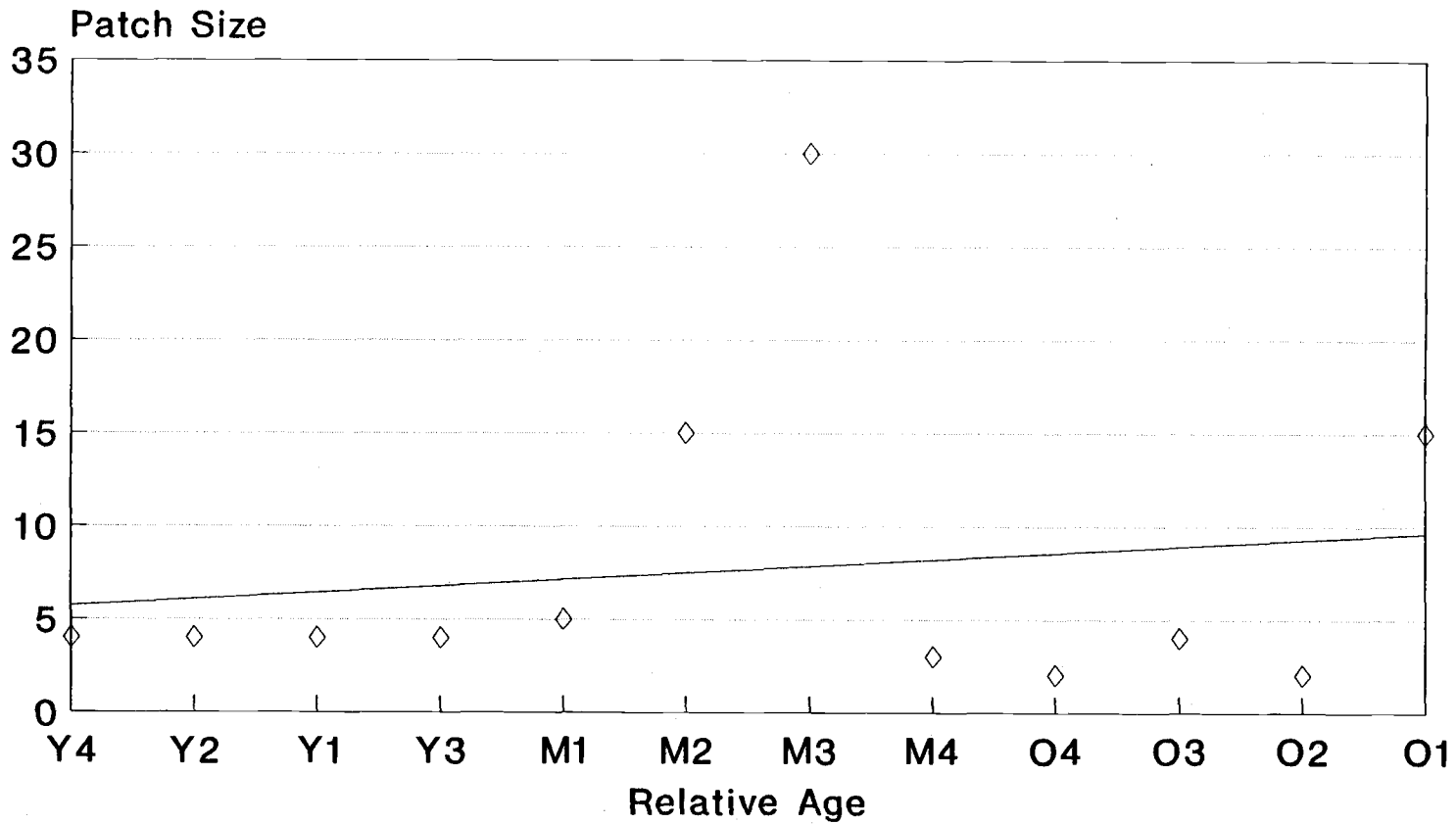


Figure 5.14 Wavelet variance for hemlock seedling in all twelve stands.



**Figure 5.15** Scale at which maximum wavelet variance occurs in meters (average patch size) as a function of relative stand age for hemlock seedling class.



**Figure 5.16** Scale at which maximum wavelet variance occurs in meters (average patch size) as a function of relative stand age for total woody debris class.

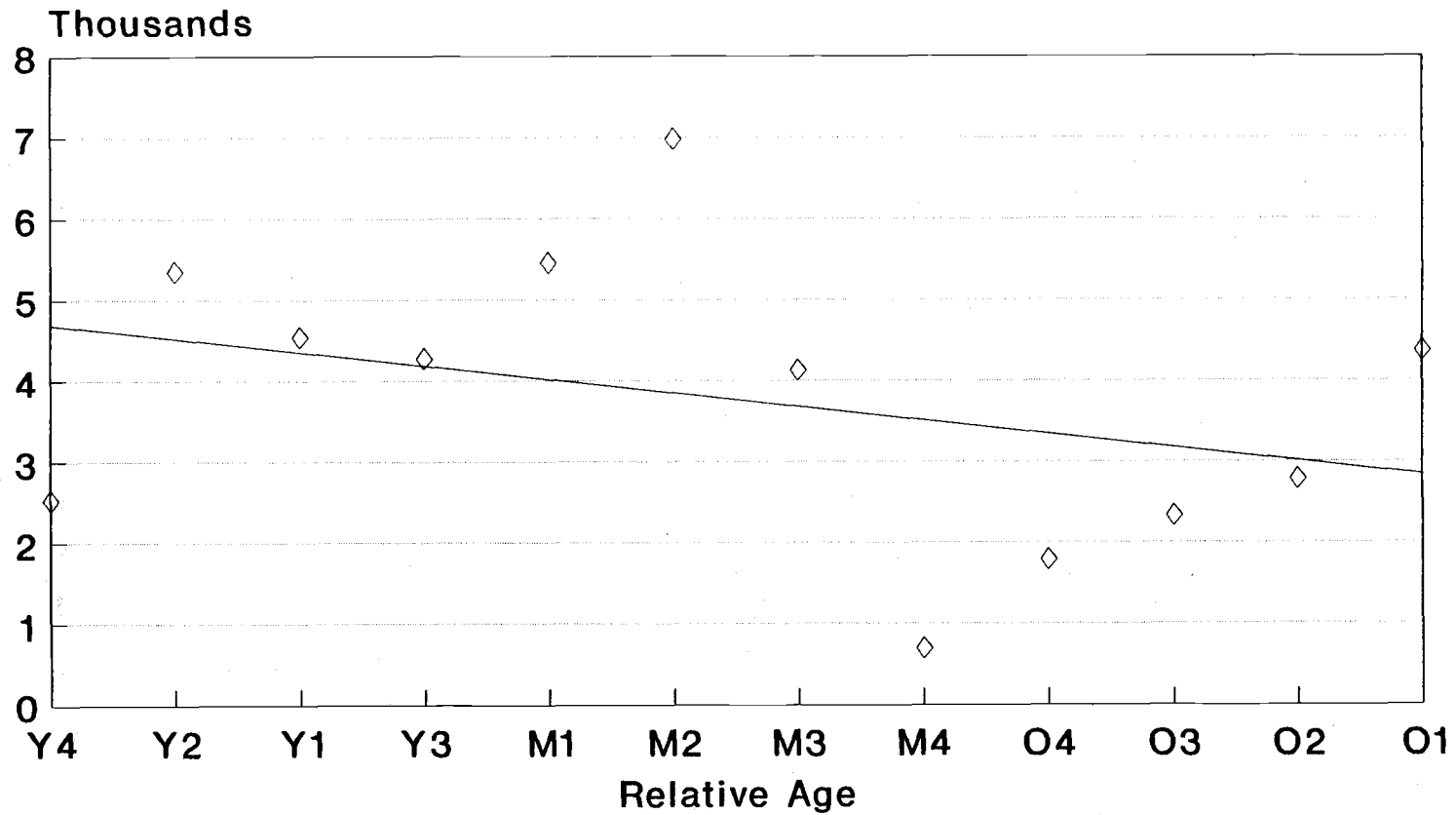


**Figure 5.17** Total wavelet variance for total woody debris class as a function of stand age. Total wavelet variance is in units of (%<sup>2</sup> cover).

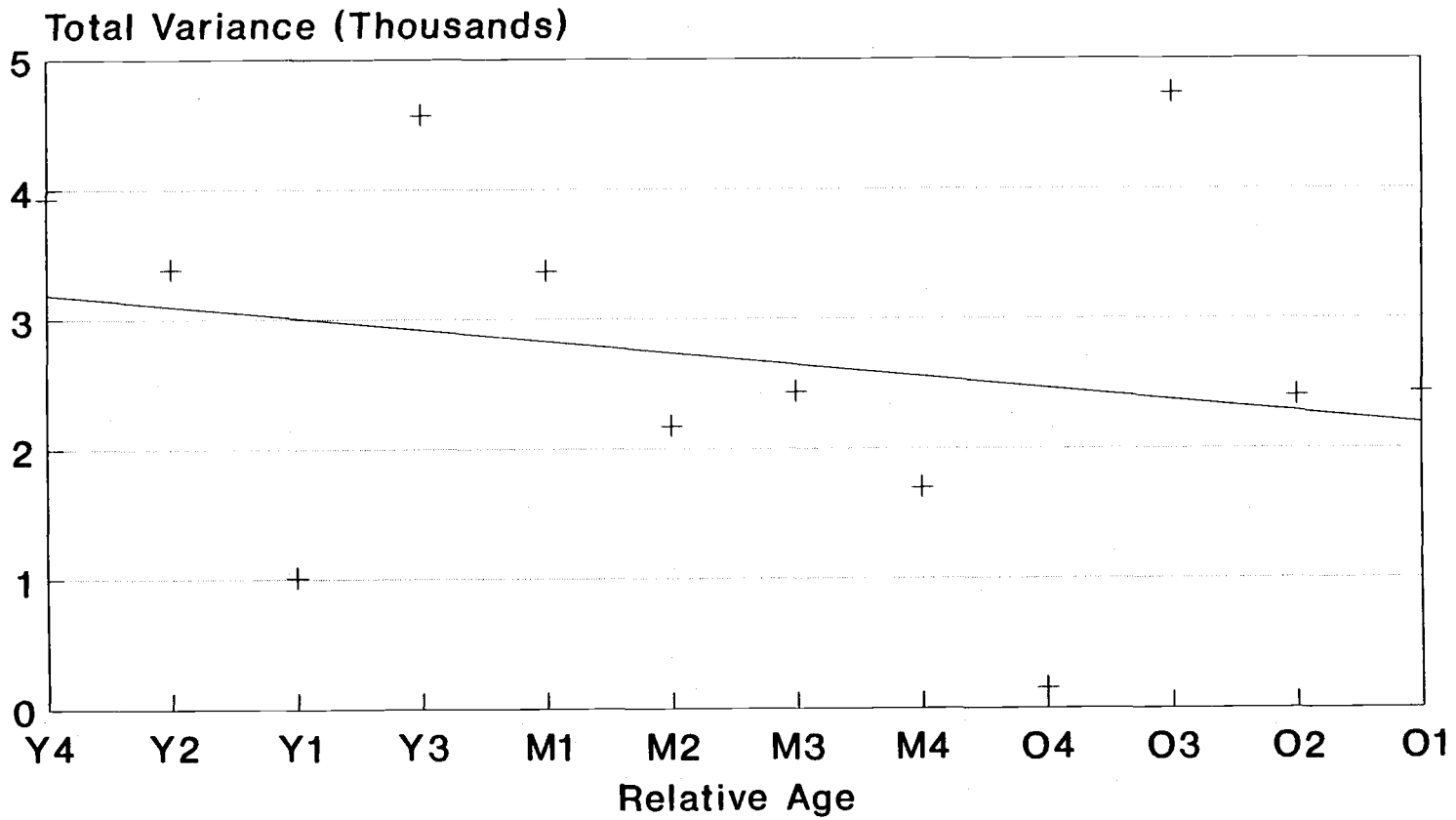


**Figure 5.18** Total wavelet variance for low shrub class as a function of stand age. Total wavelet variance is in units of ( $\%^2$  cover).

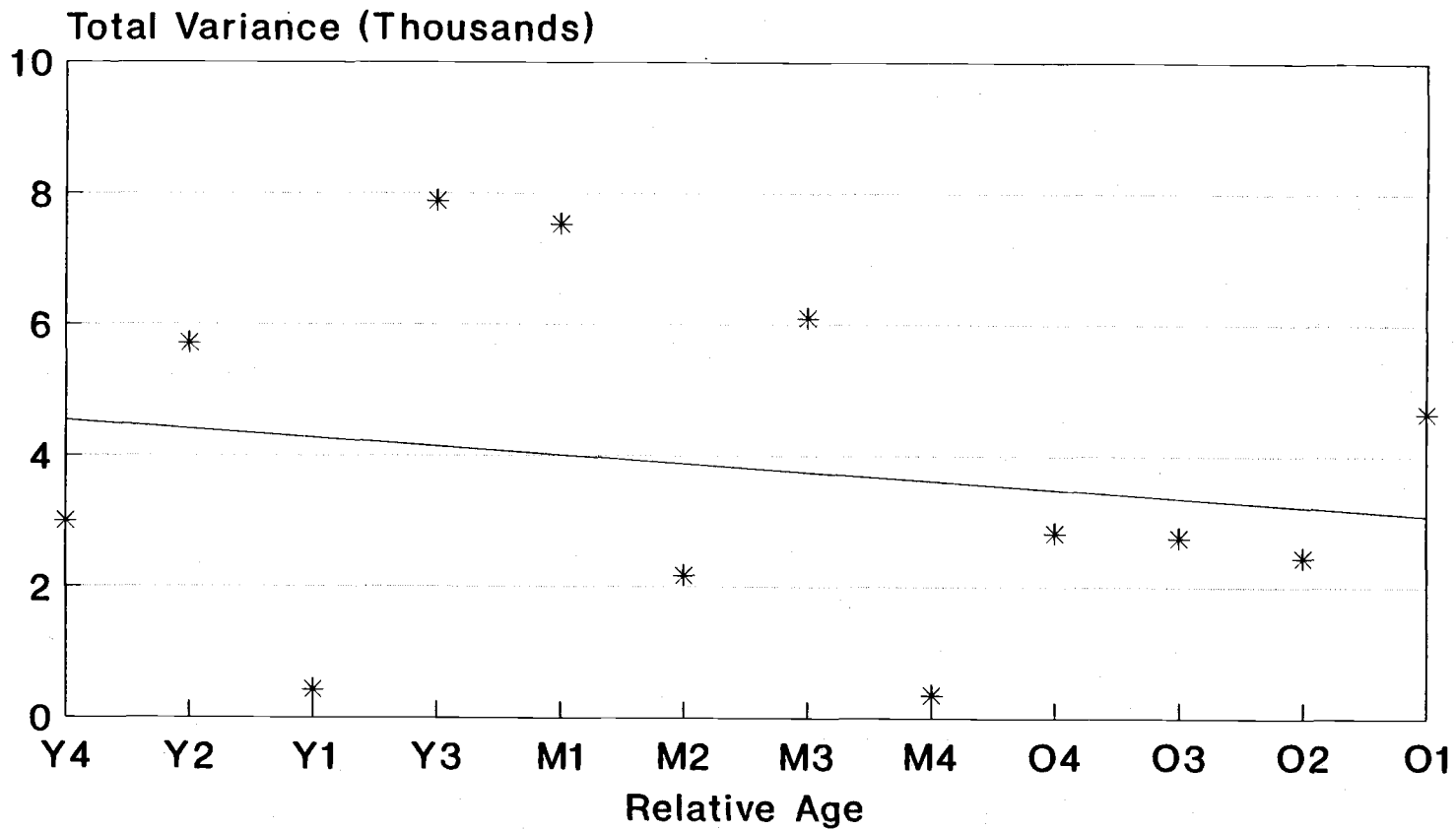


**Figure 5.19** Total wavelet variance for tall shrub class as a function of stand age. Total wavelet variance is in units of ( $\%^2$  cover).

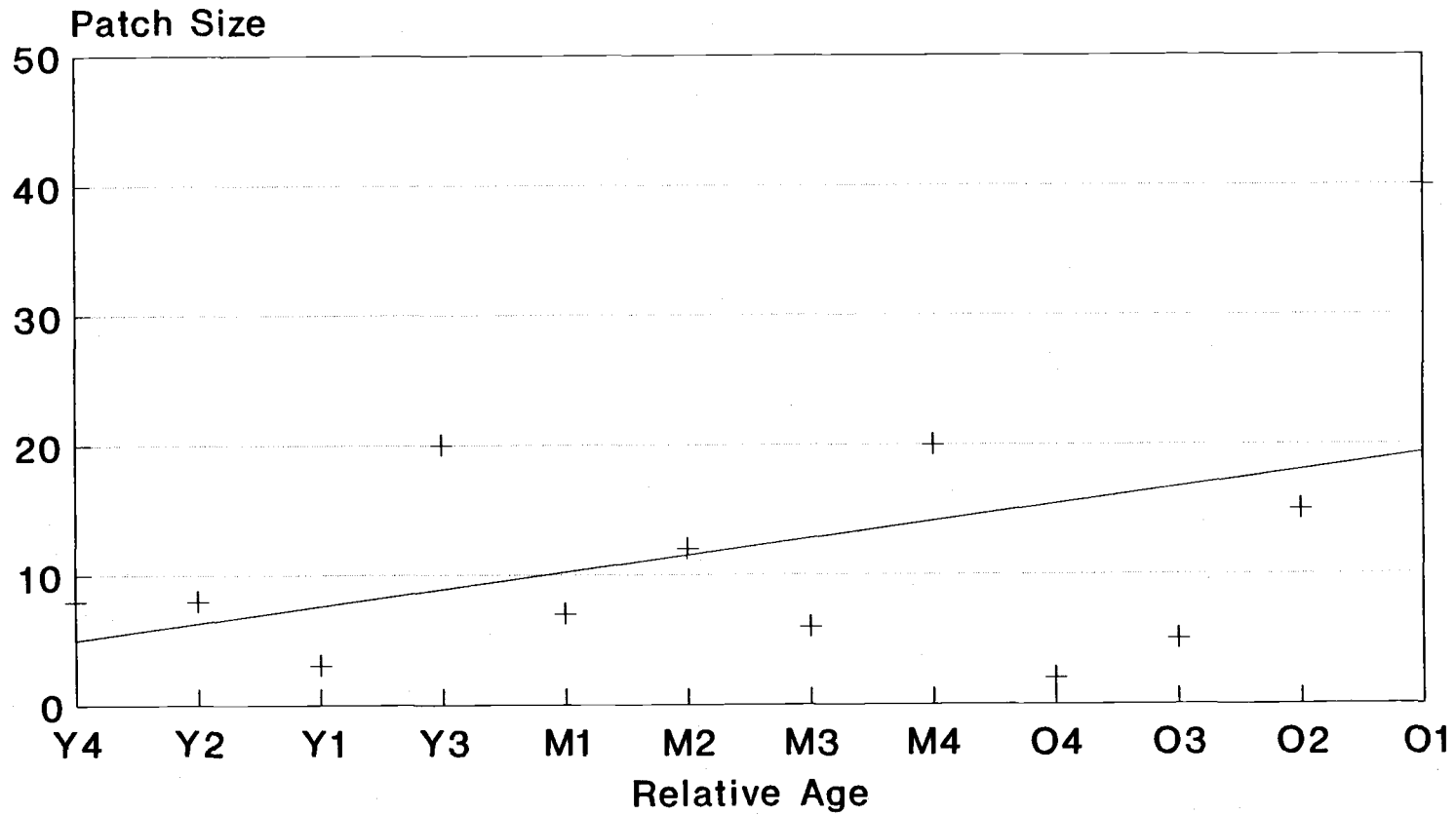


**Figure 5.20** Scale at which maximum wavelet variance occurs in meters (average patch size) as a function of relative stand age for low shrub class.

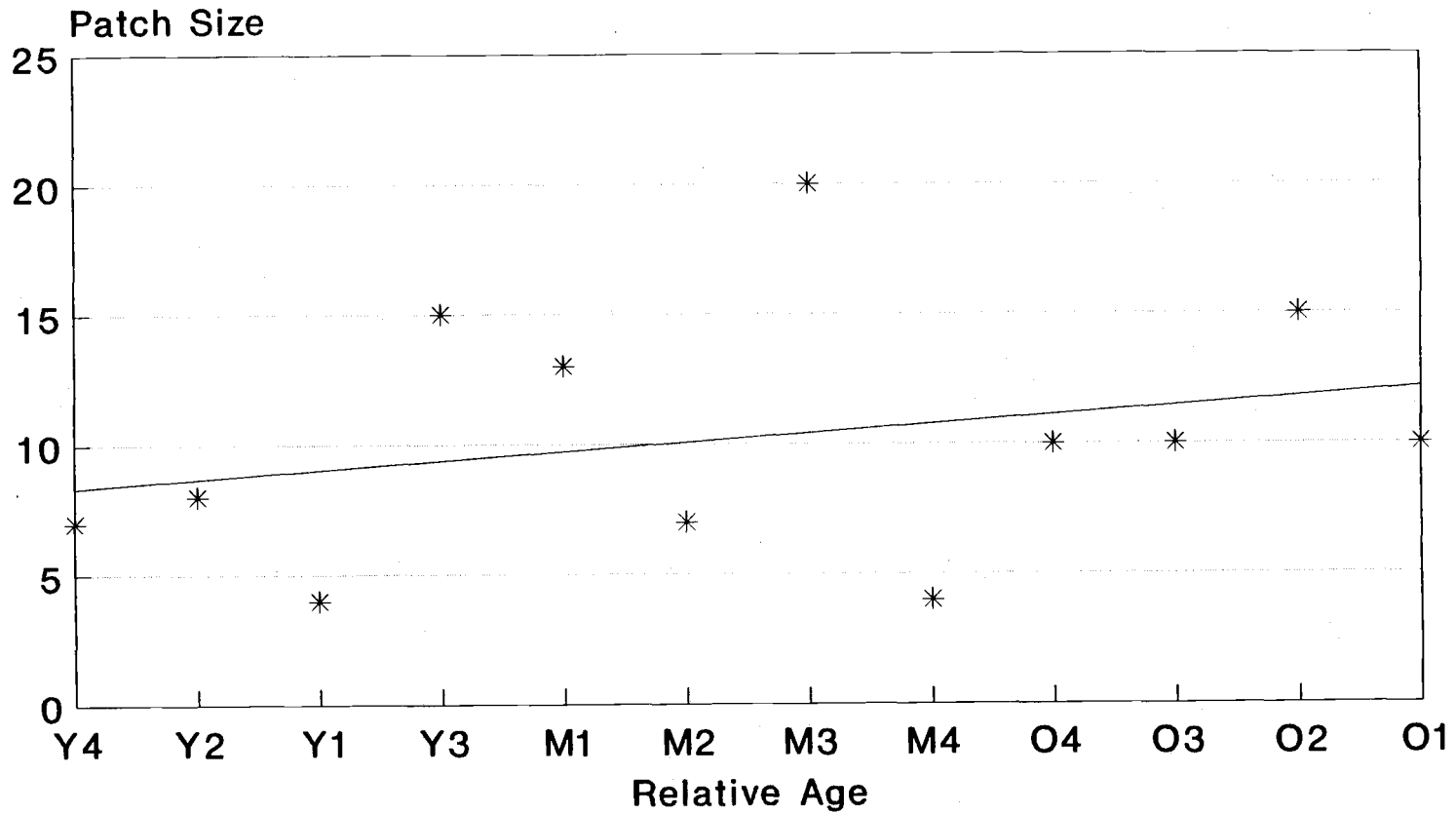


**Figure 5.21** Scale at which maximum wavelet variance occurs in meters (average patch size) as a function of relative stand age for tall shrub class.

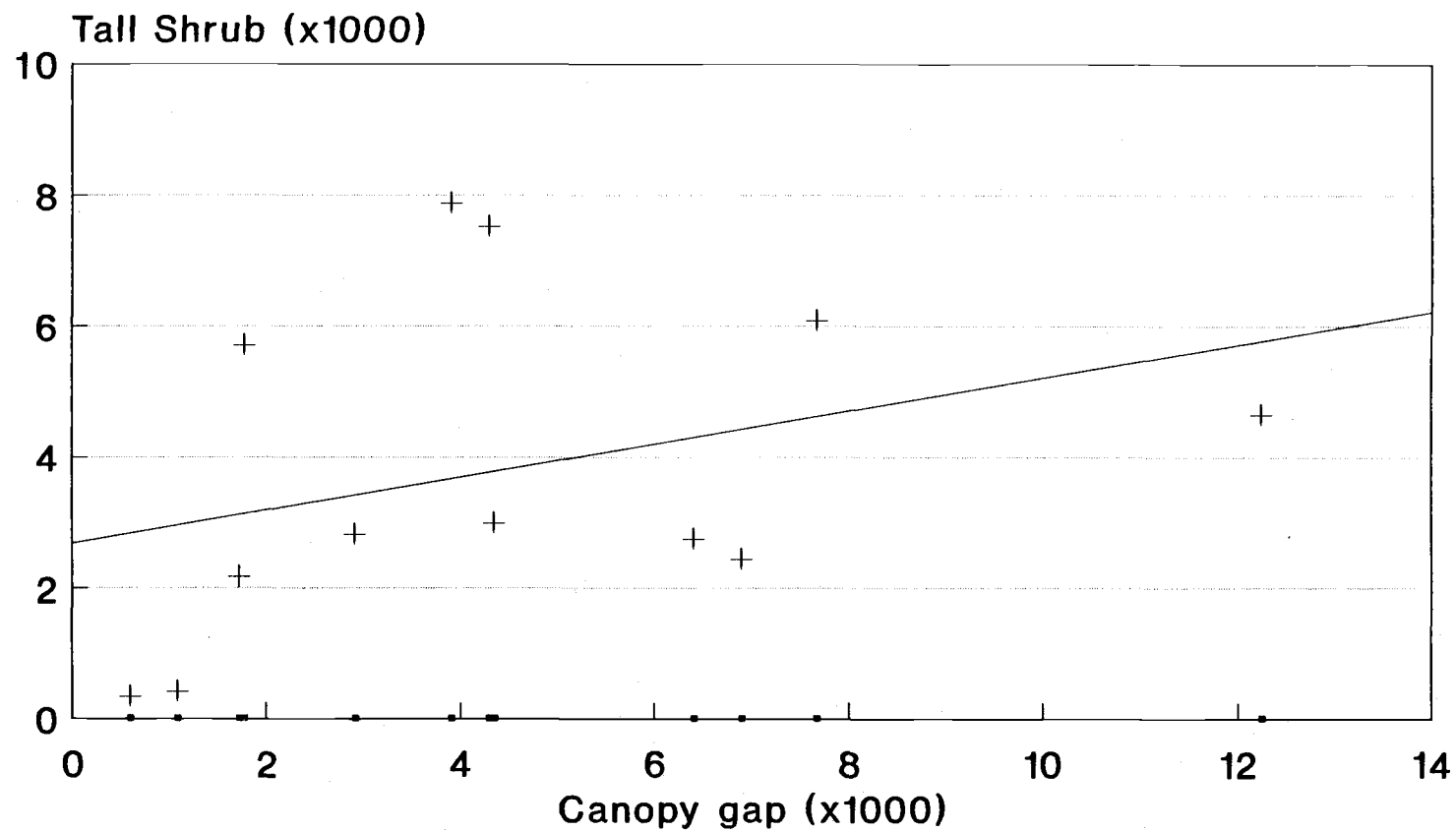


**Figure 5.22** Total wavelet variance of tall shrub cover versus total wavelet variance of canopy gap opening (%<sup>2</sup>).

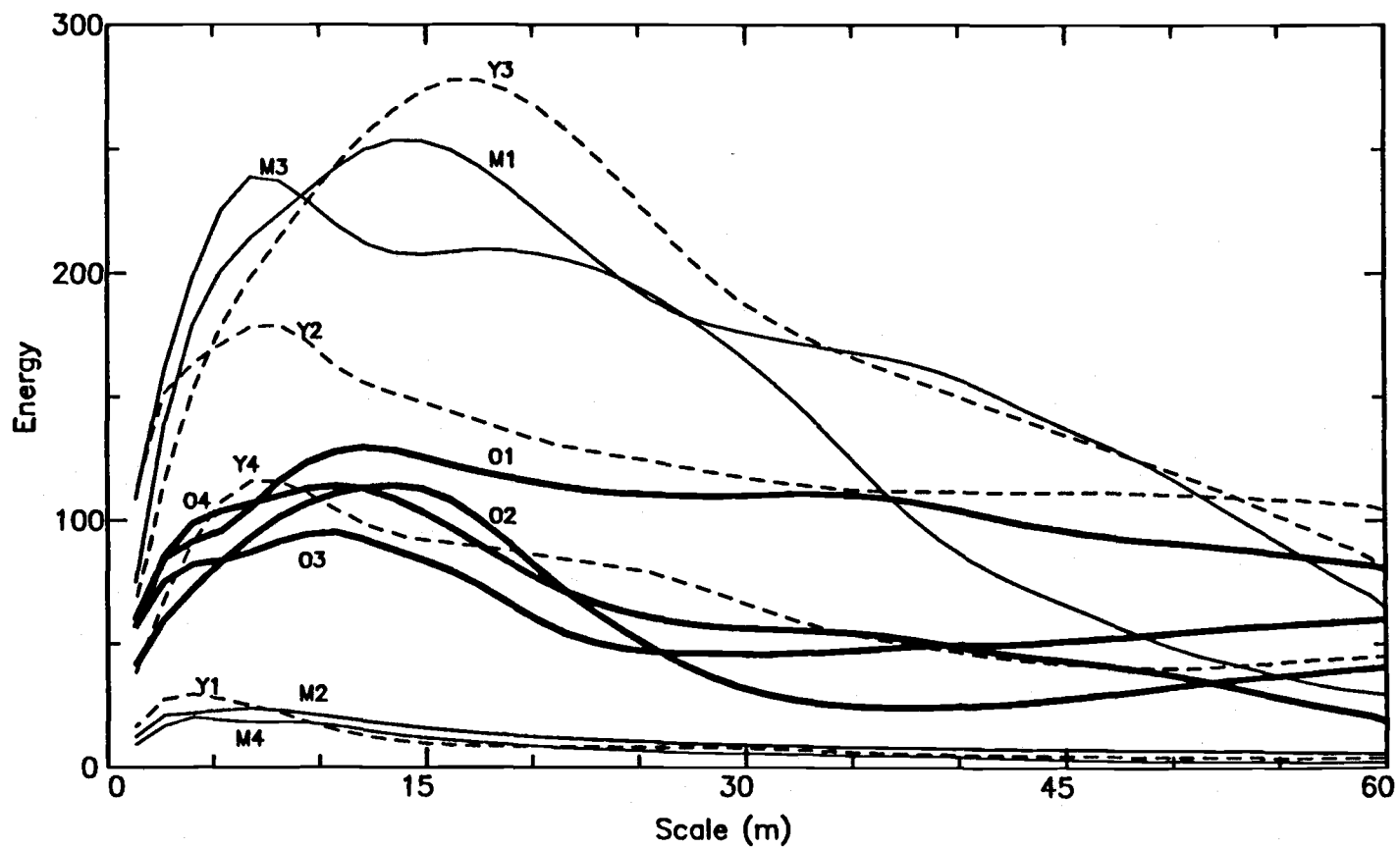
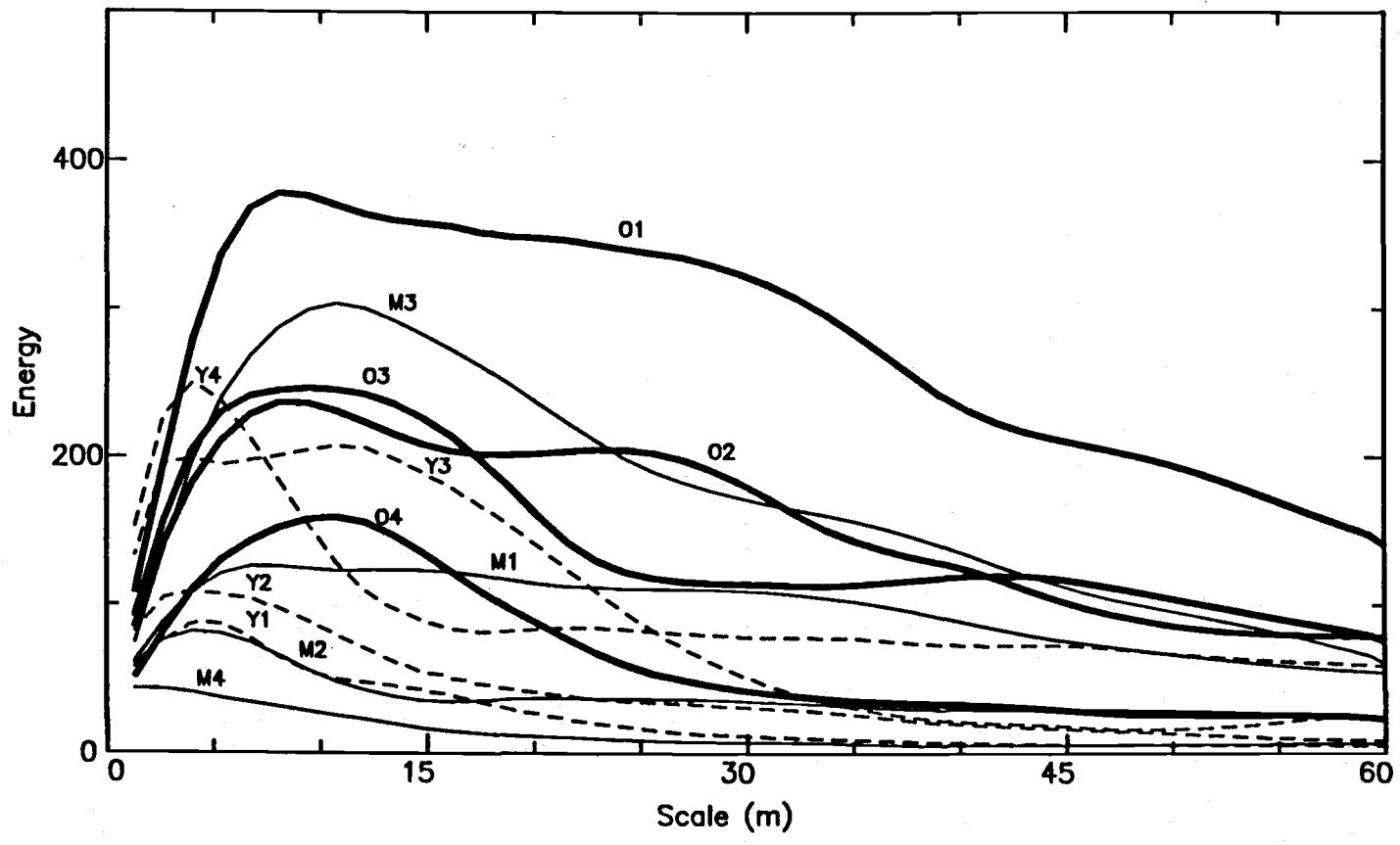
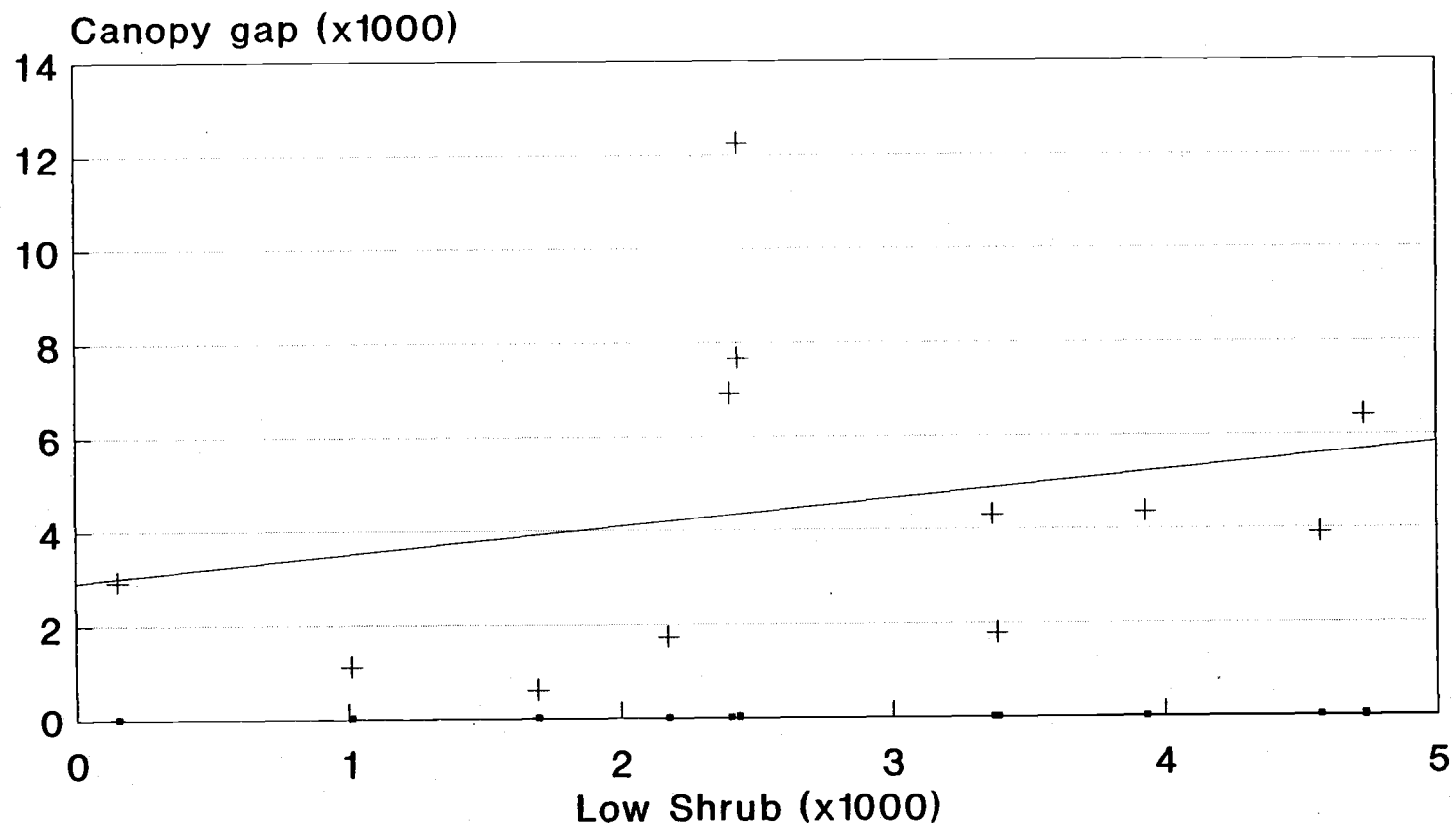


Figure 5.23 Wavelet variance for tall shrub in all twelve stands.



**Figure 5.24** Wavelet variance for canopy gap opening in all twelve stands.



**Figure 5.25** Total wavelet variance of canopy gap opening versus total wavelet variance of canopy gap opening (%<sup>2</sup>).

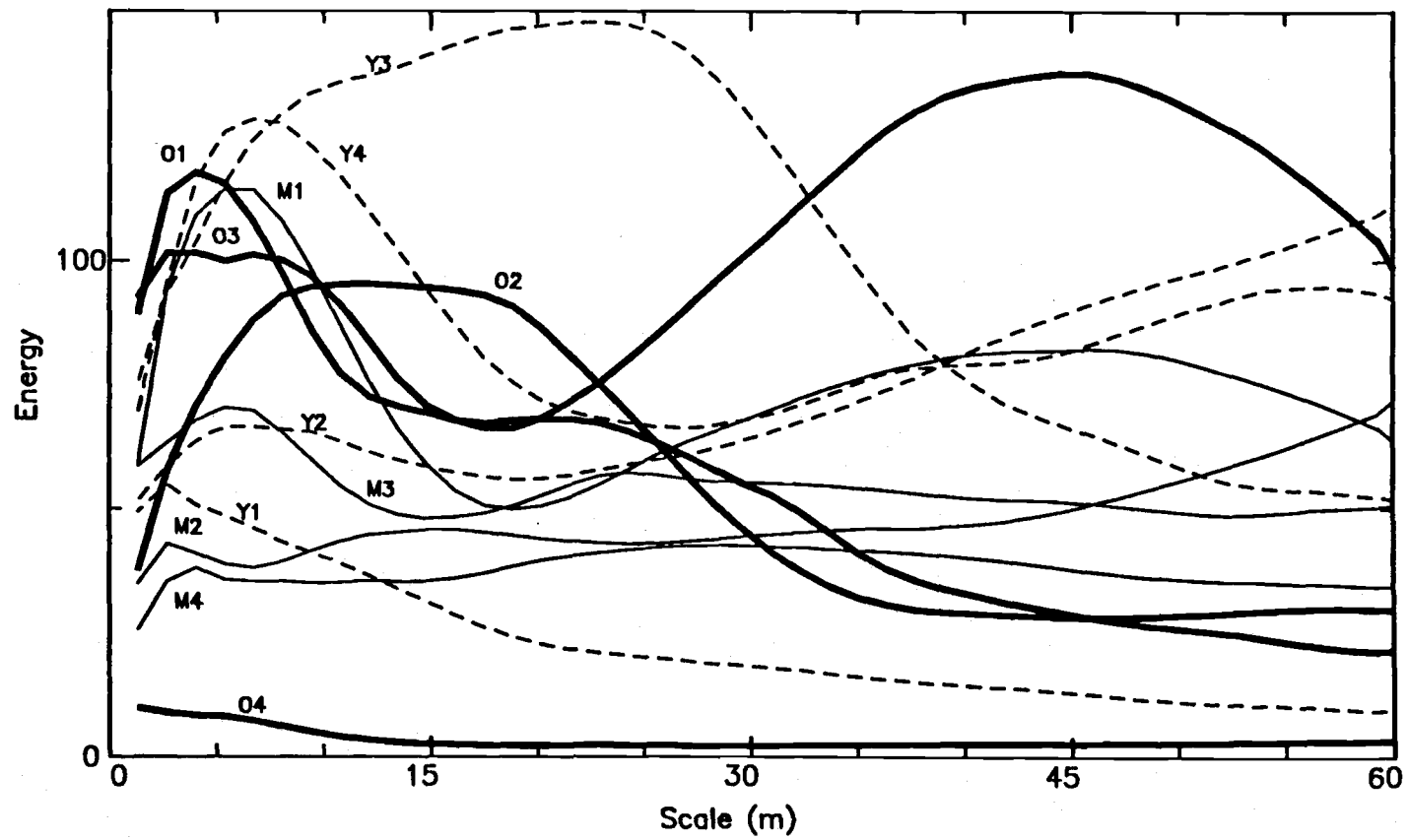


**Figure 5.26** Wavelet variance for low shrub class in all twelve stands.

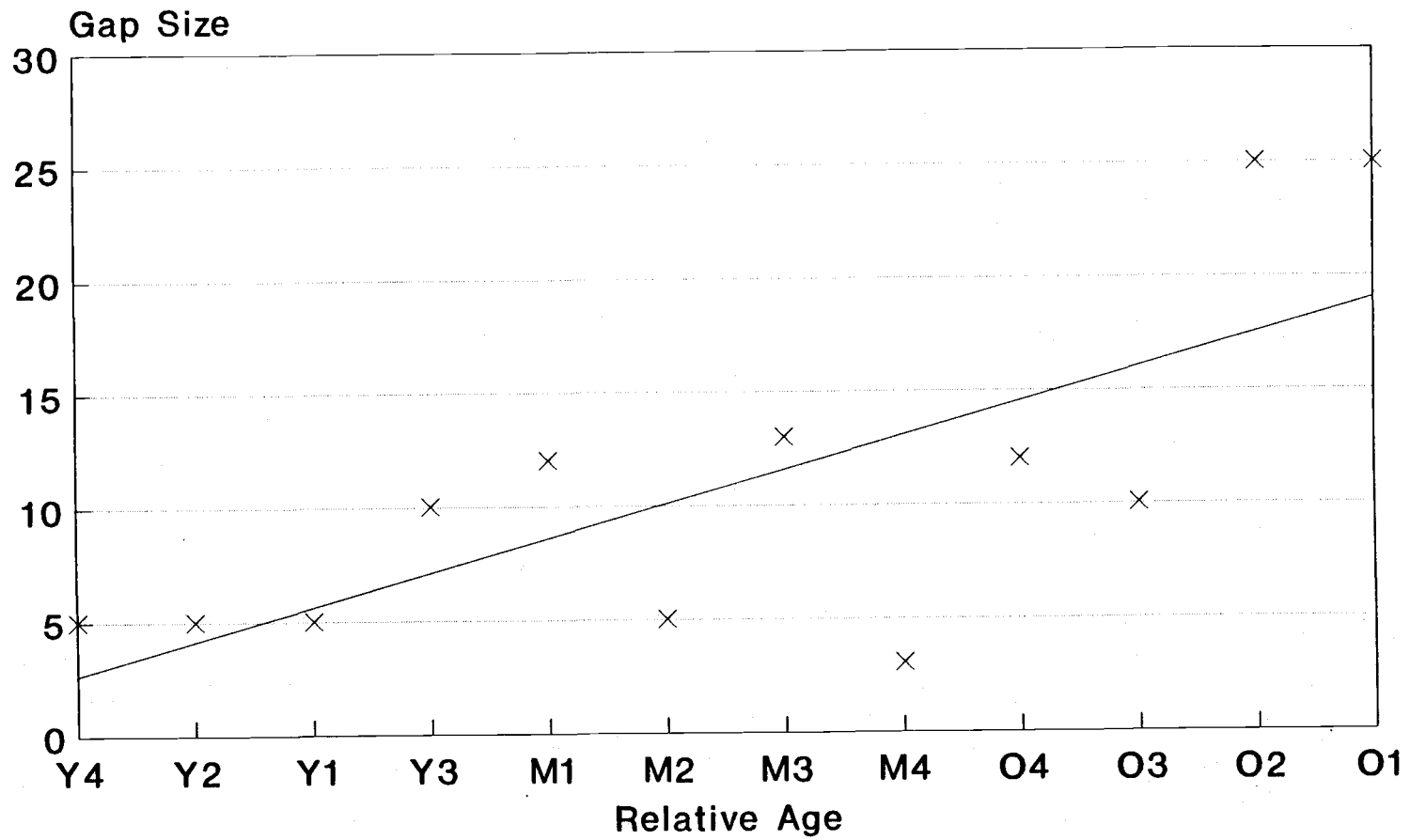


**Figure 5.27** Scale at which maximum wavelet variance occurs in meters (average patch size) as a function of relative stand age for canopy gap opening.

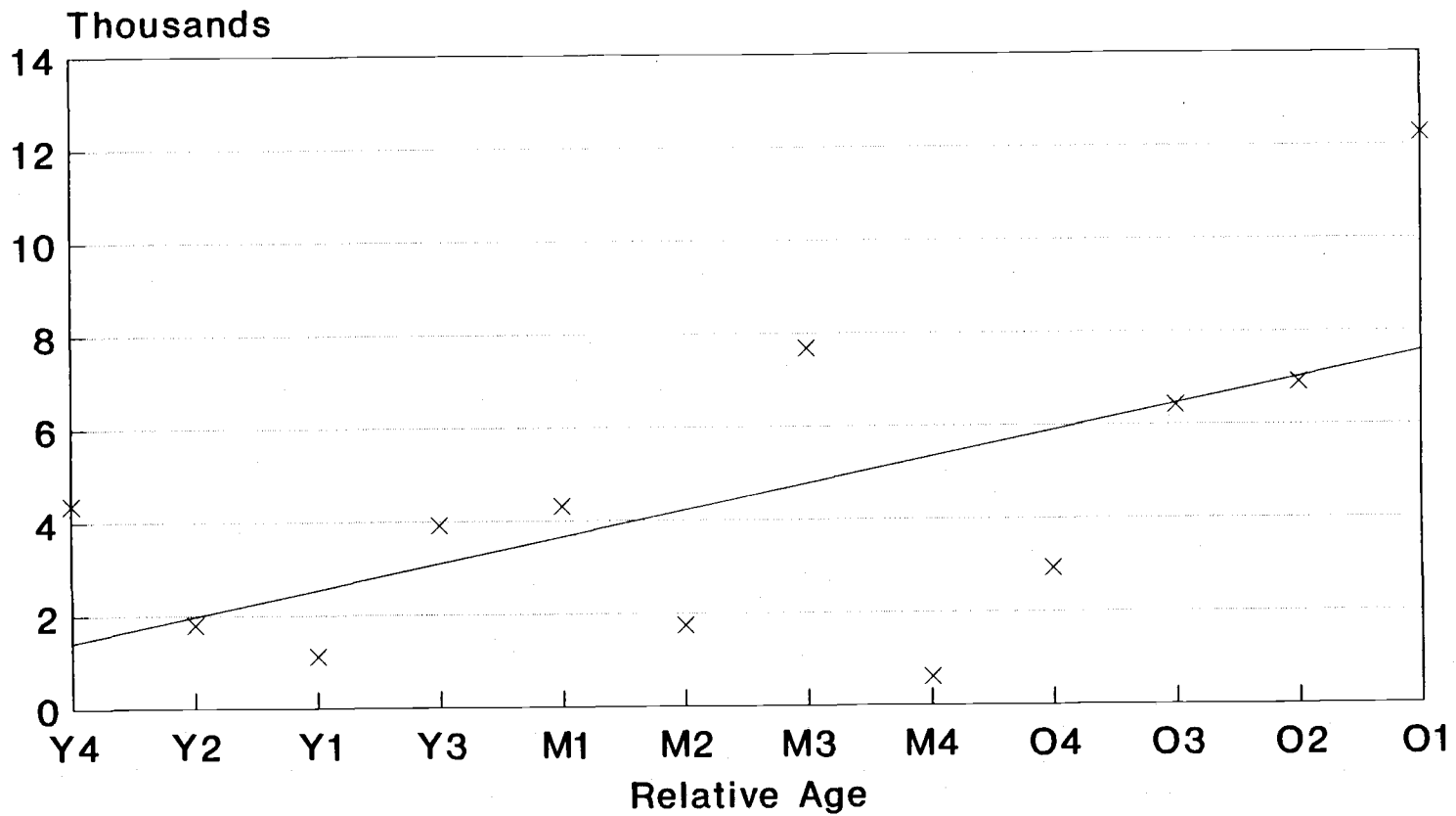


**Figure 5.28** Total wavelet variance for canopy gap opening as a function of stand age. Total wavelet variance is in units of (%<sup>2</sup> cover).

**Figure 5.29** Wavelet cross-covariance between canopy gap and low shrub cover for young stand Y1. x-axis corresponds to the lag or offset between the two variables in meters; the y-axis corresponds to the scale at which the variables are correlated. The grey-scale bar at the right of the figure indicates the magnitude of the spatial covariance. Positive covariance values are dark grey while negative correlations are white.

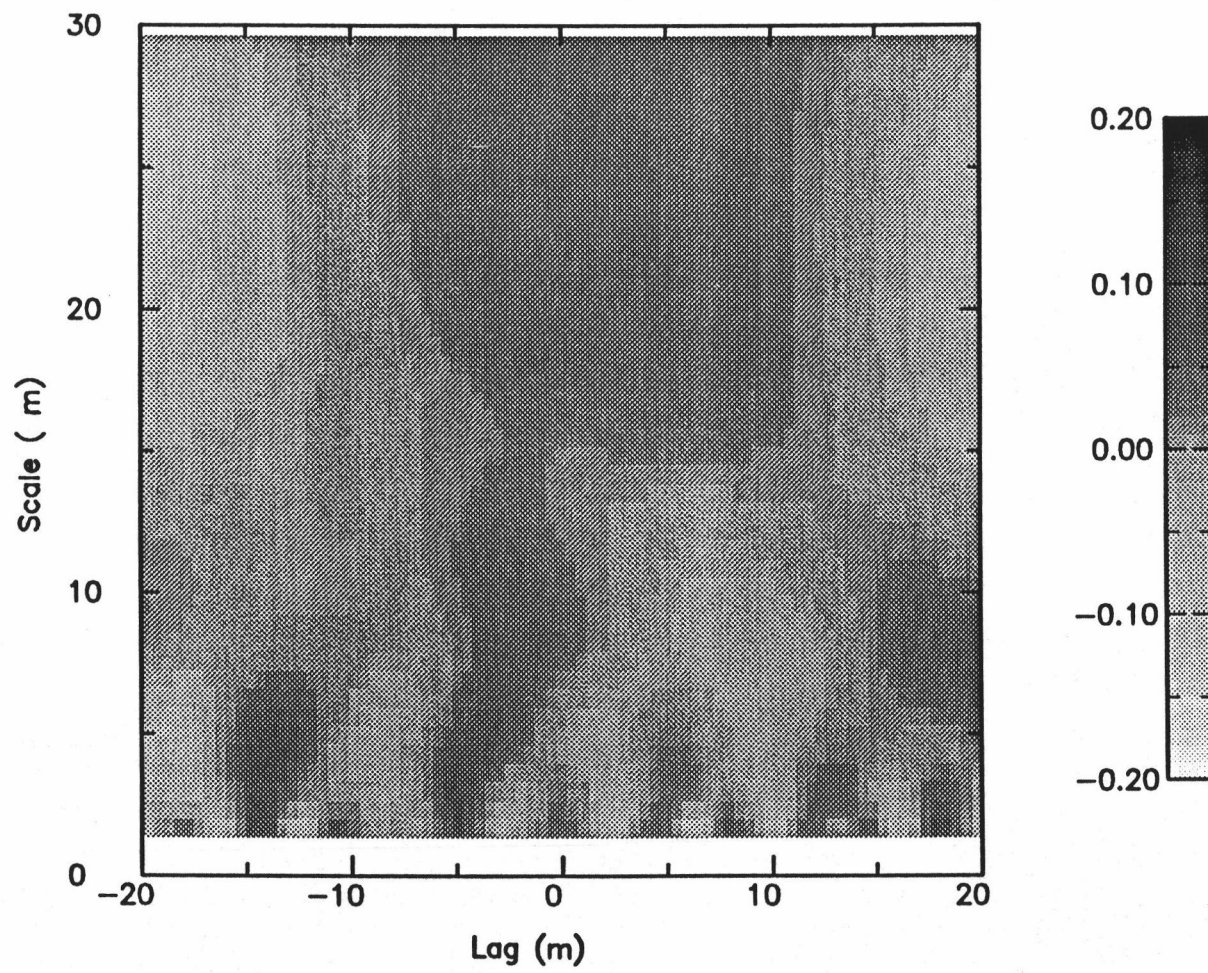
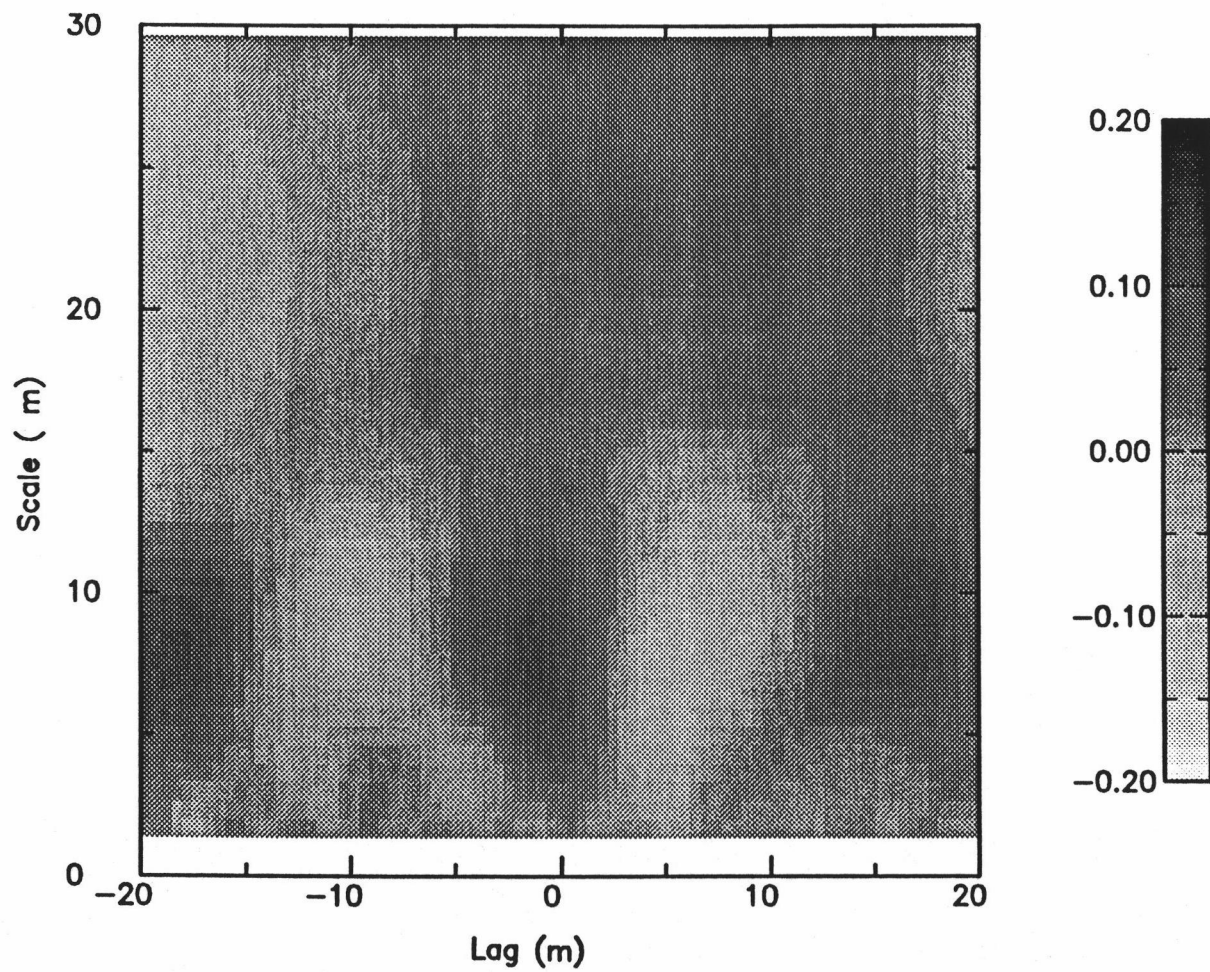
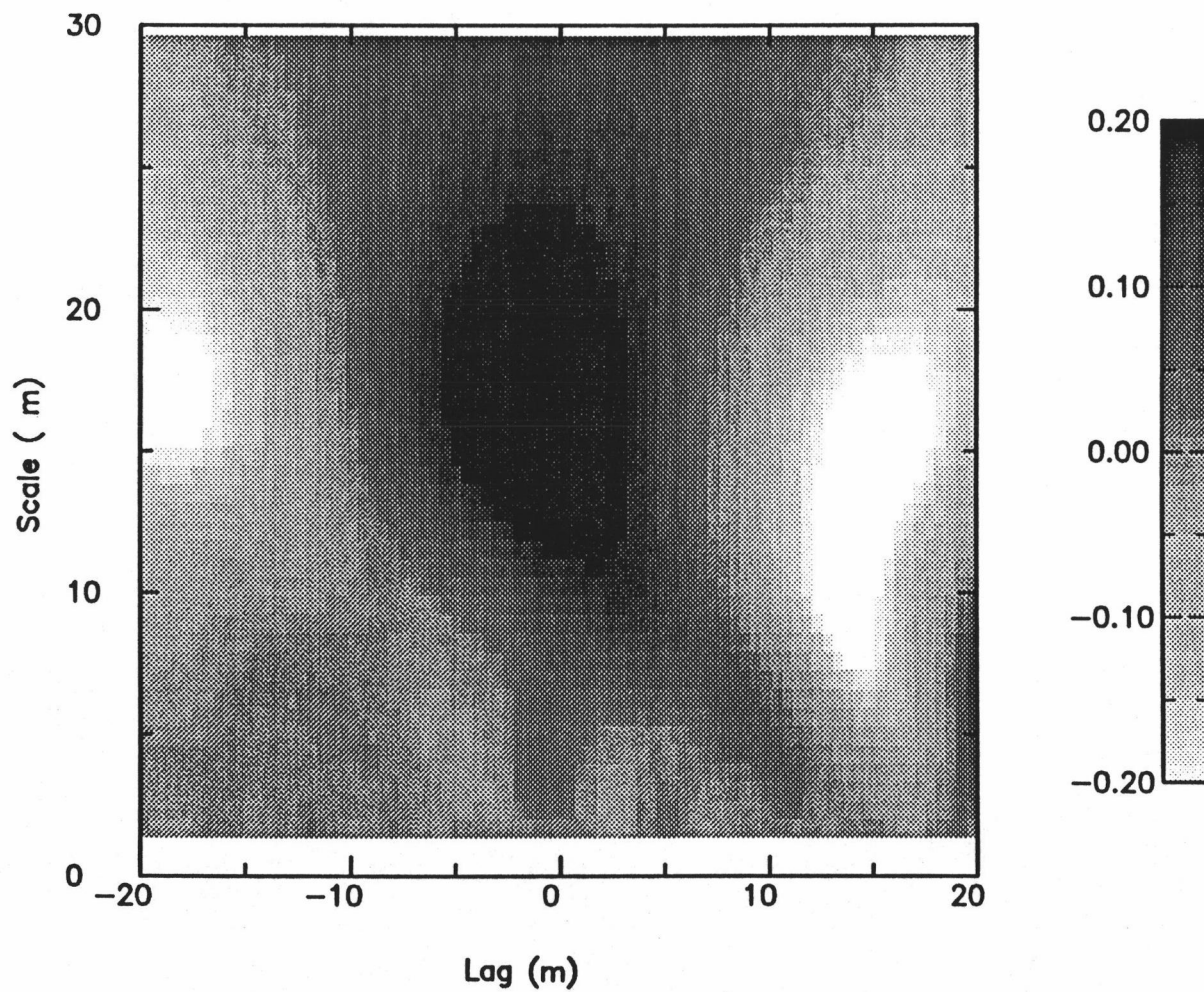


Figure 5.29



**Figure 5.30** Wavelet cross-covariance between canopy gap and low shrub cover for mature stand M3.



**Figure 5.31** Wavelet cross-covariance between canopy gap and low shrub cover for old growth stand O1.

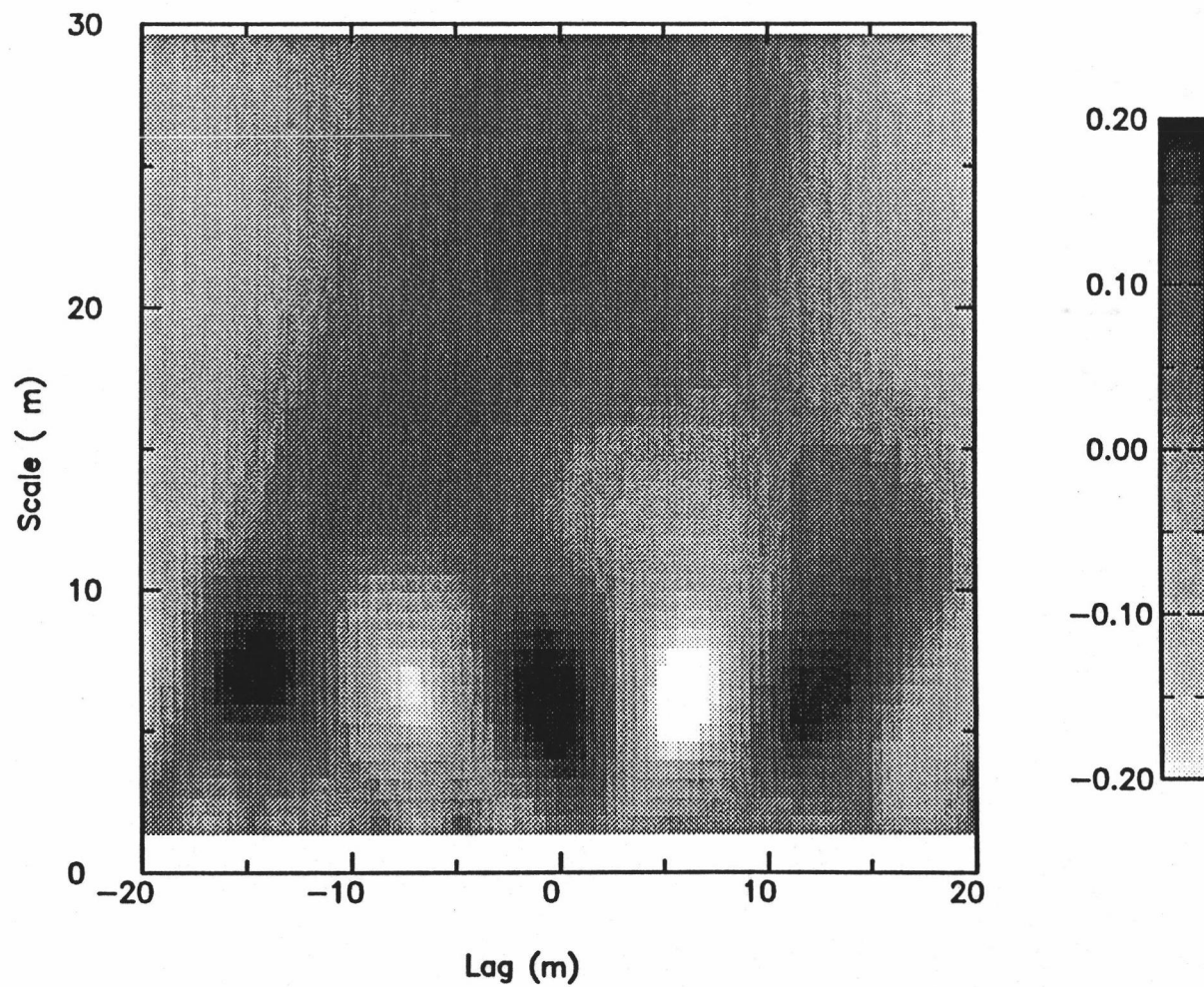


**Figure 5.32** Wavelet cross-covariance between canopy gap and tall shrub cover for young stand Y4.

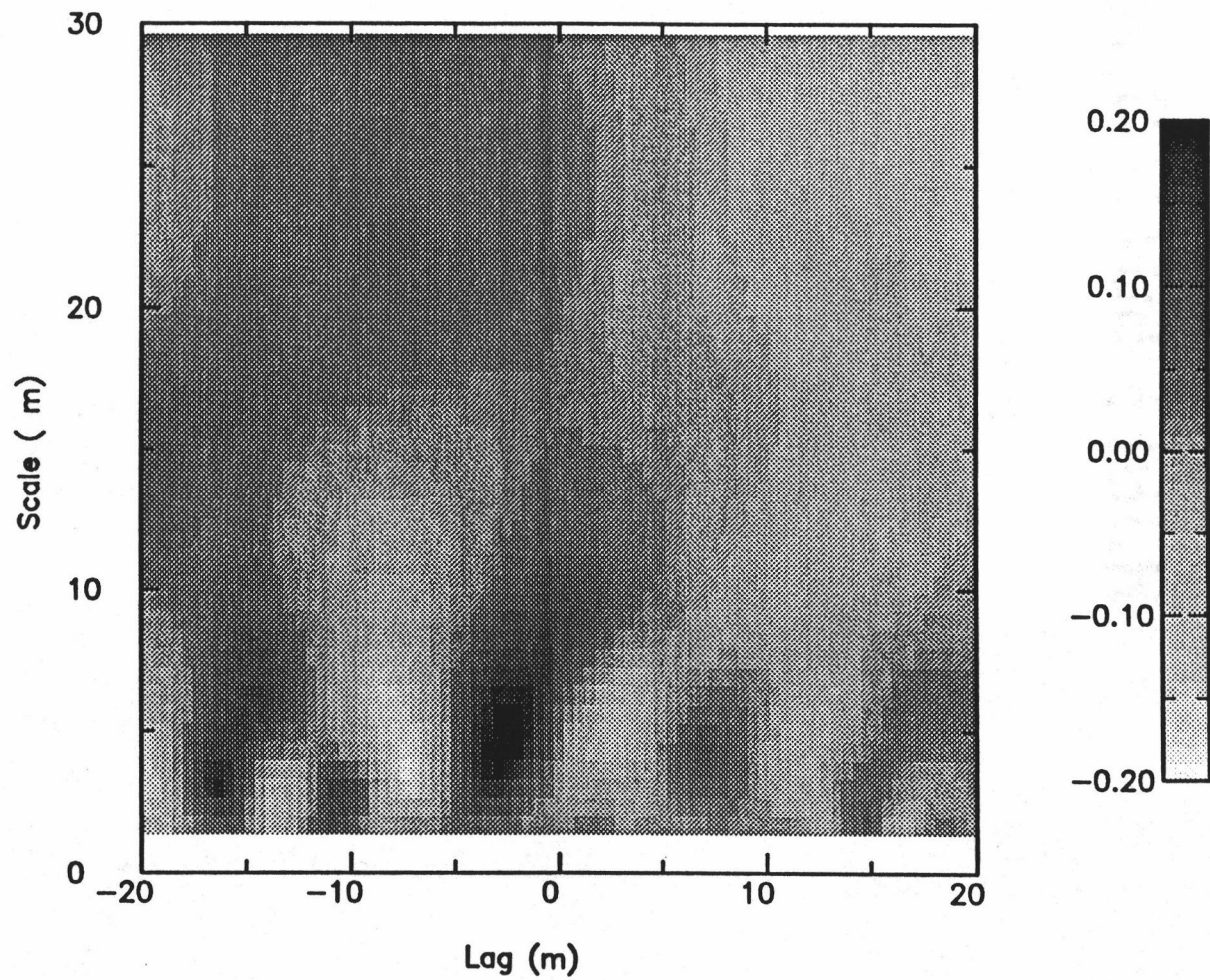


**Figure 5.33** Wavelet cross-covariance between canopy gap and tall shrub cover for young stand Y1.

**Figure 5.34** Wavelet cross-covariance between canopy gap and hemlock seedlings for old growth stand O1. Note two distinct scales of interaction at 5 and 25 meters.

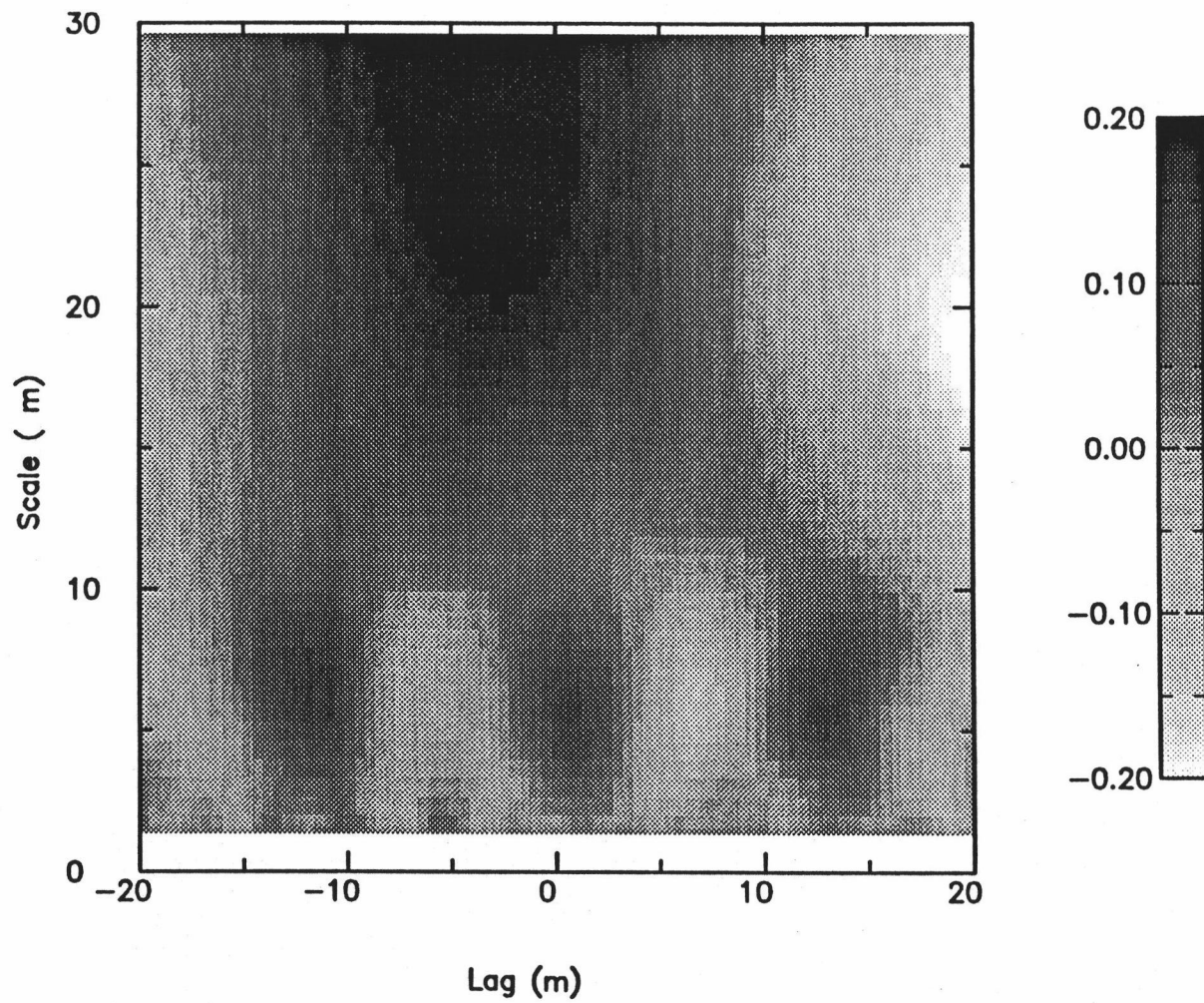


Figure 5.34

**Figure 5.35** Wavelet cross-covariance between woody debris and hemlock seedlings for stand O1. Note two distinct scales of pattern.

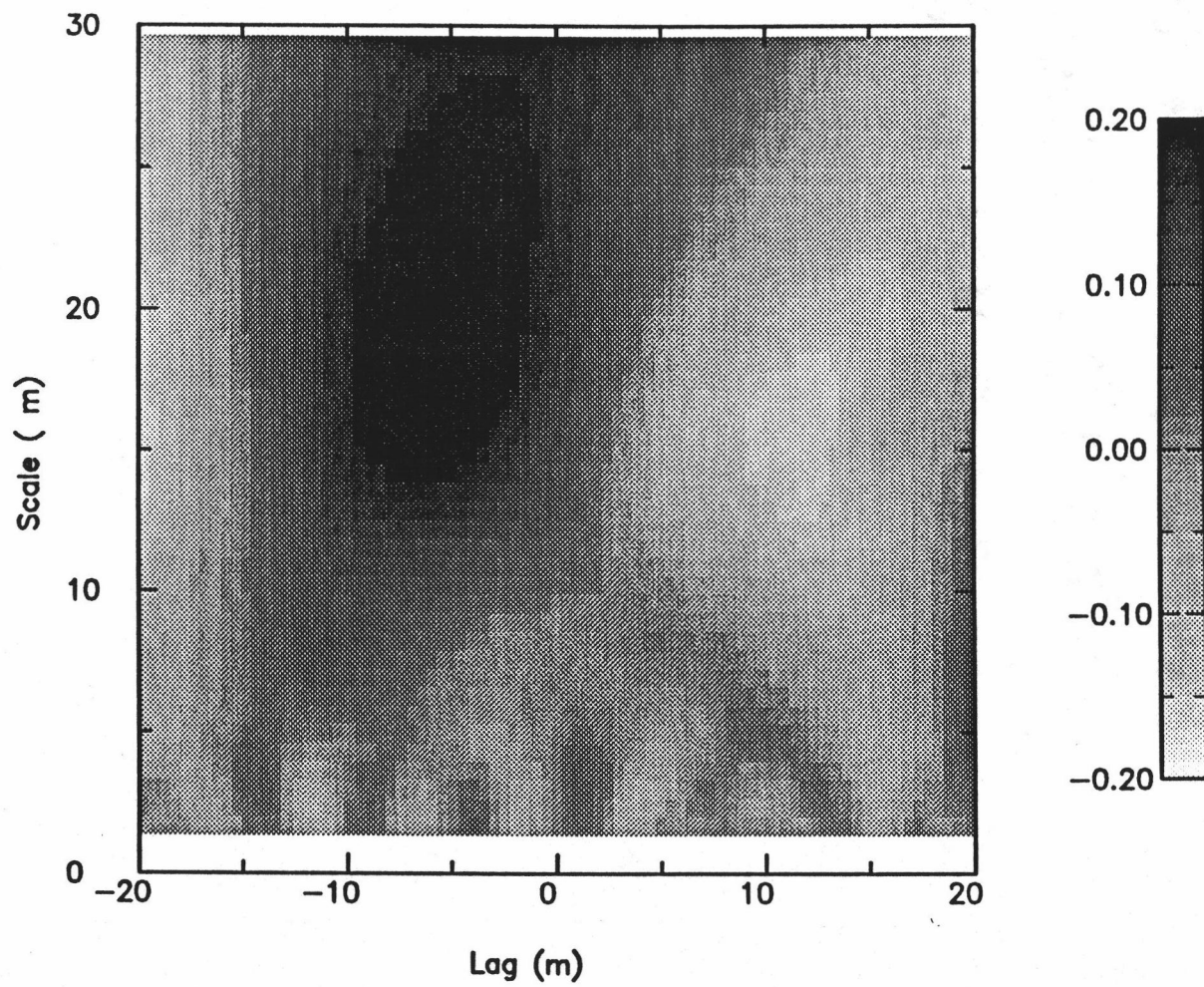
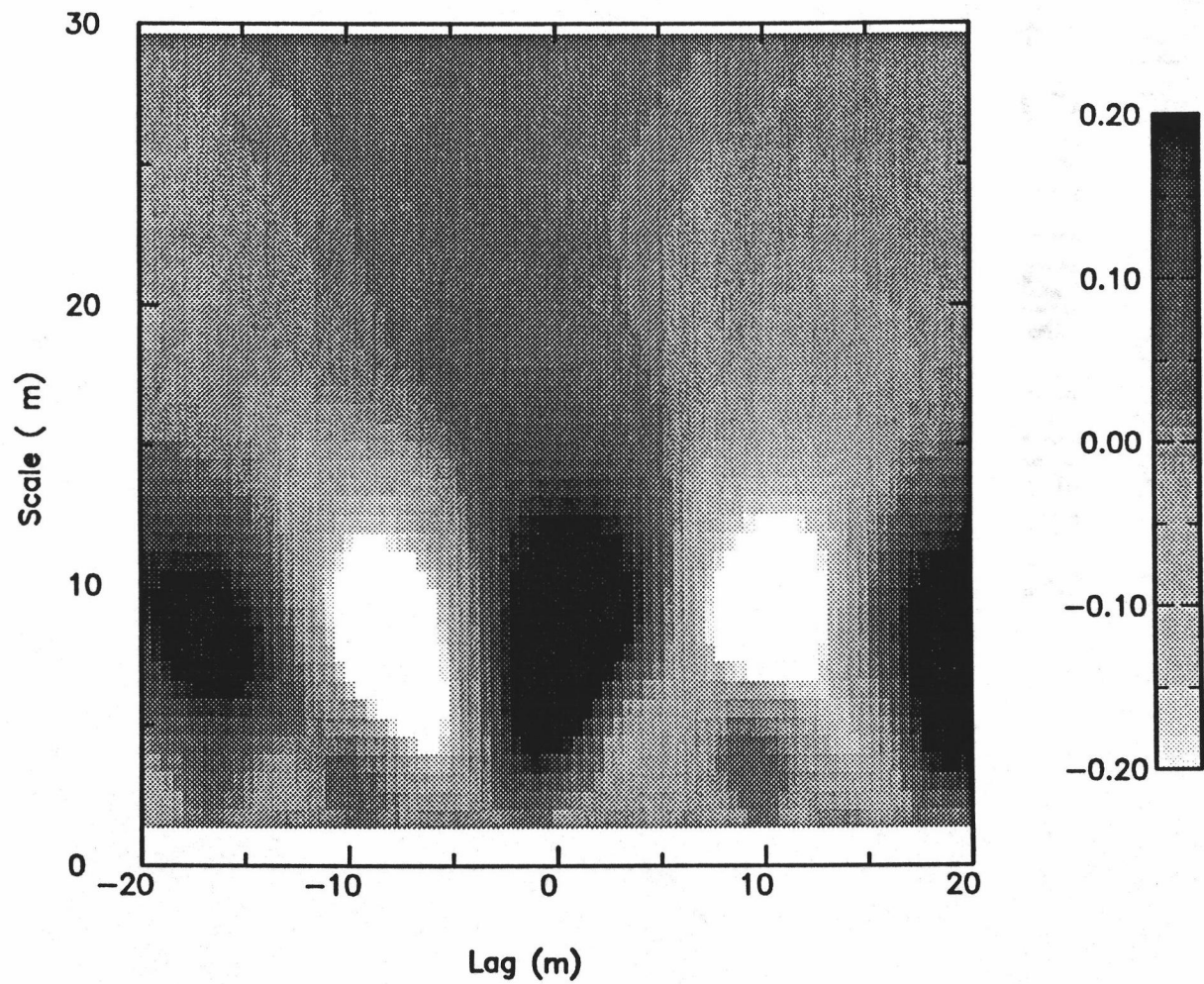
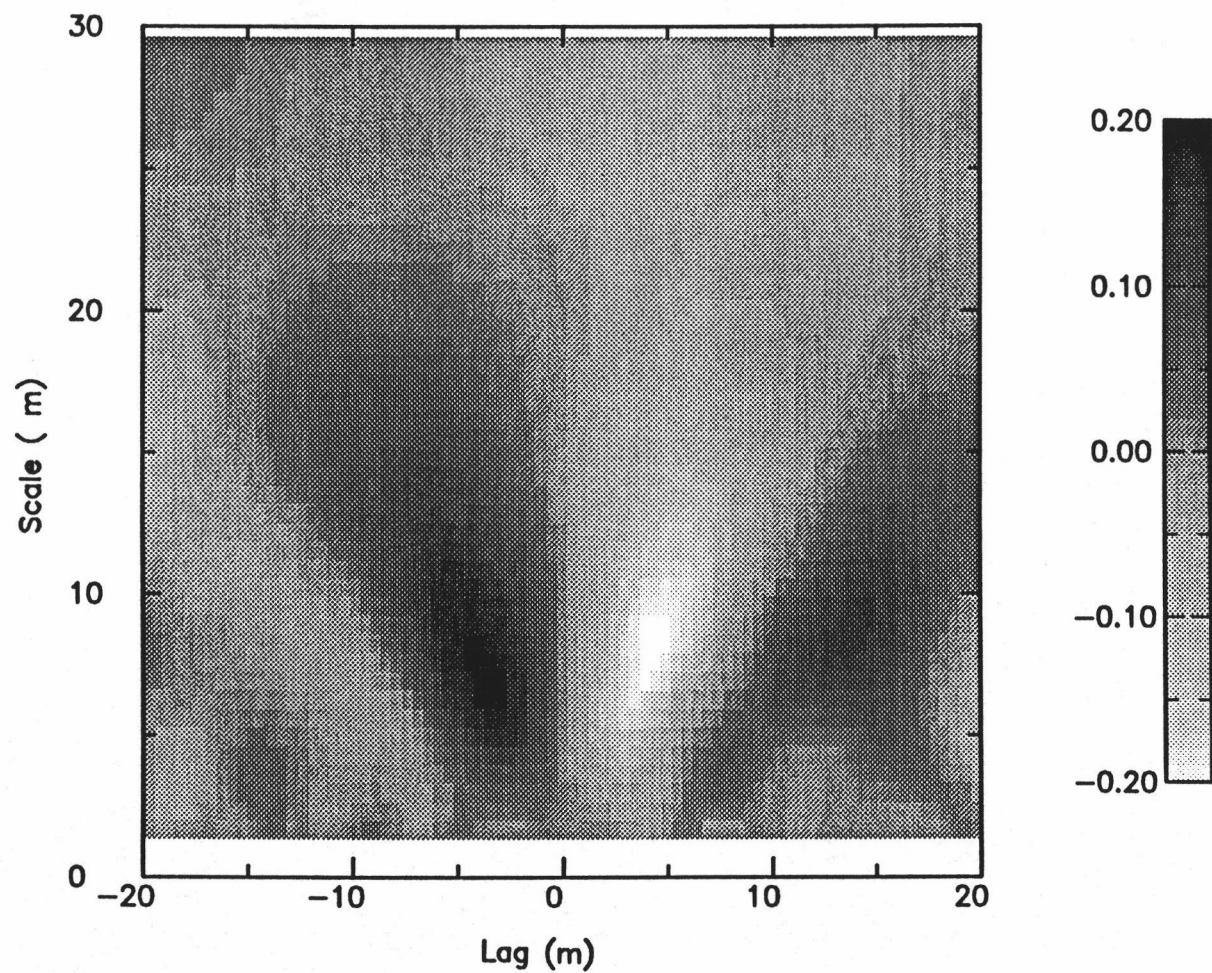


Figure 5.35



**Figure 5.36** Wavelet cross-covariance between woody debris and hemlock seedlings for mature stand M1.



**Figure 5.37** Wavelet cross-covariance between canopy gap and hemlock seedlings for mature stand M1.

**Figure 5.38** Wavelet cross-covariance between canopy gap and hemlock seedlings for mature stand M3. Note lack of structure.

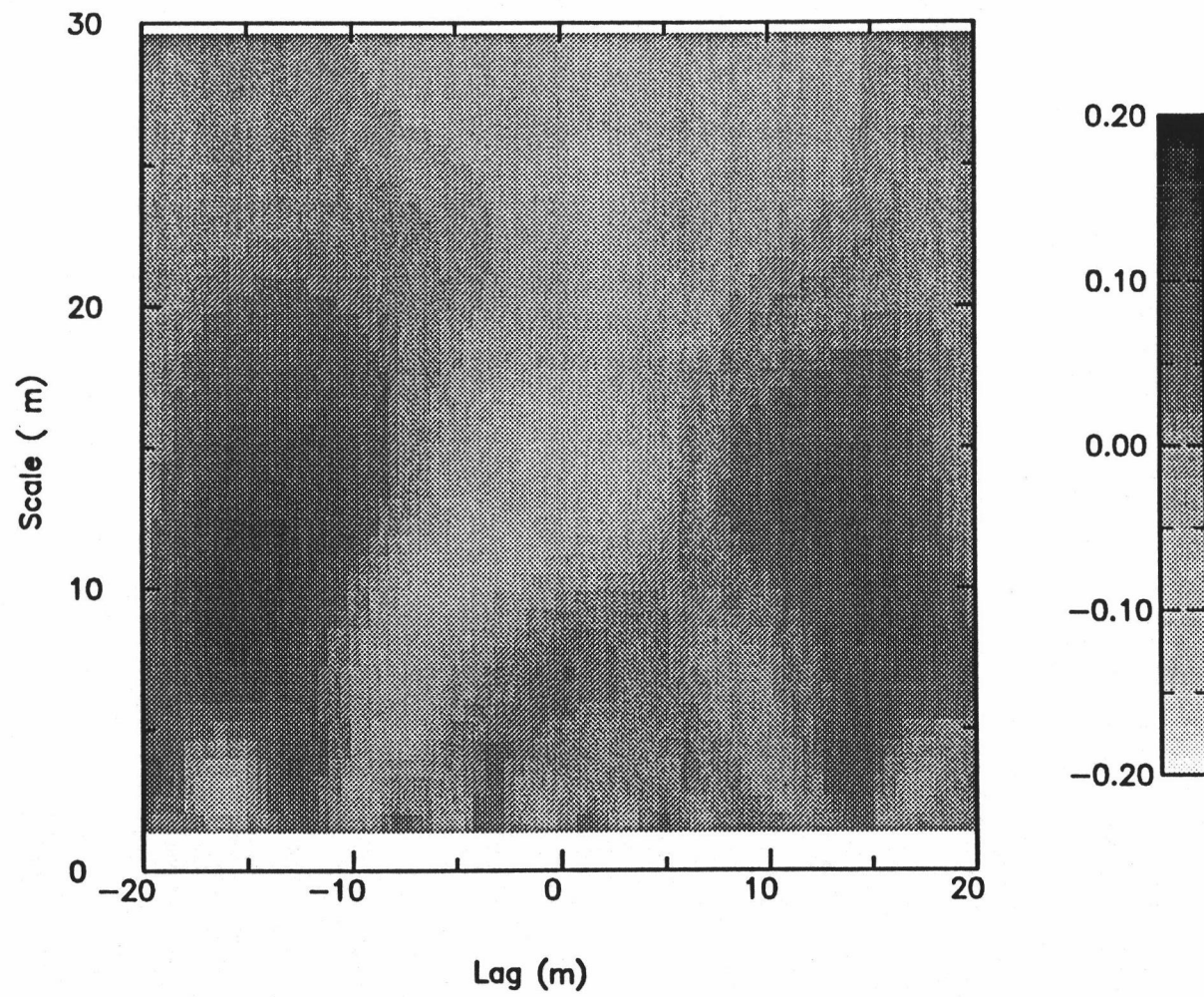


Figure 5.38

## LITERATURE CITED

- Agee, J., 1989, "The historical role of fire in the Pacific Northwest Forests". in "Natural and Prescribed Fires in Pacific Northwest Forests, 1990, Oregon State University Press, 317 pp.
- Alaback, P. B., 1981, "Forest community structural changes during secondary succession in southeast Alaska". in "Forest Succession and Stand Development Research in the Northwest, Proc. Symposium 26 March, 1981, Corvallis, Oregon, FRL, Oregon State University.
- Alaback, P.B. and F.R.Herman, 1988, "Long-term response of understorey vegetation to stand density in Picea-Tsuga forests". Canadian Journal of Forests Resources. 18: pp. 1522-1530.
- Beatty, S.W., 1984, "Influence of microtopography and canopy species on spatial patterns of forest understory plants". Ecology. 65(5), pp. 1406-1419.
- Connell, J.H. and R.O. Slatyer, 1977, "Mechanisms of succession in natural communities and their role in community stability and organization". American

Naturalist. 111, pp. 1119-1144.

Daubenmire, R.F., 1968, "Plant communities: a textbook of plant synecology". Harper and Row, New York, 300 pp.

Franklin, J.F. and C.T. Dyrness, 1984, "Natural Vegetation of Oregon and Washington". Oregon State University Press. 452 pp.

Halpern, C.B., 1989, "Early successional patterns of forest species: interactions of life history traits and disturbance". Ecology, vol 70(3), pp. 704-720.

Halpern, C.B. and J.F. Franklin, 1989, "Physiognomic development of Pseudotsuga forests in relation to initial structure and disturbance intensity". Journal of Vegetation Science. 1: pp. 475-482.

Hermans, Martin, 1988, "Correlation between forest layers in mixed deciduous forests in Flanders (Belgium). in "Diversity and pattern in plant communities, ed. H.J. During, M.J.A. Werger, and J.H. Willems Academic Publishing, The Hague, Netherlands.

Mueller-Dombois, D. and H. Ellenberg, 1974, "Aims and methods of Vegetation ecology". John Wiley and Sons. 547 pp.

Oliver, C.D. and B.C. Larson, 1990, "Forest stand dynamics". McGraw-Hill. 467 pp.

Spies, T.A. and J.F. Franklin, 1990, "Gap characteristics and vegetation response in coniferous forests of the Pacific Northwest". Ecology, vol 70(3), pp.543-545.

Spies, T.A., J.F. Franklin, and T.B. Thomas, 1988, "Coarse woody debris in Douglas-fir forests of western Oregon and Washington". Ecology: 69(6), pp.1689-1702.

Waring, R.H. and W. Schlesinger, 1985, "Forest ecosystems: concepts and management". Academic Press. 340 pp.

Yoccoz, N.G., 1991, "Use, overuse, and misuse of significance tests in evolutionary biology and ecology". Bulletin of the Ecological Society of America. 72(2): pp. 106-110.

Zamoro, B.A., 1981, "Understorey development in forest succession: an example from the inland northwest". in Forest Succession and stand development research in the Northwest, Proc. Symposium, 26 March, 1981, Corvallis, Oregon.

## Chapter 6

### CONCLUSIONS

This dissertation has presented the use of a method called wavelet analysis to quantify spatial pattern and infer related processes from ecosystem transect data. While wavelet analysis is one of many methods which can be used for pattern quantification, it offers an alternative approach for non-uniform and hierarchically structured data. The main advantage of the wavelet is its ability to preserve the relationship between pattern scale and location.

When three time series methods were compared using a set of stationary processes, the resolution capabilities of each method was comparable in the majority of cases. However, both the wavelet variance and power spectrum were found to be superior to the semi-variogram in cases where the data is characterised by a repeating, single-scale structure. Both the power spectrum and the wavelet variance were found to be sensitive to data morphology and the relative scales of pattern in the data. The appropriate choice between methods will depend on consideration based on specific data morphology, ratio of the dominant scale of patterns which characterise the data, and study objectives. Once again, the ratio of the "dominant" scale of patterns must be applied

relative to the given set of data and study objectives. This ration will vary as a function of such variables as signal contrast (amplitude) and period.

The wavelet cross-covariance function was developed and introduced as a method to describe the spatial correlation of two variables as a function of scale and offset. A two-dimensional contour plot of the maximum values of the function identifies the scale and the offset at which both variables are correlated. The analysis effects a scale by scale comparison of pattern in multivariate data.

To illustrate the concept and method of multi-scale analysis using the wavelet transform, both satellite imagery and forest stand-level data were employed. Results from both the understory-canopy and remote sensing studies demonstrate the importance of the spatial relationship between the components of the ecosystem in addition to their abundance or composition. A disregard for the spatial heterogeneity of a system may result in a skewed interpretation of the results.

Using satellite imagery at three resolutions, wavelet analysis was performed to identify major landscape and sub-landscape features in the western Cascade area of Oregon. The structure of the western Cascades was dominated by various scales of features ranging from 100 meters to several kilometers. These patterns were inferred to result from recent human disturbance (i.e. varying land practices as a function of ownership). In contrast, the major factor governing the

dominant scale of biomass pattern in the Starkey Experimental Forest of northeastern Oregon, was inferred to reflect a topographically-linked response to a steep environmental gradient or critical moisture threshold restricting vegetation distribution. Scales at which these patterns dominated differed according to location within the state. The pattern found in Starkey was in marked contrast to the Douglas-fir stands of the western Cascades where vegetation appears more uniform and less closely coupled to topographic trends. Although representing an undersampling of the landscape, these preliminary results encourage an extension to two-dimensions. In the two-dimensional context, the wavelet cross-covariance may be used with GIS (geographical information systems) maps of such variables as elevation and aspect.

Wavelet analysis was also used to explore within-stand variability among age-classes in Douglas-fir forests in the western Cascades. Results indicate that while canopy gap structure appears to follow stand development, small to intermediate disturbance events significantly influence canopy gap structure. Calculation of the wavelet variance facilitated comparison between stands of varying ages and stand histories allowing for the identification of disturbance and age-related trends. Spatial patterns of understory vegetation generally followed canopy gap structure trends. Deviations from age-related trends were identified with differences in the abundance of overstory hemlock and disturbance-derived gaps.

The wavelet cross-covariance function was able to elucidate these patterns which other, more traditional methods failed to distinguish.

As the availability of satellite imagery and mapped data increases, it will become more important to be able to perform such an analysis in the according dimensionality. A two-dimensional wavelet analysis should be formulated to capture all aspects of the pattern in the remotely sensed image. Transects cannot capture the scope of a two-dimensional pattern. The incorporation of spatial information may prove essential in the analysis of resource management at the landscape scale. For example, wavelet cross-covariance analysis may be a useful means by which spatial information can elucidate scale-dependent physical processes governing vegetation distributions by using such data as classified satellite imagery and digital terrain maps to quantify topographic-spectral relationships. Similarly, wavelet analysis may be helpful identifying wildlife movement patterns as measured by radio telemetry in relationship to vegetation distribution.

With increased dimensionality, the interpretation and display of the analysis will become more complex. These are obstacles which can be addresses with increasingly flexible computer graphics. It remains to the scientist to be able to comprehend the results.

**BIBLIOGRAPHY**

Agee, J., 1990, " The historical role of fire in the Pacific Northwest fires", in " Natural and Prescribed fires in Pacific Northwest Forests". Oregon State University Press. 317 pp.

Agee, J., 1989, "The historical role of fire in the Pacific Northwest Forests", in "Natural and Prescribed Fires in Pacific Northwest Forests, 1990, Oregon State University Press, 317 pp.

Alaback, P. B., 1981, "Forest community structural changes during secondary succession in southeast Alaska", in "Forest Succession and Stand Development Research in the Northwest, Proc. Symposium 26. March, 1981, Corvallis, Oregon, FRL, Oregon State University.

Alaback, P.B. and F.R.Herman, 1988, "Long-term response of understory vegetation to stand density in Picea-Tsuga forests". Canadian Journal of Forests Resources. 18: pp. 1522-1530.

- Argoul, F., A. Arneodo, G. Grasseau, Y. Gagne, E.J.  
Hopfinger, U.Frisch, 1989, "Wavelet analysis of  
turbulence reveals the multifractal nature of  
the Richardson cascade", Nature. 338: 51-53.
- Baldwin, E.M., 1976, "Geology of Oregon. Kendall/Hunt  
Publishing Co. 147 pp.
- Barbour, M.G., J.H. Burk, and W.D. Pitts, 1980,  
"Terrestrial Plant Ecology". Benjamin/Cummings  
Pubs. , 604 pp.
- Beatty, S.W., 1984, "Influence of microtopography and  
canopy species on spatial patterns of forest  
understorey plants". Ecology. 65(5), pp. 1406-  
1419.
- Bracewell, R.N., 1978, "The Fourier transform and its  
applications. McGraw Hill, New York, 444 pp.
- Carpenter, S.R. and J.E. Chaney, 1983, "Scale of pattern:  
four methods compared". Vegetatio 53: 153-160.
- Chatfield, C., 1989, "The analysis of time series: an  
introduction", 4th edition, Chapman and Hall.  
241 pp.

- Cohen, W, B., T.A. Spies and G.A. Bradshaw, 1990, "Semi-variograms of digital imagery of conifer canopy structure", Remote Sensing of the Environment. 34: pp.167-178.
- Connell, J.H. and R.O Slatyer, 1977, "Mechanism of succession in natural communities and their role in community stability and organization". American Naturalist, 111. pp. 1119-1144.
- Curran, P., 1988, "The semi-variogram in remote sensing". Remote Sensing of the Environment. vol 24, pp. 620-628.
- Curran, P., 1980, "Multi-spectral remote sensing of vegetation amount". Progress in Physical Geography, 4(3), pp. 315-341.
- Dale, M. R. T. and D.A. MacIssacs, 1989, "New methods for spatial analysis of pattern in vegetation". Journal of Ecology. 77: 78-91.
- Daubechies, I, 1988, " Orthonormal bases of compactly supported wavelet. Communications of Pure and Applied Mathematics. 41: pp.909-996.

- Daubechies, I., A. Grossman, and Y.J. Meyer,  
(1986). "Painless non-orthogonal expansions".  
Journal of Mathematical Physics. 27: pp. 1271-  
1283.
- Daubenmire, R.F., 1968, "Plant communities: a textbook of  
plant synecology". Harper and Row, New York,  
300 pp.
- Ford, E.D. and E. Renshaw (1984). "The interpretation of  
process from pattern using two-dimensional  
spectral analysis". Vegetatio 56: pp. 113-123.
- Forman, R.T.T. and M. Godron, 1986, "Landscape Ecology".  
John Wiley. 354 pp.
- Franklin, J.F. and C.T. Dyrness, 1984, "Natural vegetation  
of Oregon and Washington". Oregon State  
University Press. 452 pp.
- Franklin, J.F. and R.T.T. Forman, 1987, "Creating landscape  
patterns by cutting: ecological consequences  
and principles". Landscape Ecology, 1, pp. 5-  
18.

Gamage, N.K.K., 1990, "Detection of coherent structures in shear induced turbulence using the wavelet transform methods". AMS Symposium on Turbulence and Diffusion, Roskilde, Danmark, April 1990.

Gholz, H.L., S.A. Vogel, W.P. Cropper, K. McKelvey, K.C. Ewel, R.O. Teskey, and P.J. Curran, 1991, "Dynamics of canopy structure and light interception in Pinus stands, North Florida". Ecological Monographs, 61(1), pp. 33-54.

Grieg-Smith, P., 1964, "Quantitative Plant ecology". 2nd edition, Butterworth, London.

Halpern, C.B., 1989, "Early successional patterns of forest species: interactions of life history traits and disturbance". Ecology, vol 70(3), pp. 704-720.

Halpern, C.B. and J.F. Franklin, 1989, "Physiognomic development of Pseudotsuga forests in relation to initial structure and disturbance intensity". Journal of Vegetation Science. 1: pp. 475-482.

- Harris, L.D., 1984, "The Fragmented Forest: Island biogeography theory and the preservation of biotic diversity". University of Chicago Press. 211 pp.
- Hemstrom, M.A. and S.E. Logan, 1986, "Plant association and management guide, Siulslaw National Forest". USDA Forest Service, R6-Ecol 220-1986a.
- Hermly, Martin, 1988, "Correlation between forest layers in mixed deciduous forests in Flanders (Belgium). in "Diversity and pattern in plant communities, ed. H.J. During, M.J.A. Werger, and J.H. Willems. Academic Publishing, The Hague, Netherlands.
- Journel, A.G. and Ch. J. Huijbregts, 1978, Mining Geostatistics, Academic Press, 600 pp.
- Jupp, D. L. B., A.H. Strahler, and C.E. Woodcock, 1988, "Autocorrelation and regularization in digital images: I. Basic Theory." IEEE Transactions. Geosci. Remote Sens., vol. 26, pp. 463-473.

Kenkel, N.C. "Spectral Analysis of hummock-hollow pattern in a weakly minerotrophic mire". *Vegetatio* 78: pp. 45-52.

Knipling, E.B., 1970, "Physical and physiological basis for the reflectance of visible and near-infrared radiation from vegetation", *Remote Sensing of the Environment*. 1: pp. 155-159.

Legendre, P. and M.-J. Fortin, 1989, "Spatial pattern and ecological analysis", *Vegetatio* 80: pp.108-138.

Levin, D.A. and H.W. Kerster, 1971, "Neighborhood structure in plants under diverse reproductive methods". *American Naturalist* 105: pp. 345-354.

Levin, S.A., 1988, "Patterns, scale, and variability". *Lecture Notes in Biomathematics*. Springer-Verlag, pp.1-12.

Liebermann, M.D., D. Liebermann, and R. Peralta (1989). "Forests are not just swiss-cheese: canopy stereogeometry of non-gaps in tropical forests". *Ecology*. 70(2), pp. 550-552.

Lillesand, T.M. and R.W. Kiefer, 1987, "Remote Sensing and Image Interpretation" (second edition). John Wiley. New York.

MacIntosh, R. P., 1985, "The background of ecology".  
Cambridge Studies in Ecology. 382 pp.

Mallet, S.G. (1988). "Review of multi-frequency channel decompositions of images and wavelet models".  
Robotics report no. 178, Courant Institute  
of Mathematical Sciences, New York  
University, New York.

Milne, B.T., 1988, "Measuring the fractal geometry of landscapes". Applied Mathematical Computing.  
27, pp. 67-79.

Moloney, K.A., S.A. Levin, N.R. Chiariello, and L. Buttel,  
in review, "Pattern and Scale in a Serpentine  
Grassland." Moloney, K.A., A. Morin and  
S.A. Levin, in press, "Interpreting  
ecological patterns generated through simple  
stochastic processes", Landscape Ecology.

Mueller-Dombois and H. Ellenberg (1974). "Aims and Methods of Vegetation Ecology". John Wiley and Sons, New York. 546 pp.

Neilsen, R.P. and L.H. Wullstein, 1983, "Biogeography of two southwest American oaks in relation to atmospheric dynamics", Journal of Biogeography. 10: 275-97.

Oliver,, C.D. and B.C. Larson, 1990, "Forest stand dynamics". McGraw-Hill. 467 pp.

Pickett, S.T.A. and P.S. White, eds, 1985, "The ecology of natural disturbance and patch dynamics". New York, Academic Press. pp.189-209.

Pielou, E.C., 1977, "Mathematical Ecology". Wiley, New York. 214.pp.

Platt, T. and K.L. Denman, 1975, "Spectral analysis in ecology". Ann. Rev. Ecol. Syst. 6: 189-210.

Powell, T. M., 1989, "Physical and biological scales of variability in lakes, estuaries, and the coastal ocean". in 'Perspectives in ecological theory', eds., J. Roughgarden, R.M. May, and S.A. Levin. Princeton University Press, 394 pp.

Priestley, M.B., 1981, "Spectral analysis and time series". (volumes 1 and 2), London, Academic Press.

Renshaw, E. and E.D. Ford, 1984, "The description of spatial pattern using two-dimensional spectral analysis". *Vegetatio* 56: 75-85.

Ripley, B.D., 1981, "Spatial Statistics". Wiley, New York.

Ripple, W.J., G.A. Bradshaw, and T.A. Spies, 1991, "Measuring landscape patterns in the Cascade Range of Oregon, U.S.A.". *Biological Conservation*. 57: pp.73-88.

Sears, P.B., 1955, "Some notes on the Ecology of Ecologists". *The Scientific Monthly*. July. pp.22-27.

Spies, T.A. and J.F. Franklin, in press. "The structure of natural young, mature, and old-growth forests in Washington and Oregon". in Old Growth Symposium GTR, 1989.

Spies, T.A. and J.F. Franklin, 1990, "Gap characteristics and vegetation response in coniferous forests of the Pacific Northwest". Ecology, vol 70(3), pp.543-545.

Spies, T.A., J.F. Franklin, and T.B. Thomas, 1988, "Coarse woody debris in Douglas-fir forests of western Oregon and Washington". Ecology: 69(6), pp.1689-1702.

Spies, T.A., J.F. Franklin, and M. Klopsch (1990). "Canopy gaps in Douglas-fir forest of the Cascade Mountains". Canadian Journal of Forest Research. 20: pp. 649-659.

Tucker, C.J., I. Y. Fung, C.D. Keeling, and R.H. Gammon, 1986, "Relationship between atmospheric CO<sub>2</sub> variations and a satellite-derived vegetation index". Nature. 319: pp.195-199.

- Turner, S.J., R.V. O'Neill, W. Conley, M. Conley, and H. Humpheries (1991). "Pattern and Scale: statistics for landscape ecology". in M.G. Turner & R.H. Gardner, editors, "Quantitative Methods & Landscape Ecology". Springer Verlag.
- Waring, R.H., 1989, "Ecosystems: Fluxes of matter and energy", in "Ecological Concepts: The contribution of ecology to an understanding of the natural world", 29th Symposium, British Ecological Society, 1988. Blackwell Sci. Pubs. pp. 17-41.
- Waring, R.H. and W. Schlesinger, 1985 , "Forest ecosystems: concepts and management". Academic Press. 340 pp.
- Yahner, R.H., 1988, "Changes in wildlife communities near edges". Conservation Biology. 2: pp. 333-339.
- Yoccoz, N.G., 1991, "Use, overuse, and misuse of significance tests in evolutionary biology and ecology". Bulletin of Ecological Society of America. 72(2): pp. 106-110.

Zamoro, B.A., 1981, "Understory development in forest succession: an example from the inland northwest". in Forest Succession and stand development research in the Northwest, Proc. Symposium, 26 March, 1981, Corvallis, Oregon.